A ROLE FOR DEFERASIROX AS AN ANTI-NEOPLASTIC AND CHEMOSENSITISING AGENT IN GASTROINTESTINAL CANCER

MATTHEW ROBERT BEDFORD

A thesis submitted to

The University of Birmingham

for the degree of

DOCTOR OF PHILOSOPHY

School of Cancer Sciences

College of Medical and Dental Sciences

University of Birmingham

February 2015

Abstract

Cancer of the gastrointestinal tract remains a significant cause of morbidity and mortality. Although surgical resection of the primary tumour remains the cornerstone of curative treatment, chemotherapy forms an increasingly important component of the management armamentarium. Response to therapy, however, is by no means uniform and thus the development of new agents is highly desirable.

There is a significant body of evidence implicating iron in the malignant progression of gastrointestinal cancer. Tumours acquire an excess of iron which in turn propagates their malignant phenotype. This project aimed to demonstrate that a strategy to deplete tumour cells of iron using the licensed iron chelator Deferasirox was effective in the treatment of oesophageal and colorectal cancer.

Deferasirox significantly impedes cellular viability and proliferation both *in-vitro* and *in-vivo* in oesophageal and colorectal cancer models. The drug can overcome established chemotherapy resistance and may also act as a chemosensitiser. The disturbance of normal intracellular iron homeostasis and increased dependence of gastrointestinal tumour cells on iron means chelation may offer targeted therapy. Certain iron regulatory proteins may also serve as biomarkers for treatment efficacy. Deferasirox therefore represents an effective and well tolerated adjunct to existing therapies that should be considered for future clinical trials.

Dedication

This thesis is dedicated to my beautiful wife Laura and my little boy Henry. Laura, you are my inspiration and without your constant help and support throughout the period of this PhD (and beyond) I simply would not have completed it. Henry, thank you for smiling and laughing at me every time I come home, regardless of what sort of a day I've had!

Acknowledgements

I am indebted to my supervisor and friend Dr Chris Tselepis for the patience, guidance and intellect shown to me throughout the duration of this project. Without his input and support it would simply not have been possible. Chris, for that I will be forever grateful. I would also like to acknowledge the support of my co-supervisors Professor Derek Alderson and Mr Samuel Ford.

The remainder of the Tselepis group (in particular Richard, Elisabeth and Dan) have been a constant pillar of support throughout this project and I have really enjoyed our time working together. Thanks also go to Dr Mat Coleman and Mr Andrew Beggs for their help with the vector and statistical work respectively. Sarah Evans completed her BSc project during the course of this PhD and contributed to the work on IRP2. Her enthusiasm and hard work were an asset to the group.

Finally, I would like to acknowledge the vital support of my funders the Royal College of Surgeons of England (for a Surgical Research Fellowship), the Royal College of Surgeons of Edinburgh (for a Small Research Support Grant) and the University of Birmingham (for a Preliminary Data Award). I offer my sincere thanks to all of these organisations and to the wonderful people who support them.

Contents

List of Abbreviations

APC	Adenomatous polyposis coli
Bax	Bcl-2-like protein 4
BM	Barrett's metaplasia
B-raf	Murine sarcoma viral oncogene homolog B
Brdu	5-bromo-2'-deoxyuridine
CDC4	Cell division control protein 4
CDK	Cyclin dependent kinase
CDKI	Cyclin dependent kinase inhibitor
cDNA	Complementary deoxyribonucleic acid
Ct	Cycle threshold
Dcytb	Duodenal cytochrome b
DFO	Desferrioxamine
DMEM	Dulbecco's Modified Eagles Medium
DMSO	Dimethyl sulfoxide
DMT1	Divalent metal transporter 1
DNA	Deoxyribonucleic acid
Dp44mT	Di-2-pyridylketone-4,4-dimethyl-3-thiosemicarbazone
ECF	Epirubicin, Cisplatin and 5-Fluorouracil
ECL	Enhanced chemiluminescence
EDTA	Ethylenediaminetetraacetic acid
EGFR	Epidermal growth factor receptor
EOC	Epirubicin, Oxaliplatin and Capecitabine
ERK	Extracellular signal-regulated kinases
FACS	Fluorescence-activated cell sorting
FBC	Full blood count
FCS	Foetal calf serum
FPN	Ferroportin
GORD	Gastro-oesophageal reflux disease
GSK	Glycogen synthase kinase
Hb	Haemoglobin
HCP1	Haem-carrier protein 1
HEPES	4-(2-hydroxyethyl)-1-piperazineethanesulfonic acid
HER2	Receptor tyrosine-protein kinase erbB-2

HFE	Haemochromatosis gene
HIF	Hypoxia-inducible factor
HIF1α	Hypoxia-inducible factor 1-alpha
HO1	Haem oxygenase 1
IGF2R	Insulin-like growth factor 2 receptor
IHC	Immunohistochemistry
IRE	Iron responsive element
IRP1	Iron regulatory protein 1
IRP2	Iron regulatory protein 2
kDa	Kilo Dalton
K-ras	Kirsten rat sarcoma
MAPK	Mitogen activated protein kinase
MEK	Mitogen activated protein kinase kinase
mRNA	Messenger ribonucleic acid
mTOR	Mammalian target of rapamycin
MTT	3-(4,5-dimethylthiazol-2-yl)-2,5-diphenyltetrazolium bromide
Ndrg1	N-myc downstream regulated gene 1
NF-κB	Nuclear factor κB
NOD-SCID	Non-obese diabetic-severe combined immunodeficiency
OAC	Oesophageal adenocarcinoma
PBS	Phosphate buffered saline
PI	Propidium iodide
PIK3CA	Phosphatidylinositol-4,5-bisphosphate 3-kinase, catalytic subunit alpha
PVDF	Polyvinylidene difluoride
qRT-PCR	Quantitative real-time polymerase chain reaction
REDD1	Regulated in development and DNA damage response
RIPA	Radio-immuno-precipitation buffer
ROS	Reactive oxygen species
RPMI	Roswell Park Memorial Institute medium
rRNA	Ribosomal ribonucleic acid
SCC	Squamous cell carcinoma
SDS	Sodium dodecyl sulphate
SDS-PAGE	Sodium dodecyl sulphate -Polyacrylamide Gel Electrophoresis
siRNA	Short interfering ribonucleic acid

SMAD4	Mothers against decapentaplegic homolog 4
SPSS	Statistical Package for the Social Sciences
SRB	Sulforhodamine B
TBS	Tris-buffered saline
TBST	Tris-buffered saline tween
Tf	Transferrin
TfR1	Transferrin receptor 1
TGFBR2	Transforming growth factor beta receptor 2
TNM	Tumour, Node and Metastasis
TP53	Tumour protein p53
VEGF	Vascular endothelial growth factor
VEGFR	Vascular endothelial growth factor receptor
WB	Western blotting

List of Figures

List of Tables

Chapter 1. Introduction

1.1 Gastrointestinal Cancer

Cancer is a disease characterised by uncontrolled growth and spread of structurally and biologically abnormally differentiated cells that can originate from any tissues within the body. [1]

On a worldwide basis, there are over 12.5 million new cases of cancer each year and the disease is responsible for over 7.5 million deaths. [2] In the United Kingdom (UK), cancer is a major cause of morbidity and mortality with over 300,000 people per year diagnosed. [3] The disease is responsible for more than 1 in 4 deaths in the UK; a figure significantly greater than those caused by ischaemic heart disease or stroke. [4]

The gastrointestinal tract runs from the mouth to the anus and includes organs such as the oesophagus, stomach, small intestine, colon and rectum. [5] Cancer of the gastrointestinal tract encompasses a range of heterogeneous malignancies arising from different organs which, when grouped together, accounts for approximately 20% of all new cancer diagnoses each year. [6]

Within this thesis two specific forms of gastrointestinal malignancy have been focused upon; the first being cancer of the oesophagus (a disease whose incidence has increased dramatically over recent decades) and the second, cancer of the colon and rectum (the second largest cause of cancer related death in the UK). [7, 8]

1.2 Cancer of the Oesophagus

1.2.1 Structure and Function of the Oesophagus

The oesophagus is a muscular tubular structure, approximately 25 cm in length, joining the pharynx to the stomach. [5] Its primary function is the conduction of food from the mouth to the stomach through the action of peristalsis. [5] It is lined predominantly by squamous epithelium and (apart from some striated muscle in the upper cricopharyngeal sphincter) is comprised of smooth muscle under autonomic control. [9] The distal oesophagus is protected against the regurgitation of acidic gastric contents by a 'functional' lower oesophageal sphincter assisted by the constricting muscle bands of the diaphragm and an acute angle of entry into the stomach. [9] The final 1.5-2 cm of the oesophagus is situated below the diaphragm and is lined my columnar epithelium. [9] The transition point from squamous to columnar epithelium occurs at around 40 cm (from the incisor teeth) and is clearly visible on endoscopy. [9]

1.2.2 Oesophageal Cancer

Owing to the different types of epithelium found within the oesophagus there are two main forms of oesophageal carcinoma – squamous cell carcinoma (SCC, which tends to arise in the upper two thirds of the oesophagus) and adenocarcinoma (OAC, which typically arises in the lower third). [9] Other less common subtypes include melanoma, leiomyosarcoma and small-cell carcinoma. [10]

Cancer of the oesophagus is a global health problem and was the 6th most common cancer on a worldwide basis in 2002. [11] It is characterised by a worldwide geographical variation in incidence, being the 4th most common tumour in developing countries but only the 15th in developed countries. [12]

Over the past 30 years the relative incidence of oesophageal carcinoma has risen dramatically, largely driven by an unprecedented increase in cases of the OAC subtype. [13] In the UK, oesophageal carcinoma is now the 9th most common cancer (by incidence) with over 8,000 new cases per year. [14] There is a strong male to female preponderance with an incidence ratio of 2:1 in favour of males. [14] Overall 5 year survival rates remain poor (13%). [14] This compares with rates of 20% in China and 15.4% in the United States. [15] The disease is uncommon below the age of 50. [16]

1.2.2.1 Squamous Cell Carcinoma

Squamous cell carcinoma (SCC) of the oesophagus remains the predominant histological type of oesophageal carcinoma worldwide. [17] It typically arises in the upper two thirds of the oesophagus and risk factors for its development are well documented (Table 1.1). Heavy alcohol intake is associated with at least a 20 fold greater risk and smokers have at least 5 times the risk of non-smokers. [16]

Rates of SCC are highest in the so called Asian belt encompassing Turkey, north eastern Iran, Kazakhstan and northern and central China. [17] Incidence rates in these areas are greater than 100 cases per 100 000 population annually. [17] SCC rates are also high in certain parts of southern and eastern Africa. [17]

1.2.2.2 Oesophageal Adenocarcinoma

OAC typically arises in the lower third of the oesophagus. [9]

The main risk factors for OAC are listed in Table 1.1. Symptomatic gastro-oesophageal reflux disease (GORD) is one of the strongest risk factors, although preceding symptoms are said to be infrequent or absent in more than 40% of patients who develop the disease. [18] Obesity, which is increasing dramatically worldwide, is also a risk factor for both OAC in its own right and for GORD. [19, 20]

In cases of longstanding GORD, the lower oesophagus may come to be lined by columnar mucosa, a condition referred to as Barrett's oesophagus or Barrett's metaplasia (BM). [9] At endoscopy, proximal extension of pink columnar mucosa can be seen replacing the pearly-white squamous epithelium of the lower oesophagus. [9] Initially, this transformation in epithelium is in the form of tongues extending up from the gastric cardia, but as it develops it may come to represent a complete cylinder of columnar epithelium that can occupy much of the distal half of the oesophagus. [9]

Microscopically, BM consists of columnar epithelium, containing goblet cells and intervening mucus-producing cells which both secrete intestinal-type mucins (a form of intestinal metaplasia). [9] Whilst the initial change from squamous epithelium to a gastric-type mucosa is accepted as being a response to acid reflux, the development of intestinal-type features cannot be explained solely as a response to acid. [9] Other factors, such as bile reflux, are also likely to play a role. [9]

The reported prevalence of BM in the general population is 1.6%. [21] In patients undergoing endoscopy for GORD type symptoms it is 10-15%. [22] As well as GORD, abdominal obesity is a risk factor for the development of BM. [23]

BM is the strongest risk factor for OAC and its presence is estimated to increase the risk of developing OAC by 30 to 125 fold. [24, 25, 26] The annual conversion rate of BM to OAC has been estimated to be as high as 0.5% per year with the risk being greatest in patients with high-grade dysplasia of the oesophagus (which progresses to OAC in 16-59% of cases). [17, 27, 28, 29,] Genetic abnormalities present in BM (e.g. chromosomal instability, cell cycle abnormalities, expression of the proto-oncogene c-Myc, p53 mutational status and KI67 staining) have all been postulated as potential biomarkers of progression to OAC although none have been conclusively validated. [17, 30]

Table 1.1 Risk factors for oesophageal SCC and OAC

Squamous Cell Carcinoma (SCC)	Adenocarcinoma (OAC)
Tobacco use	Symptomatic gastro-oesophageal reflux disease
Alcohol consumption	Barrett's oesophagus
Mutations in alcohol metabolising enzymes	Obesity
Achalasia	Tobacco use
Caustic injury	Previous thoracic radiation
Previous thoracic radiation	Diet low in vegetables and fruit
Poor oral hygiene	Increased age
Nutritional deficiencies	Male sex
Non-epidermolytic palmoplantar keratoderma	Medications that relax lower oesophageal sphincter
Low socioeconomic status	Family history

Adapted from Pennathur A, Gibson MK, Jobe BA, Luketich JD. Oesophageal carcinoma. The Lancet 2013; 381: 400-12. [17]

1.2.3 The Genetic Basis of Oesophageal Cancer

Understanding of the molecular events surrounding the development and progression of oesophageal carcinoma has until recently been somewhat limited. Recent progress in molecular biology, however, has revealed a number of genetic and epigenetic alterations that are found in both the SCC and OAC subtypes. [31]

Commonly mutated genes within both SCC and OAC include Tumour Protein p53 (TP53) and Phosphatidylinositol-4,5-bisphosphate 3-kinase catalytic subunit alpha (PIK3CA).[31] TP53 is a major tumour suppressor gene whilst PIK3CA is a kinase activator of the phosphoinositide 3-kinase (PI3K)/AKT pathway. [31 32 33]

Of note, comparisons of mutated genes found within non-dysplastic Barrett's epithelium, high grade dysplasia and OAC revealed that the majority of recurrently mutated genes in OAC, with the exception of TP53 and SMAD4, were also mutated in non-dysplastic Barrett's epithelium. [34] SMAD4 (Mothers against decapentaplegic homolog 4), like TP53 is known to function as a tumour suppressor. [31]

A number of genes have also been shown to undergo amplification or loss of heterozygosity in oesophageal carcinoma. [31] Of note, epidermal growth-factor receptor (EGFR), Myc, K-ras and PIK3CA have all demonstrated amplification in SCC, whilst TP53, cyclin-dependent kinase inhibitor 2A (CDKN2A) and the adenomatous polyposis coli (APC) gene have shown loss of heterozygosity. [31] Again, all of the latter genes function as tumour suppressors. In addition, amplification or overexpression of the oncogene human epidermal growth-factor receptor 2/neu (ERBB2) has been observed in around 25% of OAC. [35]

Epigenetic alterations arising from hyper or hypo methylation of genes (including APC and CDKN2A) and also manipulation of gene expression through the action of microRNAs (small, noncoding RNA molecules that can also induce epigenetic modifications) have also been demonstrated in both SCC and OAC. [31]

1.2.4 The Management of Oesophageal Cancer

1.2.4.1 Diagnosis and Staging

Dysphagia (difficulty in swallowing) is the most common symptom of oesophageal carcinoma although this often develops insidiously. [16, 17] In patients with SCC, the most common presentation is dysphagia, typically associated with a history of smoking, long-term alcohol intake and accompanied by weight loss [16]

Patients with OAC are typically white men with a history of GORD who have recently developed dysphagia. [17] Physical examination often reveals little, except in advanced cases where wasting, hepatomegaly (due to metastasis), a Virchow's node in the left supraclavicular fossa or hoarseness (as a result of recurrent laryngeal nerve involvement) may be present. [16]

Definitive diagnosis is reached through direct visualisation of the tumour at endoscopy and subsequent biopsy and histological confirmation. [17]

Once the diagnosis of oesophageal carcinoma is made, accurate staging of the disease must be performed in order to determine disease extent, plan appropriate treatment and define prognosis.

The staging work-up involves a number of approaches including history, physical examination, endoscopy, endoscopic ultrasonography (EUS, to assess the local extent of the tumour into the oesophageal wall) , computerised tomography (CT) scans of the chest and abdomen (to assess local disease and metastasis), positron emission tomography (PET) scans (to assess distant metastasis), and bronchoscopy (to assess thoracic invasion). [36] Laparoscopy may also be performed to exclude occult distant metastasis prior to consideration of definitive surgical resection. [17]

Oesophageal cancer is staged using the tumour, node and metastasis (TNM) classification (Table 1.2). [37]

Table 1.2 The TNM staging system for oesophageal carcinoma

Primary tumour (T)	
TX	Primary tumour cannot be assessed
T0	No evidence of primary tumour
Tis	High-grade dysplasia
T1	Tumour invades lamina propria, muscularis mucosa, or submucosa
T1a	Tumour invades lamina propria or muscularis mucosa
T1b	Tumour invades submucosa
T2	Tumour invades muscularis propria
T3	Tumour invades adventitia
T4	Tumour invades adjacent structures
T4a	Resectable tumour invading pleura, pericardium, or diaphragm
T4b	Unresectable tumour invading other adjacent structures, such as the aorta, vertebral body and trachea
Regional lymph nodes (N)	
NX	Regional lymph node(s) cannot be assessed
N0	No regional lymph node metastasis
N1	Metastasis in 1-2 regional lymph nodes
N2	Metastasis in 3-6 regional lymph nodes
N3	Metastasis in 7 or more regional lymph nodes
Distant metastasis (M)	
M0	No distant metastasis
M1	Distant metastasis

Adapted from the National Comprehensive Cancer Network (NCCN) clinical practice guidelines in oncology. Oesophageal and oesophagogastric junction cancers. Available at http://www.nccn.org/professionals/physician_gls/pdf/esophageal.pdf. [38]

1.2.4.2 Treatment of Oesophageal Cancer

Locally advanced disease, as defined by the extent of the primary tumour and involvement of loco-regional lymph nodes (higher than stage T2, node positive without distant metastasis, or both) is generally treated with curative intent comprising a multimodal approach that includes surgical resection of the tumour. [17] Advanced (metastatic or disseminated) and recurrent disease are treated with palliative intent through chemotherapy to extend survival or local therapies, such as radiotherapy and endoscopically sited stents, to relieve dysphagia. [17]

1.2.4.2.1 Neoadjuvant Therapy

Chemotherapy prior to surgical resection (neoadjuvant) can be used to control the early spread of systemic disease. [39] The UK Medical Research Council Oesophageal Cancer Working Group study demonstrated that the use of chemotherapy before surgery significantly improved 3 year survival compared to surgery alone. [40] In this study, the group of patients given Cisplatin and 5-fluorouracil (5-Fu) in 2 cycles followed by surgery had a median survival of 16.8 months compared to 13.3 months in the group undergoing surgery alone. [40] These results were supported by the MAGIC trial which demonstrated that the administration of Epirubicin, Cisplatin and 5-Fu (ECF) for 3 cycles pre and post surgery significantly improved 5 year survival compared to surgery alone (36 vs. 23%, P=0.009). It was also noted that the resected tumours were significantly smaller and less advanced in the group given chemotherapy. [41]

A number of studies have also investigated the role of chemoradiotherapy followed by surgery compared with surgery alone in patients with potentially resectable oesophageal carcinoma. [42, 43, 44, 45, 46, 47, 48] Most thus far have demonstrated non-significant results, although a meta-analysis of over 1200 patients demonstrated a significant 13% absolute difference in survival at 2 years in patients

given neoadjuvant chemoradiotherapy followed by surgery compared with those receiving surgery alone. [48] This compared with an absolute survival benefit of 7% at 2 years in patients given chemotherapy alone followed by surgery. [48]

1.2.4.2.2 Adjuvant Therapy

Adjuvant chemotherapy for oesophageal carcinoma treated with primary resection may be of benefit, especially in patients with node positive disease. [17] A study of 556 patients randomised to either surgery alone or surgery followed by chemoradiotherapy (5-Fu, Leucovorin and radiotherapy) demonstrated both increased median survival in the group given adjuvant therapy (36 vs. 27 months) and reduced risk of relapse. [49]

Randomised trials of adjuvant therapy with radiation alone have been inconclusive and its indication is currently restricted to positive resection margins or residual disease following resection. [17]

1.2.4.2.3 Advanced Disease

A significant proportion of patients with oesophageal carcinoma have advanced or metastatic disease at diagnosis (approximately 50-75%).[50, 51] In these patients curative treatment is not possible and median overall survival with best supportive care is around 3 months. [52] Palliative chemotherapy may be given and is chosen on the basis of projected efficacy, the patient's co-morbidities and the side effect profiles of proposed chemotherapy agents. [17]

Few palliative regimens have been validated in phase III trials. The REAL-2 study of 1002 patients with oesophagogastric cancers assessed three-drug regimens that included Epirubicin plus either Oxaliplatin or Cisplatin and 5-Fu or Capecitabine. [52] Median survival in the group given Epirubicin

plus Oxaliplatin and Capecitabine (EOC) was greatest, although still only 11.2 months. A recent Cochrane review comparing chemotherapy with best supportive care for advanced oesophageal carcinoma did not demonstrate any survival benefit with chemotherapy. [51] Furthermore, the authors concluded that there was no consistent benefit of any specific chemotherapy regimen utilised and that there is a need for well designed, adequately powered, phase III trials comparing chemotherapy versus best supportive care for patients with metastatic oesophageal cancer. [51]

There is without doubt a need for the development and investigation of new drugs and treatment regimens to improve prognosis in these patients. With this in mind, agents containing small molecules and antibodies that have been created on the basis of tumour biology are being incorporated into multimodal therapies. [53] The most commonly used agents include the angiogenesis inhibitor Bevacizumab and the epidermal-growth-factor receptor (EGFR) inhibitors Panitumumab and Cetuximab. [17]

The REAL-3 study compared chemotherapy with EOC to EOC plus Panitumumab in patients with untreated, metastatic or locally advanced oesophagogastric adenocarcinoma. [54] Median overall survival was actually shorter in the group given Panitumumab (8.8 months vs. 11.3 months) and the combination was significantly less well tolerated than the standard EOC regime.

The ToGA trial investigated the efficacy of Trastuzumab (Herceptin, a monoclonal antibody directed at HER-2) in combination with Cisplatin and fluoropyrimidine chemotherapy in 594 patients with HER-2-positive advanced gastric or oesophagogastric junction adenocarcinoma. [55] The combination of the antibody with chemotherapy significantly improved overall survival (median 13.8 vs. 11.1 months) without additional toxicity or adversely affecting quality of life. [55] Although promising, however, it should be noted that only around 25% of patients with oesophageal cancer are HER-2 positive and many patients exhibit either primary or acquired resistance to Trastuzumab. [56]

1.3 Cancer of the Colon and Rectum

1.3.1 Structure and Function of the Colon and Rectum

The large intestine comprises the caecum, appendix, colon (further divided into ascending, transverse, descending and sigmoid components) and rectum. [5] Its primary function includes the storage and elimination of food residues, the maintenance of fluid and electrolyte balance and the degradation of complex carbohydrates (and other nutrients) by luminal bacteria. [9]

The colon and rectum are lined predominantly by columnar epithelium. [9] The mucosa itself is devoid of villi and instead comprises perpendicular crypts extending from the flat surface down to the muscularis mucosae, separated by a little lamina propria. [9]

1.3.2 Colorectal Cancer

Over 40,000 people are diagnosed with colorectal cancer in the UK each year making it the 4th most common cancer by incidence (after breast, lung and prostate). [3] The disease is also responsible for over 16,000 deaths which means that, although it carries an overall 5-year survival rate of 55% (significantly more favourable than that for oesophageal cancer), it is still the 2nd leading cause of cancer related death. [8, 57]

Approximately 30% of colorectal cancers arise in the rectum, 25% in the caecum and ascending colon and 20% in the sigmoid colon (with the remainder spread between the transverse colon, splenic and hepatic flexures, descending colon, appendix and anus). [58] Microscopically, colorectal tumours are predominantly of the adenocarcinoma type and display varying degrees of mucin production and differentiation. [9]

Whilst approximately 5-10% of colorectal cancers arise secondary to inherited genetic defects, diet and lifestyle are without doubt the main contributing factors to the high incidence of the disease, particularly in Western countries. [59] Of note, individuals consuming high fat, high protein, low fibre diets and diets that contain significant proportions of red and processed meat have an increased risk of developing the disease. [9, 60, 61] Other recognised and modifiable risk factors for colorectal cancer include smoking, alcohol intake, physical inactivity and obesity. [9, 60]

1.3.3 The Genetic Basis of Colorectal Cancer

The genetic aberrations which accumulate en-route to the development of colorectal cancer have been well studied. [62] Mutations can occur through chromosomal instability, defects in DNA repair pathways and or aberrant methylation of DNA, leading to the functional silencing of tumour suppressor genes or the amplification of oncogenic pathways. [62]

The majority of colorectal adenocarcinomas arise in pre-existing adenomas, the so-called adenoma→carcinoma sequence, as first proposed by Vogelstein and colleagues (Figure 1.1). [63] Evidence for this sequence comes from an understanding of the genetic and molecular events surrounding the inherited condition Familial Adenomatous Polyposis (FAP) and also from epidemiological data. [9] FAP is an autosomal dominant condition resulting from an inherited point mutation on the long arm of chromosome 5 leading to deletion of one copy of the adenomatous polyposis coli (APC) gene which encodes the tumour suppressor protein APC. [62] Loss of one copy of APC is inherently followed by loss of the other during life and thus the accumulation of APC loss within intestinal cells leads to hyperproliferation within the intestinal crypts and the formation of multiple polyps. [9, 62] Subsequent acquirement of additional mutations in other tumour suppressors and oncogenes (the so-called 'two hit' theory) leads to the malignant transformation of these polyps in almost all untreated cases by the age of 30-40. [9]

In terms of epidemiological evidence supportive of the adenoma → carcinoma progression, the marked geographical variation in the incidence of polyps correlates strongly with the incidence of colorectal carcinoma. Furthermore, adenomas and carcinomas are frequently found together in resected specimens. [9] Increasing polyp size, villous growth pattern and degree of dysplasia are known to correlate with risk of malignancy within polyps.

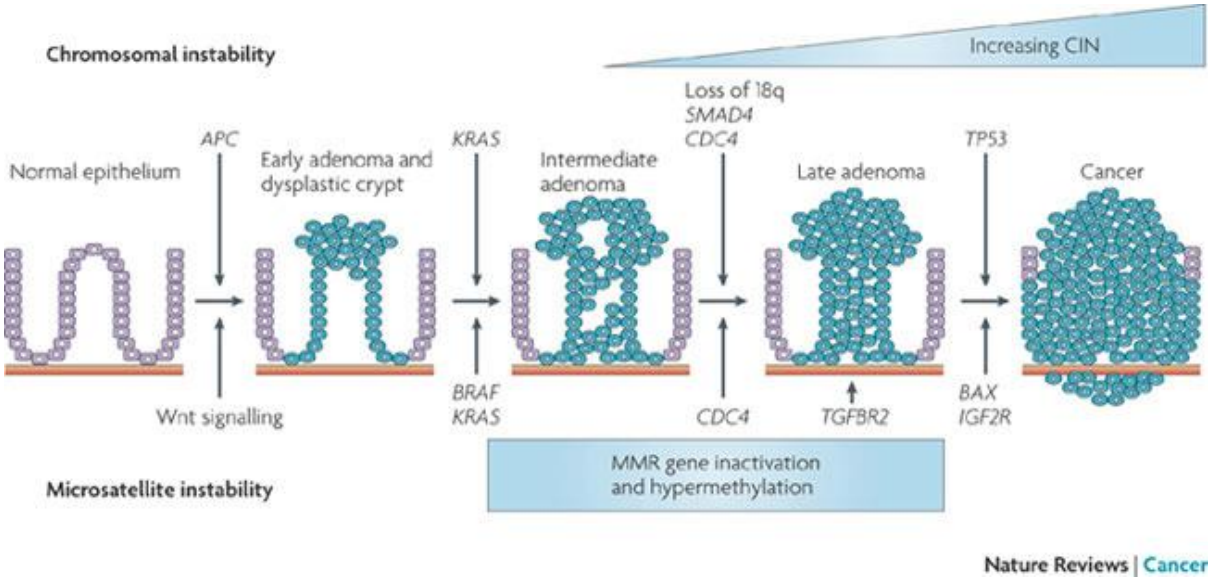

Figure 1.1 The colorectal adenoma → carcinoma sequence

The initial step in colorectal tumourigenesis is that of adenoma formation, associated with loss of the tumour suppressor adenomatous polyposis coli (APC). Larger adenomas and early carcinomas typically acquire mutations in K-ras, followed by loss of chromosome 18q and SMAD4 and mutations in p53 (often the key step in the transition to invasive adenocarcinoma). Mutations in B-raf are usually mutually exclusive to those in K-ras.

Adapted from Walther A, Johnstone E, Swanton C *et al*. Genetic prognostic and predictive markers in colorectal cancer. Nat Rev Cancer. 2009; 9(7): 489-99. [64]

Loss of APC leads to polyp formation through activation of the Wnt signalling pathway (Figure 1.2). [62] Wnt signalling occurs when the onco-protein β-catenin translocates to the nucleus (following its accumulation within the cytoplasm) and binds to members of the T-cell factor-lymphocyte enhancer factor (TCF-LEF) family to create a transcription factor that regulates a number of genes ultimately involved in cellular growth and proliferation (including c-Myc). [62, 65, 66] The normal functioning of APC is crucial for the abrogation of Wnt signalling through its formation of a destruction complex (alongside glycogen synthase kinase 3β and AXIN (axis inhibitor)) which phosphorylates β-catenin, targeting it for ubiquitination and proteasomal degradation. [65] In the absence of APC, β-catenin is able to evade degradation and thus accumulates within the cytoplasm, precipitating subsequent translocation to the nucleus and activation of transcription factors.

As well as in FAP, APC is known to be mutated in approximately 85% of sporadic cases of colorectal cancer and is the initiating mutation in the vast majority of instances. [62] In addition, a small subgroup of tumours that retain functioning wild-type APC have been shown to harbour mutations in β-catenin itself that renders the protein resistant to the Wnt degradation complex. [62]

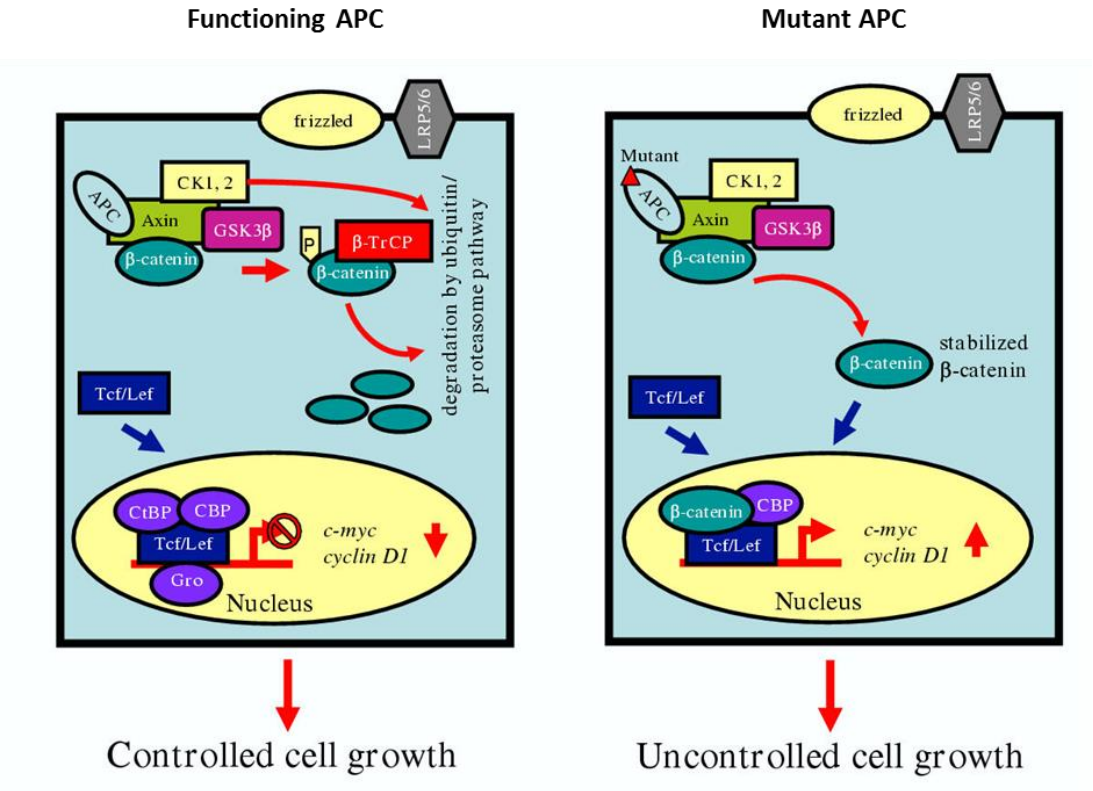

Figure 1.2 The Wnt signalling pathway

In the presence of Wnt signalling and functioning APC, β-catenin associates with a multi-protein destruction complex comprising APC, AXIN and GSK3β. β-catenin is phosphorylated by CK1/CK2 and GSK3β leading to its ubiquitination (through binding to β-TrCP) and degradation by the proteasome. Members of the TCF/LEF family remain bound in the nucleus by repressors that belong to the GRO (groucho-related gene) family and are therefore inactive. In the absence of APC (i.e. in the presence of an APC mutation), the destruction complex is no longer functional, preventing the phosphorylation of β-catenin, thus allowing its accumulation within the cytoplasm and subsequent translocation to the nucleus where it activates TCF/LEF. This in turn leads to the transcription of pro-proliferative proteins such as c-Myc and cyclin D1.

Adapted from Narayan S, Roy D. Role of APC and DNA mismatch repair genes in the development of colorectal cancers. Mol Cancer 2003; 2: 41. [67]

Inactivation of the tumour suppressor protein p53 through mutation of TP53 is the second key genetic step in the development of colorectal cancer. [62] In most tumours, the two TP53 alleles are inactivated, usually by a combination of missense mutation that inactivates the transcriptional activity of p53 and a 17p chromosomal deletion that eliminates the second TP53 allele. [62] Wild-type p53 mediates cell-cycle arrest and a cell-death checkpoint, which can be activated by multiple cellular stresses, including DNA damage, ultraviolet light and oxidative stress. [62] The inactivation of TP53 (present in around 35-55% of tumours) often coincides with the transition of large adenomas into invasive adenocarcinomas. [68]

Mutational inactivation of the tumour suppressing TGF-β signalling pathway is a third crucial step in the progression to colorectal cancer. [62] Mutational inactivation of TGFBR2 and/or mutations altering expression of its downstream target SMAD4 (present in around 30% of cancers) also coincide with the transition from adenoma to high-grade dysplasia or carcinoma. [62]

The mitogen activated protein kinase (MAPK) signalling cascade (Figure 1.3) can also become constitutively active during the development of colorectal cancer through oncogenic mutations in K-ras and B-raf (occurring in 37 and 13% of cases respectively) resulting in the activation of numerous transcription factors (such as the Ets family and c-Myc). [62, 69] K-ras mutations activate the GTPase activity that signals directly to raf. B-raf mutations in turn signal B-raf serine-threonine kinase activity, which then further drives the MAPK signalling cascade. [62] This pathway can be further perturbed through over-expression or mutation of the epidermal growth factor receptor (EGFR; the up-stream regulator of MAPK) which is present in 27-77% of colorectal cancers. [69] Aberrant EGFR signalling (and mutations in K-ras) can also lead to constitutive activation of the phosphatidylinositol 3-kinase (PIK3CA) signalling pathway resulting in cell-survival signalling and suppression of apoptosis. [62] In addition, mutation of the tumour suppressor PTEN (present in 10-15% of colorectal cancers) also results in constitutively active PIK3CA signalling. [62]

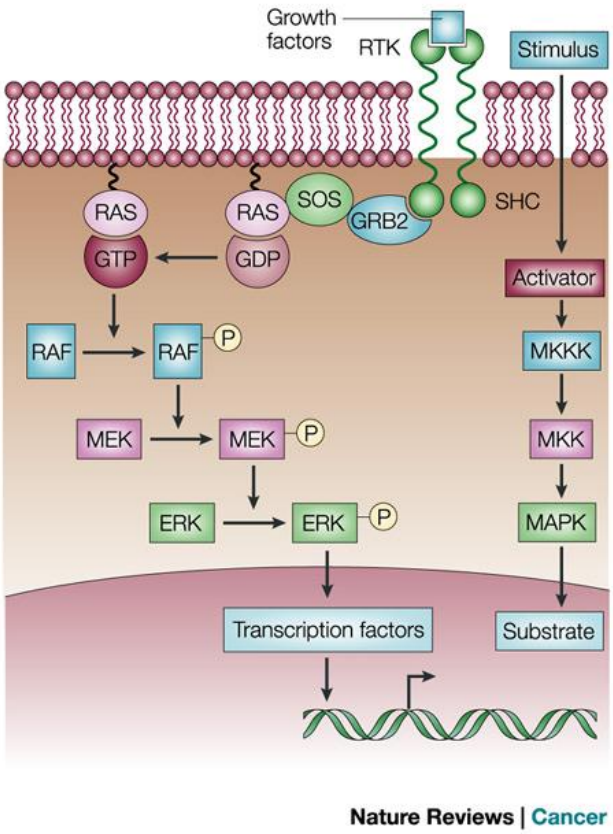

Figure 1.3 The MAPK signalling cascade

The MAPK (mitogen activated protein kinase) signaling cascade (also known as the RAS–RAF–MEK–ERK pathway) forms a phospho-relay system that translate a plethora of extracellular signals into diverse cellular responses. After binding of ligands, such as growth factors, to their respective receptor tyrosine kinase (RTK), receptor dimerization triggers the intrinsic tyrosine-kinase activity. This is followed by auto-phosphorylation of specific tyrosine residues on the intracellular portion of the receptor. These phosphorylated tyrosine residues then bind the sequence homology 2 (SH2) domains of adaptor proteins such as GRB2. Such a complex formation recruits SOS (son of sevenless, a cytosolic protein) into close proximity to RAS on the plasma membrane. Like other G proteins, RAS (H-ras, N-ras and K-ras) cycles between the GDP-bound inactive form and the GTP-bound active form. In the quiescent state, Ras exists in the GDP-bound form. The binding of SOS to Ras causes a change in conformation leading to the dissociation of GDP and binding of GTP. GTP-bound Ras is the activator of this signalling module. It initiates the signal cascade by phosphorylating Raf (A-raf, B-raf

or C-raf). Raf in turn phosphorylates the MEKs (MEK1 and MEK2) which then phosphorylate the ERK MAPKs (extracellular signal-regulated kinases, ERK1 and ERK2). Activated ERKs then translocate into the nucleus where they phosphorylate specific substrates that are involved in the regulation of various cellular responses. In addition, ERK-mediated transcription can result in the up-regulation of RTK ligands (such as TGFα), thus creating an autocrine feedback loop.

Adapted from Chin L. The genetics of malignant melanoma: lessons from mouse and man. Nature Reviews Cancer 2003; 3**:** 559-570. [70]

1.3.4 The Management of Colorectal Cancer

1.3.4.1 Diagnosis and Staging

Patients with suspected colorectal cancer typically present electively (with abdominal bloating and pain, change in bowel habit, bleeding per rectum, loss of appetite, weight loss or iron deficiency anaemia) or as an emergency (with bowel obstruction or perforation secondary to the tumour). [9] Patients may also present with symptoms secondary to the metastatic spread of the primary tumour. [9] In the UK, a screening programme has now been established meaning asymptomatic patients may also present following a positive faecal occult blood test. [71]

A definitive diagnosis of colorectal adenocarcinoma is achieved through histological examination of a biopsy (obtained through colonoscopy) or through examination of the resected tumour specimen (if an emergency operation was necessitated). [72] Following confirmation of the diagnosis, the cancer is then staged using CT of the chest, abdomen and pelvis and, additionally for rectal cancer, an MRI scan of the pelvis. [72]

As in the oesophagus, colorectal cancer is staged using the TNM system (Table 1.3). [73]

Table 1.3 The TNM staging system for colorectal carcinoma

Primary tumour (T)	
TX	Primary tumour cannot be assessed
T0	No evidence of primary tumour
Tis	Carcinoma in situ
T1	Tumour is confined to submucosa
T2	Tumour invades muscularis propria
T3	Tumour invades through muscularis propria (but does not penetrate) serosa
T4	Tumour has penetrated serosa and peritoneal surface
T4a	Tumour penetrates to the surface of the visceral peritoneum
T4b	Tumour directly invades or is adherent to other organs or structures
Regional lymph nodes (N)	
NX	Regional lymph node(s) cannot be assessed
N0	No regional lymph node metastasis
N1	Metastasis in up to 3 regional lymph nodes
N2	Metastasis in 4 or more regional lymph nodes
Distant metastasis (M)	
M0	No distant metastasis
M1	Distant metastasis (including lymph node metastasis to non-regional lymph nodes)

Adapted from The National Institute for Health and Care Excellence (NICE). Staging colorectal cancer. Available at http://pathways.nice.org.uk/pathways/colorectal-cancer. [73]

1.3.4.2 The Treatment of Colorectal Cancer

Surgical resection of the primary tumour remains the cornerstone of curative treatment for colorectal cancer. [72] Laparoscopic resection has become increasingly popular in recent years, both for colonic and rectal lesions. [74] In addition, local excision of early stage (T1 and T2) rectal tumours through trans-anal endoscopic microsurgery (TEMS) is also now being offered by some centres. [75]

1.3.4.2.1 Neoadjuvant Therapy

Short course radiotherapy or long cause chemoradiotherapy is now routinely offered to patients pre-operatively with rectal cancer with the aim of decreasing local recurrence rates. [72] A recently published meta-analysis assessed the safety and effectiveness of neoadjuvant (chemo)radiotherapy in rectal cancer. [76] Although neoadjuvant radiotherapy was shown to decrease local recurrence (hazard ratio, HR = 0.59; 95%CI: 0.48-0.72) compared to surgery alone, it had only a marginal benefit on overall survival (HR = 0.93; 95%CI: 0.85-1.00) and was associated with increased perioperative mortality (HR = 1.48; 95%CI: 1.08-2.03). Neoadjuvant chemoradiotherapy improved local control as compared to radiotherapy alone (HR = 0.53; 95%CI: 0.39-0.72), but again had no influence on long-term survival. [76]

Neoadjuvant therapy for colon cancer is currently not routinely used, although preliminary results from trials investigating its efficacy in locally advanced (T3 and T4) tumours show much promise. [77]

1.3.4.2.2 Adjuvant Therapy

Adjuvant therapy is currently advocated for the post-operative treatment of colorectal cancer patients with positive lymph node involvement (Stage III) or with high risk Stage II disease (T3 and T4

lesions). [72] Current regimens are based largely around Oxaliplatin and 5-Fu (+/- folinic acid) with variable results. [72, 78] Metastatic colorectal cancer is also treated systemically with the aforementioned agents in combination with Irinotecan. [72]

1.3.4.2.3 Advanced Disease

As well as the standard chemotherapeutic agents already mentioned, advanced (metastatic) colorectal cancer has also been the focus for the introduction of new systemic treatments targeted against specific features of the tumour's biology.

The monoclonal antibodies Cetuximab, Panitumumab and Bevacizumab have all been utilised (often in combination with existing reagents) with variable results. Cetuximab and Panitumumab are monoclonal antibodies directed against EGFR, whilst Bevacizumab is an anti VEGFR antibody. All have shown improvement in survival when given alongside existing chemotherapy regimens in metastatic colorectal cancer although the presence of mutations within individual tumours has been shown to influence response to therapy (e.g. K-ras or B-raf in the case of EGFR monoclonal antibodies). [79] Furthermore, tumours that were initially sensitive to the effects of these agents have also been shown to subsequently develop resistance. [79] Further work is undoubtedly needed within this area to conclusively identify biomarkers predictive of therapy response and also to delineate mechanisms for overcoming established therapy resistance (be it primary or secondary).

1.4 Iron

1.4.1 Iron Absorption and Metabolism

Iron plays a crucial role in the regulation of numerous cellular functions and is thus essential for life. [80] The ability of iron, through redox cycling, to function as both an electron donor and acceptor means that it serves as a co-factor within the active site of several key enzymes in a number of critical biochemical pathways including ATP generation, oxygen transport, cell cycling and DNA synthesis. [80]

Iron exists in the diet in either the organic (heme, e.g. from red meat) or in-organic (from various legumes) form. The absorption of both occurs within the small intestine, predominantly in the duodenum. [81] There is no iron absorption within the colon or rectum. [81]

1.4.1.1 In-organic Iron

In-organic iron is absorbed through a process which begins with the reduction of dietary ferric iron (Fe^{3+}) to ferrous iron (Fe^{2+}) through the action of the ferrireductase duodenal cytochrome b (DCYTB) which is highly expressed on the enterocyte brush border (Figure 1.4). [82, 83] Some reduction of ferric iron also takes place within the stomach secondary to the action of hydrochloric acid. [80]

Following reduction by DCYTB, ferrous iron is then transported into the enterocyte by divalent metal transporter 1 (DMT1, also known as NRAMP2/DCT1), which is found at the apical membrane. [84, 85] Once inside the enterocyte the iron is either i) immediately utilised within the various cellular processes in which it participates, ii) stored in an inert form for later use bound to the protein ferritin or iii) exported out of the enterocyte into the systemic circulation. [86]

Exit from the enterocyte requires the ferroxidase hephaestin (HEPH) and the basolateral iron transporter ferroportin (FPN, also termed IREG1 or metal transporter protein 1). [87, 88, 89] Iron is then transported in the serum bound to transferrin (Tf), which can bind two atoms of ferric iron. Tf-bound iron then interacts with transferrin receptor 1 (TfR1) on the plasma membrane of cells which take up iron. Finally, the iron/Tf/TfR1 complex is internalised by receptor mediated endocytosis and iron is released from transferrin by a mechanism requiring endosomal acidification. [90] Within the endosome, the acidic environment triggers the release of ferric iron from Tf and its subsequent reduction to ferrous iron through the ferrireductase activity of STEAP3 (six transmembrane epithelial antigen of the prostate 3). The Tf/TfR1 complex then recycles back to the cell surface, where transferrin can take part in further rounds of iron uptake. Finally, ferrous iron is transported out of the endosome into the cytosol by DMT1 where it joins the labile iron pool and, as in the enterocyte, is either used in a multitude of cellular processes or stored as ferritin. [92]

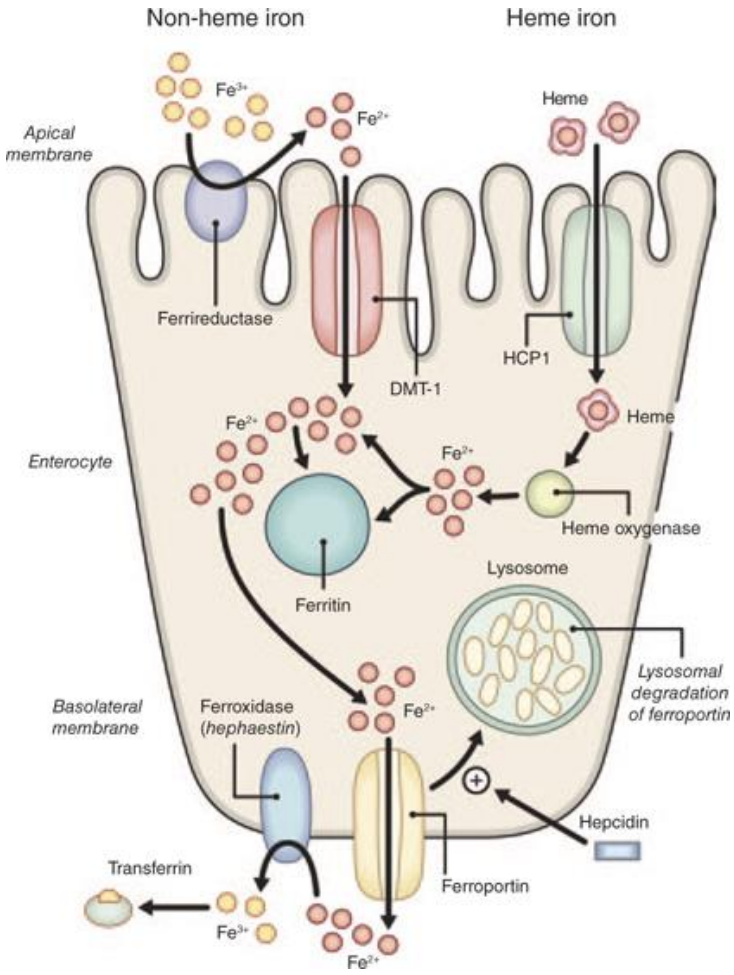

Figure 1.4 The intestinal absorption of iron

Iron is absorbed across the apical membrane of the enterocyte as either heme or non-heme iron. Once within the cell it is either immediately used for the plethora of intracellular processes for which it is required, stored for later use in ferritin or exported out of the cell across the basolateral membrane.

Adapted from Rizvi S, Robert E Schoen RE. Supplementation with oral vs. intravenous iron for anaemia with IBD or gastrointestinal bleeding: Is oral Iron getting a bad rap? The American Journal of Gastroenterology 2011; 106: 1872-1879. [91]

1.4.1.2 Organic Iron

Organic (heme) iron is absorbed from the small intestine through a process only recently characterised and distinctly separate to that of in-organic iron. [92] Originally it was thought that heme was absorbed through passive diffusion, however, the heme carrier protein (HCP1) has now been shown to function within the small intestine and represents the best candidate for a heme transporter. [80, 93] Interestinlgy, HCP1 has also been shown to act as a folate transporter, intimating that folate and heme may in fact compete for absorption through this mechanism and that consequently there may still be other heme absorption proteins yet to be discovered. [92, 94] Once within enterocytes, heme is broken down into biliverdin and iron(II) by heme oxygenase-1 (HO-1). [95] From this point, the ferrous iron obtained from heme is regulated and transported in the same fashion as its in-organic counterpart.

1.4.1.3 Regulation of Iron Metabolism

As the human body possesses no direct capacity to excrete iron (other than small amounts through desquamation) it has adapted several mechanisms to regulate iron absorption and thus maintain an appropriate iron balance. [96]

1.4.1.3.1 Iron-regulatory Proteins

The uptake, usage and storage of iron is maintained within tight limits by the regulation of the various iron transport proteins at the post-transcriptional level according to the intracellular concentration of iron. [80] The iron regulatory proteins 1 and 2 (IRP1 and IRP2) bind to iron responsive elements (IREs) located in the 5'- or 3'- untranslated regions of the mRNA of the iron metabolism proteins (e.g. TfR1, DMT1, ferritin and ferroportin) dependent on the intracellular iron concentraton

(Figure 1.5). [97, 98] At times of iron depletion, the IRPs bind with IREs located at the 3' end of the iron uptake protein's mRNA (stabilising its translation) and the 5' end of iron storage protein's mRNA (inhibiting translation). This ultimately results in an increase in expression of TfR1 (and to a certain extent DMT1) and a reduction in the expression of ferritin and ferrportin. [97, 98] Conversely, in iron-replete cells, IRPs are unable bind to these same IREs leading to a reduction in iron uptake and an increase in iron storage (IRP1 instead functions as a cytosolic acinotase whilst IRP2 is degraded). [97, 98]

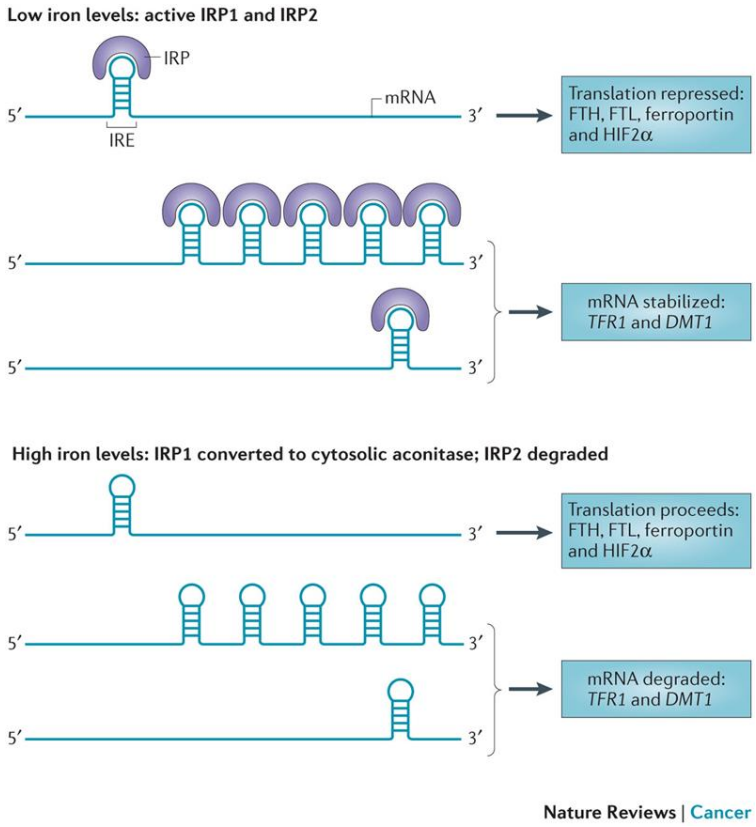

Figure 1.5 Iron-regulatory protein interactions respond to intracellular iron levels

IRP1 and IRP2 bind to IREs present in either the 5′ or the 3′ UTR of mRNAs. IREs are found in the 5′ UTR of mRNAs encoding ferritin, ferroportin and hypoxia-inducible factor 2α (HIF2α), and also in the 3′ UTR of mRNAs encoding TFR1 and IRE-containing isoforms of DMT1. Binding of IRPs to 5′ IREs inhibits translation, whereas binding to 3′ IREs stabilizes mRNA. IRPs bind to IREs under conditions of low iron levels; under conditions of high iron levels, IRP1 loses its IRE-binding activity and acquires enzymatic activity as a cytosolic aconitase, whereas IRP2 is degraded. Thus, under conditions of low iron levels, the IRE–IRP system functions to increase iron uptake (by stabilizing mRNAs that encode TFR1 and DMT1) and decreases iron storage and efflux (by inhibiting the translation of ferritin and ferroportin). Binding of IRPs to mRNAs encoding HIF2α is thought to function as a feedback loop to inhibit erythropoiesis when iron levels are low.

Adapted from Torti S, Torti F. Iron and cancer: More ore to be mined. Nature Reviews Cancer 2013; 13: 342-55. [99]

1.4.1.3.2 Hepcidin

Hepcidin is a peptide secreted by the liver that acts as a systemic iron regulatory hormone. [100] It binds to ferroportin 1, thus trigerring its internalisation and lysosomal degradation. This results in the inhibition of iron release from iron exporting cells (such as enterocytes and also macrophages) and a subsequent decrease in serum iron levels. [101]

1.4.2 The Redox Activity of Iron

Iron possesses the unique ability to cycle between two stable configurations, the ferric (Fe^{3+}) and ferrous (Fe^{2+}) states. [80] This allows it to act as both an electron donor and acceptor.[80]

$$Fe^{2+} + H_2O_2 \rightarrow Fe^{3+} + OH^{\bullet} + OH^{-}$$

Figure 1.6 The Fenton Reaction

In the Fenton reaction (Figure 1.6), a hydroxyl free radical is produced through the donation of an electron from the ferrous iron. [99] This highly reactive free radical is able to induce cell death through the initiation of a series of chemical reactions ultimately resulting in DNA oxidation, mitochondrial damage and the peroxidation of membrane lipids. [80] In addition, excess free iron can also react with unsaturated lipids to produce alkoxyl and preoxyl radicals. [80] All of these oxidative reactions result in the impairment of cellular function and lead to the damage of cells, tissues and organs.

1.4.3 Iron in Health and Disease

Iron is essential for life; it plays a crucial role in oxygen transport and storage (where both haemoglobin and myoglobin contain iron) and is equally as vital for processes such as ATP generation, effective DNA synthesis and cell cycle progression. [80, 102] As iron is so important within the body, deviation from the normal tight regulation of its metabolism can have deleterious effects. This is best exemplified by the clinical syndrome of iron deficiency anaemia, a condition that occurs when the body has insufficient amounts of iron to meet its metabolic demands. [103] The consequences of iron deficiency include compromised immunity, physical impairment (e.g. lethargy, shortness of breath) and poor cognition. [104]

Conversely, as the body does not possess a system for its effective excretion, excess systemic iron (as in the iron storage disease Hereditary Haemochromatosis or in iron-overload conditions such as β-thalassemia and Friedrich's Ataxia) leads to iron deposition in a number of organs including the heart, pancreas and liver. [105] This in turn causes irreversible tissue damage and fibrosis through the action of reactive oxygen species generated by the iron. [106, 107] As such, excess iron has been implicated in a number of diseases including ischaemic heart disease, diabetes mellitus and neurodegenerative disorders. [108, 109, 110]

1.4.4 Iron and Cancer

Iron has also been implicated in the development of cancer. [111] This is perhaps not entirely surprising since iron is essential for ATP production, DNA synthesis and cell cycle progression; all activities that are increased in cancer cells. [112] Neoplastic cells therefore have a higher requirement for iron and it has been shown that the perturbation of cellular iron uptake proteins arrests cell

growth *in-vitro* and *in-vivo*. [113] Iron may also accelerate tumour initiation by enhancing the formation of free radicals which, as outlined earlier, damage cells and are potentially mutagenic. [99]

1.4.4.1 Epidemiological Studies

In an early study examining the association between biochemical markers of iron stores and cancer, Stevens *et al* analysed more than 14,000 participants in the first US National Health and Nutrition Examination Survey. [99, 114, 115] The authors demonstrated that transferrin saturation at the time of enrolment into the study was significantly higher in men who subsequently developed cancer than in those who did not.

Studies have also investigated the incidence of cancer in patients with Hereditary Haemochromatosis (HH), a condition characterised by iron overload, particularly in the parenchymal cells of the liver, heart and endocrine organs (such as the pancreas and pituitary).[116, 117] There is a 20-200 fold increased risk of hepatocellular carcinoma in HH patients and individuals which carry mutations in haemochromatosis (HFE), one of the mutated genes that underlies HH, may also be at an increased risk of certain extrahepatic cancers, including breast and colorectal. [118, 119, 120]

Conversely, a 2008 study by Zacharski and colleagues demonstrated that repeated phlebotomy over a period of 4.5 years in elderly men with peripheral arterial disease (inferring a reduction in total body iron levels) reduced both overall cancer risk (HR 0.65, p=0.036) and cancer specific mortality (HR 0.49; p=0.009). [121] Although the authors interpreted their results with caution, their findings were consistent with other observations of a decreased cancer risk of several cancers (such as liver, lung, colon, stomach and oesophageal) in individuals who frequently donate blood. [99, 122]

A meta-analysis of 33 studies assessing iron intake and colorectal cancer risk revealed that approximately 75% of the studies included associated higher iron intake with an increased risk of colorectal cancer. [123] A recent study by Ward and colleagues also demonstrated an increased risk of oesophageal adenocarcinoma amongst individuals with a higher intake of heme iron or total iron from meat. [124]

1.4.4.2 Human Tissue Studies

The up-regulation of the pertinent cellular iron transport proteins has been demonstrated in a number of cancers including oesophageal, colon and breast. [24, 82, 125]

Boult and colleagues studied human samples of BM and OAC. [24] DMT1, DCYTB and TfR1 were found to be overexpressed in OAC tumour samples relative to BM and increased iron acquisition occurred as a result. [24] Interestingly, DMT1 expression was also shown to correlate with the presence of metastatic OAC.

A similar phenomenon has also been noted in colorectal cancer, where Brookes and colleagues demonstrated increased iron acquisition in human colorectal tissue along the progression from adenoma to carcinoma. [82] In addition, the authors also demonstrated over expression of the cellular import proteins DCYTB, DMT1 and TfR1 along with internalisation of the iron exporter ferroportin. It was concluded that these adaptations along the pathway from adenoma to carcinoma favour the acquisition of intracellular iron which in turn is likely to drive proliferation and repress cell adhesion. [82] Increased iron acquisition along the progression to colorectal cancer has been demonstrated in other studies also. [126]

Finally, Pinnix and colleagues demonstrated an association between decreased ferroportin gene expression and reduced metastasis free and disease specific survival in breast cancer patients. [125] Paradoxically, high ferroportin and low hepcidin gene expression in samples of breast tumour identified a cohort of patients with >90% 10 year survival.

1.4.4.3 Animal Studies

A number of animal models have demonstrated the ability of iron to drive tumourigenesis, particularly in the presence of underlying genetic mutations. [102, 127, 128, 129]

Of note, Chen *et al* demonstrated that administration of intra-peritoneal iron dextran to rats that had undergone oesophagogastroduodenal anastomosis (to simulate reflux) caused an increase in the rate of OAC formation compared to rats without iron supplementation. [129] Interestingly, all of the tumours which developed occurred at the squamo-columnar junction, the area where iron deposition was greatest.

Radulescu *et al* investigated the effect of dietary iron intake in combination with a pre-existing mutation in the tumour suppressor gene APC on intestinal tumourigenesis. [102] It was demonstrated that the administration of an iron deficient diet to mice genetically predisposed to the development of intestinal tumours (through loss of APC) significantly increased rates of apoptosis within intestinal crypts resulting in decreased tumour proliferation and increased survival. Conversely, administration of excess dietary iron was found to significantly increase rates of tumourigenesis (compared to controls) and negatively influence survival. [102] Furthermore, analysis of murine intestinal tissue revealed an up-regulation in the expression of the iron import proteins TfR1 and DMT1 following loss of APC. Up-regulation of DMT1 was also noted in the intestinal tumours of $APC^{Min/+}$ mice with

activated HIF-2α in a separate study, leading the authors to postulate that dysregulation of iron homeostasis was a critical factor in the progression of colorectal tumourigenesis. [130]

1.4.4.4 Cell Based Studies

Several *in-vitro* studies have demonstrated a dysregulation of iron homeostasis in cancer cells. [99, 131] Perturbation of normal iron metabolism has been demonstrated in colorectal, oesophageal, breast, lung, renal, hepatocellular, prostate, melanoma, pancreatic and haematological cell lines. [99]

Of note, iron administration has been shown to increase proliferation rates in oesophageal and colorectal cell lines. [24, 82] In addition, iron has also been shown to amplify Wnt signalling (the major oncogenic signalling pathway in the colon) in APC deficient colorectal cells resulting in elevated levels of c-Myc and suppression of the cell adhesion protein E-cadherin. [132] In B-cell lymphoma cell lines, c-Myc has been shown to increase the expression of TfR1, subsequently leading to an increase in cellular proliferation. [133]

'Knockdown' of IRP2 has been shown to increase ferritin expression whilst decreasing TfR1 expression in lung and breast cancer cells. [134, 135] Moreover, suppression of IRP2 significantly impaired the subsequent growth of lung and breast cell xenografts. [135, 136]

Interestingly, down-regulation of ferritin has been shown to increase the sensitivity of breast cancer cells to the chemotherapeutic agents Doxorubicin and Cisplatin *in-vitro*. [137, 138]

Thus, a dysregulation of iron metabolism appears to be intimately linked to tumourigenesis; cancerous cells acquire an excess of iron which drives their malignant phenotype both directly (through DNA synthesis and ATP generation) and indirectly (through ROS generation and the

amplification of Wnt signalling). Furthermore, the increased expression of proto-oncogenes such as c-Myc (associated with Wnt) may, it seems, further enhance cellular iron acquisition (through increased IRP2) leading to a self-perpetuating cycle of increased tumourigenesis.

1.4.5 Iron Chelators as Anti-cancer Agents

Given the association between dysregulated iron metabolism and cancer, there is now significant interest in the investigation and development of iron chelating drugs (aimed at depriving tumour cells of iron) as anti-neoplastic agents. [80, 92]

1.4.5.1 Experimental Iron Chelators

A number of synthetic iron chelators have been created and subjected to pre-clinical testing to evaluate their anti-neoplastic effects. These include O-Trensox, Tachypyridine, the thiosemicarbazones and Triapine. [92] Several mechanisms have been proposed for the anti-neoplastic effects of these agents including iron depletion, induction of apoptosis, cell cycle modulation and redox cycling. [92]

Of particular note, the agent Dp44MT (a member of the thiosemicarbazone family of iron chelators) developed by Richardson and colleagues has shown great promise as an anti-neoplastic agent in a number of *in-vitro* and *in-vivo* studies. [139, 140] The drug has demonstrated anti-proliferative effects in over 28 different human cell lines (including lung, melanoma and breast) *in-vitro* and of note, is also able to overcome Etoposide and Vinblastine resistance in breast and epidermoid carcinoma cell lines respectively. [92] *In-vivo*, Dp44mT markedly inhibits the growth of human lung carcinoma, neuroepithelioma and melanoma tumour xenografts in nude mice. [139] These positive findings,

however, have so far been largely negated by a number of significant side effects (including weight loss and cardiac fibrosis) associated with the drug in experimental models. [92]

More recently, the 2-benzoylpyridine thiosemicarbazone (BpT) chelators have been synthesized in an attempt to overcome some of the side effects seen with Dp44MT. [141] *In-vitro* studies using these agents have shown them to have greater anti-proliferative activity than Desferrioxamine and Triapine (but crucially not Dp44MT) in SK-N-MC neuroepithelioma cell lines. [141] *In-vivo*, the agent Bp44MT is also able to reduce tumour growth and decrease levels of cyclin D1 expression in DMS-53 lung carcinoma xenografts relative to control. [142]

Thus far, however, despite these promising findings, the clinical application of all experimental iron chelators remains limited. As such, interest has been stirred in the anti-neoplastic potential of iron chelating agents that are already licensed and employed safely in other diseases. [80, 92]

1.4.5.2 Approved Iron Chelators as Anti-cancer Agents

At present there are 3 chelating agents in routine clinical use; Desferrioxamine (DFO) is the longest serving agent and requires subcutaneous infusions; Deferiprone and Deferasirox are newer chelators and have the advantage over DFO of oral administration. [80]

1.4.5.2.1 Desferrioxamine

DFO was the first iron chelating agent to be introduced into clinical practice and has been used in the treatment of the iron overload associated with β-thalassemia for a number of years. [80] It is a hexadentate chelator capable of binding iron in a 1:1 ratio (Figure 1.7). The drug has poor membrane permeability (it is hydrophilic rather than lipophilic) which, when combined with its short

half-life and rapid metabolism, means it must be given as a subcutaneous infusion several times a week in order to effectively chelate iron. [92]

As early as 1988, it was noted that DFO demonstrated anti-tumour effects upon human neuroblastoma cells most likely through iron deprivation in a time and dose dependent manner. [143] Subsequent studies have demonstrated DFO to have similar effects in several gynaecological malignancies and also in leukaemia. [144, 145, 146]

Results from clinical trials of DFO as an anti-cancer agent are varied and this, coupled with its laborious method of delivery, accounts for why it is unlikely to be taken forward as an anti-cancer agent. [147]

1.4.5.2.2 Deferiprone

Deferiprone (Ferriprox® / L1 / CP20) was the first orally administered iron chelator introduced into clinical use (Figure 1.7). [92] Like DFO, it has demonstrated promising anti-proliferative effects in a number of cancer cell lines *in-vitro* including neuroblastoma, hepatocellular carcinoma, cervical carcinoma and leukaemia. [144, 148, 149, 150, 151]

Unfortunately, the drug's *in-vitro* anti-neoplastic effects have not been replicated with the same magnitude *in-vivo* and this, combined with a list of potentially significant side effects seen when used in humans (including agranulocytosis, neutropenia, arthralgia, liver fibrosis and gastrointestinal disturbances), means further investigation of the drug in this context has been limited thus far. [151, 152, 153]

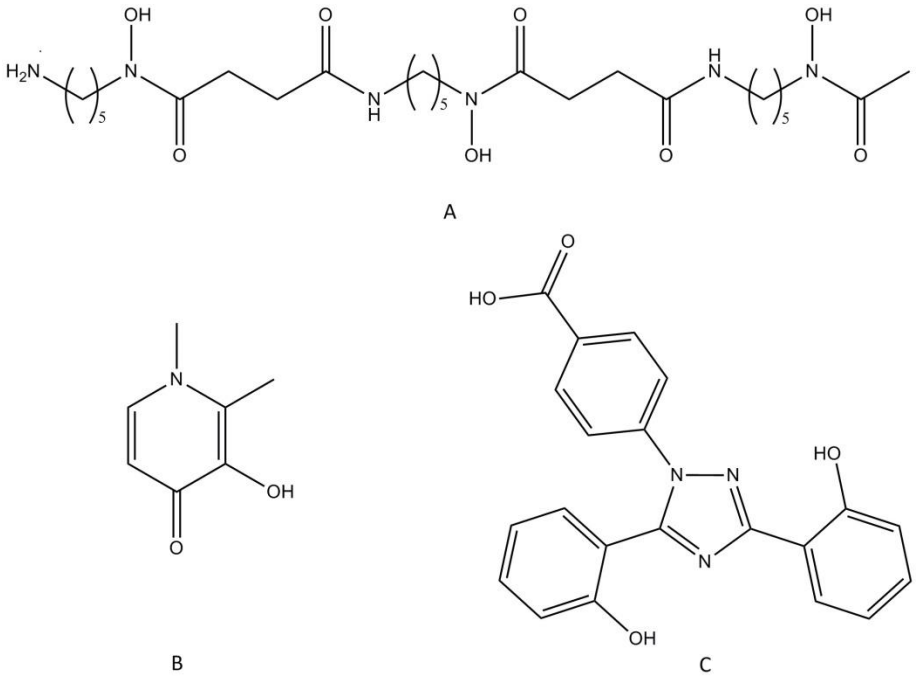

Figure 1.7 The Chemical Structure of the Approved Iron Chelators Desferrioxamine (A), Deferiprone (B) and Deferasirox (C)

1.4.5.2.3 Deferasirox

Deferasirox (Exjade® / ICL670A) is also an orally administered iron chelator and was first approved for the treatment of transfusional iron overload associated with β-thalassaemia major in adults and children over the age of 6. [154, 155]

Deferasirox is a hydroxyphenyl-triazole, tridentate chelator and as such two molecules are required to form a stable complex with a single iron ion. [156] The active molecule (ICL670A, Figure 1.7) is, unlike DFO, highly lipophilic and 99% albumin bound. Deferasirox has a high affinity for iron (approximately 14 and 21 times greater than its affinity for copper [Cu^{2+}] and zinc [Zn^{2+}] respectively). [156]

In-vivo animal pharmacokinetic studies have demonstrated that Deferasirox is rapidly absorbed from the gut and is capable of mobilising iron from various organ systems including hepatocytes and cardiomyocytes. [156, 157]

Phase 1 clinical trials for the use of Deferasirox in iron overloaded individuals demonstrated that its serum concentration is directly proportional to the dose administered. [158] Unbound Deferasirox has a mean half-life of 11–19 hours and plasma levels are maintained within a therapeutic range over a 24-hour period (20 mg/kg/day: peak levels approximately 60–100 μmol/L, trough levels approximately 15–20 μmol/L), providing constant chelation activity. [159]

The proof of concept for Deferasirox treatment in humans was achieved through a dose escalation study in patients with β-thalassemia and transfusional iron overload. [159] The study demonstrated chelation efficiency for the drug of up to 20.5%, establishing an effective dose between 20–30

mg/kg/day. Data from subsequent phase II and III comparative studies in transfusion dependent β-thalassemia patients provided evidence that Deferasirox's efficacy is comparable to DFO. [160, 161]

Furthermore, the recently published results of a 3 year multicentre trial assessing the efficacy of Deferasirox in myelodysplastic syndrome has shown that it significantly reduced serum ferritin and serum labile iron pool in all transfusion dependent patients with elevated levels upon treatment commencement. [162]

Deferasirox has been shown to be generally well tolerated in both adults and children. [161] A total of 652 patients received Deferasirox during core clinical trials with the most frequent adverse events being transient gastrointestinal disturbances (nausea, vomiting, abdominal pain, constipation and diarrhoea) and skin rashes. [161, 163, 164] These events rarely required drug discontinuation and many resolved spontaneously. [161] Mild, non-progressive increases in serum creatinine were also observed in 34% of patients.

The incidence of serious adverse events as a result of Deferasirox treatment appears to be low. [162] The EPIC study reported serious drug related adverse events in 14 of 327 (4.3%) patients given Deferasirox. [164] Likewise, the eXtend and eXjange study documented 7 events in a total of 167 (4.2%) patients. [165] Serious adverse events experienced with the drug include cases of gastrointestinal haemorrhage, myocardial infarction, neutropenia, thrombocytopenia, lens opacity, derangement in liver function and acute renal failure. [165] As such, all patients commenced on the drug require baseline evaluation of their renal and hepatic function with subsequent monitoring during therapy. The drug should be discontinued if increases in creatinine greater than 33% of baseline in 2 consecutive readings are recorded with subsequent reintroduction at a lower dosage followed by monitored escalation. [166]

1.4.5.2.3.1 Deferasirox as an Anti-neoplastic Agent

Over the past few years, the potential for Deferasirox to act as a cytotoxic agent has been investigated. [167, 168] At present results are predominantly limited to *in-vitro* and *in-vivo* laboratory studies. [167, 168, 169] Human data currently comprises only small case series and anecdotal case reports. [170, 171, 172]

1.4.5.2.3.1.1 *In-vitro* and Pre-clinical Effects of Deferasirox

Deferasirox administration has been shown to decrease cellular viability, inhibit DNA replication and induce DNA fragmentation (all with a greater *in-vitro* cytotoxic effect than the chelator O-trensox) in both human hepatoma cell lines and normal human hepatocyte primary cultures. [167] Interestingly, in contrast to other iron chelators, Deferasirox also induces cell cycle blockade during S-phase rather than G_1. [167] Furthermore, much higher concentrations of Deferasirox are required to induce cytotoxicity in primary hepatocyte cultures compared to hepatoma cells (25 μM versus >200 μM) suggesting that malignant lines may be more sensitive to Deferasirox exposure than benign tissues; an observation previously seen with DFO, Deferiprone and O-Trensox. [143, 167, 168]

Exposure to Deferasirox has also been shown to cause a marked reduction in polyamine synthesis; possibly through inhibition of ornithine decarboxylase (ODC) mRNA levels which in turn results in decreased cellular viability and DNA replication. [173] Natural polyamines (e.g. putrescine, spermidine and spermine) are (like iron) required for cell proliferation to occur effectively. They are considered to be critical for the regulation of cell growth, differentiation and death and, unsurprisingly, their intracellular levels and uptake are significantly enhanced in tumour cells. [174] In turn, the enzyme ODC is a crucial component of the polyamine biosynthesis pathway and has been labelled a putative proto-oncogene by some. [174]

The anti-neoplastic effect of Deferasirox upon lung tumour xenografts was recently assessed. [169] Oral Deferasirox was found to significantly reduce xenograft size with no effects seen on mouse health, haemoglobin levels or biochemical parameters. [169] Deferasirox increased expression of the metastasis suppressor protein, n-Myc downstream regulated gene-1 (NDRG1) and up-regulated the cyclin-dependent kinase inhibitor $p21^{CIP1/WAF1}$. In line with previous findings in myeloid leukaemia cells, the drug also increased the expression of apoptosis markers, including caspase-3 (a serine protease that induces apoptosis). [169, 175, 176]

The potential impact of Deferasirox upon the nuclear factor kappa-light-chain-enhancer of activated B cells (NFκB) pathway has also been investigated. [177] NFκB plays a pivotal role in the pathogenesis of a number of cancers by regulating several fundamental cellular processes such as apoptosis, proliferation, differentiation and tumour migration. [178] It has been shown to be constitutively active in most tumour cell lines and has also been identified in tumour tissue from patients with multiple myeloma, acute myeloid leukaemia, prostate cancer and breast cancer. [178, 179, 180, 181, 182] Deferasirox was found to dramatically reduce NFκB activity in both leukaemia cell lines and blood samples from patients with myelodysplastic disorders. [177] Furthermore, the addition of ferric hydroxyquinoline during incubation did not reinstate NFκB activity suggesting that the effect produced by Deferasirox may be independent of chelation induced cell iron deprivation. [177] In addition, inhibition of the NFκB pathway was seen solely with Deferasirox (it did not occur with either DFO or Deferiprone). Interestingly, it was also noted that pre-incubation of cells with Deferasirox followed by subsequent incubation with Etoposide lead to an increase in the number of apoptotic cells compared to both drugs alone. [177]

Deferasirox also appears to be capable of repressing signalling through the mammalian target of rapamycin (mTOR) pathway by enhancing expression of the regulated in development and DNA damage response protein (REDD1, also known as HIF-1 responsive protein) to give anti-proliferative

effects on myeloid leukaemia cells. [183] The mTOR pathway is known to demonstrate aberrant activity in a number of cancers including ovarian, breast, colon, brain and lung.[184] Over activity of this pathway culminates in de-regulation of the cell cycle and increased cellular proliferation. Conversely, inhibition of the mTOR pathway results in cytostatic effects possibly through a reduction in proteins ultimately required for cell cycle progression including the previously mentioned ODC and cyclin D. [184] REDD1 has been previously identified as a stress-response gene and is strongly induced by hypoxia. [185]

Finally, Deferasirox has been shown to attenuate Wnt signalling (a major oncogenic signalling pathway in a number of cancers, most notably colorectal) through an iron dependent mechanism. [102, 186]

1.4.5.2.3.1.2 Human Studies

A number of studies have anecdotally described an improvement in red blood cell parameters amongst patients with myelodysplastic disorders following chelation therapy with Deferasirox. For example, post-hoc analysis of a recently published 3 year prospective multicentre trial (which was designed primarily to assess the safety and efficacy of Deferasirox as an iron chelator in myelodysplastic syndrome) revealed improvement in haematological parameters amongst a sub-group of patients within the first year of treatment. [162]

The results seen in the previous trial have been supported by a number of case reports. [170, 171, 172] Di Tucci and colleagues administered Deferasirox as chelation therapy to a patient with primary myelofibrosis and previous transfusion dependency.[170] After 2 months of therapy the patient's transfusion requirement progressively decreased and ceased completely after 5 months. Guariglia *et al*. also documented the case of a 74 year old male patient with refractory thrombocytopenia given

Deferasirox as chelation therapy who, despite persistence of the karyotypic and morphological abnormality, became transfusion independent following 6 weeks of therapy. [187] Interestingly, once treatment with Deferasirox was stopped the patient again became transfusion dependent; Deferasirox was thus restarted and the patient became transfusion independent once more.

Finally and perhaps of most interest, another case report documented that Deferasirox administration achieved complete remission in a patient with previously chemotherapy resistant acute monocytic leukaemia. [188] Following relapse and subsequent rejection of further chemotherapy, the patient underwent regular blood transfusions with the addition of Deferasirox as chelating therapy for 12 months. Four months after discontinuation of Deferasirox the patient's blood cell count normalised and the patient became transfusion-independent. Bone marrow aspiration and biopsy revealed a haematological and cytogenetic complete remission.

The mechanism by which chelation therapy with Deferasirox may induce haematological improvement remains unclear. It is known that iron chelators promote iron release from storage sites, facilitating its usage for haematopoietic tissue. [187, 188] Reduction in iron stores appears to up regulate erythropoietin response with subsequent increase in haemoglobin release. [189] In patients with myelodysplastic syndrome in particular, treatment with Deferasirox significantly reduces ROS, membrane lipid peroxidation and labile iron pools. [189] It also increases glutathione levels in red blood cells, neutrophils and platelets. [190]

1.5 Conclusion

Gastrointestinal cancer remains a significant health problem throughout the world. [2] In the UK in particular, both oesophageal cancer (with its increasing incidence and poor outcome) and colorectal cancer (as the 4th most common malignancy) place significant burdens on both the individuals affected and society as a whole. [3, 4, 7, 58] As such, the development and implementation into clinical practice of new treatments that are either solely effective or can enhance the efficacy of existing therapies would be highly desirable.

Iron is intimately involved in tumourigenesis and it has been shown to have a role in the propagation of both oesophageal and colorectal cancers. As such, iron chelation represents a promising avenue in the treatment of cancer. Although experimental chelating agents have demonstrated significant anti-proliferative and chemosensitising properties, associated side effects mean that at present approved iron chelators offer the best chance of translation into clinical practice.

Of the three chelators currently in clinical use, Deferasirox has the advantage of once daily oral administration (unlike DFO) and is well tolerated with a safety profile that appears superior to other chelators. The drug possesses potent anti-neoplastic effects in a number of pre-clinical cancer models and furthermore, these cytotoxic and anti-proliferative actions appear to be mediated through a number of different oncological pathways and are not merely restricted to the action of iron deprivation through chelation.

Considering Deferasirox's potentially multi-modal therapeutic action, ease of administration, good safety profile and anecdotal clinical experience to date, the drug makes for an attractive chemotherapeutic agent in the treatment of cancer.

1.6 Hypothesis and Aims

Normal iron metabolism is dysregulated in gastrointestinal cancer in a way that favours the propagation of tumourigenesis. As such, a strategy to starve tumour cells of iron represents a potential novel treatment worthy of further investigation. With this in mind, iron chelation therapy has shown early promise in a number of malignancies. Furthermore, iron chelators have also been shown to possess chemosensitising properties when given in combination with existing agents in experimental models. None of this has been investigated before in the context of gastrointestinal cancer, however. Thus, the aims of this thesis are:

1. To determine the efficacy of the iron chelating agent Deferasirox as an anti-neoplastic and or chemosensitising agent in oesophageal cancer.
2. To determine the efficacy of the iron chelating agent Deferasirox as an anti-neoplastic and or chemosensitising agent in colorectal cancer.
3. To determine the role of IRP2 in colorectal cancer in order to offer a predictive marker for iron chelation efficacy.
4. To determine the ability of the iron chelating agent Deferasirox to chemosensitise a panel of re-purposed drugs in oesophageal and colorectal cancer.

Chapter 2. Materials and Methods

2.1 Materials

2.1.1 Cell Lines Utilised

2.1.1.1 Oesophageal Cell Lines

OE19

Also known as JROECL19, the OE19 cell line was established in 1993 from an adenocarcinoma of the gastric cardia/gastroeosophageal junction in a 72 year old male patient. [191] The tumour was identified as pathological stage III and showed moderate differentiation.

OE33

Also known as JROECL33, the OE33 cell line was established from an adenocarcinoma of the lower oesophagus in a 73 year old female patient. [191] The cancer had developed on the background of Barrett's metaplasia. The tumour was identified as pathological stage IIa and showed poor differentiation.

OE21

Also known as JROECL21, the OE21 cell line was established from a squamous cell carcinoma of the mid oesophagus in a 74 year old male patient. [191] The tumour was identified as pathological stage IIa and showed moderate differentiation.

TE4

The TE4 cell line was a kind gift from Professor Winand Dinjens at Erasmus MC, Rotterdam, Holland. It was established from a squamous cell carcinoma of the oesophagus and has been shown to be highly resistant to chemotherapy with Cisplatin. [192]

2.1.1.2 Colorectal Cell Lines

RKO

The RKO cell line is a poorly differentiated colon carcinoma cell line taken from an 82 year old female patient. It expresses wild type APC, p53 and GADD45. [193]

SW480

The SW480 cell line was established from a primary adenocarcinoma of the colon in a 50 year old male. The line expresses constitutively active c-Myc and K-ras along with mutated p53. It also contains a truncated/mutated APC. [193]

SW620

The SW620 cell line was established from a metastatic lymph node taken from the same patient as the SW480 cell line 1 year later when the disease recurred. It is thus a colonic adenocarcinoma metastasis and is essentially isogenic with the SW480 cell line. The line expresses c-Myc and K-ras as well as mutant APC. [193]

HT29

The HT29 cell line was a kind gift from Dr Bert Vogelstein of the John Hopkins University, Baltimore, USA. It originates from a colonic adenocarcinoma in a 44 year old female and expresses the oncogenes c-Myc and K-ras. It also possesses mutant APC. [193]

This cell line was modified by Dr Vogelstein to express wild type APC following incubation with 100 μM zinc chloride for 24 hours. [63] This occurs through the action of a zinc inducible, Hygromycin B resistant APC expressing vector (pSAR-MT-APC) transfected by Dr Vogelstein and confirmed through Western blotting. [63] The cell line has subsequently been utilised in a number of studies as a model for investigating the effect of APC expression on cell phenotype behaviour. [194, 195]

HCT116

The HCT116 cell line is a colonic adenocarcinoma cell line originating from an adult male patient. It possesses wild type APC and p53 but has activated c-Myc and K-ras expression. [193]

In addition, an isogenic HCT116 p53 -/- cell line was also utilised, which was a kind gift from Dr Bert Vogelstein of the John Hopkins University, Baltimore, USA. This cell line has undergone targeted deletion of both p53 alleles and is a suitable model for studying the effects of p53 on cell growth and subsequent response to therapy. [196]

Caco-2

The Caco-2 cell line is a colonic adenocarcinoma cell line originating from a 72 year old Caucasian male. [193] In addition, when cultured under specific conditions the cells become differentiated and polarized such that their phenotype (morphologically and functionally) resembles the enterocytes lining the small intestine. [197] Thus, Caco-2 cells are most commonly cultured to a confluent monolayer on a cell culture insert filter (e.g. Transwell). When cultured in this format, the cells differentiate to form a polarized epithelial cell monolayer that provides a physical and biochemical barrier to the passage of ions and small molecules. [197] This Caco-2 monolayer model is widely used across the pharmaceutical industry as an *in-vitro* model of the human small intestinal mucosa to predict the absorption of orally administered drugs.

Colo320

The Colo320 cell line originates from a 55 year old female and is a Duke's C colonic adenocarcinoma. It possesses mutations in both the APC and p53 tumour suppressor genes but displays wild type K-ras and B-raf. [193]

Colo205

The Colo205 cell line originated from the ascitic fluid of a 70 year old male patient with colonic adenocarcinoma previously treated with 5-Fluorouracil. Like the Colo320 cell line, it possesses mutations in APC and p53, however, it also contains a BRAF V600E mutation. [193]

Table 2.1 Genetic status and oncogene expression in certain colorectal cancer cell lines utilised

Cell Line	RKO	HCT116	HT29	Colo320	Colo205	Caco-2	SW480	SW620
APC status	Wild type	Wild type	Mutated *	Mutated	Mutated	Mutated	Mutated	Mutated
p53 status	Wild type	Wild type	Mutated	Mutated	Mutated	Mutated	Mutated	Mutated
K-ras	Wild type	Mutated	Wild type	Wild type	Wild type	Wild type	Mutated	Mutated
c-Myc expression	Detected	Detected	Detected	Detected	Detected	Detected	Detected	Detected
PIK3CA	Mutated	Wild type	Mutated	Wild type	Wild type	Wild type	Wild type	Wild type
B-raf	Mutated	Wild type	Mutated	Wild type	Mutated	Wild type	Wild type	Wild type

*also wild type inducible

Adapted from American Tissue Culture Collection (ATCC). Colon cancer and normal cell lines. [193]

RGC2

The RGC2 cell line is derived from a colonic adenoma and was a kind gift from Professor Ann Williams, School of Cellular and Molecular Medicine, University of Bristol, UK. It possesses wild type APC and expresses c-Myc. [198]

AAC1

The AAC1 cell line is derived from a colonic tubular adenoma displaying mild dysplasia. [199] It has an APC mutation, expresses c-Myc and also possesses a K-ras mutation.

2.1.2 Materials Utilised

General, Cell Culture and Molecular Biology Reagents

General, cell culture and molecular biology reagents were obtained from the following sources:

Abbott, Global

Isoflurane

Amersham Pharmacia, Amersham, Buckinghamshire

ECL reagent; Hybond PVDF, Hyperfilm x-ray film, Peroxidase linked secondary antibodies;

Antec International, Sudbury, UK

Virkon

Applied Biosystems, Cheshire

96 well optical plate; optical adhesive covers; RNAlater; TaqMan ribosomal RNA control reagent

Appleton Woods, Selly Oak, Birmingham

10 ml and 25 ml pipettes; Bijou 3 ml and 7 ml tubes; Eppendorfs; Universal 15 ml and 50 ml tubes

Becton Dickinson (BD), Plymouth UK

Falcon 5 ml round bottom counting tubes; FACS tubes (5 ml 12/75 mm); BD Matrigel

Bioline, Humber Road, London, UK

SensiMix^{tm} II qRT-PCR probe kit

Bio-optica, Milano, Italy

Tris Buffered Saline, W-CAP TEC Buffer

Boehringer Mannheim, Lewes, East Sussex

Mycoplasma detection Kit

Chance Propper, Smethwick, West Midlands

Glass coverslips

DAKO UK Ltd, Cambridge, UK

DAKO Antibody Diluent; DAKO ChemMate substrate buffer; DAKO REAL DAB and Chromogen Kit; DAKO Pen

Eurogentec, Seraing, Belgium

Reverse transcriptase core kit

Fisher Scientific, Loughborough, Leicestershire

BCA protein assay

Geneflow, Southampton

Acrylamide

Invitrogen, Paisley, Renfrewshire (incorporating Gibco BRL)

Dulbecco's Modified Eagles Medium (DMEM) with Glutamax-1, pyridoxine and 4500mg/L glucose; Foetal Calf Serum; Hygromycin B; McCoy's 5A medium; Normal goat serum; Optimem medium; Penicillin and Streptomycin solution; PLUS Reagent; PureLink HiPure Plasmid Filter Purification Kits – Maxi Prep; Puromycin; Roswell Park Memorial Institute (RPMI) medium with 25 mM Hepes buffer and L-glutamine; Super Ooptimal Broth with Catabolite repression (S.O.C) media; Trizol reagent; Trypsin EDTA.

Iwaki, Stone, Staffordshire (Subsidiary of Barloworld scientific)

25, 75 and 150 cm^2 tissue culture flasks; 96 well culture plates; 12 well culture plates; 6 well culture plates

Pall Corporation, Newquay, Cornwall

0.2 μm filters

Promega, Chilworth Research Centre, Southampton

Dual-Luciferase Reporter Assay System; Nuclease free water

Roche Applied Science, Lewes, East Sussex

BrdU proliferation assay; Proteinase and phosphatase inhibitor cocktails

Sigma Chemical Company Limited, Poole, Dorset

Agarose; Ammonium acetate; Ammonium persulphate; β-mercaptoethanol; Bromophenol Blue; Calcium chloride; Citric acid (tri-sodium citrate); DAB (3,3'-diaminobenzidene tetrahydrochloride) tablets; DAPI (4',6-diaminido-2-phenylindole); Deoxynucleotide (dNTP) mix; Dimethyl Formamide; Dimethyl Sulfoxide (DMSO); Dithiothreitol (DTT); DNAse I; Ferrous sulphate; Ferrozine (3-(2-Pyridyl)-

5,6-diphenyl-1,2,4-triazine-4,4-disulfonic acid); Formalin; Glycerol; Glycine; N-[2-Hydroxethyl]piperazine-n'-[2-ethanesulfonic acid] (HEPES); H2DCF-DA (2,7-dichloro-fluorescein-diacetate); Hydrochloric acid; Hydrogen Peroxide 30% w/v; Hydroquinone (1,4-Benzenediol); LB Broth EZMix powder; Isopropanol; Lauryl sulphate; $MgCl_2$; Mayer's Haematoxylin 0.1% Solution; Methanol; MTT (3-(4,5-dimethylthiazol-2-yl)-2,5-diphenyltetrazolium bromide); NP40; Paraformaldehyde; Polyoxyethylenesorbitan monolaurate (Tween 20); Phosphate buffered saline; Potassium Acetate; 1,2-propanediol; Propidium Iodide; RNase A; Sodium Acetate; Sodium Ascorbate; Sodium Carbonate; Sodium Chloride; Sodium Citrate; Sodium dodecyl sulphate (SDS); TEMED; Trichloroacetic Acid, Tris HCl; Trizma base; Urea; Xylene

Turumo, Europe

Capijet blood tubes

2.2 Methods

2.2.1 Routine Cell Culture

Cell lines were cultured in an incubator at 37 °C and 5% CO_2 atmosphere for all experiments (apart from those involving the induction of hypoxia where a hypoxic chamber at 1% O_2, 5% CO2, and 94% nitrogen was utilised). Unless stated otherwise, cells were grown in Dulbecco's Modified Eagles Medium (DMEM) supplemented with 10% (v/v) Foetal Calf Serum (FCS), 50 U/ml penicillin and 50 µg/ml streptomycin. Colo320 and Colo205 cells were cultured in RPMI medium containing 10% (v/v) FCS, 50 U/ml penicillin and 50 µg/ml streptomycin. HT29 cells were cultured in McCoy's 5A medium containing 10% (v/v) FCS, 50 U/ml penicillin, 50 µg/ml streptomycin and also 0.6 mg/ml Hygromycin B.

All cell lines utilised grow as an adherent monolayer and were passaged at approximately 90% confluence by aspirating the culture medium, washing the monolayer in sterile phosphate buffered saline (PBS) and incubating with 5 ml of 0.05% (w/v) trypsin EDTA until cells had detached (typically 5-10 minutes). Five ml of culture media was then added and cells were disaggregated by trituration and then centrifuged at 1500 rpm for 5 minutes. The cell pellet was either re-suspended in culture media and reseeded or was re-suspended in 1 ml of freezing medium (10% (v/v) dimethyl sulphoxide (DMSO), 20% (v/v) FCS, 70% (v/v) media as appropriate) and placed in a cryovial for cryopreservation.

Vials were kept at –70 ^{o}C for 3 days before transfer to liquid nitrogen storage. Frozen cells were resurrected by rapid warming of the cryovial in a 37 ^{o}C water bath and the cells were then washed and suspended in pre-warmed culture media. Cells were seeded into tissue culture flasks and cultured in the standard manner. All cell culture procedures were performed in a laminar flow tissue

culture cabinet using aseptic technique. Mycoplasma testing was performed periodically to ensure cells remained negative.

2.2.2 Preparation of Pharmaceutical Agents

Deferasirox

A 10mM stock solution of Deferasirox (ICL670A, Exjade ®Novartis Pharmaceuticals, Switzerland) was produced by dissolving 37.34 mg of the drug in 10 ml of serum free DMEM. The resulting solution was sterile filtered prior to use and then diluted as appropriate for the experiment performed.

Cisplatin

A 100 µM stock solution of Cisplatin was prepared by adding 300 µl of 1 mg/ml Cisplatin to 9.7 ml of serum free DMEM. The stock solution was then diluted as appropriate for the experiment performed.

5-Fluorouracil

A 500 µM stock solution of 5-Fu was prepared by adding 26 µl of 25 mg/ml 5-Fu to 9974 µl of serum free DMEM. The stock solution was then diluted as appropriate for the experiment performed.

ECF

The chemotherapy combination of Epirubicin, Cisplatin and 5-Fu (ECF/ECX) is commonly used in the treatment of oesophageal cancer. [41] For the purposes of the experiments performed, the individual agents were prepared at their pre-determined IC25s of 0.5 µM (Epirubicin), 4 µM (Cisplatin) and 4

μM (5-Fu) and combined together in serum free media. The stock solution was then diluted as appropriate for the experiment performed.

Trametinib

The MEK (MEK1 and MEK2) inhibitor Trametinib was purchased from Santa-Cruz Biotechnology. Following re-suspension in DMSO the drug was added to standard media and used at the concentrations documented (typically 10 nM).

Sorafenib

The intracellular serine/threonine kinase (B-raf) inhibitor Sorafenib was purchased from Santa-Cruz Biotechnology and following re-suspension in DMSO was added to standard media to produce the documented experimental concentrations (typically 1 μM).

Ferrous Sulphate

A stock solution of 10 mM ferrous sulphate ($FeS0_4$) was prepared by dissolving 111.2 mg $FeS0_4$ in 40 ml of sterile distilled water (SDW). In addition, either 395 mg (enhanced) or 7.9 mg (standard) of sodium ascorbate (equivalent to 50 mM and 1 mM respectively) was added to prevent the iron from oxidising in solution, thus maintaining an adequate pool of Fe^{2+} for absorption by the cells. The $FeS0_4$ stock solution was then filtered and diluted in serum free media as appropriate for the particular experiment (typically 100 μM $FeSO_4$).

Zinc Chloride

Zinc chloride was dissolved in SDW and used at the previously published concentration of 100 μM for 48 hours to induce APC expression in the HT29 colonic cell line. [63]

Library of Redeployed Drugs

The library of 99 redeployed drugs was a kind gift from Professor Chris Bunce and Dr Farhat Khanim, School of Biosciences, University of Birmingham, UK. The library contains drugs from all sections of the British National Formulary (BNF). Drugs are utilised at concentrations equivalent to the peak serum concentration achieved through their standard dosing regimen as recommended in the BNF (Table 2.2). [200]

Drugs were initially prepared as stock solutions equivalent to 10,000x their reported peak serum concentration and kept at -20 ^{0}C until required. [200] For experiments, 1 μl of stock solution was added to standard DMEM containing 10% FCS (v/v) and 1% penicillin/streptomycin (v/v). Working solutions were prepared fresh for each experiment.

Table 2.2 Library of redeployed drugs

Drug	x10,000 stock (mM)	Chlorambucil	16.173
Prednisolone	716.000	Metoclopromide	2.974
Amantidine	35.000	Domperidone	0.446
Folic acid	1.041	Thalidomide	109.000
Thiamine	1.186	Chloroquine	1.980
Ranitidine	15.500	Metformin	121.000
Fluoxetine	6.820	Niclosamide	32.000
Dexamethasone	4.332	Pravastatin	0.269
DMSO	Control	Nortryptyline	4.636
Vitamin K1	0.008	Dantrolene sodium	37.000
Carbamazepine	508.000	Omeprazole	26.113
Propanolol	5.105	Diclofenac	12.570
Erythromycin	52.000	Ritodrine	1.390
Retinol	10.000	Selegiline	2.011
Bendroflumethiazide	1.186	Mebendazole	16.933
Propylthiouracil	1057.000	Flupentixol	0.118
Nicotinic acid	1000.000	Acipimox	382.000
Theophylline	110.000	Ethanol	Control
Nicotinamide	409.000	Desferrioxamine	132.000
Ascorbic acid	950.000	Imipramine	2.241
Acyclovir	222.000	Artemisinin	14.000
Allopurinol	460.000	Propantheline	0.468
Chlorpheniramine	0.409	Diltiazem	4.010
Neostigmine	0.150	Ampicillin	162.000
Alpha tocopheryl acetate	500.000	Methanol	Control
Bromocriptine	13.750	Amphotericin b	43.000
Cyclophosphamide	2000.000	Danazol	17.780
Imatinib	51.000	Penicillin V	914.000
Zinc acetate	3234.000	Mesalazine	26.120
Valproic acid	6017.000	Finasteride	1.074
Rifampicin	122.000	Colchicine	0.175
Metronidazole	760.000	Levothyroxine	1.500
Praziquantel	350.000	Methotrexate	10.000
Flutamide	62.235	Mifepristone	4.600
Clomipramine	8.540	Nicotine	2.157
Testosterone	0.400	Cefaclor	625.000
Calciferol/ergocalciferol	0.500	Vitamin B12	0.001
Doxycycline	68.000	Medroxyprogesterone acetate	2.330
Aspirin	3330.000	Bezafibrate	83.000
Ibuprofen	1939.000	Paroxetine	1.734
Norethisterone	0.294	Trimethoprim	69.000
Itraconazole	8.800	Water	Control
Methyldopa	57.200	Naloxone	0.875
Fenofibrate	26.300	Simvastatin	0.186
Clofibric acid	2330.000	Flecainide	21.000
Clobetasol propionate	0.099	Pilocarpine	3.000
Paracetamol	1323.000	Fluconazole	617.000
Alverine citrate	100.000	Acitretin	12.250
Mefenamic acid	414.000	DMEM (1)	Control
Prochlorperazine	66.000	DMEM (2)	Control

Table 2.2 Library of redeployed drugs

Drugs were utilised at concentrations equivalent to the peak serum concentration achieved through their conventional dosing regimens. [200] Stock solutions were made at 10,000x concentration (mM). Working solutions were created by adding 1 µl of stock solution to 10 ml of standard media. For compounds marked control, 1 µl of reagent (at standard concentration) was added to 10 ml standard media.

2.2.3 Cell Viability Assay

Cells were plated out and subjected to conditions as outlined within each experimental section.

After the defined time points, 3-(4,5-dimethylthiazol-2-yl)-2,5-diphenyltetrazolium bromide (MTT) assays were performed in order to determine cellular viability. The MTT assay is a colorimetric assay for measuring the activity of cellular enzymes that reduce the tetrazolium dye, MTT, to its insoluble formazan form. The more viable (and active) the cells, the more the MTT is reduced.

Briefly, 10 µl of MTT solution (5 mg/ml in sterile PBS) was added to 100 µl of culture media in each well of the 96 well plate and incubated for 3 hours. Following this period, the media (containing the MTT) was aspirated and replaced with 100 µl of dimethyl sulfoxide (DMSO) to dissolve the accumulated formazan crystals. After 15 minutes at room temperature, the plates were placed into a Bio-Tek ELx800 absorbance micro plate reader and absorbance read at 490 nM. The resulting optical densities were used to calculate percentage viability with respect to control (normalised to 1).

2.2.4 Cell Proliferation Assay

The pyrimidine analogue 5-bromo-2'-deoxyuridine (BrdU) is incorporated into cellular DNA in place of thymidine during replication and can therefore be used to quantify cellular proliferation. Incorporated BrdU can be detected by the use of a peroxidase conjugated anti-BrdU antibody followed by a colorimetric reaction involving tetramethyl-benzidien (TMB).

After the defined experimental time point, cells were labelled with BrdU (10 µl per well, diluted 1 in 100 v/v with plain media) for 4 hours at 37 ^{0}C, then fixed and DNA denatured with FixDenat solution

(200 µl per well for 30 minutes at room temperature). Cells were then incubated with anti-BrdU antibody for 90 minutes at room temperature (50 µl per well, diluted 1 in 100 with antibody diluent). Immune complexes were detected after washing, using a TMB substrate reaction (100 µl per well) with the subsequent product assessed at 405 nm (after 15 minutes) on a micro plate reader. The resulting optical densities were used to calculate percentage viability with respect to control (normalised to 1).

2.2.5 Oesophageal Cell Line Xenografts

Suspensions of OE19 cells (1 x 10^7 cells) were centrifuged and re-suspended in 50 µL of culture media. Immediately prior to injection, the cell slurry was mixed 50/50 (v/v) with Matrigel (extracellular matrix). The cell suspension was then subcutaneously injected into NOD-SCID (severely immunodeficient) mice (100 µl per mouse). After a period of tumour establishment (typically 2 weeks), mice were divided into groups and given treatments as per the experimental protocol.

Throughout the experimental period, mouse health and weight were closely monitored. Tumour growth was also measured weekly using calipers. Following the treatment period, mice were anaesthetised and exsanguinated by direct cardiac puncture and blood/plasma retained for full blood count and biochemical analysis (creatinine and serum iron). Tumours were removed and weighed to assess tumour burden. All work was carried out under Home Office approved conditions and in accordance with the United Kingdom Animals (Scientific Procedures) Act of 1986.

2.2.6 NFκB Reporter Assay

The pGL4.32 vector contains five copies of an NF-κB response element (NF-κB-RE) that drives transcription of the luciferase reporter gene luc2P and was a kind gift from Dr Chris Dawson, School of Cancer Sciences, University of Birmingham, UK.

Briefly, OE19, OE21 and OE33 oesophageal cells were plated out into 12 well plates and co-transfected the following day with the pGL4.32 vector and the CMV-Renilla plasmid (Promega) using Lipofectamine 2000 transfection reagent. Following an overnight expression period, cells were treated with either control solution (standard DMEM), TNFα (20 ng/ml in DMEM, positive control) or Deferasirox. After being returned to the incubator again overnight whilst induction took place, luciferase activity was quantified using a dual-luciferase® reporter assay system the following day.

After reading the plates on a Victor plate reader, the reading of the luciferase signal was corrected with the reading of the Renilla (as per manufacturer's instruction). Fold change in luciferase reporter activity (NFκB activity) was then calculated using the formula:

$$\text{Fold Induction} = \frac{\text{Average relative light units of induced cells (either TNFα or Deferasirox)}}{\text{Average relative light units of control cells}}$$

Data was thus expressed as a fold change relative to control NFκB levels (normalised to 1).

2.2.7 Protein Quantification Assay

A protein assay was performed on cellular lysates in order to determine protein concentration prior to Western blotting, the ferrozine assay and the ferritin ELISA.

Protein concentration of samples was determined using a BCA™ (bicinchoninic acid) protein assay and compared with bovine serum albumin at standard concentrations between 0 and 2 mg/ml. 10 µl of each standard, or 10 µl of each cell lysate, were aliquoted in triplicate onto a clear flat bottomed 96-well plate. 200 µl of BCA™ working reagent (reagent B 1:50 in reagent A) was added to each well and incubated for 30 minutes at 37 °C. Absorbance was then measured at 550 nm using a Bio-Tek ELx800 absorbance microplate reader. The sample protein concentrations were then derived from a graph of standard concentrations plotted against optical density at 550 nm.

2.2.8 Western Blotting

Cells were cultured in 6 well plates as per the desired experimental conditions. For lysate preparation, the media was removed and cells washed 3 times with 1 ml PBS. 160 µl RIPA lysis buffer (1% (w/v) NP40 (nonyl phenoxypolyethoxylethanol) (5 g); 0.5% sodium deoxycholate (2.5 g); 0.1% SDS (0.5 g) in 500 ml deionised water) containing protease and or phosphatase inhibitor cocktail tablets (as required) was then added to each well. Lysates were prepared on ice, subjected to ultrasound probe sonication and stored at -4°C prior to use.

Prior to sample preparation a protein assay was performed (as outlined previously) so that equal volumes of lysate could be loaded (typically 10 or 20 µg). Lysates were mixed with loading dye (500 µl 4x SDS + 200µl β-mercaptoethanol) at a ratio of 4:1 and then boiled for 5 minutes at 100 °C.

Standard 10% resolving gels were made for all antibodies except ferritin (for which a 12.5% gel was utilised). The 10% resolving gel comprises 1-2 mg of ammonium persulphate; 3.5 ml deionised water; 10 ml gel stock 2 (0.75 M TRIS + 1 g SDS made up to 500 ml with deonised water, pH 8.8); 6.5 ml 30% acrylamide/ 8% bisacrylamide and 60 µl TEMED). Once set, stacking gels were made (1-2 mg ammonium persulphate, 3.7 ml deionised water, 5 ml gel stock 1 (0.25 M TRIS + 1 g SDS made up to

500 ml with deionised water; pH 6.8), 1.3 ml acrylamide and 60 µl TEMED). The 12.5% resolving gel comprised the same components as the 10% gel except it contains 1.9 ml of deionised water and 8.1 ml of 30% acrylamide/ 8% bisacrylamide.

For 10 lane gels 20 µg of protein was loaded per well into the gel (10 µg for 15 lane gels), with one lane containing 2.5 µl of PageRuler^{TM} Plus Prestained Protein Ladder (ThermoScientific) per gel. Samples were stacked for 10 minutes at 100 V then run at 180 V until proteins had migrated fully (typically 45 minutes). Running buffer comprised 10x buffer stock (30 g TRIS, 144 g glycine, 10 g SDS in 1 L water, (pH 8.3)) diluted 1:10 with deionised water.

After samples had been run, proteins were transferred from the gel onto a polyvinylidene difluoride (PVDF) membrane. Transfer was carried out in 1x transfer buffer (100 ml 10x transfer buffer (30.28 g Tris base + 144 g glycine +1 g SDS in 1 L); 700 ml deionised water and 200 ml methanol) for 100 minutes at 100V. Following transfer, membranes were blocked for 1 hour with 5% skimmed milk powder (w/v) dissolved in 1x TBST (10x TBST: 200 mls 1 M TRIS pH 8; 175.5 g NaCl; 10 ml Tween20 made up in 1.8 L deionised water) on a horizontal mixing plate.

Following blocking, membranes were incubated overnight at 4 °C with primary antibodies (as outlined in Table 2.3) dissolved in either 5% milk: 1xTBST (w/v) or 5% BSA: 1xTBST (for phosphorylated antibodies).

After overnight incubation the primary antibody was removed and the membrane washed x4 in 1xTBST (x1 immediate wash followed by x3 washes of ten minutes each). The membrane was then incubated for 1 hour at room temperature in either an anti-mouse or anti-rabbit secondary antibody as appropriate (diluted 1 in 10,000 v/v in either 5% milk:1xTBST or 5% BSA:1xTBST. After 1 hour the secondary antibody was removed and the membrane washed x4 as previously outlined prior to the

application of the ECL developing reagent (typically 4 ml ECL per membrane for 5 minutes). The membranes were finally placed on hyperfilm x-ray film in a darkroom and developed.

Films were subsequently scanned and analysed semi-quantitatively using ImageJ analysis software (Softonic®) and Microsoft Excel 2010 (Microsoft). In all cases, band intensity for the antibody of interest was expressed relative to expression of the ubiquitously expressed protein β-actin.

Table 2.3 Primary antibodies utilised in Western blotting protocols

Target Antigen	Molecular weight	Source	Antibody class	Optimal Dilution
β-actin	42 kDa	Abcam Ab8226	Mouse IgG anti-human	WB: 1/10000
β-catenin	94 kDa	BD Biosciences 562505	Mouse IgG anti-human	WB: 1/2000
B-raf	95 kDa	Santa-Cruz Biotechnology SC-5284	Mouse IgG anti-human	WB: 1/200
Ferritin	20 kDa	Abcam Ab7332	Rabbit IgG anti-human	WB: 1/5000
HIF-1α	120 kDa	BD Biosciences 610958	Mouse IgG anti-human	WB: 1/250
IRP2	105 kDa	Source Bioscience Lifesciences LS-B675	Rabbit IgG anti-human	WB: 1/500
p-ERK 1/2	p-ERK 1 44 kDa p-ERK 2 42 kDa	Cell Signalling Technology 9101	Rabbit IgG anti-human	WB: 1/500
p-IκB-α	41 kDa	Santa-Cruz Biotechnology SC-101713	Rabbit IgG anti-human	WB: 1/500
TfR1	190 kDa dimer, 95 kDa subunit	Invitrogen 13-6800	Mouse IgG anti-human	WB : 1/1000

2.2.9 Quantification of Intracellular Iron Levels by Ferrozine Assay

The ferrozine assay permits the quantification of intracellular iron levels. Ferrozine forms a stable, water soluble, magenta complex with divalent iron that is suitable for colorimetric quantification.

Cells were cultured in 6 well plates with media as per the experimental conditions. After a pre-determined incubation period the monolayer was washed three times with 1 ml PBS. After thorough aspiration of the PBS, 160 µl of HEPES saline (10 mM HEPES in 0.9% (w/v) sodium chloride at pH 7.4) was added to the well in order to lyse the cells. The cell monolayer was then separated from the plate bottom using a cell scraper. 90 µl of the lysate suspension was removed and added to 200 µl 20% (w/v) trichloroacetic acid in 4% (w/v) sodium pyrophosphate (TCA) This was boiled for 5 minutes then re-centrifuged for a further 5 minutes at 12000 RPM. 200 µl of the supernatant was aspirated and added to 600 µl of Ferrozine stock solution (100 µl of 0.23 M sodium ascorbate, 80 µl of 10 mM ferrozine and 420 µl of 2 M sodium acetate). This solution was thoroughly mixed and 200 µl aliquots placed in triplicate in a flat-bottomed clear 96 well plate. The colorimetric change in each sample was measured using a Bio-Tek ELx800 plate reader at 550 nm. The absorbance in the blank was used to correct each sample. The protein concentration (analogous to overall cell number) in each sample was determined (by performing a protein assay on the remaining 60 µl of lysate, as outlined previously) allowing the iron content of each sample to be expressed as a function of protein content (ng Fe / µg protein).

2.2.10 Quantification of Cellular Ferritin Concentration by Ferritin ELISA

The Spectro Ferritin MT ELISA kit (Ramco Laboratories Inc) was utilised as an alternative method (to Western blotting) of quantifying intracellular ferritin protein expression.

Cells were plated out and treated as per the desired experimental conditions. Following this, lysates were extracted using HEPES saline lysis buffer (as described in the ferrozine assay) and a protein assay performed (as previously outlined). Briefly, 10 or 5 µl (depending on protein concentration) of sample was then loaded per well along with the ferritin calibrator solutions (provided with the kit) at 6, 20, 60, 200, 600 and 2000 ng/ml. To this, 200 µl of unconjugated antihuman ferritin was then added before incubating on a horizontal mixing plate for 2 hours. Wells were then washed with deionised water before the addition of 200 µl substrate solution. Following incubation for 30 minutes at room temperature, 100 µl of 0.24% (w/v) potassium ferricyanide was added to develop the colour and the plate was then read at reading at 490/595 nm using the Victor^2 Multilabel Counter (Perkin Elmer).

A595 values were subsequently subtracted from A490 values for each sample and compared to the calibration curve. Values were then corrected for protein concentration and expressed as ng ferritin / µg protein.

For all iron based experiments, cells were plated out in 6 well plates at a concentration of $2x10^5$/well. The following day cells were challenged for 1 hour with either standard media (control), media containing 100 µM $FeSO_4$ (+500 µM Na ascorbate) or media containing Deferasirox 40 µM + 100 µM $FeSO_4$. Where the ability of Deferasirox to remove iron from pre-loaded cells was being assessed, an additional group treated with 100 µM $FeSO_4$ for 1 hour followed by Deferasirox (40 µM) for 1 hour was also included. The ferrozine assay was performed immediately after the treatment period ended. In the case of the western blot and ferritin ELISA, standard media was placed back on the cells and left overnight to permit translation of ferritin protein.

2.2.11 Transwell Radio-labelled Iron Uptake Studies

Cell culture plates (6 well) were coated overnight in rat-tail collagen and placed in ultra-violet (UV) light for 24 hours. Permeable transwell inserts (Corning) were then placed into each well, upon which Caco-2 cells were seeded at 2 x 10^5 cells/ml. DMEM (2 ml) supplemented with 10% (v/v) FCS, 50 U/ml penicillin and 50 μg/ml streptomycin was then added to both the apical and basolateral chambers. Cells were then cultured for 14 days with a fresh media change taking place every 2 days. After this time the Caco-2 cells were sufficiently differentiated to form a confluent monolayer, complete with microvilli and tight junctions.

At 24 hours prior to iron uptake experiments being performed the culture media was removed and replaced with minimal essential media (MEM, Sigma) containing epidermal growth factor (20 mg/L), triiodothyronine (0.05 μM/L), PIPES (piperazine-N,N'-bis[2-ethanesulfonic acid]) (10mM/L), hydrocortisone (11 μM/L), sodium selenite (0.02 μM/L) and insulin (0.87 μM/L).

After the 24 hours period cells were then stimulated with media containing $^{59}FeCl_3$ (with or without Deferasirox at the concentrations specified within individual experiments) for 1 hour before it was removed and replaced with standard DMEM. The transwell inserts were finally removed 24 hours later and cells were washed twice with 2 ml Versene (0.2 g/L EDTA in PBS) before being lysed with RIPA buffer (as outlined previously). 200 μl of each lysate was subsequently removed and transferred to a scintillation tube where 2 ml of OptiPhase HiSafe scintillation fluid (Perkin Elmer) was added prior to reading on a beta/gamma counter. Counter readings were expressed as counts per minute (CPM) and normalised to sample protein content (using the protein assay as previously outlined).

2.2.12 Cell Cycle Analysis

Fluorescence-activated cell sorting (FACS) with propidium iodide (PI) labelling was utilised in order to determine treatment effect upon the cell cycle.

Cell lines were seeded into T25 flasks such that a confluence of 70% would be achieved at time of FACS. Cells were cultured as per the experimental conditions. Following treatment, the cells were trypsinised and centrifuged at 1500 rpm for 5 minutes. The cell pellet, following media aspiration, was washed by re-suspension in PBS containing 1% FCS (v/v) and then centrifuged at 1500 rpm for 5 minutes. Upon re-suspension, cells were adjusted to $1x10^6$ cells per 1 ml PBS. 1 ml of PBS containing cells was then vortexed whilst 1 ml of ice cold 95% ethanol (v/v) was added drop wise whilst to fix the cells. Cell suspensions were then stored at -20 ^{0}C prior to use.

Prior to preparing the cells for analysis, the following solutions were made up:
10x PI stock solution (0.5 mg/ml) – 0.5mg PI dissolved in 0.038 M sodium citrate (pH 7.0), covered and stored at 4 ^{0}C.
10 ml PI working solution (50 µg/ml) - 1ml PI stock solution, 100 µl 1 M TRIS (pH 7.5), 50 µl 1 M $MgCl_2$, 20 µl RNase A (20 mg/ml), 8.9 ml diethylpyrocarbonate (DEPC) H_2O, covered and stored at 4 ^{0}C.

For analysis, cells were centrifuged at 2000 rpm for 5 minutes and the supernatant aspirated. The pellet was washed in PBS and centrifuged at 2000 rpm and the supernatant aspirated for the final time. The pellet was then resuspended in 500 µl PI working solution, transferred to FACS tubes and incubated at 37 ^{0}C for 30 minutes in the dark. Cells were then gently vortexed immediately prior to being analysed on a Coulter® EPICS XL® analyser and Multicycler for Windows. Cells were sorted into G0-G1 and S-G2-M pools.

2.2.13 Mouse Models of Colorectal Tumourigenesis

A number of transgenic murine models of in-situ colorectal tumourigenesis were utilised in order to test drug effects upon intestinal phenotype and mouse survival.

The Villin-CreER^{+} Apc$^{fl/fl}$ mouse contains a lox-flanked APC allele on an oestrogen inducible Cre background. Following induction of the Cre recombinase with a single dose of intraperitoneal Tamoxifen (80 mg/kg), both copies of the APC gene are lost throughout the whole intestine (villus and crypt). As a result, a hyper-proliferative phenotype develops over the following 4 days where the normal crypt-villus architecture is distorted, such that crypt like cells occupy the vast majority of the crypt-villus axis. [201] Mice are taken on day 5 as they would become rapidly unwell if left beyond this. This model permits analysis of the effects of a single dose of a drug upon the intestinal phenotype through quantification of the number of mitotic figures and apoptotic bodies present within the crypts. [102]

Lgr5-CreER^{+} APC$^{fl/fl}$ mice are similar to Villin-CreER^{+} Apc$^{fl/fl}$ mice except that the Apc deletion which occurs post Tamoxfen induction (80 mg/kg intraperitoneal injection on 2 consecutive days) is solely within the intestinal stem cells. [202] Again, this represents a rapid model of intestinal tumorigenesis with an increase in crypt size seen and mice subsequently developing numerous adenomas within 50 days following Cre induction. [102] As this is a less aggressive model of intestinal tumorigenesis than the Villin-CreER^{+} Apc$^{fl/fl}$, it permits analysis of the effect of multiple doses of a drug on both intestinal phenotype and ultimately mouse survival (as used in this project).

Lgr5-CreER^{+} APC$^{fl/fl}$ Pten$^{fl/fl}$ mice also have an inducible deletion in the Pten tumour suppressor gene which becomes activated (along with the APC deletion) upon injection of a single dose of intraperitoneal Tamoxifen (80 mg/kg intraperitoneal x1). [203] This is a more aggressive model of

tumourigenesis than the Lgr5-CreER^{+} APC$^{fl/fl}$ as the superimposed Pten deletion permits the development of invasive adenocarcinomas. [203] Again, this model can be used to examine the effect of multiple doses of a drug on both intestinal phenotype and ultimately mouse survival (as used in this project).

Mice were gavaged Deferasirox as per the individual experimental conditions and all work was carried out under Home Office approved conditions.

2.2.14 Immunohistochemistry

Murine Tissue

Murine intestines (duodenum, small intestine and colon) were harvested immediately after the animal was culled. Guts were washed with tap water (using a 200 µl pipette tip and 5 ml syringe), opened longitudinally and placed on filter paper before being submerged in methacarn (4 parts methanol : 2 parts chloroform : 1 part acetic acid) for at least 4 hours. Following this period, the guts were rolled longitudinally in a proximal to distal intestinal direction and placed in formalin. Samples were then transferred to the University of Birmingham Human Biomaterials Resource Centre (HBRC) where they were embedded into paraffin blocks.

When required for immunohistochemistry, slides were sectioned at 5 µm intervals and applied to SuperFrost glass slides. Slides were dewaxed via submersion in xylene for 10 minutes (x2) before being hydrated in successive ethanol washes (2 x 5 minutes in 100% ethanol, 1 x 5 minutes in 95% ethanol, 1 x 5 minutes in 70% ethanol and 1 x 5 minutes in tap water).

Antigen retrieval was achieved via submersion of slides in dilute citrate buffer (27 mls of 21% (w/v) citric acid added to 123 mls of 2.9% (w/v) sodium citrate in a total volume of 1.5 L deionised water, ph 6) in a microwavable pressure cooker. Once the pressure had been optimised, the slides were removed from the pressure cooker and permitted to cool for 30 minutes at room temperature (whilst remaining in the citrate buffer).

Slides were then blocked for 20 minutes using Envision+ 2% (v/v) hydrogen peroxide solution prior to being washed x3 in PBS and then incubated for 45 minutes in 10% (v/v) normal goat serum.

The primary antibody (activated/cleaved caspase-3, 1 in 800 dilution with 1% BSA, rabbit polyclonal, R&D Systems, AF835; phospho-histone H3, 1 in 500 dilution with 1% BSA, rabbit polyclonal, Cell Signalling Technology, 9701) was then left on overnight at 4 ^{0}C.

Slides were then removed from the primary antibody and washed x3 in PBS before incubation with the secondary antibody (Envision+ labelled polymer HRP-conjugated) for 1 hour at room temperature. Slides were then washed again x3 in PBS.

Positive staining was visualised using the DAB+ chromogen (3,3´-diaminobenzidine tetrahydrochloride) in DAB substrate buffer (1 drop of chromogen : 1ml of solution substrate buffer), with approximately 200 µl applied to each slide for approximately 5 minutes. Slides were then washed x3 in PBS before being transferred to water.

Counterstaining was performed with 0.1% Mayer's haemotoxylin (for 30 seconds) prior to the slides being dehydrated in increasing concentrations of ethanol (1 x 2 minutes in 70% ethanol, 1 x 2 minutes in 95% ethanol, 2 x 2 minutes in 100% ethanol and finally 2 x 5 minutes in xylene). Slides were then mounted with Depex and a coverslip applied.

NB For haemotoxylin and eosin staining, slides are dewaxed and hydrated as previously described. Slides are then stained with 0.1% Mayer's hemotoxylin (for 30 seconds) prior to being rinsed in running tap water and then submersed in 0.3% acid alcohol (700 ml ethanol, 300 ml deionised water, 3 ml hydrochloric acid). Slides are then washed again in running tap water and submersed in Scott's tap water substitute (2 g sodium hydrogen carbonate, 20 g magnesium sulphate, 1 L deionised water) before being rinsed in tap water again and finally stained for 2 minutes in 1% eosin. Slides were then dehydrated and mounted as previously described.

Images were visualised from paraffin sections using a Nikon Eclipse E600 microscope and digital image captured using a Nikon DXM1200F camera (Surrey, UK). Nikon ACT-1 version 2.62 software was used for image acquisition (Surrey, UK).

Slides were analysed blindly and scored by expressing the total number of mitotic figures and apoptotic bodies per half crypt as a percentage of the total number of cells within that crypt (50 half crypts scored for each hematoxylin and eosin (H&E) stained slide). [102] For slides stained with cleaved caspase-3 and or phosphor-histone H3 antibodies the total number of positive cells per crypt (for 25 whole crypts) were expressed as a percentage of total cell number in the same crypt.

Human Tissue

Paraffin embedded sections from 32 patients with colorectal adenocarcinoma undergoing surgical resection were collated from archive and processed by the University of Birmingham Human Biomaterials Resource Centre (HBRC) for use in immunohistochemistry. Full ethical approval to use the samples was obtained by Dr Chris Tselepis, School of Cancer Sciences, University of Birmingham.

Slides were stained using automated Ventana® platforms (Roche) using the *Ultra*View Universal DAB Detection Kit (Roche) at Birmingham Heartlands Hospital. Antigen retrieval was carried out using the high pH, cell conditioning 1, setting for 64 minutes at 99 °C. Following treatment with Universal DAB inhibitor, containing 3% hydrogen peroxide solution, slides were incubated for 32 minutes at 37 °C with IRP2 primary antibody (Table 2.3). A secondary antibody multimer, active against mouse, goat and rabbit IgG and labelled with horseradish peroxidase was used to oxidise universal DAB+ chromogen detector. Between each stage, sections were washed by the Ventana platform and evaporation minimised by application of a liquid coverslip.

Following preparation, slides were independently scored by a Consultant Histopathologist based on intensity of staining (0- none, 1- mild, 2- moderate, 3-strong staining) and percentage of cells stained (0, 0-24%; 1, 25-49%; 2, 50-74%; 3-75-100%). The assigned values were then multiplied to give a total score for each section out of nine. [24] Chi-Square analysis was then performed using Minitab® 17.0 (Minitab Inc).

2.2.15 RNA Extraction and cDNA Generation

RNA extraction from frozen tissue

Matched frozen tumour and normal tissue obtained from 41 patients with colorectal adenocarcinoma undergoing resection was thawed on ice and homogenised in 750 µl Trizol reagent using a PolyTurrax homogeniser.

Samples were then incubated for 5 minutes at room temperature to allow complete dissociation of nucleoprotein complexes. 100 µl of chloroform was added and vortexed for 15 seconds and then incubated at room temperature for 15 minutes. Samples were then centrifuged at 12,000 g for 15

minutes at 4 °C and the upper aqueous phase harvested. RNA was precipitated by addition of 250 µl isopropanol and incubated for a further 10 minutes at room temperature. RNA was pelleted by centrifugation at 12,000g at 4 °C for 10 minutes and washed with 75% ethanol. The 75% ethanol was then aspirated and the residual volume allowed to evaporate followed by RNA re-suspension in 10 µl of nuclease free water. Optical density of the re-suspended RNA was measured at 260 nm on a spectrophotometer and the concentration of RNA calculated using the equation 1 OD unit= 40 µg/ml RNA. RNA was stored at -80 °C.

RNA extraction from cells

Cells were cultured in 6 or 96 well plates as per experimental conditions. Following removal of media, cells were washed twice with filter sterilised PBS and 100 or 500 µl Trizol was added to each well of 96 or 6 well plates respectively. Cells were incubated for 10 minutes at room temperature before aspirating well contents; samples were stored at -20 °C until use and then processed for RNA as per tissue samples.

cDNA Generation

cDNA was synthesized from RNA using a reverse transcription system (Eurogentec). A Nanodrop-1000 spectrophotometer (Thermo Scientific) was used to determine the mRNA concentration of samples extracted from Trizol. 1 µg RNA was used per sample, dissolved in a total volume of 14 µl nuclease free water. 6 µl of SuperScript®VILO® mastermix (4 µl 10x SuperScript®Enzyme mixed with 2 µl of 5x VILO™ Reaction Mix) (Invitrogen™) was added to each sample. Samples were run on a thermal cycler (MyCycler®, Bio-rad) at 25 °C for 10 minutes, 42 °C for 60 minutes and 85 °C for 5 minutes before storage at -20 °C.

2.2.16 qRT-PCR

TaqMan® Gene Expression Assays (Applied Biosystems®) were used to detect IRP2 and TfR1 mRNA expression. Master-mixes comprised 0.04 µl ROX solution 25 µM (Bioline Reagents Ltd), 7.5 µl SensiMix® II Probe (SensiMix® II Probe Kit (Bioline Reagents Ltd)), 1 µl of TaqMan® probe, 0.075 µl 18s yy probe 6.5 µM (Eurogentec), 0.15 µl 18s primer mix 10 µM (Eurogentec) and 5.235 µl nuclease free water per reaction. 14 µl was added to 1 µl template in separate wells of a 96 well plate; the plate was then sealed and centrifuged at 1200 rpm for 2 minutes prior to reading. PCR was carried out using ABI FAST Realtime PCR and 7500 RT PCR Systems (both Applied Biosystems®) using the following cycle: 50 °C for 2 minutes, 95 °C for 10 minutes, 40 repeats of 95 °C for 15 seconds and 60 °C for 1 minute**.** All experiments were carried out in triplicate.

Cycle threshold (ct) values were normalised relative to 18s control to give dCt. Fold changes relative to control were calculated based on 2^{-ddCt} (where ddCt is dCT of cancer minus dCT of normal for each pair) and statistical analysis of differences between groups performed as appropriate.

2.2.17 IRP2 siRNA 'Knockdown'

Cells were seeded at $5x10^4$/ml in 96 well plates or $5x10^5$/ml in 6 well plates. IRP2 Silencer®siRNA (Life Technologies®, sequence: (5'-3') GGAACAUUUUCUUCGCAGAtt; antisense UCUGCGAAGAAAAUGUUCCtg) was re-suspended in nuclease free water to create a 100 µM stock solution. A 10 µM working stock was made using nuclease free water immediately prior to use. siRNA and lipofectamine®2000 were diluted in Opti-MEM® Medium (Gibco®, Life Technologies®) before being combined to give a final concentration of 20 pmol SiRNA to 6 µl lipofectamine per 100 µl and left for 5-10 minutes at room temperature. 10 µl or 250 µl of working solution was then added to cells in a 96 or 6 well plate respectively. Cells were harvested at 24 hours.

Silencer® Select Negative Control siRNA #1 was prepared in exactly the same way and used as a control in all experiments.

All ddCt values were calculated relative to negative control SiRNA. Expression levels were compared by conducting statistical analysis on 1 divided by the average dCT value for each group.

2.2.18 Preparation of B-raf V600E Inducible Cell Lines

A construct containing a B-Raf V600E mutation was successfully created and transfected into HCT116 colorectal adenocarcinoma cell lines. In short, a doxycycline-inducible HA epitope-tagged B-Raf V600E cDNA was constructed in a puromycin resistant pTIPZ lentiviral vector using a pEF-myc-B-Raf^{V600E} construct kindly donated by Dr Richard Marais (Institute of Cancer Research, London, United Kingdom).

Following PCR amplification of B-Raf^{V600E} from pEF-myc-B-Raf^{V600E} using primers encoding a HA-epitope tag at the N-terminus the PCR product was digested with Sbf1 and Asc1 restriction enzymes and ligated into pTIPZ lentiviral vector which had also been cut at the same sites. Samples were transformed into competent bacteria by heat shock before plating on agar plates containing 100 μg/ml ampicillin and incubation at 32 ^{0}C overnight. Bacterial clones were inoculated into broth and grown overnight at 37 ^{0}C and 150 rpm before isolation of pTIPZ plasmid DNA using a Qiagen Miniprep kit. Successful ligation of the vector and B-Raf V600E insert was confirmed through gel electrophoresis (1% agarose gel) following Sbf1/Asc1 diagnostic digest. Positive clones were sent for DNA sequencing to definitively confirm the presence of the correct HA-B-Raf V600E insert.

pTIPZ HA-B-Raf V600E and a control empty pTIPZ vector (EV) were delivered into the HCT116 colorectal cell line via lentiviral infection. Lenti-viruses were manufactured by 293T cells following

transfection of the pTIPZ HA-B-Raf V600E and pTIPZ EV constructs with viral packaging plasmids. Viral supernatant from transfected HEK293T cells was collected two days later and diluted 1:1 with normal growth media. The target HCT116 cells were seeded into 6 well plates at a concentration of $4x10^5$ cells per well 24 hours prior to the infection. On the day of infection, the standard media was aspirated from each well and replaced with viral supernatant. The plates were incubated at 37°C for 12-18 hours before the viral media was aspirated and replaced with standard media containing antiobiotic selection. The pTIPZ plasmid contains a puromycin resistant gene to allow for selection of virus infected cells. Selection of infected HCT116 cells was achieved with 0.5 µg/ml of puromycin in standard growth media.

Following successful outgrowth of puromycin resistant cells a doxycycline dose response curve was performed and Western blotting carried out in order to confirm increasing HA-B-Raf V600E expression with increasing doxycycline concentration.

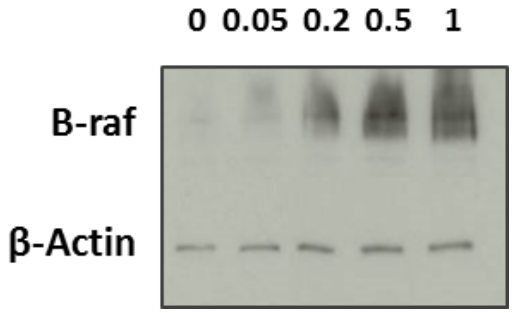

Figure 2.1 HCT116 V600E doxycycline dose response curve

Western blot demonstrating increasing B-raf expression with increasing concentration of doxycycline. Cells were incubated for 48 hours, lanes indicate doxycycline concentration in µg/ml.

2.2.19 Sulforhodamine Colorimetric (SRB) Assay

The SRB cytotoxicity assay permits cell density determination through quantification of cellular protein content. [204] Cells were seeded into 96 well plates at an approximate density of $5x10^4$/ml and treated as per the experimental conditions outlined. At the end of the experimental period cells were fixed through the addition of 20 µl 20% trichloroacetic acid (w/v) and incubated at 4 ^{0}C for 30 minutes. The excess solution was then removed from each well and the plates washed x3 with deionised water before being left to dry for at least 2 hours at room temperature. 100 µl of 0.4% SRB was then added per well and left for 10 minutes at room temperature before the SRB was removed and the wells washed using 1% acetic acid (v/v). The plates were then left again to dry for several hours, before 200 µl of 50 mM Tris solution (pH 8.8) was added to each well to dissolve the SRB crystals. Once all crystals had fully dissolved, the absorbance was read at 510 nm using a microplate reader.

Values were expressed as a fold change relative to the control group's mean absorbance (normalised to 1).

2.2.20 Statistical Analysis

Analyses of data were performed using Minitab 17.0 (Minitab Inc. 2013) and Microsoft Excel 2010 (Microsoft 2010). Kolmogorov-Smirnov testing was performed to ascertain if data conformed to the normal distribution. Normally distributed data was then analysed using Student's T-test and non-parametric data analysed using the Mann-Whitney U test or the 1-sample Wilcoxon test as appropriate. Comparison between categorical variables was made using the Chi-squared test and formal correlation assessed with Spearman's Rank co-efficient. Significance was accepted at α-level

of 5% ($p \leq 0.05$) and all data means presented with ± standard error of the mean (SEM). Where shown, univariate and multivariate analyses were performed using Strata 12.1 (Stata Corp LP®).

Chapter 3. A Role for Deferasirox as an Anti-neoplastic and Chemosensitising Agent in Oesophageal Carcinoma

3.1 Introduction

Carcinoma of the oesophagus is an increasingly significant cause of morbidity and mortality. In 2008 alone there were approximately 482,300 new cases worldwide and the disease was responsible for over 400,000 deaths. [205] In the United Kingdom, overall 5 year survival rates remain around 13% as most patients have advanced disease on presentation meaning that only around 25% can undergo potentially curative surgical resection. [14, 206, 207]

There are two main histological types of oesophageal carcinoma; squamous cell carcinoma (SCC) and oesophageal adenocarcinoma (OAC). Of note, there is now an emerging body of evidence implicating iron in the development and propagation of OAC. [119, 129, 208, 209, 210, 211]

Data from a number of human studies identifies a positive association between increased intake of heme iron from red meat and OAC risk. [124, 212, 213, 214] Of note, a higher intake of haem iron (quartile 4 versus quartile 1 for intake) from meat sources was associated with an odds ratio of 3.04 (95% confidence interval 1.2-7.72) for the development of OAC in one population-based case-control study. [124] Furthermore, in terms of specific daily intake of red meat, a 2013 meta-analysis demonstrated an increased relative risk for OAC of 1.45 (95% confidence interval 1.09-1.93) per 100 g/day increase in red meat intake. [212]

In further support of an association between iron and OAC, the conversion of BM into OAC has been shown to be associated with increased cellular iron loading and overexpression of the cellular iron import proteins DMT1 and TfR1 in human tissue samples. [24] Excess iron has also been shown to

exacerbate OAC tumourigenesis in animal models and cause an increase in OAC cell line proliferation *in-vitro*. [24, 82, 129] All of these associations are not entirely surprising, since iron is essential for a number of key cellular processes including DNA synthesis, ATP generation and cell cycle progression; all activities that are increased in cancer. [112]

Iron chelating agents have demonstrated anti-neoplastic effects in a number of previous studies. [80, 92] To date, however, the majority of this data has been derived from experimental iron chelators which possess a number of potential side effects and remain unlicensed for human use. [139]

A number of licensed iron chelators are already in routine clinical use, however, albeit limited to the treatment of iron overload associated with conditions such as β-thalassaemia and multiple blood transfusions. Of these, the orally administered iron chelator Deferasirox® (Novartis, Switzerland) has shown promise as an anti-neoplastic agent in a number of pre-clinical studies and anecdotal case reports of clinical experience. [167, 169, 170, 171, 172, 175, 177] Of note, a recent paper from our group demonstrated that Deferasirox can inhibit cellular iron uptake (by as much as 20-50%) and reduce intracellular iron levels in oesophageal cancer both *in-vitro* and *in-vivo*. [215]

Interestingly, Deferasirox appears to have an increased efficacy against malignant cells (compared to their 'normal' counterparts) and may achieve its anti-neoplastic effects via a number of different mechanisms (not merely just iron deprivation by chelation alone) including inhibition of the nuclear factor kappa-light-chain-enhancer of activated B cells (NFκB) signalling pathway (which is known to be dysregulated and influence response to therapy in OAC). [175, 177, 216, 217, 218]

The efficacy of Deferasirox in oesophageal malignancy (particularly OAC) is therefore worthy of further investigation.

3.2 Chapter Aims

The value of licensed iron chelators and in particular the orally administered agent Deferasirox in oesophageal carcinoma have not been fully addressed, thus the aims of this chapter are:

1. To assess the efficacy of the licensed oral iron chelator Deferasirox as an anti-neoplastic agent in oesophageal carcinoma (*in-vitro* and *in-vivo*).
2. To assess the efficacy of the licensed oral iron chelator Deferasirox as a chemosensitising agent in oesophageal carcinoma (*in-vitro* and *in-vivo*).
3. To assess the effect of the licensed oral iron chelator Deferasirox on the NFκB signalling pathway in oesophageal carcinoma.
4. To assess the iron status of patients presenting with oesophageal adenocarcinoma in order to determine suitability for a future trial of Deferasirox in humans.

3.3 Results

3.3.1 The efficacy of Deferasirox as an anti-neoplastic agent in oesophageal carcinoma *in-vitro*

3.3.1.1 Overview

The OAC cell lines OE19 and OE33 and the SCC cell line OE21 were seeded into 96 well plates and cultured in media with or without Deferasirox at varying doses (0-40 μM) for 24, 48 and 72 hours. Cells were counted and seeded ($4x10^4$/ml following optimisation) such that an approximate confluence of 70% was achieved in the control group (0 μM Deferasirox) at time of assay.

After the defined time points, MTT assays were performed in order to determine cellular viability (as previously outlined) relative to the control group.

3.3.1.2 Results

Following 24 hours incubation, Deferasirox did not reduce cellular viability across any of the oesophageal cell lines tested (Figure 3.1). Indeed, at doses of 2 (OE19 and OE21), 10 (OE19 and OE21) and 20 μM (OE21) a statistically significant increase in MTT readout was actually seen. This enhancement in viability, however, did not persist in any of the cell lines beyond 24 hours.

By 48 hours, Deferasirox had significantly reduced cellular viability at concentrations of 10-40μM. The largest reduction in viability seen was 57.5% at 40 μM in the OE19 OAC cell line (38.1 and 50.0% at the same concentration in the OE33 and OE21 lines respectively, all $p<0.05$ vs. control).

At 72 hours, 40μM Deferasirox had significantly reduced cellular viability by 73.2, 58.4 and 69.2% in the OE19, OE33 and OE21 cell lines respectively (all $p<0.05$ vs. control).

Across all 3 cell lines tested, the approximate IC50 of the drug equated to 40 μM at 48 hours and 20 μM at 72 hours.

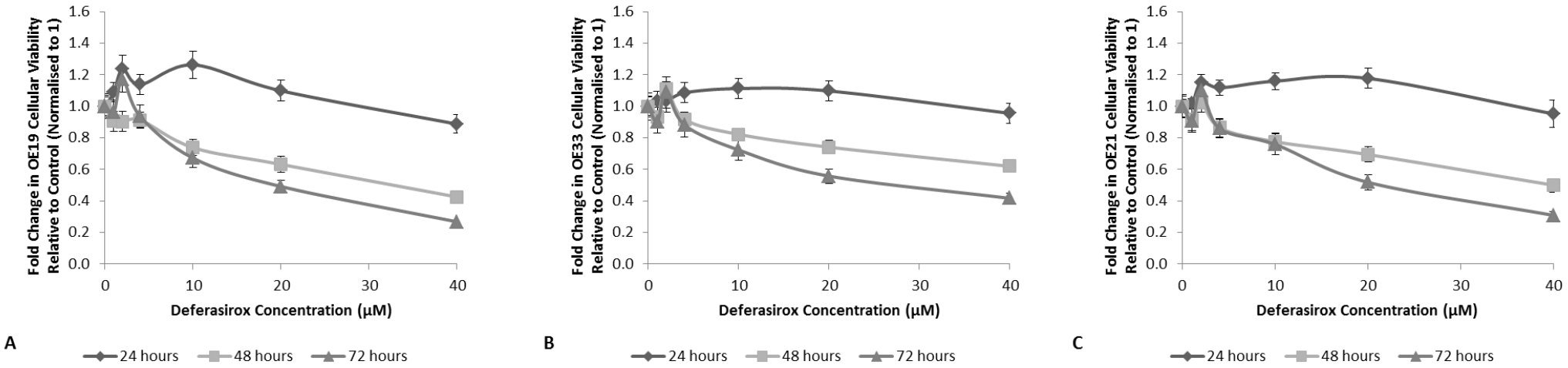

	OE19			OE33			OE21		
Deferasirox (µM)	**24**	**48**	**72**	**24**	**48**	**72**	**24**	**48**	**72**
1	0.307	0.347	0.724	0.688	0.444	0.392	0.755	0.420	0.357
2	0.037	0.339	0.120	0.728	0.204	0.508	0.032	0.803	0.238
4	0.127	0.357	0.527	0.330	0.308	0.319	0.082	0.156	0.115
10	0.019	0.008	0.001	0.212	0.022	0.016	0.025	0.018	0.014
20	0.282	0.000	0.000	0.278	0.002	0.000	0.030	0.001	0.000
40	0.188	0.000	0.000	0.617	0.000	0.000	0.623	0.000	0.000

D

Figure 3.1 Deferasirox decreases OAC and SCC cellular viability *in-vitro*

The OAC cell lines OE19 (A) and OE33 (B) and the SCC cell line OE21 (C) were co-cultured alongside increasing doses of Deferasirox (as specified) for a period of 24-72 hours. Deferasirox did not suppress cellular viability within the first 24 hours of incubation, however, it did cause a significant reduction in cell viability across all 3 cell lines in a time and dose dependent manner beyond the 48 hour time point. Data presented as mean fold change relative to standard media control normalised to 1, error bars denote ±SEM, p values for corresponding fold changes are shown in (D) where shaded boxes represent $p<0.05$.

3.3.2 The efficacy of Deferasirox as a chemosensitising agent in oesophageal carcinoma *in-vitro*

3.3.2.1 Overview

The chemotherapy regimen of Epirubicin, Cisplatin and 5- Fluorouracil (ECF) is typically used in the treatment of OAC and SCC with variable results. [41] Cellular viability (MTT) and proliferation (BrdU) assays were performed in order to assess whether pre and or concomitant treatment with Deferasirox (20 or 2 μM) could enhance the efficacy of this regimen.

Various treatment combinations (as outlined in Table 3.1) were administered to OE19, OE21 and OE33 cells over 24-72 hours before MTT and BrdU assays were performed (as previously outlined) to assess cellular viability and proliferation respectively.

Table 3.1 Treatment regimens applied to cells for the ECF combination chemotherapy experiment

Regimen	Day 2 (24 hours)	Day 3 + 4 (48-72 hours)
1	Control media	Control media
2	Control media	ECF
3	Deferasirox	ECF
4	Control	Deferasirox + ECF
5	Deferasirox	Deferasirox + ECF
6	Deferasirox	Control media
7	Control media	Deferasirox
8	Deferasirox	Deferasirox

Deferasirox was used at a concentration of 20 or 2 μM. Epirubicin, Cisplatin and 5-Fluorouracil were used at their pre-determined IC25 of 0.5, 4 and 4 μM respectively. MTT (viability) and BrdU (proliferation) assays were performed after 72 hours treatment in total.

3.3.2.2 Results

All 3 of the oesophageal cell lines tested demonstrated a marked and highly significant sensitivity to 48 hours of treatment with ECF therapy in terms of both viability and proliferative activity (mean reduction of 46.4 and 64.0% in viability and proliferation respectively across all 3 cell lines, Figure 3.2). Despite this, pre-incubation with 20 μM Deferasirox for 24 hours prior to the ECF alone for the following 48 hours further reduced cellular viability and proliferation across all 3 cell lines compared to ECF alone (mean additional reduction of 28.2 and 25.0% on MTT and BrdU respectively). Interestingly, pre-treatment with the lower dose of 2 μM Deferasirox also resulted in a significantly enhanced reduction in OE19 and OE21 cellular viability and OE19, OE33 and OE21 cellular proliferation compared to ECF alone.

Of note, at both of the Deferasirox concentrations tested, there was no additional statistical advantage in continuing the chelator alongside ECF in any of the cell lines after it had already been given as a pre-treatment (Deferasirox/Deferasirox+ECF). Likewise, there also appeared to be no additional advantage in giving Deferasirox alongside ECF (Control/Deferasirox+ECF) to the OAC cell lines at either of the doses tested. This was not the case in OE21 SCC cell line, however, where an additional reduction in cellular viability of 24.5 and 17.6% was seen with 20 and 2 μM Deferasirox respectively.

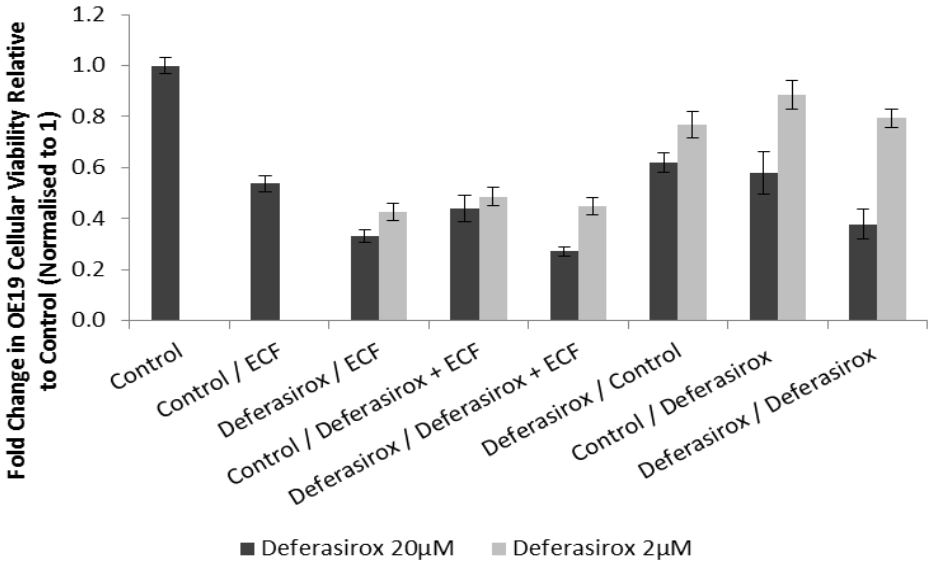

A

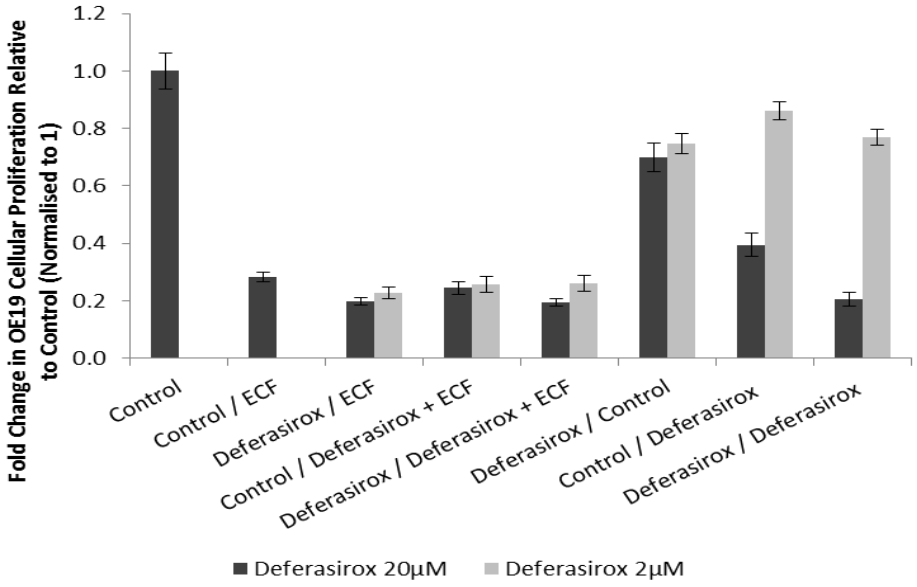

B

OE19					
Treatment		Deferasirox 20µM		Deferasirox 2µM	
1st 24 hours	2nd 48 hours	Viability	Proliferation	Viability	Proliferation
Control	Control	1.000	1.000	1.000	1.000
Control	ECF	0.536 *	0.282 *	0.536 *	0.282 *
Deferasirox	ECF	0.332 * #	0.197 * #	0.425 * # $	0.227 * # $
Control	Deferasirox + ECF	0.439 *	0.244 *	0.486 * $	0.257 * $
Deferasirox	Deferasirox + ECF	0.270 * #	0.193 * #	0.447 * # $	0.261 * $
Deferasirox	Control	0.619 * $	0.698 * # $	0.769 * #	0.747 * #
Control	Deferasirox	0.578 *	0.394 * # $	0.883 #	0.861 # $
Deferasirox	Deferasirox	0.377 * #	0.204 * #	0.793 * #	0.768 * #

C

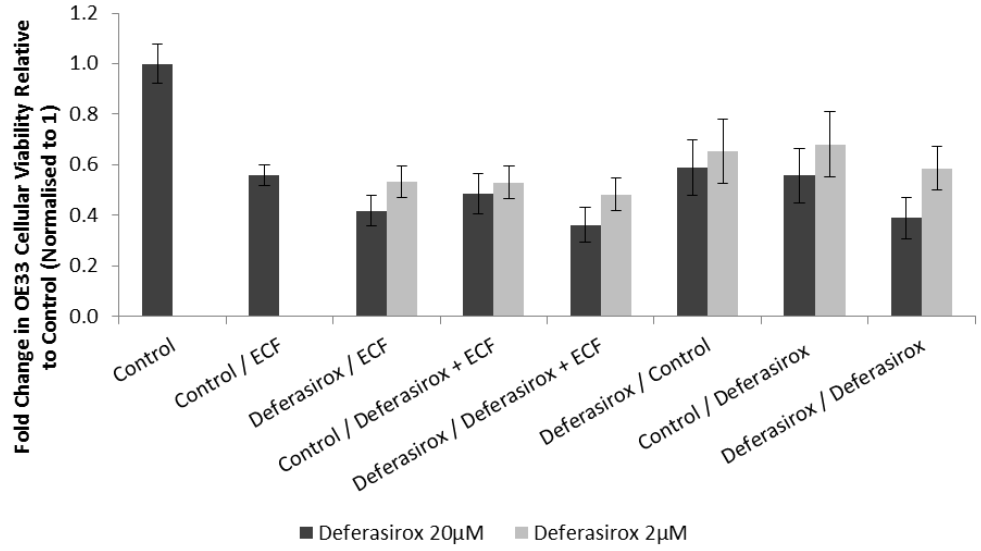

D

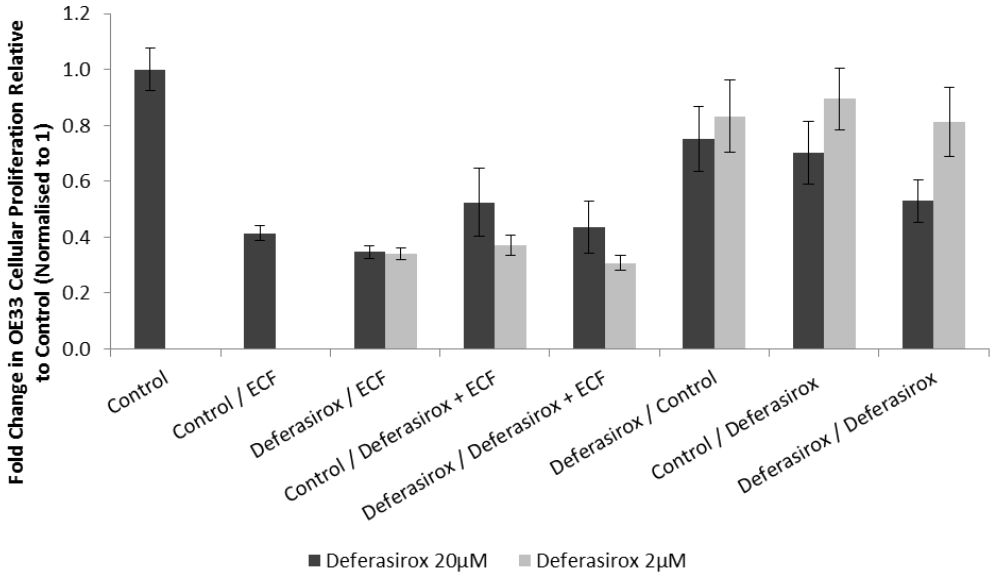

E

OE33					
Treatment		Deferasirox 20µM		Deferasirox 2µM	
1st 24 hours	2nd 48 hours	Viability	Proliferation	Viability	Proliferation
Control	Control	1.000	1.000	1.000	1.000
Control	ECF	0.561 *	0.414 *	0.561 *	0.414 *
Deferasirox	ECF	0.417 * #	0.347 * # $	0.534 *	0.339 * # $
Control	Deferasirox + ECF	0.486 *	0.525 *	0.530 *	0.369 * $
Deferasirox	Deferasirox + ECF	0.363 * #	0.436 *	0.483 *	0.308 * # $
Deferasirox	Control	0.589 *	0.751	0.654 *	0.833 #
Control	Deferasirox	0.557 *	0.701 * #	0.681	0.894 #
Deferasirox	Deferasirox	0.389 *	0.529 * #	0.586 *	0.811 #

F

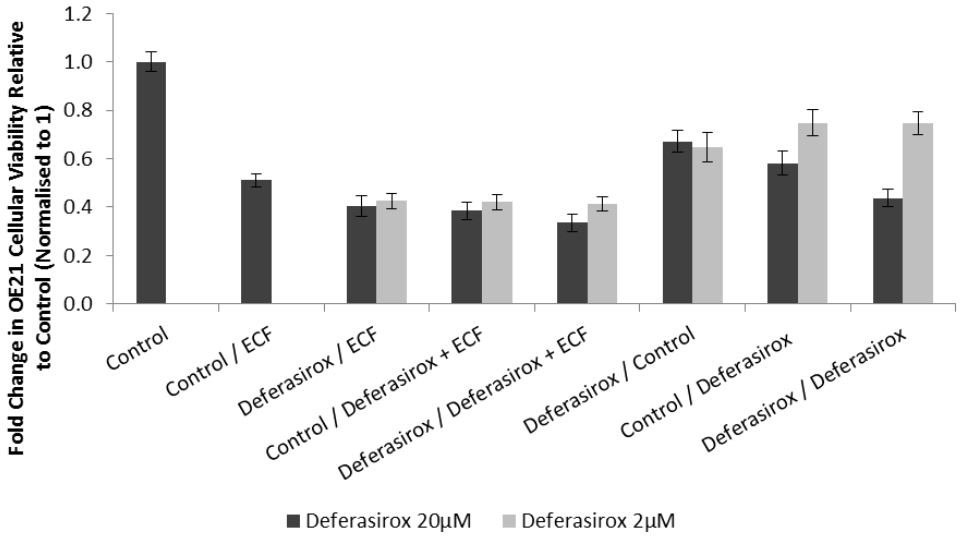

G

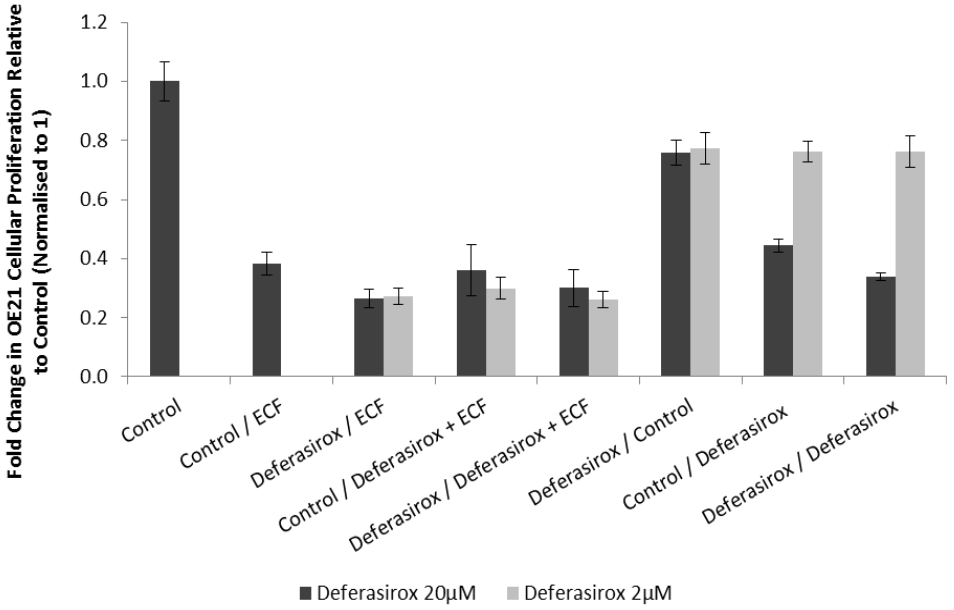

H

OE21					
Treatment		Deferasirox 20µM		Deferasirox 2µM	
1st 24 hours	2nd 48 hours	Viability	Proliferation	Viability	Proliferation
Control	Control	1.000	1.000	1.000	1.000
Control	ECF	0.510 *	0.383 *	0.510 *	0.383 *
Deferasirox	ECF	0.405 * #	0.265 * #	0.425 * # $	0.273 * # $
Control	Deferasirox + ECF	0.385 * #	0.361 *	0.420 * # $	0.300 * $
Deferasirox	Deferasirox + ECF	0.335 * #	0.300 *	0.412 * # $	0.262 * # $
Deferasirox	Control	0.672 * # $	0.759 * # $	0.647 *	0.773 * #
Control	Deferasirox	0.581 * $	0.444 * $	0.748 * #	0.762 * #
Deferasirox	Deferasirox	0.438 *	0.338 *	0.747 * #	0.761 * #

I

Figure 3.2 Pre-treatment of OAC and SCC cell lines with Deferasirox can enhance subsequent response to chemotherapy with ECF *in-vitro*

OE19 (A-C), OE33 (D-F) and OE21 (G-I) cell lines were subjected to various treatment regimens (as outlined) for a total period of 72 hours prior to cellular viability (MTT) and proliferation (BrdU) assays being performed. The chemotherapy regimen of Epirubicin, Cisplatin and 5-Fluorouracil (ECF) was utilised, comprising each of the constituent drugs at their pre-determined IC25. The addition of Deferasirox for 24 hours as a pre-treatment before ECF administration significantly enhanced the reduction in cellular viability and proliferation seen, even at the lower dose of 2 μM Deferasirox.

Data presented as mean fold change relative to standard media control normalised to 1, error bars denote ±SEM, treatment given for first 24 hours indicated prior to / and treatment given for subsequent 48 hours indicated post /. Corresponding fold changes shown in (C), (F) and (I) where * denotes $p<0.05$ vs. control, # $p<0.05$ vs. control/ECF and $ $p<0.05$ vs. Deferasirox/Deferasirox.

As expected, administration of Deferasirox alone at a concentration of 20 μM (for a total of 72 hours) resulted in a significant reduction in both cellular viability and proliferation across all of the lines tested that was at least comparable to 48 hours of ECF alone. In the OE19 OAC cell line, Deferasirox monotherapy for 72 hours was actually statistically more efficacious that ECF alone, this was not the case, however, in either the OE33 or OE21 cell line.

Of note, Deferasirox monotherapy at 20 μM for 72 hours was broadly statistically comparable to the Deferasirox/ECF pre-treatment regimen in terms of the effect on both cellular viability and proliferation. This was not the case, however, with the lower Deferasirox dose of 2 μM, where, as would be expected, monotherapy was broadly significantly less efficacious than both ECF alone and the Deferasirox/ECF pre-treatment regimen.

Interestingly, unlike in the previous experiment (Figure 3.1, page 92) where Deferasirox concentrations of 20 μM (OE21) and 2 μM (OE19 and OE21) for 24 hours did show stimulatory activity, this was not seen in this experiment in any of the cell lines tested. This may be related to the timing of assay, as in the previous experiments the assay was performed immediately after the 24 hour time period, whereas in this series of experiments the drug was removed and replaced with standard media at 24 hours but the assay was not performed until 72 hours in total had passed. This indicates Deferasirox may still have an effect on cell viability and proliferation even after its removal.

3.3.3 The ability of Deferasirox to overcome established chemotherapy resistance in oesophageal carcinoma *in-vitro*

3.3.3.1 Overview

In order to assess whether Deferasirox therapy may be effective in overcoming established chemotherapy resistance (both as monotherapy and in combination with existing agents), a Cisplatin resistant 'clone' of OE33 OAC cells was created by co-culturing them alongside progressively increasing doses of the drug over several months. In addition, the Cisplatin resistant TE4 oesophageal SCC line was also utilised. [192]

For experiments, cells were again seeded into 96 well plates and cultured alongside standard media, media containing Cisplatin, media containing Deferasirox and Cisplatin and media containing Deferasirox alone for 72 hours. MTT assays (as previously described) were utilised to determine cellular viability after 72 hours of treatment.

3.3.3.2 Results

The OE33 OAC 'clone' cell line demonstrated Cisplatin resistance up to 2 μM at 72 hours (Figure 3.3A). The cell line retained sensitivity to 20 μM Deferasirox alone (9% reduction in viability, $p<0.05$ vs. control), however, the drug appeared less efficacious than when used at an equivalent dose in the parental oesophageal cell line in previous experiments (sections 3.3.1 and 3.3.2). When Deferasirox (20 μM) and Cisplatin (2 μM) were given in combination, however, a highly significant 39.8% reduction in cellular viability was seen. This was statistically significant ($p<0.05$) compared to control and both Cisplatin and Deferasirox alone. A similar reduction in cellular viability (40%) was seen when Deferasirox was given in combination with the higher dose of 4 μM Cisplatin.

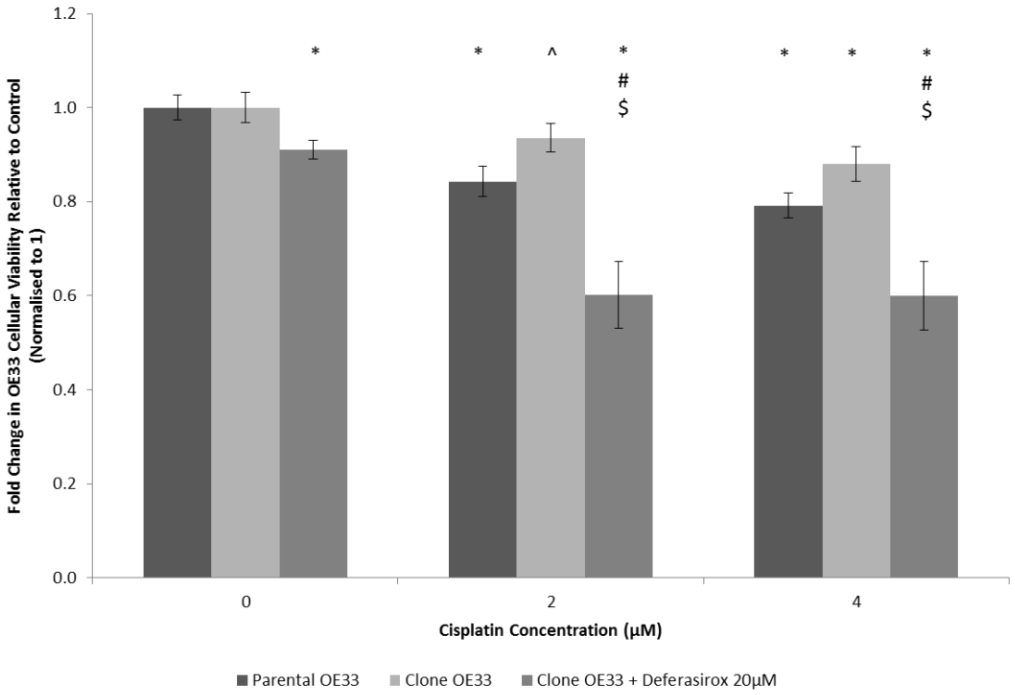
Fold Change in OE33 Cellular Viability Relative to Control (Normalised to 1)
1.2
1.0
0.8
0.6
0.4
0.2
0.0
* * ^ * * * * * * # $ # $
0 2 4
Cisplatin Concentration (µM)
Parental OE33
Clone OE33
Clone OE33 + Deferasirox 20µM

A

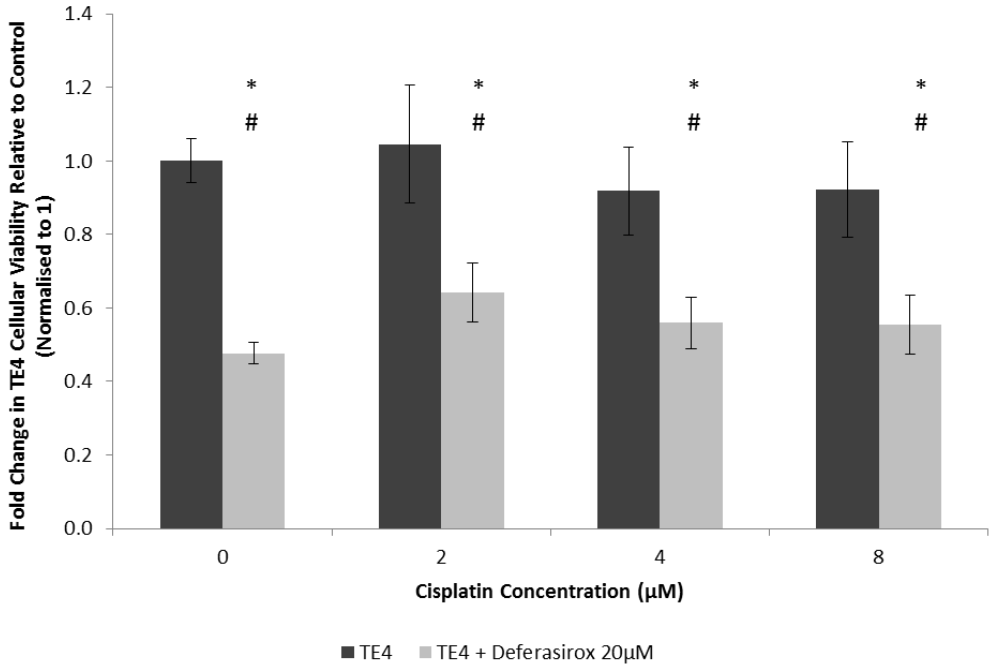
Fold Change in TE4 Cellular Viability Relative to Control (Normalised to 1)
1.4
1.2
1.0
0.8
0.6
0.4
0.2
0.0
* * * * # # # #
0 2 4 8
Cisplatin Concentration (µM)
TE4
TE4 + Deferasirox 20µM

B

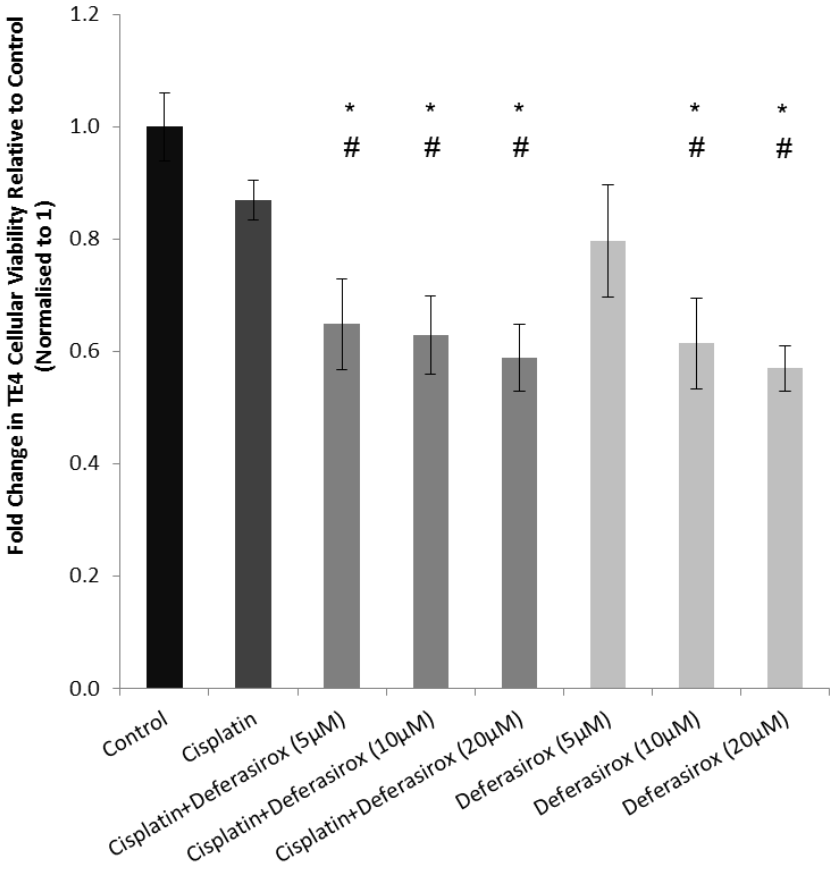

C

Figure 3.3 Treatment with Deferasirox can overcome established Cisplatin resistance in OAC and SCC cell lines *in-vitro*

Cell viability assay (MTT) demonstrating ability of Deferasirox to overcome Cisplatin resistance when given alone and or alongside Cisplatin at the concentrations specified to a 'clone' OE33 cell line (A) and the TE4 SCC cell line (B and C). Data shown represent mean fold change relative to standard media (normalised to 1), error bars denote ±SEM, *p<0.05 vs. control, # p<0.05 vs. equivalent dose of Cisplatin, $ p<0.05 vs. equivalent Deferasirox alone, ^ p<0.05 vs. parental cell line. Cisplatin utilised at specified concentrations apart from in C, when used at 2 μM throughout.

As expected, the TE4 cell line demonstrated no significant reduction in cellular viability when treated with Cisplatin alone (up to a concentration of 8 μM, Figure 3.3B). Again, however, Deferasirox alone (20 μM) significantly reduced viability by 52.3% compared to control. Interestingly, in this cell line, there was no additional effect seen by giving Deferasirox (20 μM) alongside any of the Cisplatin doses tested (2, 4 and 8 μM). A significant combinatorial reduction in cellular viability (35.2%) was seen, however, when a sub-therapeutic dose of Deferasirox (5 μM) was combined with low dose, sub-therapeutic Cisplatin (2 μM, Figure 3.3C).

3.3.4 Deferasirox as an anti-neoplastic and chemosensitising agent in a murine xenograft model of oesophageal adenocarcinoma

3.3.4.1 Overview

In order to assess the potential for Deferasirox to act as an anti-neoplastic and or chemosensitising agent *in-vivo* (and validate our previous *in-vitro* findings) a murine xenograft model using OE19 OAC cells was created.

Briefly, suspensions of OE19 cells (1 x 10^7 cells) were centrifuged and re-suspended in 50 μL of culture media. Immediately prior to injection, the cell slurry was mixed 50/50 (v/v) with Matrigel (extracellular matrix). The cell suspension was then subcutaneously injected into NOD-SCID mice (100 μl per mouse under general anaesthesia) and following a period of tumour establishment, mice were divided into groups and given one of 6 treatment regimens:

1. Control vehicle
2. Deferasirox alone (20 mg/kg on alternate days for 3 weeks via oral gavage)
3. Cisplatin alone (0.75 mg/kg every 3rd day for 3 weeks by intra-peritoneal injection; a pre-determined sub-optimal dose)
4. Deferasirox (20 mg/kg on alternate days) and Cisplatin (0.75 mg/kg every 3rd day) in combination for 3 weeks
5. Deferasirox (20 mg/kg) alone on alternate days for 1 week followed by 3 weeks of Cisplatin treatment alone (0.75 mg/kg every 3rd day)
6. Deferasirox (20 mg/kg) alone on alternate days for 1 week (commenced at the same time as 5.) followed by no further treatment during the experimental period

The vehicle for gavage consisted of 30% 1,2-propanediol/70% sterile 0.9% sodium chloride solution; Cisplatin was dissolved in sterile distilled water. Following treatment, mice were anaesthetised and exsanguinated by direct cardiac puncture and blood/plasma retained for full blood count and biochemical analysis (urea, creatinine and serum iron). Tumours were removed and weighed to assess tumour burden. All work was carried out under Home Office approved conditions.

3.3.4.2 Results

Deferasirox administration alone on alternate days for 3 weeks resulted in a significantly smaller final xenograft size compared to the control group (83.5% reduction, 35.5 mg vs. 214.9 mg, p=0.032) without any effect on haemoglobin, serum iron or creatinine levels (Figure 3.4). At the dose used, Cisplatin alone for 3 weeks also reduced xenograft size although this failed to reach the threshold for statistical significance (68.0 mg vs. 214.9 mg, p=0.064).

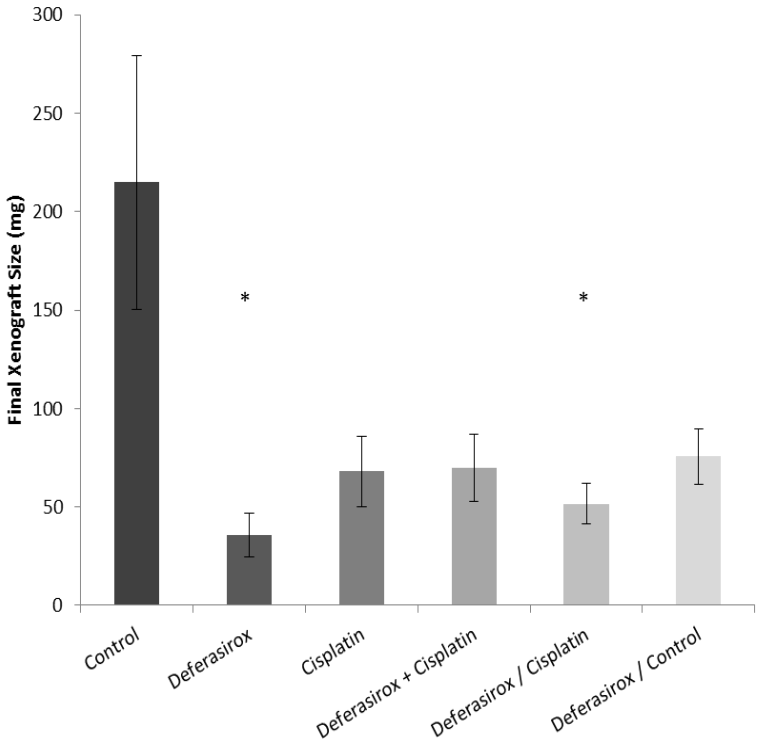

A

Treatment Group	Final Animal Weight (mg)	Final Haemoglobin (g/dL)	Serum Iron (µM/L)	Serum Creatinine (µM/L)
Control	26.77 (± 2.51)	10.93 (± 0.59)	39.06 (± 2.15)	35.83 (± 0.62)
Deferasirox	24.38 (± 1.21)	10.54 (± 1.88)	42.25 (± 4.46)	38.54 (± 1.26)
Cisplatin	24.22 (± 0.87)	9.81 (± 0.89)	42.80 (± 2.38)	36.40 (± 0.69)
Deferasirox + Cisplatin	24.40 (± 1.32)	10.76 (± 0.64)	46.04 (± 2.65)	36.02 (± 0.62)
Deferasirox / Cisplatin	25.84 (± 1.59)	11.30 (± 0.55)	40.70 (± 3.69)	38.18 (± 0.62) *
Deferasirox / Control	26.59 (± 2.17)	11.31 (± 0.95)	43.18 (± 2.13)	37.42 (± 0.44)

B

Figure 3.4 Deferasirox significantly reduces murine OE19 xenograft size when administered orally for 3 weeks

Deferasirox (20 mg/kg) given orally on alternate days for 3 weeks resulted in a significantly smaller xenograft size relative to control (83.5% reduction, p=0.032, (A)). Pre-treatment of mice with oral Deferasirox for just 1 week followed by 3 weeks of Cisplatin therapy (0.75 mg/kg) administered intra-peritoneally every third day also resulted in a significantly smaller xenograft relative to control (75.9% reduction, p=0.044), however, this was not significantly smaller than the group given Cisplatin alone (23.9% reduction relative to Cisplatin alone, p=0.455). Deferasirox was well tolerated by the mice as indicated by the parameters shown in (B) (error bars denote ±SEM, *p<0.05 vs. control).

The combination of Deferasirox with Cisplatin for 3 weeks did not improve tumour response compared to either control, Cisplatin alone or Deferasirox alone (69.9 mg Deferasirox + Cisplatin vs. 214.9 mg control, p=0.067 vs. control, p=0.941 vs. Cisplatin alone, p=0.124 vs. Deferasirox alone). Pre-treatment of mice for 1 week with Deferasirox prior to 3 weeks of Cisplatin monotherapy did, however, result in a significantly smaller xenograft compared to control (51.71 mg vs. 214.9 mg, p=0.044) albeit at the expense of a small rise in serum creatinine levels (38.18 vs. 35.83 µM/L, p=0.045 vs. control).

Treatment of mice for 1 week with Deferasirox resulted in a final xenograft size of 75.7 mg (p=0.075 vs. control) which was statistically larger than the group given 3 weeks of Deferasirox monotherapy (75.7 mg vs. 35.5 mg, p=0.047).

3.3.5 The effect of Deferasirox upon the NFκB signalling pathway in oesophageal carcinoma

3.3.5.1 Overview

In order to assess the potential efficacy of Deferasirox upon the NFκB signalling pathway in oesophageal carcinoma a dual luciferase reporter assay was utilised using the OE19, OE33 and OE21 cell lines. In addition, Western blotting was performed against the phosphorylated form of the IκBα protein. IκBα forms a complex with NFκB, keeping it in an inactive state; phosphorylation of the protein at Ser32 and Ser36 leads to activation of NFκB. Thus, p-IκBα can be used as a surrogate marker of NFκB activity. [219]

3.3.5.2 Results

All 3 oesophageal carcinoma cell lines demonstrated activation of the NFκB signalling pathway. TNFα is known to be a potent inducer of NFκB activity (as demonstrated in Figure 3.5 where TNFα (20 ng/ml) significantly induced NFκB activity in all 3 oesophageal cell lines tested). Of note, the induction in NFκB by TNFα was greatest in the OE21 SCC cell line (10.64 fold) compared to 1.07 and 1.92 in the OE19 and OE33 OAC lines respectively.

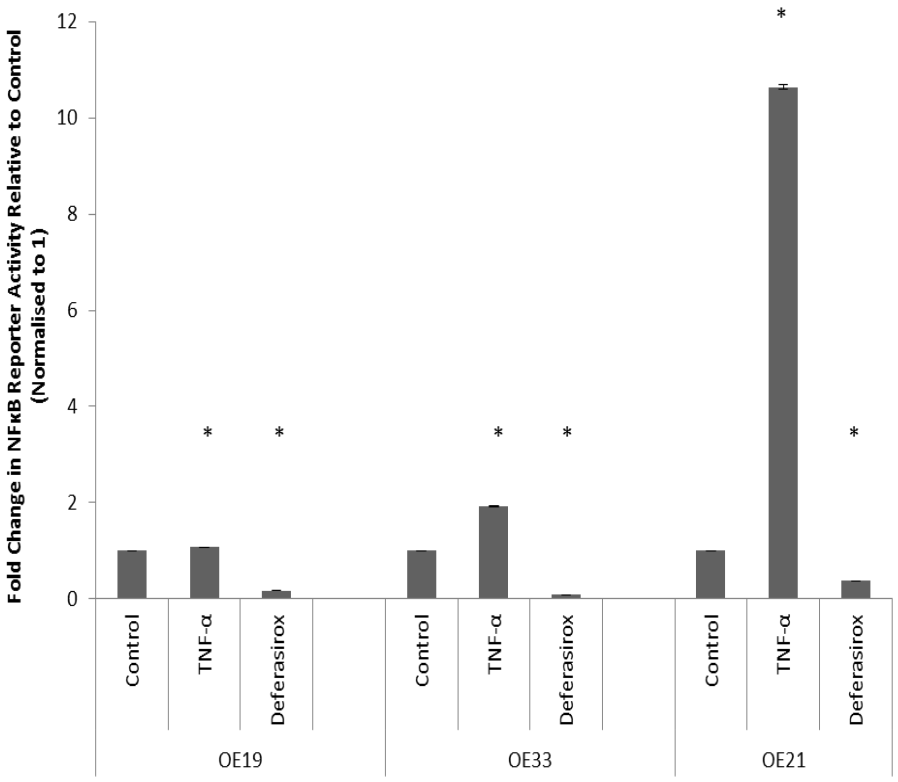

Figure 3.5 Deferasirox reduces NFκB activity in OAC and SCC *in-vitro*

Dual luciferase reporter assay demonstrating that 24 hours Deferasirox administration significantly reduces NFκB signalling activity compared to control across all 3 cell lines tested. Data presented as mean fold change in NFκB reporter activity relative to standard media control, error bars denote ±SEM, *p<0.05 vs. control.

Deferasirox administration (160 μM overnight) significantly reduced NFκB reporter activity in all 3 cell lines (0.18, 0.09 and 0.38 fold in OE19, OE33 and OE21 lines respectively, $p<0.05$ vs. control).

Western blotting for p-IκBα was then performed on the OE19 OAC cell line as this had shown the highest baseline activity in the reporter assay (as inferred by response to TNFα). Deferasirox (20 μM) administration significantly reduced p-IκBα protein expression after 48 hours (71.6% reduction, $p<0.05$ vs. control, Figure 3.6).

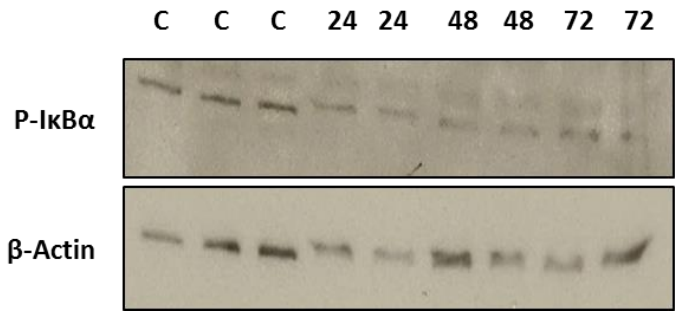
C C C 24 24 48 48 72 72
P-IκBα
β-Actin

A

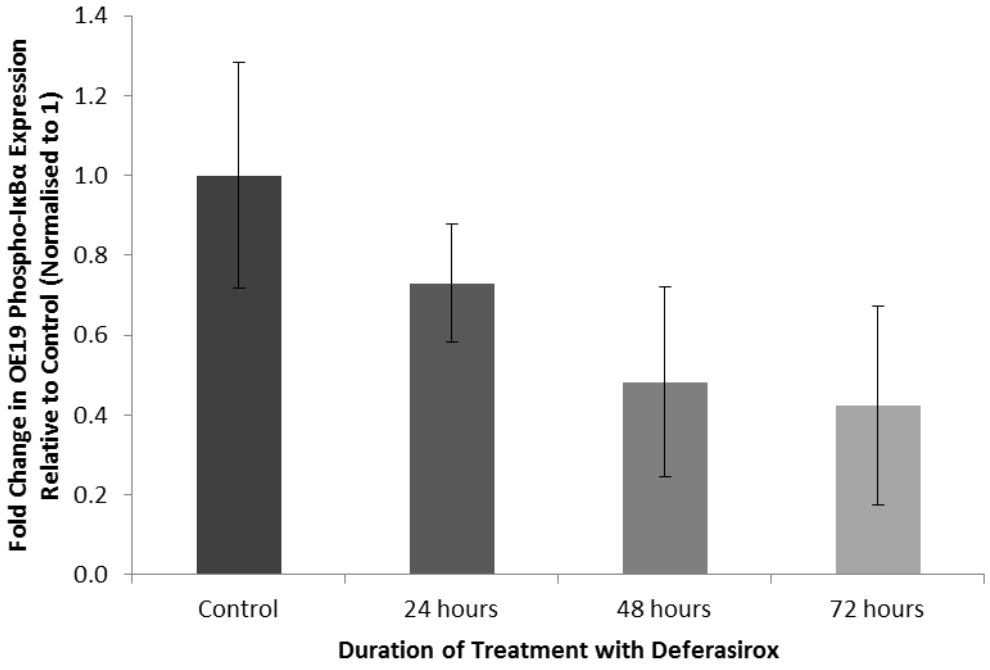
Fold Change in OE19 Phospho-IκBα Expression Relative to Control (Normalised to 1)
1.4
1.2
1.0
0.8
0.6
0.4
0.2
0.0
Control
24 hours
48 hours
72 hours
Duration of Treatment with Deferasirox

B

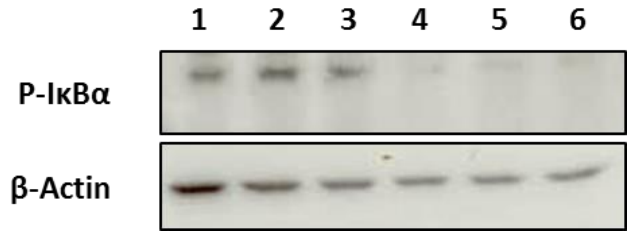

C

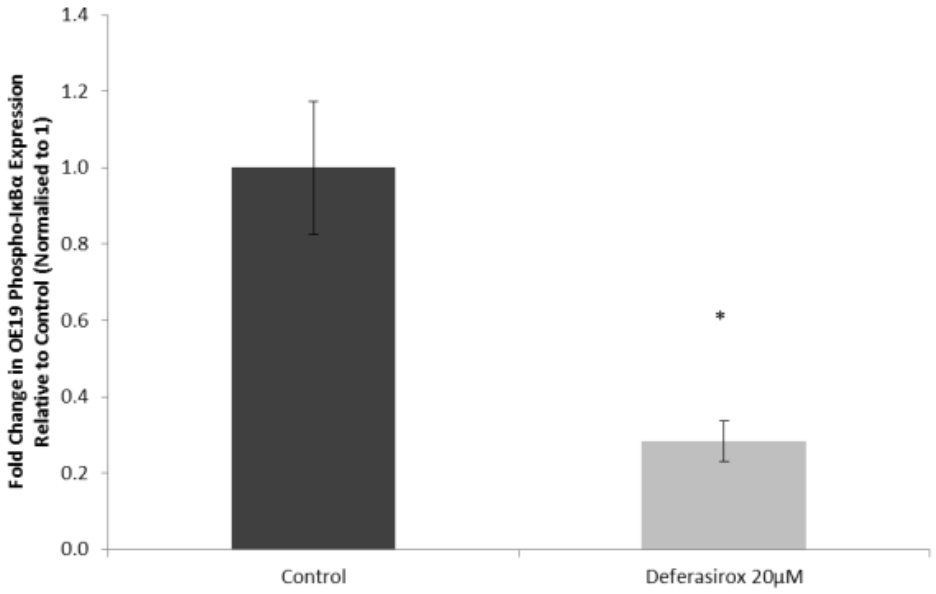

D

Figure 3.6 Deferasirox administration reduces P-IκBα expression in OE19 OAC cells

Western blot (A and C) demonstrating that administration of Deferasirox (20 μM) reduces P-IκBα expression in OE19 OAC cells. In blot (A), Deferasirox was administered for 24, 48 and 72 hours at 20 μM. In blot (C), Deferasirox was administered for 48 hours at 20 μM (lanes 1-3 = control media, lanes 4-6 = Deferasirox). P-IκBα expression was normalised to β-actin and displayed as a fold change (B and D) relative to control (normalised to 1). Error bars denote ±SEM, *$p<0.05$ vs. control.

3.3.6 Determination of the iron status of patients presenting with oesophageal adenocarcinoma

3.3.6.1 Overview

Deferasirox has been shown to significantly reduce serum ferritin and serum labile iron pool in patients with iron overload. [162] The drug appears to be well tolerated across these groups with a low incidence of serious adverse events to date. [162] The haematological and biochemical effects of iron chelator administration to a non-systemically iron overloaded group of patients, however, are not known. As such iron chelators may have the potential to induce anaemia; a state known to be associated with gastrointestinal cancers. [220]

Previous studies in oesophageal cancer have estimated the incidence of anaemia on presentation to range from 20-45%. [221, 222] Clearly, any benefit seen for patients treated with iron chelation therapy through Deferasirox in terms of anti-neoplastic activity or chemosensitisation would be substantially negated by the development of iron-deficiency and or anaemia and its associated side effects. The incidence of anaemia and or iron-deficiency in patients presenting with OAC thus needs to be formally quantified before any hypothetical trial of iron chelation therapy could commence.

The determination of the systemic iron status of patients presenting with OAC to a tertiary upper gastrointestinal resectional centre was therefore achieved through a retrospective analysis of prospectively collected haematological and biochemical data. Inclusion criteria were all patients presenting with oesophageal OAC (including Siewert types I, II and III) in a 2 year period (2008-10). All patients had histologically proven malignancy and were included in the study with informed consent and regional ethics approval. Patient demographics were recorded and blood samples taken at presentation for haematological and biochemical iron parameters. Patients were followed through the normal multidisciplinary team cancer evaluation and treatment pathways. All

haematological and biochemical quantification was performed on automated high through put analysers at the host institution's department of haematology and biochemistry. Data collected included haemoglobin, serum ferritin, serum iron and soluble transferrin receptor (sTfR). The soluble transferrin receptor – ferritin index (sTfR-F index) was also calculated by sTfR/log ferritin. Derivation of sTfR-F was performed as it has been shown to accurately distinguish between iron-replete and iron-deplete anaemic patients and also to detect the non-anaemic stages of iron deficiency. [223]

The normal reference ranges used were:

Haemoglobin concentration (Hb): male 13.5-18 g/dL and female 11.5-16.5 g/dL

Serum ferritin: 18-360 µg/L and female 10-320 µg/L

Serum iron: male 10-32 µmol/L and female 5-30 µmol/L

sTfR: male and female 2.0-3.6 mg/L

sTfR-F index: male and female >1.8 equates to storage iron depletion, >2.2 indicates iron deficient erythropoiesis and >2.8 iron deficiency anaemia [223]

3.3.6.2 Results

In total, 71 patients presenting with OAC were included with a mean age of 65.5 years.

Fifty-five (78%) OAC patients were male. Mean Hb for male OAC patients was 13.8 g/dL and 11.8 g/dL for females. Mean serum ferritin was 265 µg/L and 91 µg/L for males and females respectively and serum iron 13.4 µmol/L and 12.3 µmol/L. Mean sTfR was 2.64 mg/L for males and 2.92 mg/L for females. Mean sTfR-F index values were 1.35 for males and 1.72 for females, both within normal reference ranges.

No significant difference in any tested parameter was observed between resectable and advanced OAC at presentation.

A full iron profile was available for 11 patients in total who underwent neoadjuvant chemotherapy with Epirubicin, Cisplatin and 5-Fluorouracil/Capecitabine (ECF/ECX). A significant fall in mean Hb concentration was evident post neoadjuvant treatment (13.9 g/dL to 12.5 g/dL; p=0.019 pre vs. post treatment respectively). No significant differences were observed in mean serum ferritin (161 µg/L vs. 280 µg/L; p=0.34), serum iron (13.1 µmol/L vs. 13.8 µmol/L; p=0.81) or sTfR (2.63 mg/L vs. 2.79 mg/L; p=0.33). Although a significant drop in mean Hb was noted pre and post chemotherapy, no change in mean sTfR-F index values was seen (1.47 vs, 1.43; p=0.89 for pre and post treatment values) indicating systemic iron levels remained unchanged.

Table 3.2 Patients presenting with OAC are systemically iron replete

	Haemoglobin (g/dL)		Serum Ferritin (µg/L)		Serum iron (µmol/L)		Soluble Transferrin Receptor (mg/L)		sTfR-F index	
OAC by Gender	**Male**	**Female**	**Male**	**Female**	**Male**	**Female**	**Male**	**Female**	**Male**	**Female**
	13.8 (1.8)	11.8 (1.4)	265 (239)	91 (68)	13.4 (5.3)	12.3 (4.9)	2.64 (0.5)	2.92 (0.6)	1.35 (0.7)	1.72 (0.9)
Resectable OAC vs Advanced OAC	**Resectable**	**Advanced**	**Resectable**	**Advanced**	**Resectable**	**Advanced**	**Resectable**	**Advanced**	**Resectable**	**Advanced**
	13.2 (1.8)	13.6 (2.4)	236 (278)	317 (258)	13.6 (5)	11.3 (4.3)	2.78 (0.52)	2.35 (0.35)	1.5 (0.78)	1.11 (0.50)
Neoadjuvant ECX for OAC	**Pre**	**Post**	**Pre**	**Post**	**Pre**	**Post**	**Pre**	**Post**	**Pre**	**Post**
	13.9 (1.6)	12.5 (1.3) *	161 (57)	280 (217)	13.1 (3.7)	13.8 (4.2)	2.63 (0.48)	2.79 (0.33)	1.47 (0.65)	1.43 (0.71)

Key haematological parameters pertaining to systemic iron status were obtained from 71 patients with OAC presenting to a tertiary referral centre. Chemotherapy administered is known as ECX and comprised Epirubicin, Cisplatin and Capecitabine (pro-drug converted to 5-Fluorouracil). Data presented as mean, () denotes standard deviation, * $p<0.05$ vs. pre ECX.

NB Section 3.3.6 has been adapted from Ford SJ, Bedford M, Pang W *et al*. A comparative study of the iron status of patients with oesophageal adenocarcinoma to determine suitability for a clinical trial of iron chelation therapy. Annals of the Royal College of Surgeons of England 2014; 96(4): 275-8.

I gratefully acknowledge Dr Weehaan Pang for data collection, Mr Samuel Ford for assistance with data analysis/interpretation and Ms Olga Tucker for overall conception, design and lead of this study.

3.4 Discussion

The incidence of oesophageal carcinoma and in particular the OAC subtype is increasing at an alarming rate. [13, 14] The disease continues to carry an abysmal 5 year survival rate of around 13%, largely driven by the high percentage of patients presenting with advanced, irresectable disease and the subsequent paucity of systemic reagents effective against it. [14, 17, 40, 41, 43, 45, 47, 54, 55] Thus, the discovery and development of new agents that are solely effective against the disease or can enhance the efficacy of existing therapies would be highly desirable.

Iron metabolism appears to be dysregulated in the development of OAC, as illustrated by the increase in cellular iron import and deposition seen with the progression from pre-malignant BM to OAC. [24] Furthermore, iron has been to shown to both exacerbate tumourigenesis in murine models of OAC and increase OAC cellular proliferation *in-vitro*. [24, 129] Similar phenomena have also been demonstrated in other cancers, particularly breast and colorectal. [82, 99, 102, 125]

Iron chelators therefore offer great potential as anti-neoplastic agents, although there is little data available pertaining to the efficacy of pre-existing licensed agents. [80, 92] Deferasirox is one such agent and, unlike the original clinically available chelator Desferrioxamine, has an oral route of administration making it an attractive agent to investigate further in the context of cancer. [157]

It has been demonstrated in the current study that Deferasirox significantly impairs both OAC and SCC cell viability *in-vitro* in a time and dose dependent manner. The drug displays an IC50 of approximately 40 μM at 48 hours incubation and 20 μM at 72 hours. Moreover, Deferasirox also demonstrated a marked and significant suppression in OAC xenograft growth when given to mice at a dose of 20 mg/kg on alternate days for 3 weeks (83.5% reduction in tumour size, p=0.032 vs. control). Again, this was a significantly greater effect than when the drug was given to mice for just

one week (mean final xenograft size 35.5 mg vs. 75.7 mg, p=0.047), demonstrating a time dependent response to therapy. Crucially, Deferasirox monotherapy was well tolerated with no differences seen in final animal weight, haemoglobin, serum iron or serum creatinine compared to the control cohort.

These results are immensely promising and support the findings published in a recent paper from our group demonstrating that Deferasirox inhibits oesophageal cellular iron uptake (by as much as 20-50%) and is also capable of stripping iron from inside cells. [215] In addition, oesophageal xenografts harvested from mice given Deferasirox (20 mg/kg) for 3 weeks had a significantly reduced iron content (up to 57%) which was also reflected by significant up-regulation in TfR1 expression and concomitant down-regulation in H-ferritin and ferroportin expression (at both the mRNA and protein levels). [215] Deferasirox has also demonstrated efficacy in *in-vivo* models of lung cancer and leukaemia thus indicating that the effects of the drug are not cell line dependent. [169, 183]

Iron is essential for a number of key cellular processes including DNA synthesis, ATP generation and cell cycle progression; all of these are activities that by definition are increased in cancer and thus malignant cells are known to have a higher requirement for iron than their normal counterparts. [112] The fact that Deferasirox is able to both inhibit cellular iron uptake and facilitate the removal or iron from within oesophageal cancer cells means that the primary mechanism for its anti-neoplastic effects when given as a monotherapy is likely to be cellular iron deprivation through chelation. It is known that cellular iron depletion results in cell cycle arrest at the G1/S checkpoint and subsequent induction of apoptosis. [224] Iron deprivation is also known to inhibit activity of the R2 subunit of the enzyme ribonucleotide reductase (which catalyzes the conversion of ribonucleotides into deoxyribonucleotides during DNA synthesis) and decrease expression of cyclins A, B and D (all of which are vital for cell cycle progression). [225]

Current response rates to chemotherapy in oesophageal carcinoma are variable, as such the finding that Deferasirox can overcome established Cisplatin resistance, both as a monotherapy and when given at low 'sub-optimal' doses in combination with Cisplatin, in both OAC and SCC cell lines *in-vitro* is of significant interest. [52] Furthermore, the demonstration that pre-treatment of oesophageal cell lines with Deferasirox, even at low concentrations, *in-vitro* for 24 hours prior to administration of the ECF chemotherapy regimen results in a significant additional reduction in both cellular viability and proliferation raises the potential that the drug may act as a chemosensitiser.

Obviously, a counter argument to this could be that Deferasirox is merely acting through a different mechanism of action to existing reagents (i.e. iron chelation rather than DNA cross-linking in the case of Cisplatin) and in the case of pre-treatment, any beneficial effects seen are merely achieved through the addition of an extra drug that has been commenced earlier, and it is not actually genuine chemosensitisation per se. There are, however, a number of additional mechanisms of action for the drug proposed in the literature which offer potential routes to chemosensitisation including upregulation of the metastasis suppressor n-Myc downstream regulated 1 (NDRG1), the cyclin dependent kinase inhibitor $p21^{CIP1/WAF1}$ and the pro-apoptotic protein Caspase-3 as well as the inhibition of polyamine synthesis, mTOR signalling, Wnt signalling and the NFκB pathway. [169, 173, 175, 177, 183, 186]

Thus, of particular interest is the demonstration in this study (by both reporter assay and Western blotting) that Deferasirox can inhibit signalling through the NFκB pathway in OAC. NFκB signalling plays a pivotal role in the pathogenesis of a number of cancers by regulating several fundamental cellular processes such as apoptosis, proliferation, differentiation and tumour migration. [178] It has been shown to be constitutively active in most tumour cell lines and has also been identified in tumour tissue from patients with multiple myeloma, acute myeloid leukaemia, prostate cancer and breast cancer. [178, 179, 180, 181, 182] In OAC, NFκB expression has been shown to increase in a stepwise

manner along the progression from normal mucosa (nil) to BM (40%) to OAC (61%). [216] NFκB activity pre-therapy (chemo/radiotherapy) for OAC has also been shown to correlate with lack of subsequent complete pathological response, increased metastatic progression and decreased disease-free and overall survival. [216, 217] NFκB has been shown to be activated in OAC *in-vitro* by common chemotherapeutic drugs (such as 5-Fu) leading to inhibition of apoptosis. [218] Interestingly, chemosensitivity can be restored following treatment with an NFκB inhibitor. [218] Furthermore, NFκB inhibitors have been shown to suppress oesophageal tumour growth both *in-vitro* and *in-vivo* and also enhance sensitivity to 5-Fu and Cisplatin *in-vitro*. [226] As such, the demonstration that NFκB signalling is active in OAC cell lines but can be significantly suppressed (by as much as 71.6%) through the administration of Deferasirox therapy at a concentration of 20μM is highly relevant and offers a mode of action for how the drug may be able to sensitise cells to chemotherapy. Previous studies have identified a link between ferritin expression and NFκB signalling. [227] Of note, ferritin has been shown to induce NFκB signalling in hepatic stellate cells, which may explain in part the ability of Deferasirox (through suppression of intracellular ferritin) to inhibit NFκB signalling. [228] Furthermore, down-regulation of ferritin has been shown to increase the sensitivity of breast cancer cells to the chemotherapeutic agents Doxorubicin and Cisplatin. [229, 230]

The data shown in the current study clearly demonstrates that Deferasirox monotherapy is highly efficacious both *in-vitro* and *in-vivo* against OAC. The drug is also effective at decreasing viability in cell lines that are resistant to therapy with Cisplatin and may enhance the efficacy of existing chemotherapeutic reagents when given as a pre-treatment or at a lower dose in combination. It should also be noted, however, that the combination of Deferasirox with either ECF (*in-vitro*) or Cisplatin (*in-vitro* and *in-vivo*) does not confer any additional benefit over chemotherapy alone and indeed in the OE19 *in-vivo* xenograft model, the addition of Cisplatin to Deferasirox actually appeared to reduce the efficacy of the chelator. This in part may be explained by previous studies looking at Cisplatin based combination therapies in germ cell tumours demonstrating that Cisplatin

induced cell death occurs predominantly in cells during G2/M of the cell cycle and that use of agents which induce G1/S arrest (which is likely to be the case with an iron chelator) is unlikely to offer any synergistic advantage. [231]

The demonstration that patients presenting with OAC are not systemically iron deplete and that chemotherapy with ECX does not negatively impact on iron levels is an important finding. Although the data presented here was from a relatively small number of patients drawn from a single, tertiary upper gastrointestinal resectional centre, these results will help to justify the design of any future clinical trial of Deferasirox therapy in patients with OAC (even though it has also been demonstrated here in mouse models that Deferasirox therapy is unlikely to impact on either haemoglobin or serum iron levels).

In conclusion, it has been demonstrated that the iron chelator Deferasirox displays significant anti-neoplastic properties both *in-vitro* and *in-vivo* in the context of OAC. Crucially, Deferasirox monotherapy was well tolerated in mice treated with the drug with no negative effects on mouse health, haemoglobin, serum iron or serum creatinine levels seen. The drug is efficacious *in-vitro* against cells that are resistant to Cisplatin and can improve subsequent response to chemotherapy when given either at a low dose alongside or as a pre-treatment prior to existing therapy regimens. The drug also appears to reduce signalling through the NFκB pathway, offering an additional mechanism of action beyond iron chelation alone. Finally, evidence within this study demonstrated that patients presenting with OAC are systemically iron replete and are therefore candidates to be entered into any future clinical trial of Deferasirox as an anti-neoplastic agent in oesophageal carcinoma.

Chapter 4. A Role for Deferasirox as an Anti-neoplastic and Chemosensitising Agent in Colorectal Adenocarcinoma

4.1 Introduction

Cancer of the colon and rectum is the 4th most common cancer in the United Kingdom overall (being the 3rd most common in men and women when analysed separately). [4] Five year survival rates for the disease are 59%, with survival being strongly correlated to disease stage at the time of presentation (93.2% of patients with Duke's A disease survive 5-years, compared to 6.6% with Duke's D disease). [232, 233]

As with oesophageal carcinoma, surgery remains the cornerstone of curative treatment for colorectal adenocarcinoma, however, for those with locally advanced or systemic disease, chemotherapy continues to comprise an important component of the treatment armamentarium. [234] Again, response to chemotherapy is variable and as such the development of new agents efficacious against the disease is highly desirable. [235]

Iron appears to be intimately linked to colorectal tumourigenesis. [82, 102] Individuals harbouring a mutation in haemochromatosis (HFE), one of the mutated genes that underlies Hereditary Haemochromatosis, have also been shown to be at an increased risk of certain extrahepatic cancers, including colorectal. [118, 119, 120] Furthermore, a meta-analysis of 33 studies assessing iron intake and colorectal cancer risk revealed that approximately 75% of the studies included associated higher iron intake with an increased risk of colorectal cancer. [123] It has also been demonstrated that men who regularly donate blood may have a lower risk for developing several cancers including colorectal. [122] Colorectal adenocarcinoma typically develops through the normal mucosa → adenoma → adenocarcinoma sequence. [236] With this in mind, increased iron acquisition has been demonstrated

in samples of human tissue taken along this progression to adenocarcinoma together with a corresponding overexpression in the cellular iron import proteins TfR1 and DMT1 and an internalisation of the main cellular iron export protein ferroportin. [82] The systemic iron regulatory hormone hepcidin (which through internalisation of ferroportin precipitates cellular iron loading) has also been shown to be ectopically expressed in colorectal cancer tissue and correlates with tumour T-stage when measured in the urine of patients with the disease. [237] Likewise, iron loading of colorectal adenocarcinoma cell lines *in-vitro* has been shown to stimulate cellular proliferation and also repression of the cell adhesion protein E-cadherin. [82]

Iron has been shown to amplify Wnt signalling (the major oncogenic pathway in the colon) *in-vitro* following loss of the tumour suppressor APC (an event which occurs in the vast majority of colorectal cancers). [132] Furthermore, an upregulation in the expression of TfR1 and DMT1 was seen in adenomas extracted from the intestines of transgenic mice harbouring an APC mutation ($APC^{Min/+}$). [102] Interestingly, the increase in TfR1 and DMT1 seen was also shown to correlate with expression of the proto-oncogene c-Myc, a known Wnt target which has also been shown to activate TfR1 transcription. [102, 238] Furthermore, in the same study it was demonstrated that $Apc^{Min/+}$ mice fed a low iron diet developed fewer tumours that were also significantly smaller. [102] Conversely, a 2-3 fold amplification in tumourigenesis was seen in mice fed a high iron diet compared to the control group. Finally, mice fed a low iron diet were shown to have increased overall survival, whereas those on a high iron diet had a significantly decreased overall survival ($p<0.05$ vs. control). [102] The authors concluded that excess luminal iron in the context of APC loss was a potent stimulator of intestinal tumourigenesis. These findings support similar observations for a propagating effect of iron (both luminal and systemic) on murine colorectal tumourigenesis that have been shown previously. [239]

Malignant cells have an increased requirement for iron, owing to its vital role in DNA synthesis, ATP generation and cell cycle progression. [112] It therefore appears that iron has a dual role in the

propagation of colorectal tumourigenesis; firstly, by acting crudely as a 'fuel in the tank' for malignant cells, driving their increased rate of proliferation through the processes it is crucial to; and secondly, through the amplification of oncogenic signalling pathways such as Wnt, further increasing cell proliferation, survival and evasion of apoptosis whilst enhancing the cell's ability to acquire further iron and drive proliferation on again (thus forming an almost self-perpetuating cycle).

It thus seems logical that iron chelation may be efficacious in the treatment of colorectal adenocarcinoma, however to date, this treatment avenue remains largely unexplored.

4.2 Chapter Aims

Given the weight of evidence implicating iron in the propagation of colorectal tumourigenesis, it is pertinent to investigate whether iron chelation represents an efficacious and novel treatment option for the disease. As such, the aims of this chapter are:

1. To assess the efficacy of the licensed oral iron chelating agent Deferasirox as an anti-neoplastic agent in colorectal adenocarcinoma *in-vitro.*
2. To delineate the effects of Deferasirox administration upon colorectal cellular iron metabolism and cell phenotype *in-vitro.*
3. To assess the ability of Deferasirox to overcome established chemotherapy resistance in colorectal adenocarcinoma *in-vitro.*
4. To assess the effect of pertinent genetic mutations and hypoxia upon Deferasirox efficacy *in-vitro.*
5. To assess the efficacy of the licensed iron chelator Deferasirox in colorectal adenocarcinoma *in-vivo.*

4.3 Results

4.3.1 Deferasirox as an anti-neoplstic agent in colorectal adenocarcinoma *in-vitro*

4.3.1.1 Overview

The colorectal adenocarcinoma cell lines RKO, SW480 and HT29 were seeded into 96 well plates and cultured in media with or without Deferasirox at varying doses (0-320 μM) for 24, 48 and 72 hours. Cells were counted and seeded ($4x10^4$/ml following optimisation) such that an approximate confluence of 70% was achieved in the control group (0μM Deferasirox) at time of assay.

After the defined time points, MTT assays were performed in order to determine cellular viability (as previously outlined) relative to the control group.

4.3.1.2 Results

Deferasirox decreased colonic cell line viability in a time and dose dependent manner (Figure 4.1).

At 24 hours the drug resulted in a significant reduction in cell viability across all 3 lines tested at a dose of 320 μM (mean viability 54.5% vs. control), with the drug surpassing the IC50 mark in the HT29 cell line. Lower doses of the drug (10 μM in the RKO and 40 μM in the HT29) also generated statistical reductions in cell viability after 24 hours.

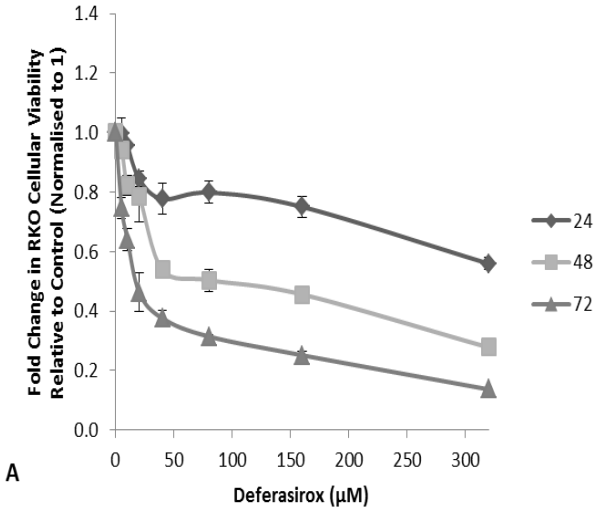

A

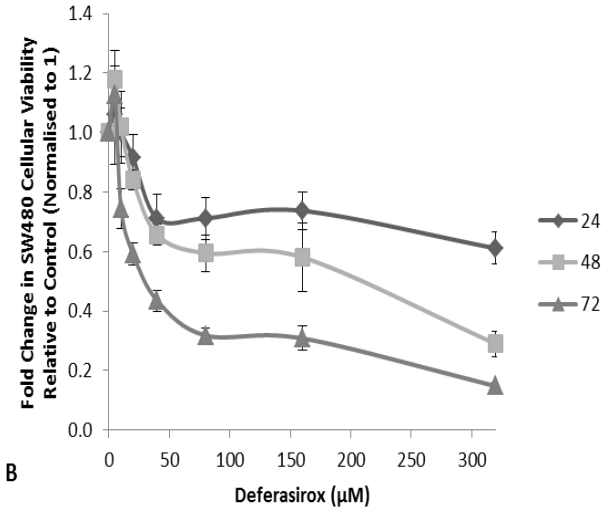

B

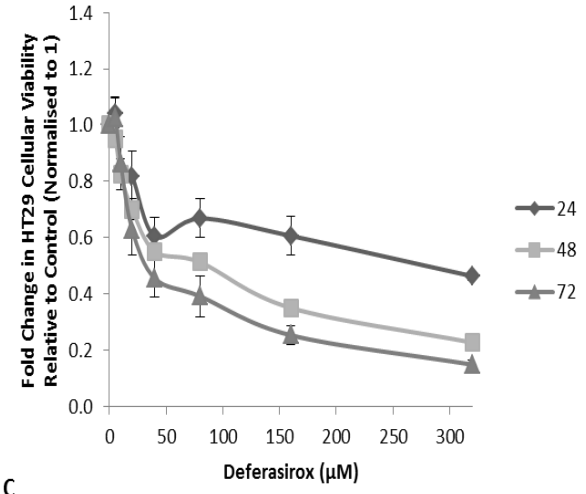

C

	RKO			SW480			HT29		
Deferasirox (µM)	24	48	72	24	48	72	24	48	72
5	0.978	0.027	0.018	0.756	0.201	0.187	0.515	0.033	0.760
10	0.022	0.033	0.011	0.993	0.894	0.063	0.064	0.015	0.284
20	0.029	0.127	0.014	0.398	0.041	0.008	0.182	0.014	0.053
40	0.052	0.002	0.002	0.073	0.010	0.004	0.026	0.004	0.014
80	0.033	0.006	0.000	0.055	0.021	0.001	0.041	0.000	0.014
160	0.019	0.002	0.000	0.053	0.069	0.003	0.029	0.000	0.002
320	0.002	0.000	0.000	0.018	0.004	0.000	0.001	0.000	0.000

D

Figure 4.1 Deferasirox administration reduces colonic adenocarcinoma cell line viability *in-vitro* in a time and dose dependent manner

MTT cell viability assay demonstrating the effect of increasing concentrations of Deferasirox on the colorectal adenocarcinoma cell lines RKO (A), SW480 (B) and HT29 (C). Data points represent mean fold change compared to standard media control (normalised to 1). Error bars denote ±SEM. P values for individual fold changes (relative to control) displayed in (D) (shaded boxes denote $p<0.05$ vs. control).

At 48 hours the drug had further decreased cell viability across all 3 cell lines. The IC50 was surpassed by 160 μM in both the RKO and HT29 cell lines (where even 5 μM registered a significant reduction) and by 320 μM in the SW480 (where 20 μM was the lowest concentration to register a significant reduction in cellular viability). The average reduction in cell viability seen was 41.8% at 40 μM Deferasirox and 46.3% at 80 μM across the 3 lines.

By 72 hours Deferasirox had reduced cell viability across all 3 lines by an average of 57.8% at 40 μM increasing to 85.5% at the highest concentration tested of 320 μM.

4.3.2 The effect of Deferasirox upon colorectal cellular iron metabolism and phenotype *in-vitro*

4.3.2.1 Overview

The effect of Deferasirox upon colorectal cellular iron loading was assessed by both ferrozine assay and through radio-labelled iron uptake studies. The ability of Deferasirox to remove iron from cells that had already been iron loaded was determined by ferrozine assay, Western blotting and a ferritin ELISA. The protocols for all of these procedures are described in chapter 2.

To delineate the effect of treatment with Deferasirox upon the cell cycle FACS was utilised. This analysis of cell phenotype was augmented by BrdU (proliferation) and MTT (viability) assays. In addition, the effect of pre-incubation of Deferasirox with iron (100 μM $FeSO_4$) upon cellular viability was assessed through the performance of an additional MTT assay over 48 hours of treatment. Finally, the ability of Deferasirox to suppress iron induced hyperproliferation of colorectal adenocarcinoma cells was assessed by performing a BrdU analysis on HT29 cells prior loaded with 25 μM $FeSO_4$ for 24 hours. HT29 cells were utilised in this section as RKO cells have previously been shown not to increase their proliferation rate in response to iron loading. [102, 132] All of the

aforementioned experimental procedures were carried out as previously outlined in the methods section.

4.3.2.2 Results

Deferasirox significantly inhibited the uptake of iron by colonic cells by both ferrozine assay and radio-labelled iron (Figure 4.2). RKO cellular iron uptake was significantly impaired when Deferasirox was co-incubated alongside $FeSO_4$ for 1 hour (49.6% reduction vs. $FeSO_4$ alone, $p<0.05$). A similar result was obtained in the radio-labelled Caco-2 trans-well system (20.4% reduction vs. $FeSO_4$ alone, $p<0.05$).

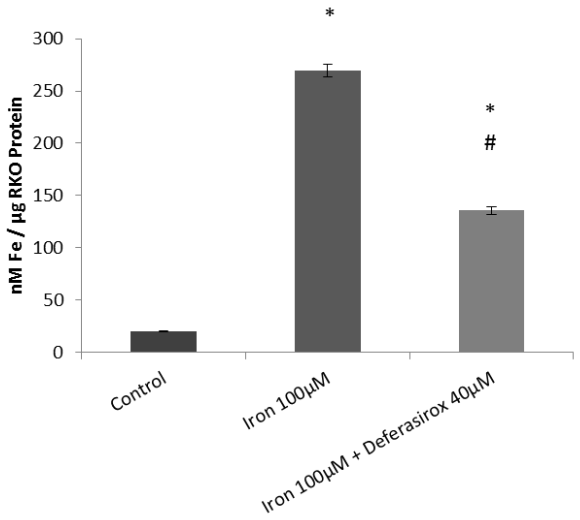

A

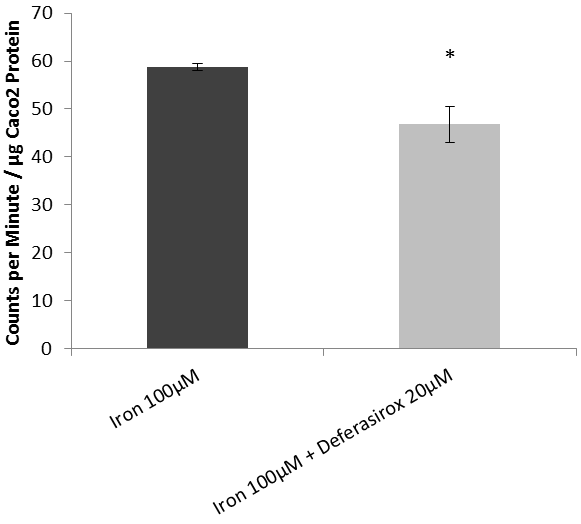

B

Figure 4.2 Deferasirox inhibits colonic cellular iron uptake *in-vitro*

Ferrozine assay demonstrating the ability of Deferasirox (40 µM) to suppress RKO cellular iron uptake when administered alongside 100 µM $FeSO_4$ for 1 hour (A). The drug also significantly suppressed the uptake of radio-labelled $FeSO_4$ (100 µM) in a trans-well model of colonic adenocarcinoma utilising Caco-2 cells (B). Error bars denote ±SEM, * $p<0.05$ vs. control.

The administration of Deferasirox (40 μM) to RKO cells that had been pre-loaded with 100 μM $FeSO_4$ resulted in a significantly reduced intracellular iron content (28.2% reduction vs. $FeSO_4$, $p<0.05$, Figure 4.3A), thus demonstrating Deferasirox's ability to strip iron from within colonic cells. This was further exemplified by a reduction in subsequent ferritin protein expression by both Western blot (62.1% reduction vs. $FeSO_4$, $p<0.05$, Figure 4.3B) and ferritin ELISA (98.2% reduction vs. $FeSO_4$, Figure 4.3C). Interestingly, in the ferritin ELISA Deferasirox decreased ferritin expression in the iron loaded cells to an even lower level than the control group.

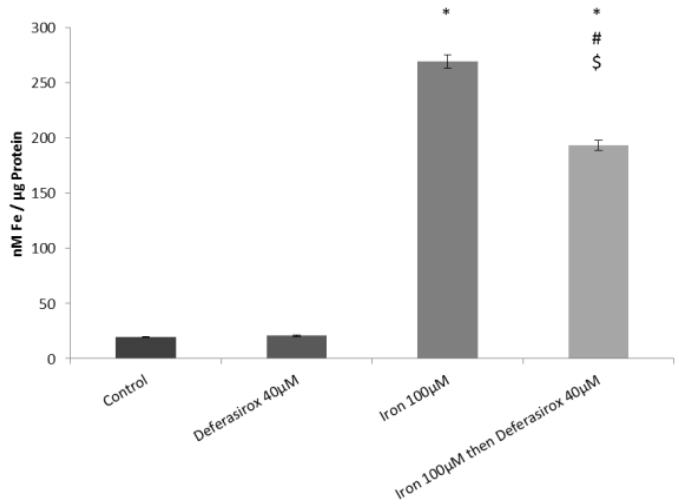
nM Fe / µg Protein
300
250
200
150
100
50
0
*
*
#
$
Control
Deferasirox 40µM
Iron 100µM
Iron 100µM then Deferasirox 40µM

A

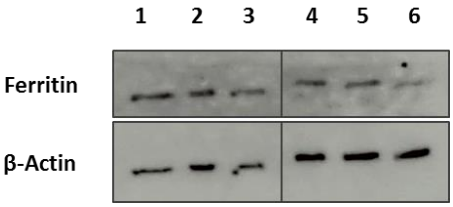
1
2
3
4
5
6
Ferritin
β-Actin

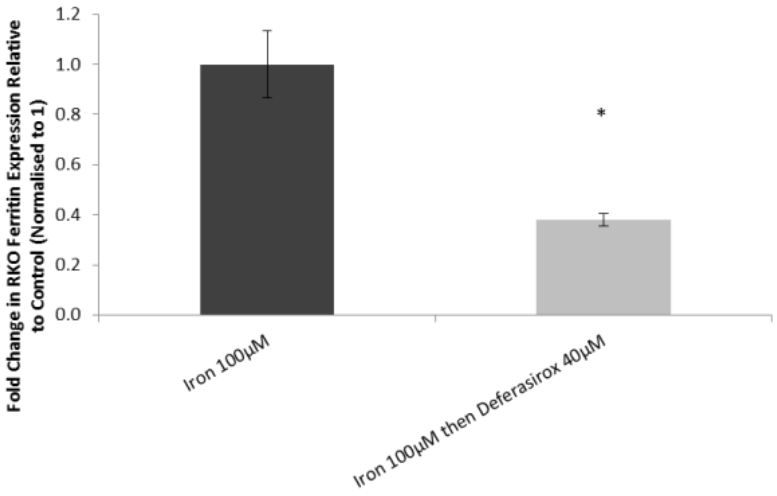
Fold Change in RKO Ferritin Expression Relative to Control (Normalised to 1)
1.2
1.0
0.8
0.6
0.4
0.2
0.0
*
Iron 100µM
Iron 100µM then Deferasirox 40µM

B

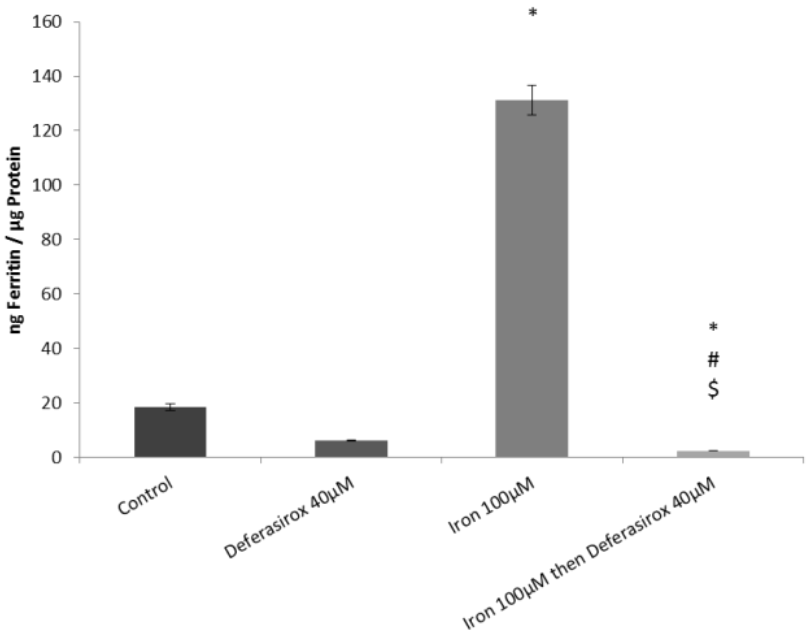

C

Figure 4.3 Deferasirox administration significantly decreases intracellular iron levels and subsequent ferritin expression

Ferrozine assay demonstrating the ability of Deferasirox (40 µM) to decrease RKO intracellular iron levels when administered to cells pre-loaded with 100 µM $FeSO_4$ (A). This is supported by decreased ferritin levels, as shown by western blot (B, lanes 1-3 100 µM $FeSO_4$, lanes 4-6 100 µM $FeSO_4$ then Deferasirox 40 µM) and ferritin ELISA (C). Semi-quantitative analysis of blots was performed through normalisation to β-actin and subsequent expression as a fold change relative to control (normalised to 1). Error bars denote ±SEM, * $p<0.05$ vs. control.

A significant increase in the proportion of cells in G1 phase of the cell cycle was seen following the administration of Deferasirox (40 μM) to RKO cells for 48 hours (83.4 vs. 57.1%, $p<0.05$ vs. control, Figure 4.4A). As expected, this was also reflected by a significant reduction in cellular proliferation as demonstrated by BrdU assay (69.1% reduction vs. control, $p<0.05$, Figure 4.4B). Finally, a significant reduction in RKO cellular viability (MTT) of 46.1% ($p<0.05$ vs. control) was also seen following the administration of Deferasirox for 48 hours (Figure 4.4C).

Deferasirox efficacy in RKO cells was maintained across all concentrations tested despite pre-incubation of the chelator with iron (Figure 4.5). At doses of 40, 80 and 360 μM, however, there was a statistical reduction in efficacy compared to when the drug was administered in the absence of iron (19.5, 12.5 and 22.2% reduction in comparative efficacy respectively, $p<0.05$).

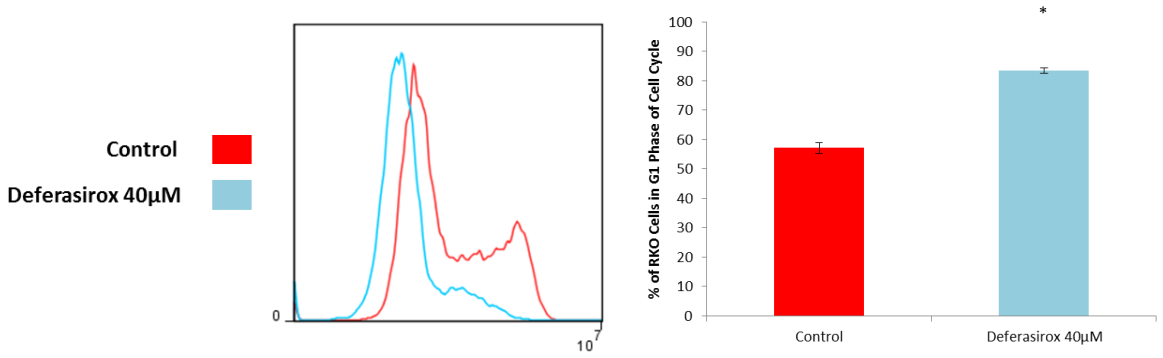
Control
Deferasirox 40µM
0
10^7
% of RKO Cells in G1 Phase of Cell Cycle
100
90
80
70
60
50
40
30
20
10
0
*
Control
Deferasirox 40µM

A

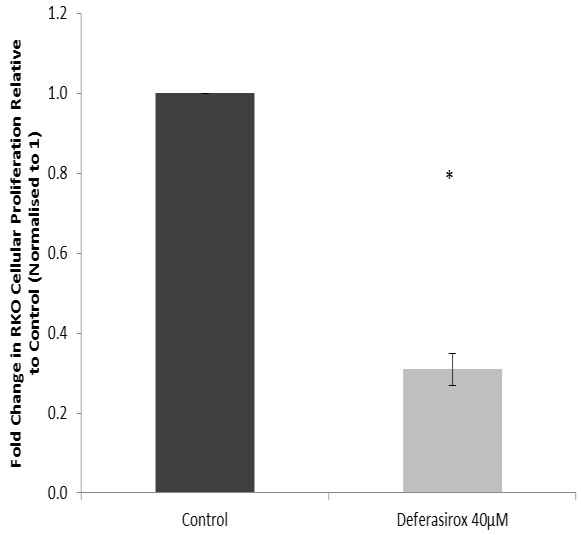
Fold Change in RKO Cellular Proliferation Relative to Control (Normalised to 1)
1.2
1.0
0.8
0.6
0.4
0.2
0.0
*
Control
Deferasirox 40µM

B

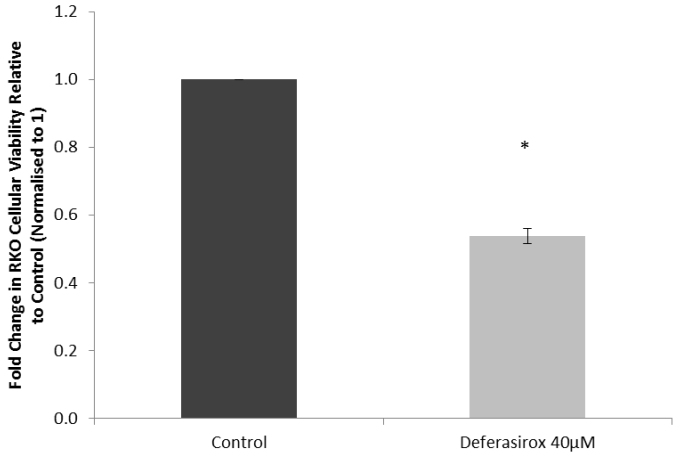
Fold Change in RKO Cellular Viability Relative to Control (Normalised to 1)
1.2
1.0
0.8
0.6
0.4
0.2
0.0
*
Control
Deferasirox 40µM

C

Figure 4.4 Deferasirox administration results in decreased proliferation through cell cycle arrest and ultimately leads to a decrease in colonic cellular viability

Cell cycle analysis through FACS (with propidium iodide) demonstrating the accumulation of RKO cells treated with Deferasirox (40 μM for 48 hours) in G1 phase of cell cycle (A). The same dosing regimen also resulted in a significant decrease in cellular proliferation (BrdU assay, (B)). Cellular viability (MTT assay, (C)) was also significantly reduced at the corresponding dose. Values plotted represent mean fold change relative to matched control (normalised to 1), error bars denote ±SEM, * $p<0.05$ vs. matched control.

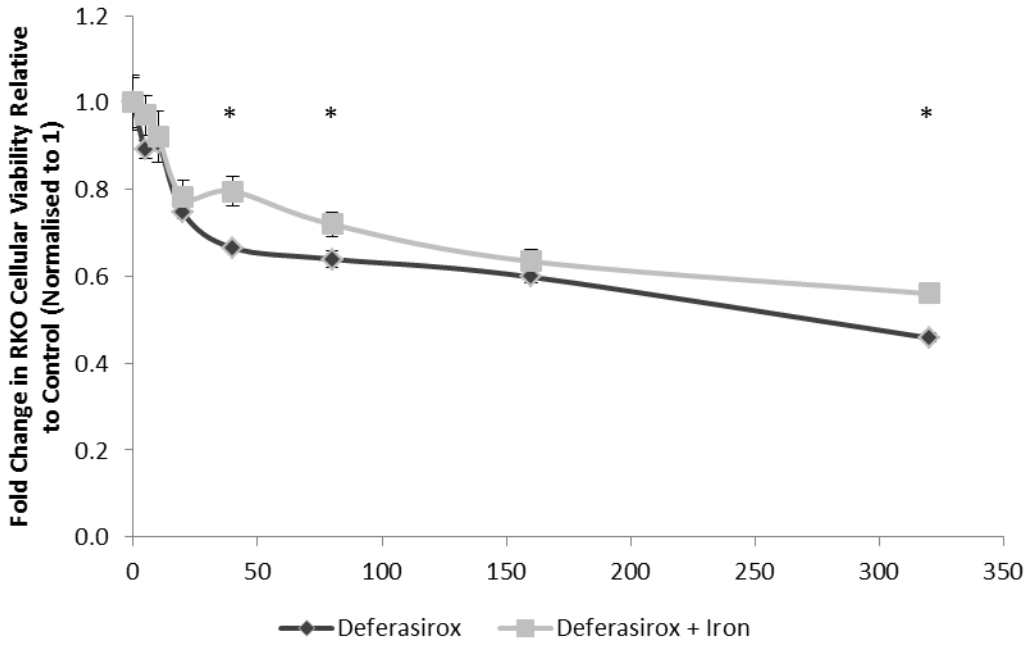

Figure 4.5 The effect of Deferasirox upon colonic adenocarcinoma cell line viability persists despite pre-incubation with iron

Cell viability assay (MTT) demonstrating that Deferasirox remains efficacious against RKO cells when administered following a period of prior incubation with 100 µM iron**.** Both regimens were statistically significant against control at all concentrations of Deferasirox >10 µM. Data points represent mean fold change vs. control, error bars denote ±SEM, * $p<0.05$ vs. equivalent dose of Deferasirox with iron.

The colonic cell line HT29 readily increased its intracellular iron content when cultured in the presence of media containing iron (Figure 4.6A). This ability to load iron was associated with a significant increase in cellular proliferation (14.3-28.9%, $p<0.05$ vs. control) as measured by BrdU assay (Figure 4.6B). Deferasirox administration for 48 hours at 40μM post iron administration, however, significantly ablated the iron induced increase in proliferation seen (reducing the proliferation of the iron loaded cells by 50.5% overall, $p<0.05$, Figure 4.6C) and crucially, reduced their proliferation to well below baseline (fold change 0.57 vs. control, $p<0.05$).

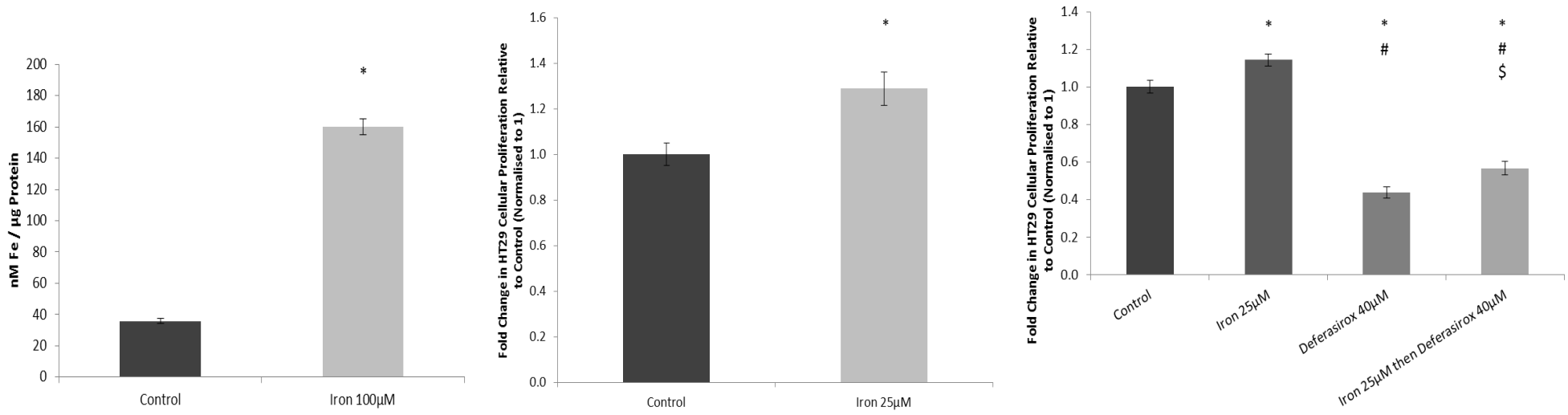

A **B** **C**

Figure 4.6 Deferasirox can suppress the iron induced increase in proliferation seen in colonic adenocarcinoma cells *in-vitro*

Ferrozine assay (A) demonstrating that the intracellular iron levels of HT29 colonic cells increase significantly when they are exposed to media containing $FeSO_4$. This is turn leads to an increase in cellular proliferation (by BrdU assay, (B)) above that seen with standard media alone. Deferasirox (40 µm for 48 hours) is capable of suppressing this enhancement in proliferation and indeed even reduces it significantly below the baseline level seen with standard media alone (C). Data points represent mean fold change relative to standard media control (normalised to 1), error bars denote ±SEM, * $p<0.05$ vs. control, # $p<0.05$ vs. iron, $ $p<0.05$ vs. Deferasirox alone.

4.3.3 The ability of Deferasirox to overcome chemotherapy resistance in colorectal adenocarcinoma *in-vitro*

4.3.3.1 Overview

The colorectal adenocarcinoma cell line SW480 and its metastatic clone SW620 were seeded into 96 well plates (100 µl per well at $4x10^4$ cells/ml) and cultured with increasing doses of the chemotherapeutic agent 5-Fu (2-128 µM) for 48 hours. In addition, the same cell lines were treated with Deferasirox at 20 or 40 µM over the same time period.

In addition, a 5-Fu resistant clone of the HT29 cell line was created by co-culturing them alongside progressively increasing doses of the drug over six months. Following this, the cells were seeded into 96 well plates and incubated with media containing 5-Fu alone (32 µM), Deferasirox (20 µM) or Deferasirox + 5-Fu for 72 hours. In addition, the parental HT29 cell line along with RKO and SW480 cells were also treated with 5-Fu for the same time period as a positive control for 5-Fu efficacy. MTT assays were again performed at the end of the treatment period to quantify effect on cellular viability.

4.3.3.2 Results

SW480 cells were significantly more sensitive to the effects of treatment with 5-Fu than their metastatic counterpart SW620 (Figure 4.7A and B). Indeed, the SW620 cells were completely 5-Fu resistant up to and including a concentration of 64 µM. Furthermore, lower concentrations of 5-Fu (2-8 µM) actually statistically increased SW620 viability by up to 24.9% ($p<0.05$ vs. control). In contrast, 8 µM 5-Fu was sufficient to decrease SW480 viability by almost 25%. At every concentration of 5-Fu tested, the SW620 line was statistically more resistant than the SW480 cell

line ($p<0.05$, Figure 4.7B). Deferasirox therapy (20 and 40 μM) resulted in a statistically significant reduction in cellular viability in both the SW480 and SW620 cell lines (Figure 4.7C), with no difference seen in efficacy between the 2 lines.

As expected, the HT29 5-Fu resistant 'clone' demonstrated no significant decrease in viability following exposure to 5-Fu at a concentration of 32 μM (Figure 4.7D). In contrast, the parental HT29, SW480 and RKO lines suffered decreased viability in the region of 60-70% (Figure 4.7D). Deferasirox monotherapy was again capable of significantly reducing viability (19.8% reduction vs. control, $p<0.05$) in the 'clone' line which was significantly enhanced further (to 29.9%) following combination with the previously ineffective 5-Fu dose of 32 μM ($p<0.05$ vs. control, 5-Fu alone and Deferasirox alone, Figure 4.7D).

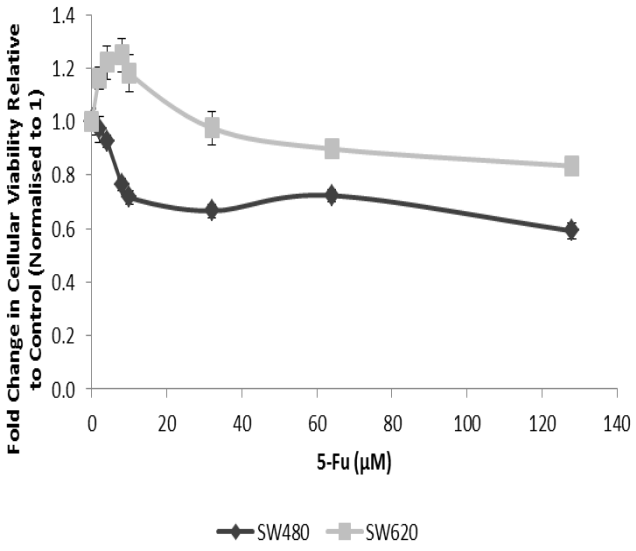

A

	P Value (vs. Matched Control)		
5-Fu (µM)	SW480	SW620	P Value (SW480 vs. SW620)
2	0.683	0.037	0.014
4	0.216	0.020	0.003
8	0.003	0.012	0.000
10	0.001	0.064	0.001
32	0.000	0.775	0.003
64	0.001	0.115	0.000
128	0.000	0.021	0.000

B

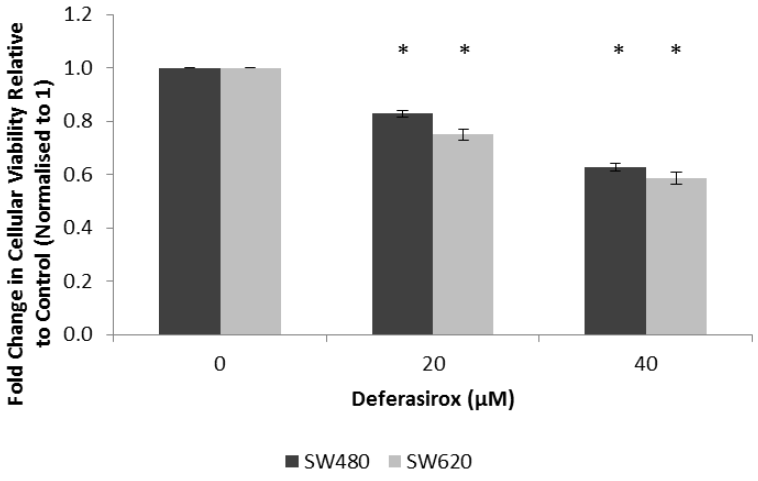

C

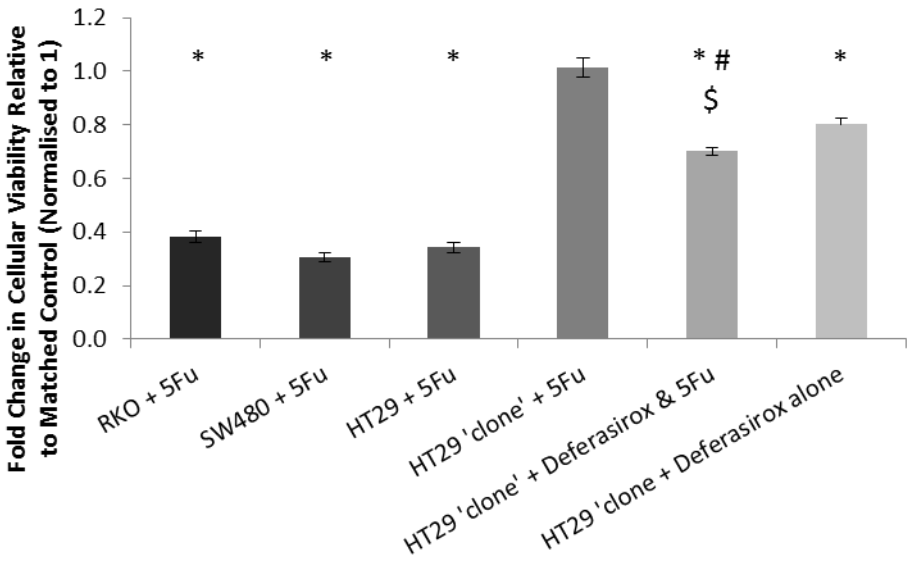

D

Figure 4.7 Deferasirox can overcome colonic 5-Fu resistance *in-vitro*

Cell viability assay demonstrating the varying response to 5-Fu seen in the colonic cell lines SW480 and SW620 (A). The SW620 cell line is 5-Fu resistant up to a concentration of 128 µM and actually increases its viability at lower doses (2-8 µM) compared to control (B). Despite this, Deferasirox induces a significant reduction in cellular viability when administered (C) with no difference in efficacy seen between the 2 cell lines at the doses tested. Deferasirox (20 µM) is also capable if inducing a significant reduction in cellular viability when administered to a 'clone' of HT29 cells that are 5-Fu resistant (up to 32 µM, (D)). In this model, the combination of Deferasirox (20 µM) with the previously ineffective 5-Fu dose of 32 µM generated a significant reduction in cellular viability greater than that seen compared to both control and Deferasirox alone. Data points represent mean fold change relative to standard media control (normalised to 1), error bars denote ±SEM, * $p<0.05$ vs. matched control, # $p<0.05$ vs. 32 µM 5-Fu alone, $ $p<0.05$ vs. Deferasirox alone.

4.3.4 The efficacy of Deferasirox in colorectal adenoma cell lines

4.3.4.1 Overview

In order to compare the efficacy of Deferasirox in colorectal adenoma and adenocarcinoma cell lines the colorectal adenoma cell lines AAC1 and RGC2 and the adenocarcinoma cell lines RKO and SW480 were treated with either standard media (control) or media containing Deferasirox (40 μM). Following 48 hours of treatment cellular proliferation was assessed by BrdU assay (as previously outlined).

4.3.4.2 Results

Deferasirox therapy had a profound effect on cellular proliferation across all 4 of the lines tested, reducing cellular proliferation to 60.3, 57.8, 30.9 and 25.6% of control in the AAC1, RGC2, RKO and SW480 cells respectively ($p<0.05$ vs. control for each, Figure 4.8). Of note, Deferasirox was statistically more effective in both the RKO and SW480 adenocarcinoma lines.

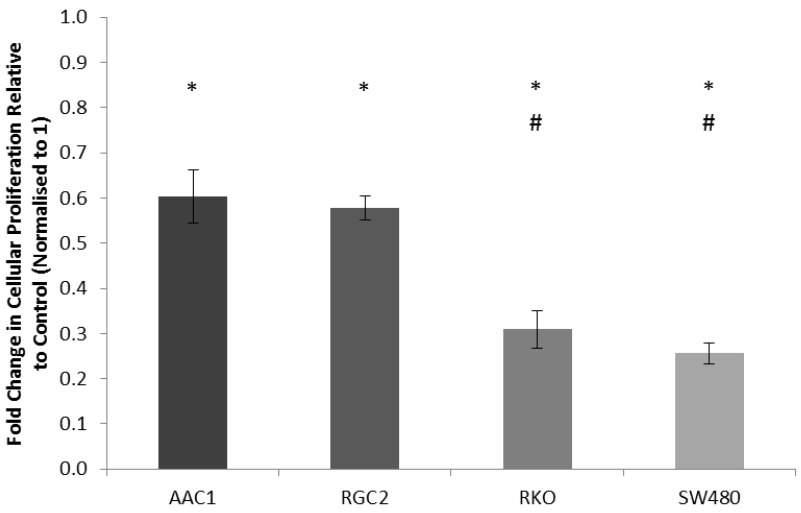

Figure 4.8 Deferasirox appears to be more efficacious in more advanced colonic adenocarcinoma cell lines

Cellular proliferation assay (BrdU) demonstrating the difference in efficacy seen when Deferasirox (40 µM for 48 hours) was administered to 2 colonic adenoma (AAC1 and RGC2) and 2 colonic adenocarcinoma (RKO and SW480) cell lines. Data points represent mean fold change relative to matched standard media control, error bars denote ±SEM, * $p<0.05$. vs. matched control for each cell line, # $p<0.05$ vs. AAC1 and RGC2.

4.3.5 The effect of pertinent genetic mutations and hypoxia upon Deferasirox efficacy *in-vitro*

4.3.5.1 Overview

Following the demonstration in section 4.3.4 that Deferasirox appeared to be more efficacious in advanced adenocarcinoma lines than it was in pre-cursor adenomas, the effect of genetic mutations key to the development of colorectal adenocarcinoma (Apc and p53) upon Deferasirox efficacy were investigated. In addition, the effect of incubation with the drug in a hypoxic environment was also investigated as this is known to play a key role in cancer therapy resistance. [240]

To delineate the effect of APC status upon Deferasirox efficacy the HT29 APC wild type inducible cell line was utilised. This cell line expresses wild type APC following incubation with zinc chloride (100 μM) for 24 hours. [63] APC expression was inferred through a Western blot of β-catenin expression (after 48 hours of treatment with zinc chloride) and a BrdU cell proliferation assay.

The effect of p53 mutation on Deferasirox efficacy was delineated by use of the isogenic cell lines HCT116 p53 wild type (WT) and HCT116 p53-/-. [196] Following confirmation of p53 status via Western blotting, both p53 WT and -/- cells were seeded into 96 well plates and subjected to increasing concentrations of Deferasirox (0-160 μM) for 48 hours. Both cell lines were also exposed to increasing concentrations of 5-Fu (0-128 μM) as a positive control for the effect of p53 status on treatment efficacy. MTT cell viability assays were then performed.

Finally, the effect of hypoxia on Deferasirox efficacy was ascertained by exposing HCT116 p53WT cells to a 1% O_2 chamber for 18-24 hours prior to treatment with the drug (0-80 μM). Induction of hypoxia was confirmed through Western blotting for HIF-1α expression. Again, a control group

treated exactly the same except for exposure to hypoxia was included. An SRB proliferation assay was then performed on both groups (as previously outlined in chapter 2.2.19).

4.3.5.2 Results

Exposure of HT29 cells to 100μM zinc chloride for 48 hours resulted in a decrease in β-catenin protein expression and a concomitant reduction in cellular proliferation as per BrdU (Figure 4.9A). When Deferasirox was administered to the HT29 APC WT and MT lines, an increase in efficacy was evident in the cells still harbouring an APC mutation compared to those now expressing APC. This increase ranged from 16.2-35.6% (depending on the dose) and was statistically significant at all doses used except 160 μM (Figure 4.9B).

HCT116 p53WT and HCT116 p53-/- are isogenic and differ only in p53 status (Figure 4.10A). P53 status significantly effected HCT116 response to treatment with 5-Fu (Figure 4.10B), with the p53-/- cells demonstrating a marked reduction in response to the drug (14.2-52.4% reduction in efficacy, $p<0.05$ vs. p53WT for all doses, Figure 4.10B). Deferasirox therapy, however, did not appear to be influenced by p53 status (Figure 4.10C), with no statistical difference seen in efficacy between any of the doses tested.

HIF-1α expression (and thus hypoxia) was markedly induced following exposure of HCT116 cells to 1% O_2 for 18-24 hours (Figure 4.11A). Although a trend for a reduction in cellular proliferation with Deferasirox under hypoxic conditions was seen across all concentrations tested, Deferasirox therapy did not achieve a statistically significant reduction compared to control at any of the doses tested (Figure 4.11B). In contrast, statistically significant suppression of cellular proliferation was achieved across all concentrations when the drug was used under normoxic conditions (Figure 4.11B).

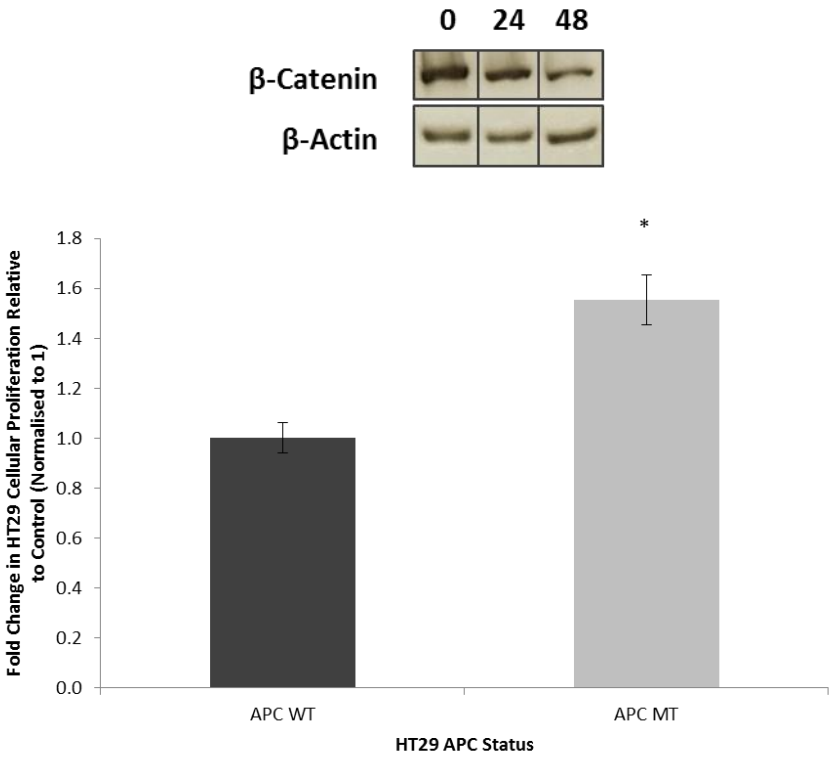

A

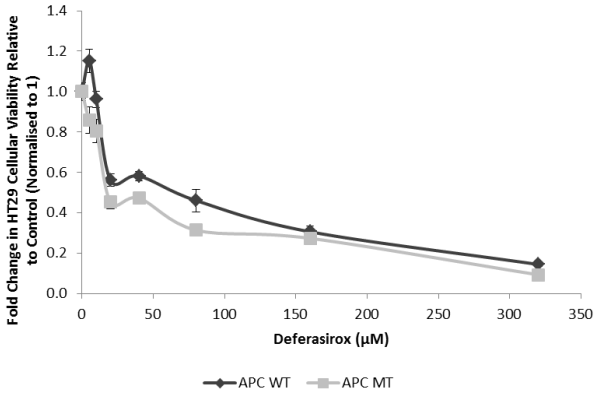

Deferasirox (μM)	APC MT % Change in Efficacy	P Value for Difference
5	25.6	0.004
10	16.2	0.045
20	19.5	0.025
40	18.8	0.006
80	31.9	0.033
160	10.6	0.273
320	35.6	0.000

B

Figure 4.9 Deferasirox appears to be more efficacious in the background of an APC mutation

Western blot (A) demonstrating reduction in β-catenin expression when HT29 cells are exposed to 100 μM zinc chloride for 24-48 hours. This reduction in β-catenin is taken as inference of restoration of APC expression and thus, as would be expected, a significant reduction in cellular proliferation (BrdU, (A)) is also seen. Subsequent cell viability assay (MTT, (B)) demonstrating the increased efficacy of Deferasirox in the presence of increased β-catenin (and thus an APC mutation). P values for % increase in efficacy with an APC mutation at equivalent doses of Deferasirox are displayed in the table in (B). Data points represent mean fold change relative to standard media control (normalised to 1), error bars denote ±SEM, * $p<0.05$ vs. standard media control.

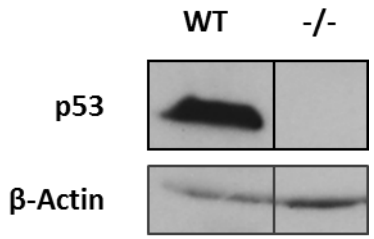

A

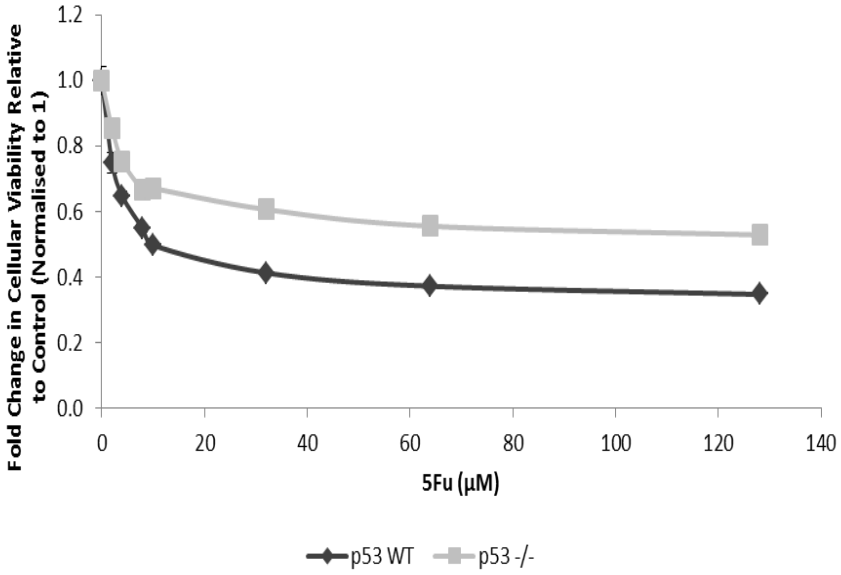

5Fu (µM)	p53 -/- % Change in Efficacy	P Value for Difference
2	-14.2	0.018
4	-16.4	0.003
8	-21.9	0.000
10	-34.8	0.000
32	-46.9	0.000
64	-49.3	0.000
128	-52.4	0.000

B

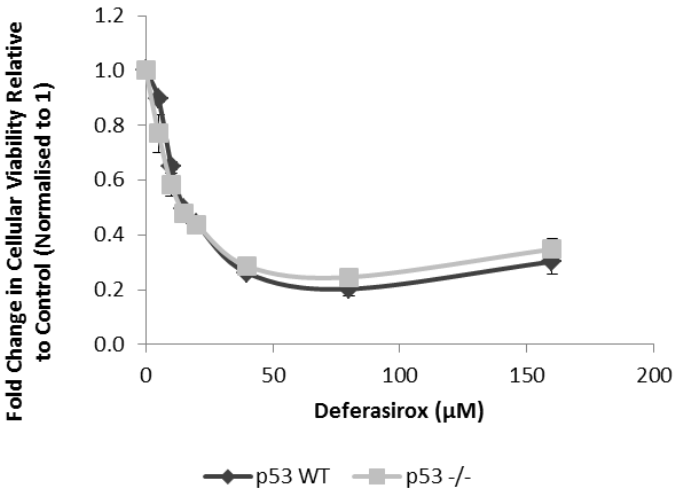

Deferasirox (µM)	p53 -/- % Change in Efficacy	P Value for Difference
5	14.0	0.209
10	10.4	0.234
15	2.8	0.522
20	0.8	0.929
40	-9.5	0.372
80	-21.2	0.330
160	-14.9	0.502

C

Figure 4.10 Deferasirox efficacy is not influenced by p53 status *in-vitro*

Western blot (A) confirming the p53 status of the isogenic cell lines HCT116 p53WT and HCT116 p53-/-. The HCT116 p53-/- cells have a significantly reduced response to 5-Fu across all concentrations tested (cell viability assay, (B)). This is not the cases with Deferasirox, however, which displayed no statistical differences in magnitude of cell viability reduction (C) dependent on p53 expression across the range of concentrations tested. Data points represent mean fold change relative to matched standard media control (normalised to 1), error bars denote ±SEM, * $p<0.05$ vs. matched control.

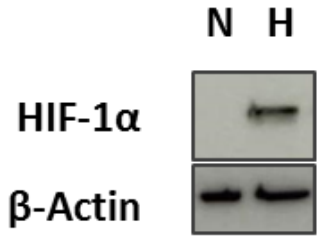

A

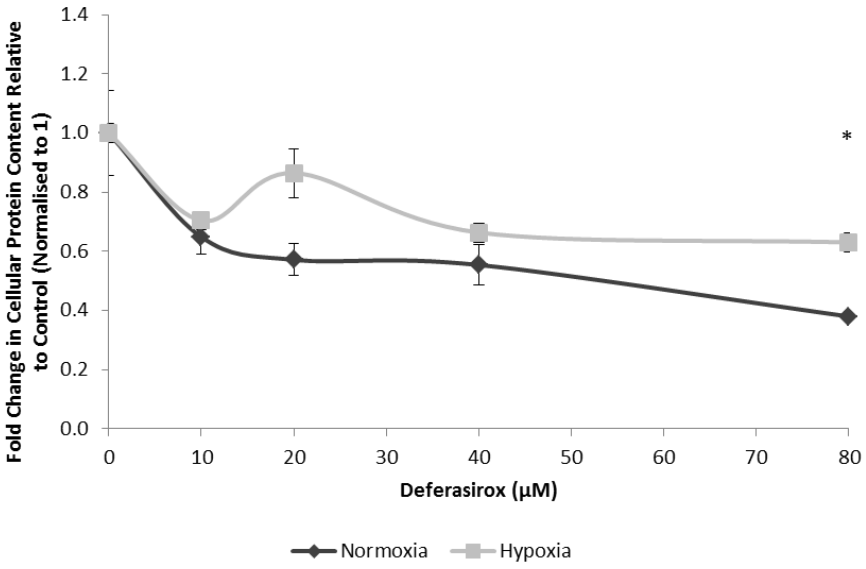

	P Value vs. Control	
Deferasirox (μM)	Normoxia	Hypoxia
10	0.003	0.133
20	0.001	0.484
40	0.002	0.099
80	0.000	0.077

B

Figure 4.11 Deferasirox did not induce a significant reduction in cellular proliferation under hypoxic conditions

Western blot demonstrating increased HIF 1α expression following exposure of HCT116 p53WT cells to 1% $p0_2$ for 24 hours (A, lane N = normoxia, lane H = hypoxia). SRB assay demonstrating the inability of Deferasirox to induce a statistically significant reduction in the same colonic cells once hypoxia had been induced (B). Data points represent mean fold change relative to standard media control (normalised to 1), error bars denote ±SEM, * $p<0.05$ vs. equivalent dose of Deferasirox in normoxia, grey boxes within table denote $p<0.05$ vs. matched control.

4.3.6 The effect of Deferasirox administration upon murine intestinal phenotype

4.3.6.1 Overview

To further delineate the efficacy of Deferasirox as a potential therapy for colorectal adenocarcinoma, the drug was administered orally to Villin-CreER^{+} Apc$^{fl/fl}$ transgenic mice. Tamoxifen administration intraperitoneally on day 1 (80 mg/kg) deletes both copies of the APC gene throughout the intestine and a hyper-proliferative phenotype rapidly develops over the ensuing days.

Deferasirox was administered orally as a single dose on day 5 and the mice were then taken 6 hours post treatment. The intestine was immediately harvested and processed for H&E, Caspase-3 and Phospho-Histone H3 staining as outlined in the methods section. Slides were then scored as previously described.

Deferasirox was administered at a dose of either 20 or 200 mg/kg as a single 200 µl oral gavage using 30% 1,2-propanediol/70% sterile 0.9% sodium chloride solution as a vehicle. In addition, the drug was also administered at a dose of 100 mg/kg in a modified vehicle of 30mM sodium carbonate / 3 mM TRIS (again 200 µl single gavage). The latter vehicle was utilised in an attempt to see if improved drug solubility improved subsequent efficacy.

4.3.6.2 Results

At a dose of 20 mg/kg Deferasirox administration did not significantly alter either mitosis or apoptosis (Figure 4.12 A + B). When utilised at the higher dose of 200 mg/kg, however, a statistically

significant suppression in mitosis (52.4% reduction vs. control, $p<0.05$, Figure 4.13) and an induction of apoptosis (65.2% increase vs. control, $p<0.05$) was seen (Figure 4.14).

The administration of Deferasirox at a dose of 100 mg/kg (in the Na_2CO_3/TRIS vehicle) to APC wild type mice significantly suppressed mitosis (Figure 4.15) but had no effect upon apoptosis. A statistically significant increase in apoptosis was seen (64.3% increase vs. control, $p<0.05$, Figure 4.16), however, when Deferasirox was utilised at a dose of 100 mg/kg in the Villin-CreER^{+} Apc$^{fl/fl}$ mice.

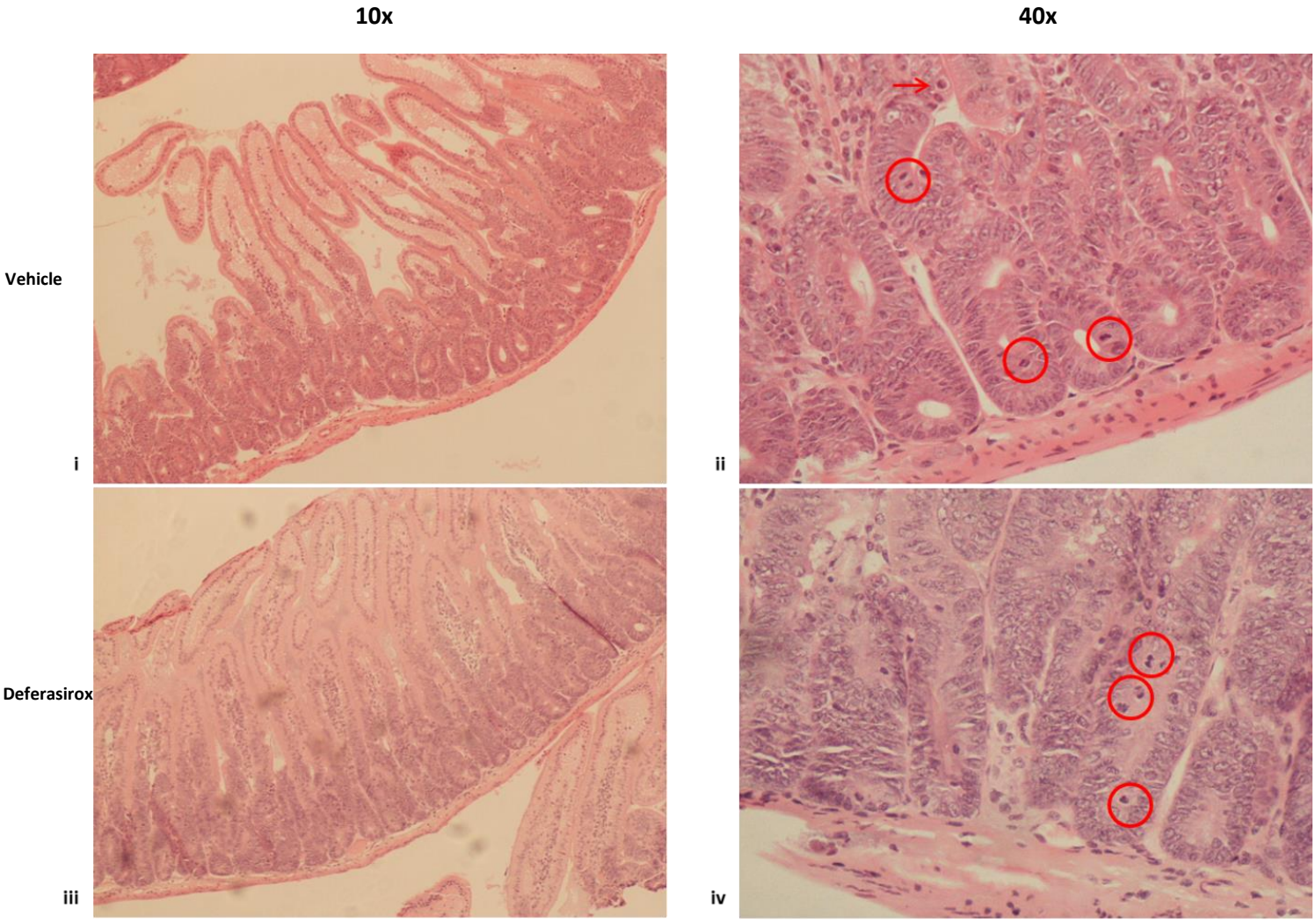
10x
40x
Vehicle
Deferasirox
i
ii
iii
iv

A

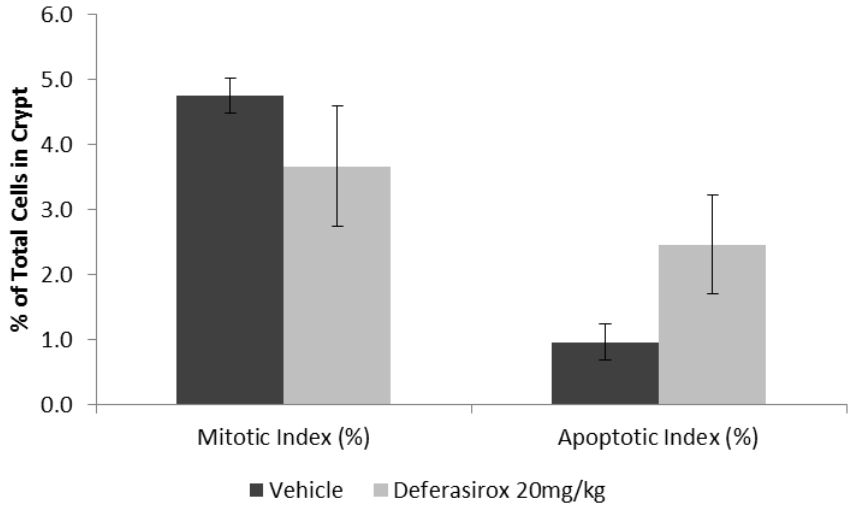
6.0
5.0
4.0
3.0
2.0
1.0
0.0
% of Total Cells in Crypt
Mitotic Index (%)
Apoptotic Index (%)
Vehicle
Deferasirox 20mg/kg

B

Figure 4.12 Deferasirox did not significantly alter intestinal proliferation when given at a dose of 20 mg/kg to Villin-CreER^{+} Apc$^{fl/fl}$ mice

Representative H&E images (A) of intestinal crypts (i and ii = Vehicle, iii and iv = Deferasirox) 6 hours post exposure to Deferasirox at a dose of 20 mg/kg orally. Circles indicate mitotic figures, arrows indicate apoptotic bodies. Mitotic and apoptotic indexes (B) indicative of proportion of cells per intestinal crypt in mitosis or apoptosis. Data points plotted indicate mean index score, error bars denote ±SEM. Higher powered images taken at 40x, lower at 10x.

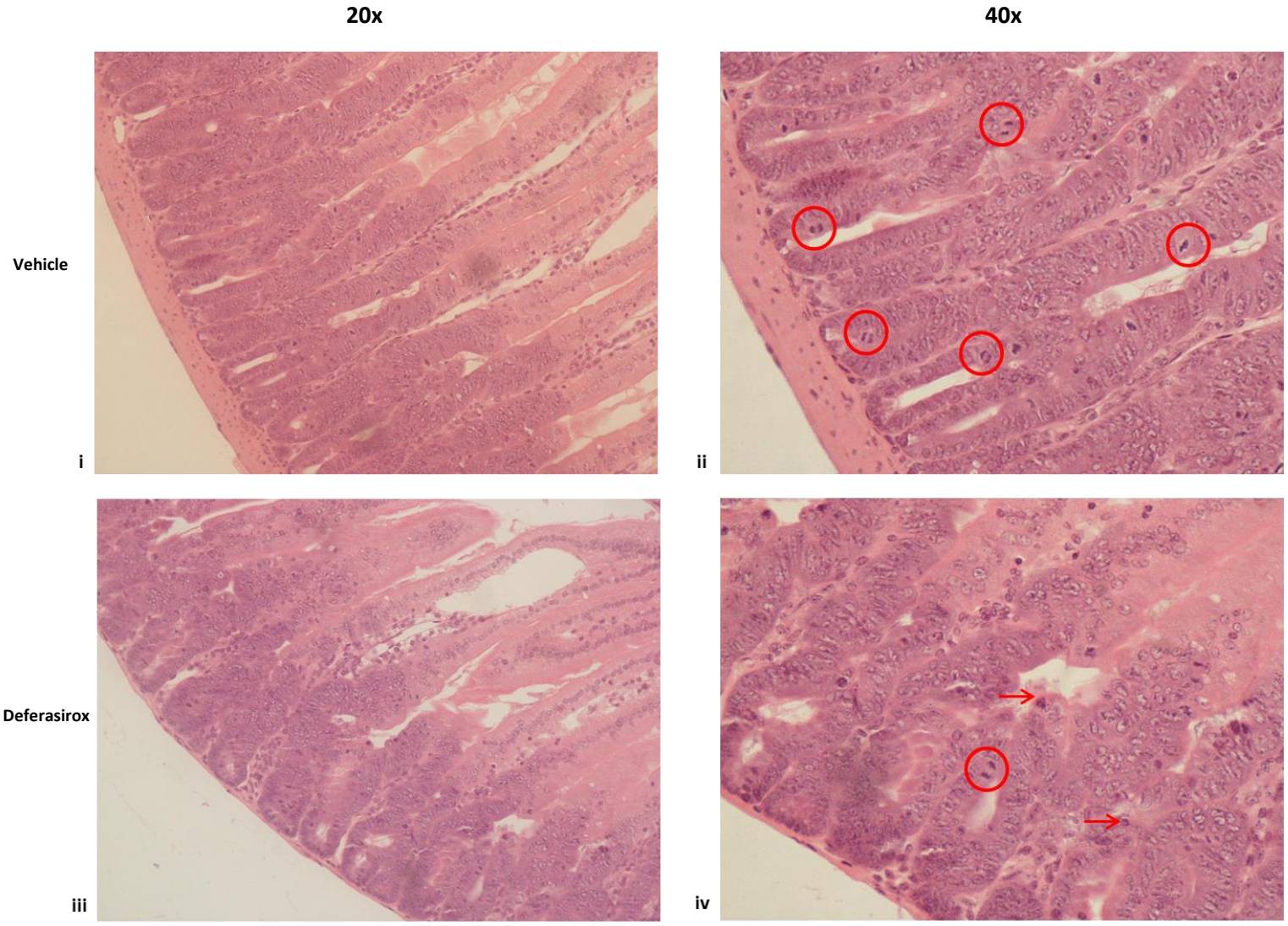
20x
40x
Vehicle
i
ii
Deferasirox
iii
iv

A

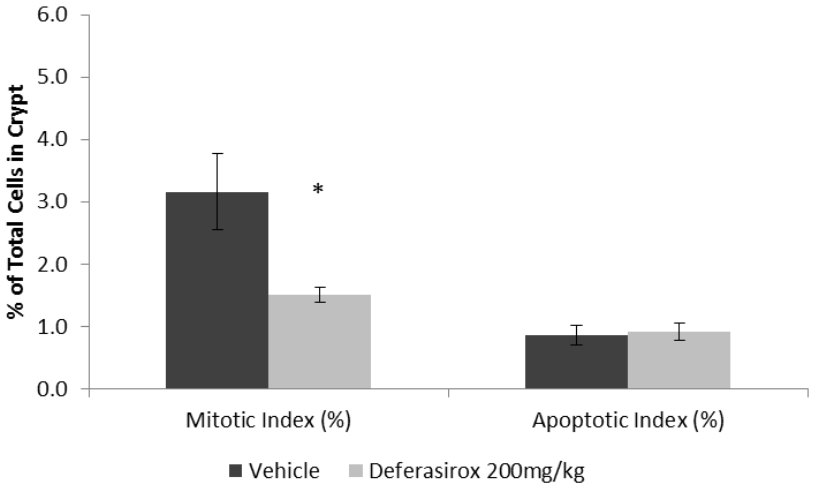
6.0
5.0
4.0
3.0
2.0
1.0
0.0
% of Total Cells in Crypt
*
Mitotic Index (%)
Apoptotic Index (%)
Vehicle
Deferasirox 200mg/kg

B

Figure 4.13 Deferasirox significantly suppresses mitosis within intestinal crypts when given at a dose of 200 mg/kg to Villin-CreER^{+} Apc$^{fl/fl}$ mice

Representative H&E images (A) of intestinal crypts (i and ii = Vehicle, iii and iv = Deferasirox) 6 hours post exposure to Deferasirox at a dose of 200 mg/kg orally. Circles indicate mitotic figures, arrows indicate apoptotic bodies. Mitotic and apoptotic indexes (B) indicative of proportion of cells per intestinal crypt in mitosis or apoptosis. Data points plotted indicate mean index score, error bars denote ±SEM, * $p<0.05$ vs. vehicle. Higher powered images taken at 40x, lower at 20x.

Phospho-Histone H3 Expression

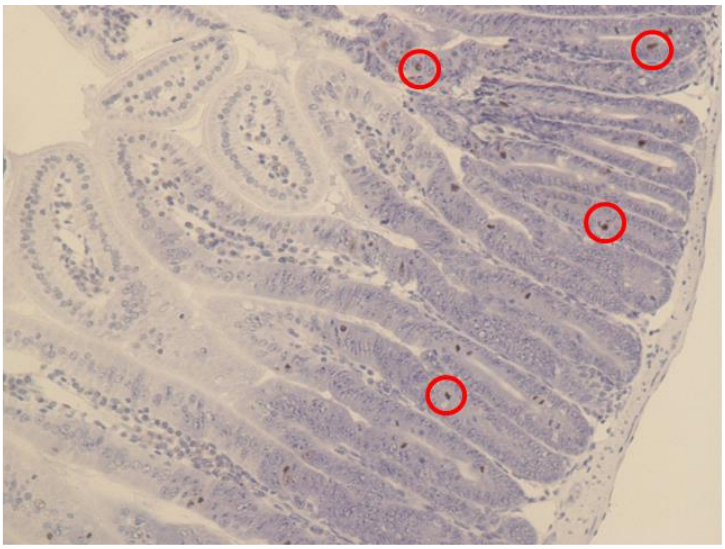

Vehicle

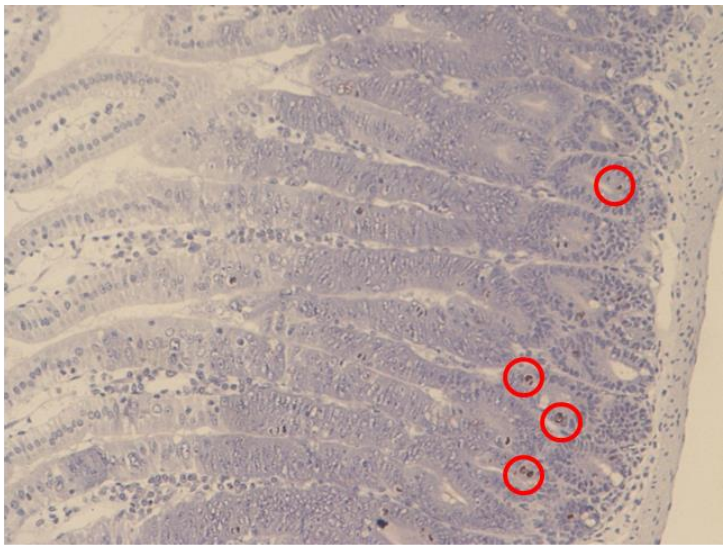

Deferasirox 200mg/kg

A

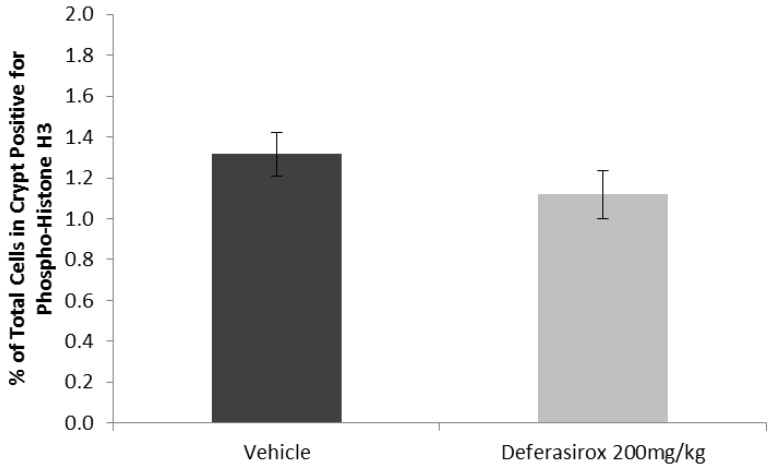

B

Cleaved Caspase-3

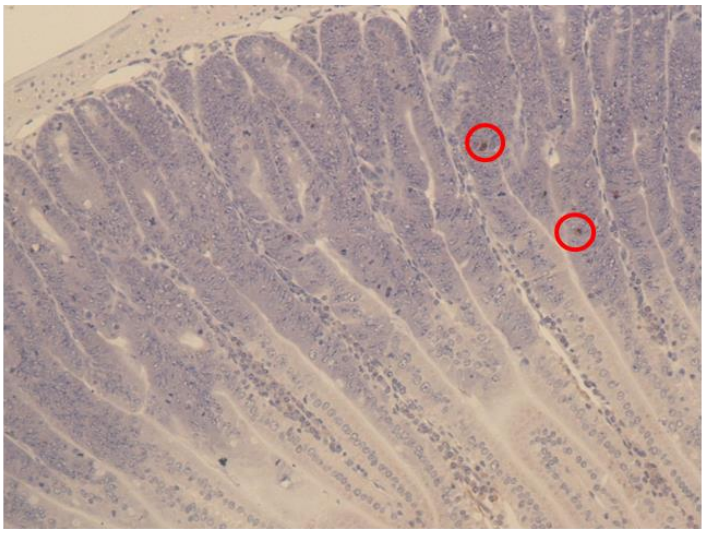

Vehicle

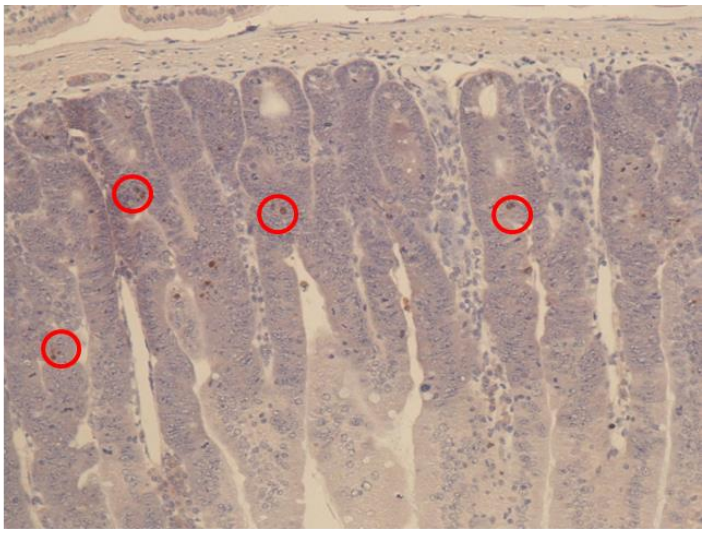

Deferasirox 200mg/kg

C

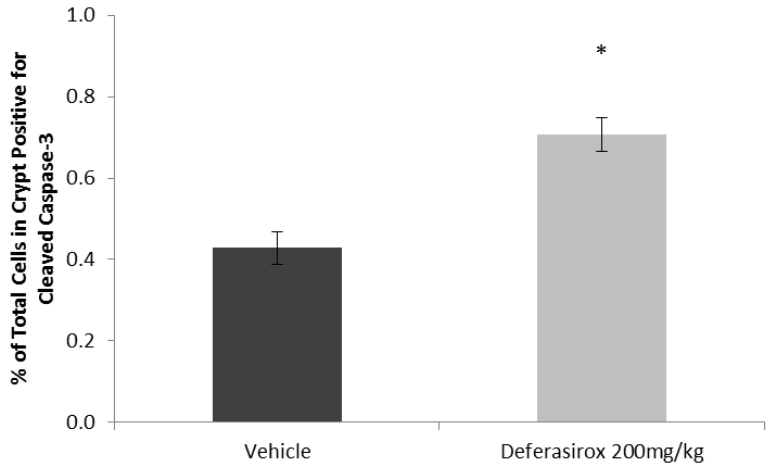

D

Figure 4.14 Deferasirox significantly stimulates apoptosis within intestinal crypts when given at a dose of 200 mg/kg to Villin-CreER^{+} Apc$^{fl/fl}$ mice

Staining of intestinal crypts for the mitosis marker Phospho-Histone H3 (A + B) and the apoptosis marker Caspase-3 (C and D) on tissue obtained 6 hours post exposure to Deferasirox at a dose of 200 mg/kg PO. Representative images (A and C) demonstrating positively stained cells within crypts (red circles delineate examples of positive staining). Error bars denote ±SEM, * $p<0.05$ vs. vehicle. Images taken at 20x.

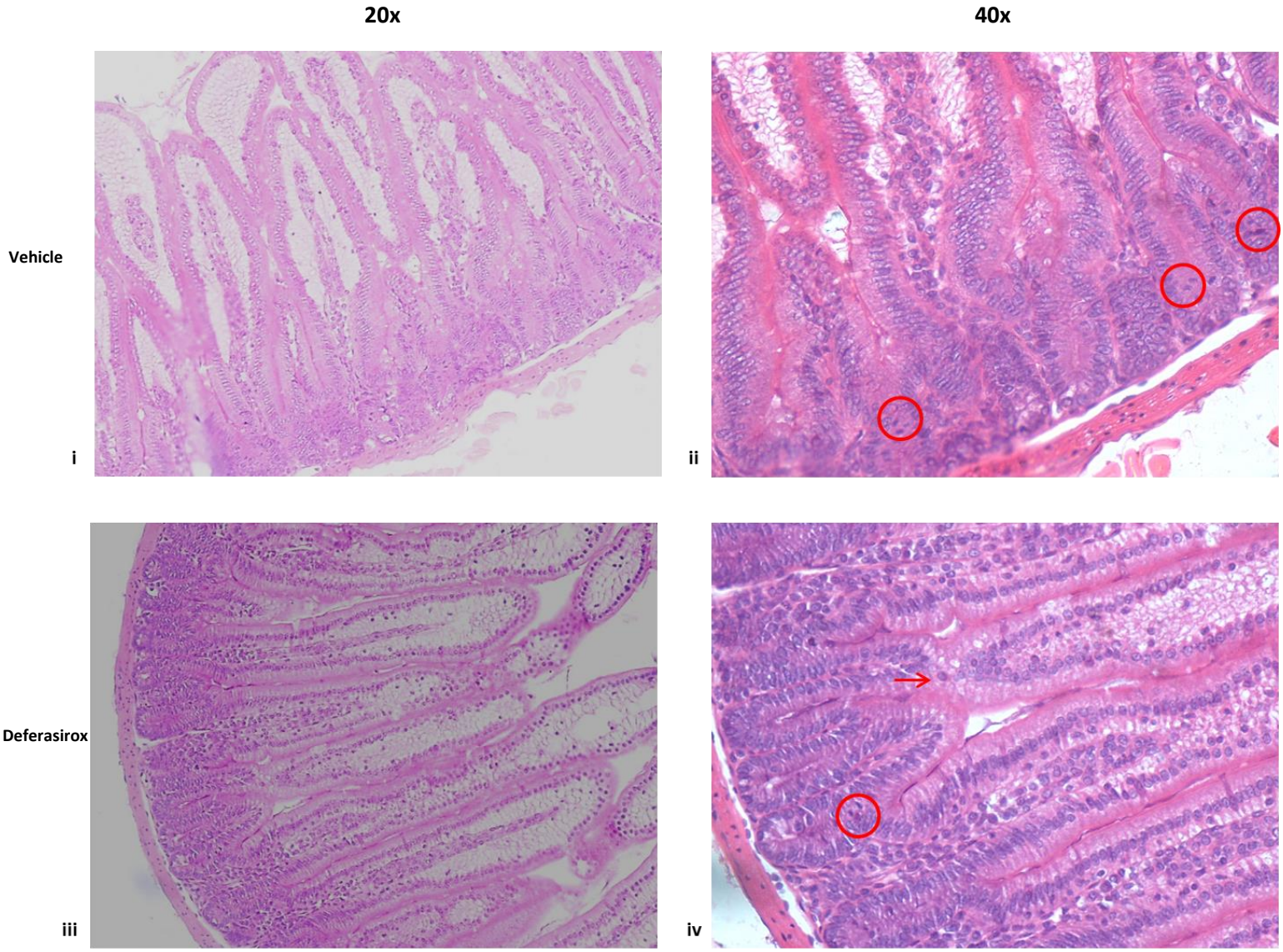
20x
40x
Vehicle
i
ii
Deferasirox
iii
iv

A

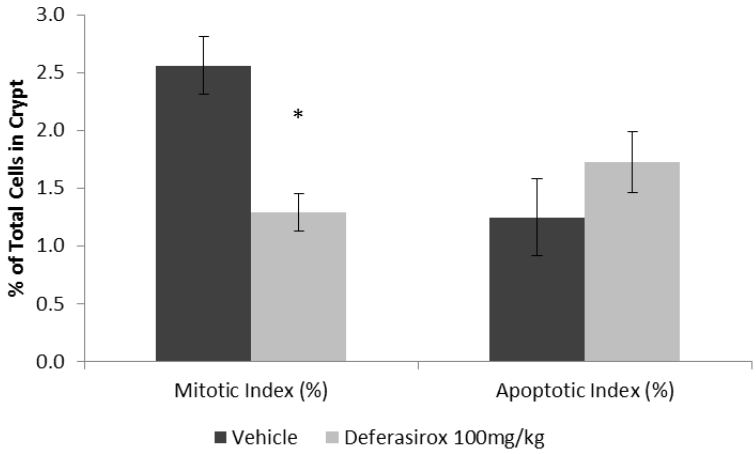
3.0
2.5
2.0
1.5
1.0
0.5
0.0
% of Total Cells in Crypt
*
Mitotic Index (%)
Apoptotic Index (%)
Vehicle
Deferasirox 100mg/kg

B

Phospho-Histone H3

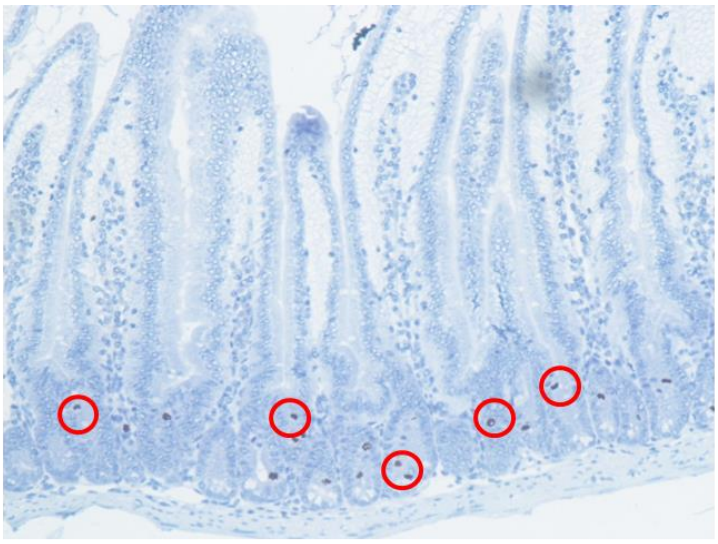

Vehicle

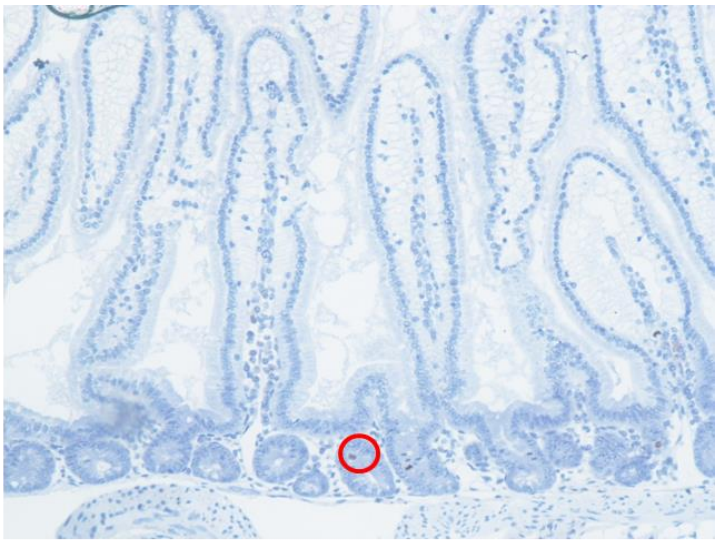

Deferasirox 100mg/kg

C

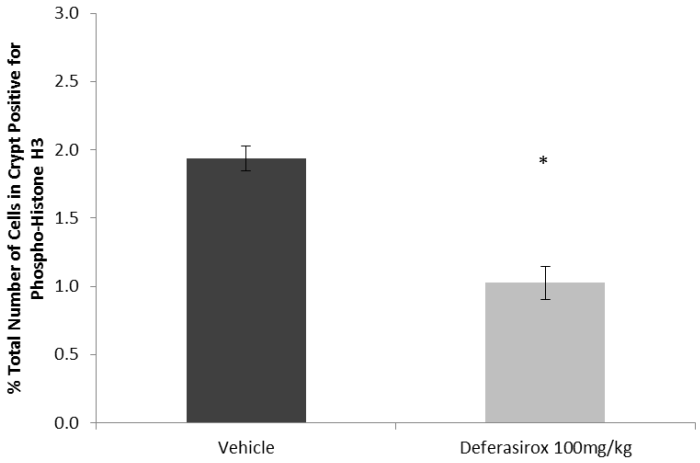

D

Cleaved Caspase-3

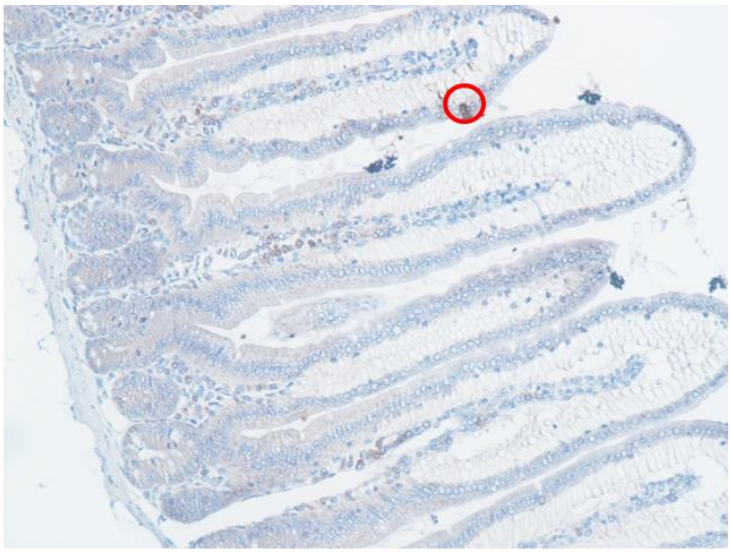

Vehicle

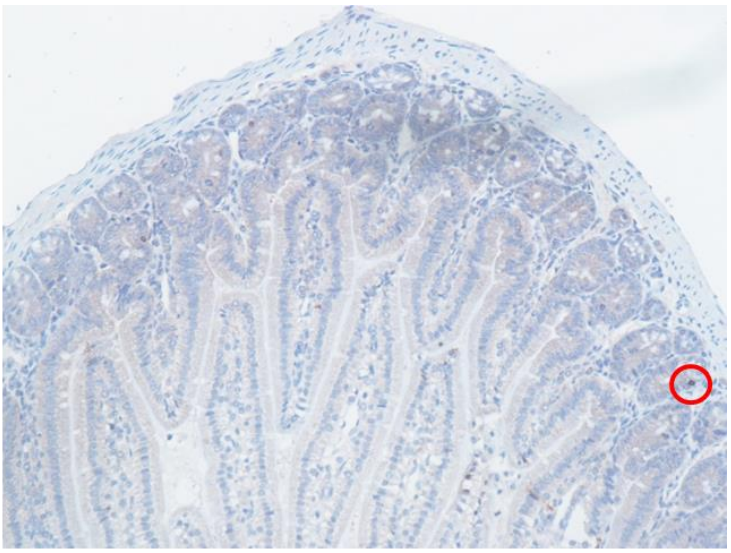

Deferasirox 100mg/kg

E

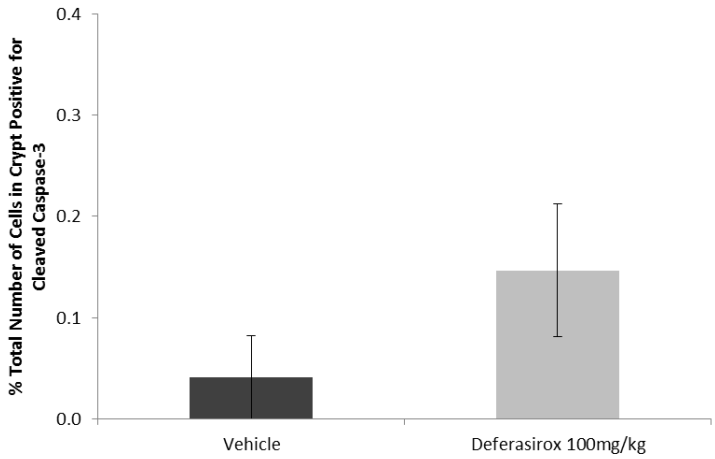

F

Figure 4.15 Deferasirox significantly suppresses mitosis within intestinal crypts when given at a dose of 100 mg/kg to WT APC mice

Representative H&E images (A) of intestinal crypts (i and ii = Vehicle, iii and iv = Deferasirox) 6 hours post exposure to Deferasirox at a dose of 100 mg/kg orally. Circles indicate mitotic figures, arrows indicate apoptotic bodies. Mitotic and apoptotic indexes (B) indicative of proportion of cells per intestinal crypt in mitosis or apoptosis.

Staining of intestinal crypts for the mitosis marker Phospho-Histone H3 (C + D) and the apoptosis marker Caspase-3 (E and F) on tissue obtained 6 hours post exposure to Deferasirox at a dose of 100 mg/kg PO. Representative images (C and E) demonstrating positively stained cells within crypts (red circles here exemplify positive staining).

Data points plotted indicate mean index score, error bars denote ±SEM, * $p<0.05$ vs. vehicle. Higher powered images taken at 40x, lower at 20x.

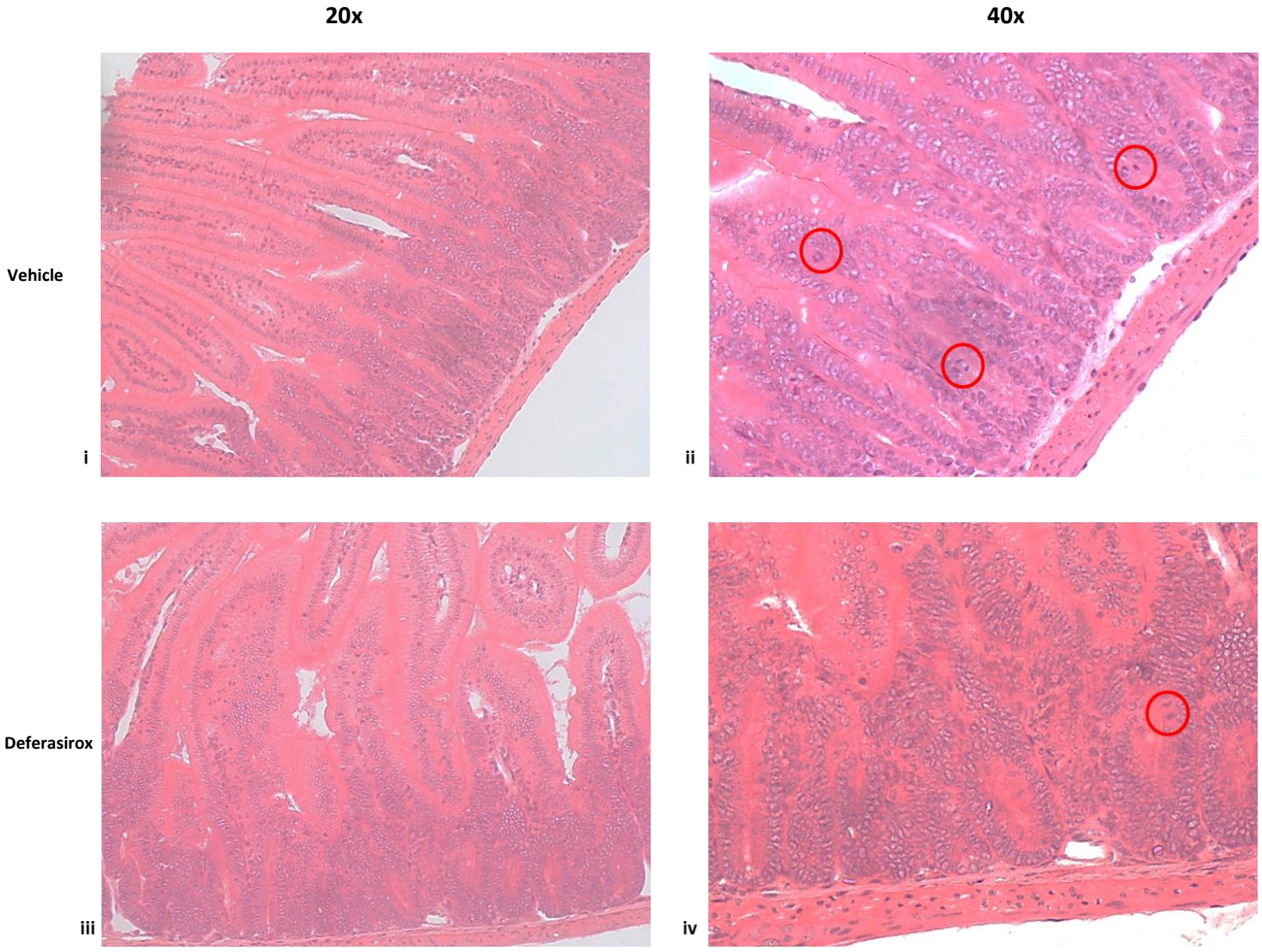
20x
40x
Vehicle
i
ii
Deferasirox
iii
iv

A

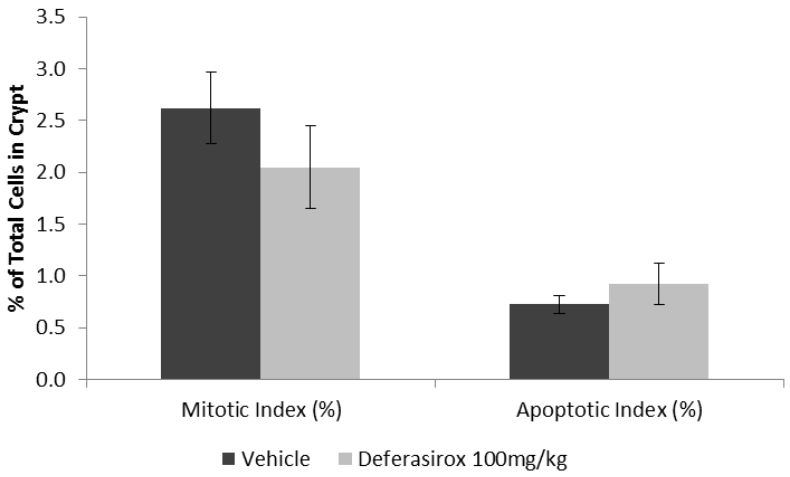
3.5
3.0
2.5
2.0
1.5
1.0
0.5
0.0
% of Total Cells in Crypt
Mitotic Index (%)
Apoptotic Index (%)
Vehicle
Deferasirox 100mg/kg

B

Phospho-Histone H3

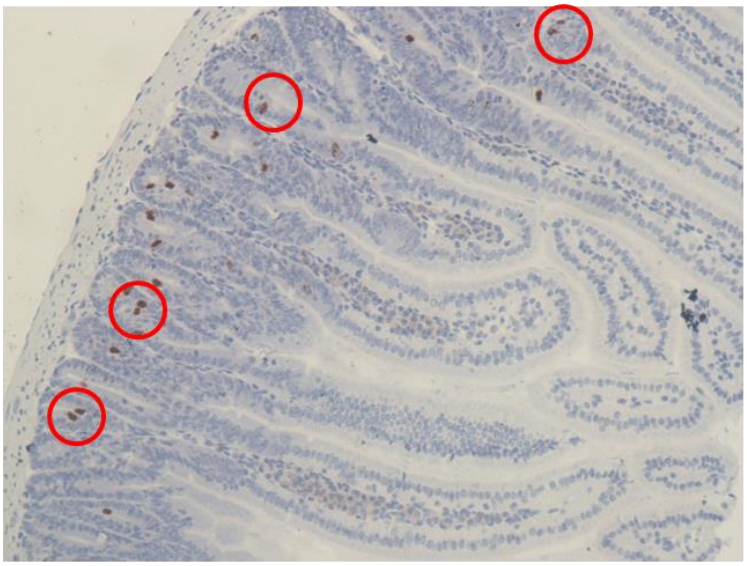

Vehicle

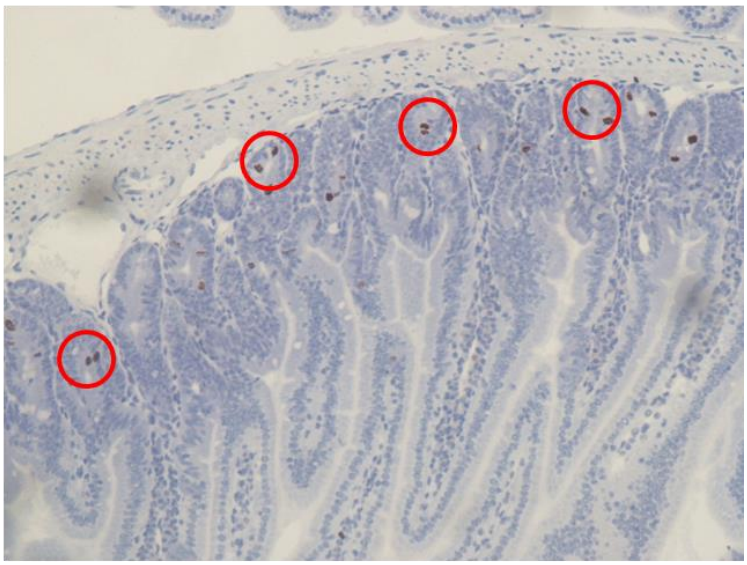

Deferasirox 100mg/kg

C

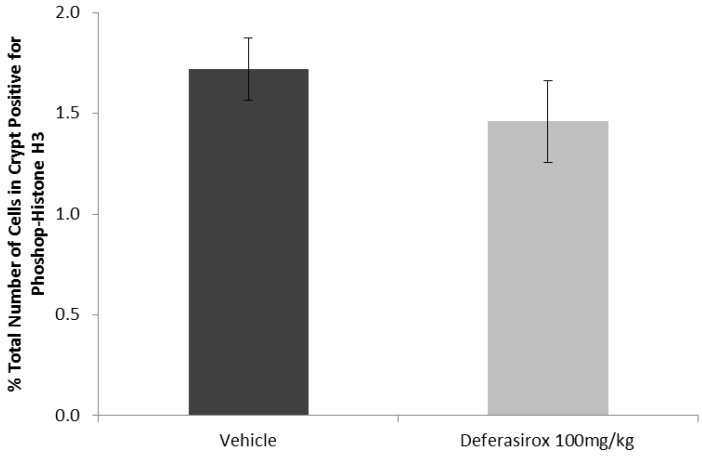

D

Cleaved Caspase-3

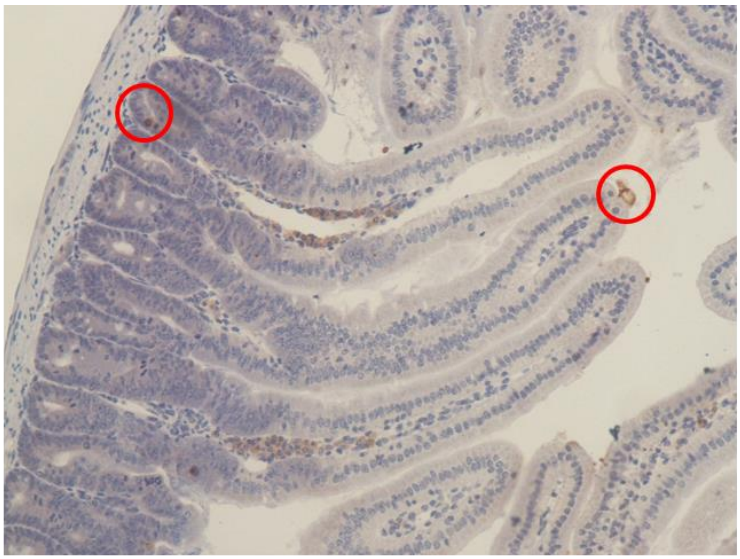

Vehicle

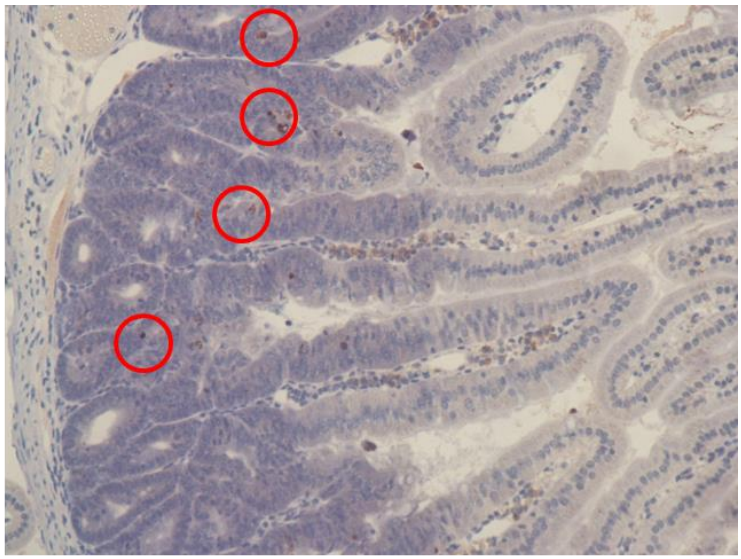

Deferasirox 100mg/kg

E

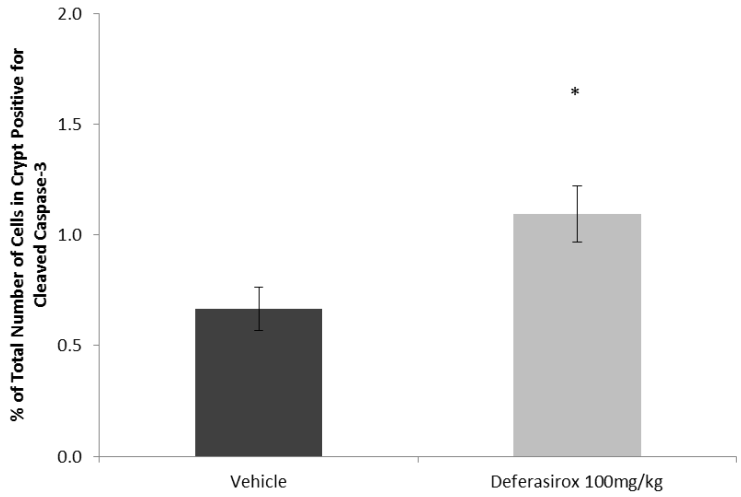

F

Figure 4.16 Deferasirox significantly stimulates apoptosis within intestinal crypts when given at a dose of 100 mg/kg to Villin-CreER^{+} Apc$^{fl/fl}$ mice

Representative H&E images (A) of intestinal crypts (i and ii = Vehicle, iii and iv = Deferasirox) 6 hours post exposure to Deferasirox at a dose of 100 mg/kg PO. Circles indicate mitotic figures, arrows indicate apoptotic bodies. Mitotic and apoptotic indexes (B) indicative of proportion of cells per intestinal crypt in mitosis or apoptosis.

Staining of intestinal crypts for the mitosis marker Phospho-Histone H3 (C + D) and the apoptosis marker Caspase-3 (E and F) on tissue obtained 6 hours post exposure to Deferasirox at a dose of 100mg/kg PO. Representative images (C and E) demonstrating positively stained cells within crypts (red circles exemplify positive stained cells).

Data points plotted indicate mean index score, error bars denote ±SEM, * $p<0.05$ vs. vehicle. Higher powered images taken at 40x, lower at 20x.

4.3.7. The effect of Deferasirox upon murine survival

4.3.7.1 Overview

In order to ascertain whether or not the effects of Deferasirox upon murine intestinal phenotype translate into increased survival, the Lgr5-CreER^{+} APC$^{fl/fl}$ and Lgr5-CreER^{+} APC$^{fl/fl}$ Pten$^{fl/fl}$ transgenic mice models were utilised.

Mice were induced with Tamoxifen (as outlined in the methods section) and commenced treatment with Deferasirox at either 200 mg/kg (30% 1,2-propanediol/70% sterile 0.9% sodium chloride solution as a vehicle) or 100 mg/kg (30 mM sodium carbonate / 3 mM TRIS vehicle) or vehicle alone (as a control) as a 200 µl oral gavage 3 times per week. Mouse health was monitored daily throughout treatment and mice were taken immediately upon showing any signs of deteriorating health.

4.3.7.2 Results

Deferasirox failed to increase murine survival in the Lgr5-CreER^{+} APC$^{fl/fl}$ murine model in either of the dosing regimens tested (Figure 4.17 and 4.18).

Interestingly, in the more aggressive Lgr5-CreER^{+} APC$^{fl/fl}$ Pten$^{fl/fl}$ model Deferasirox showed a trend towards increased survival compared to vehicle (52.3 days vs. 39.8 days)), although this was not statistically significant (p=0.512 vs. vehicle, Figure 4.19).

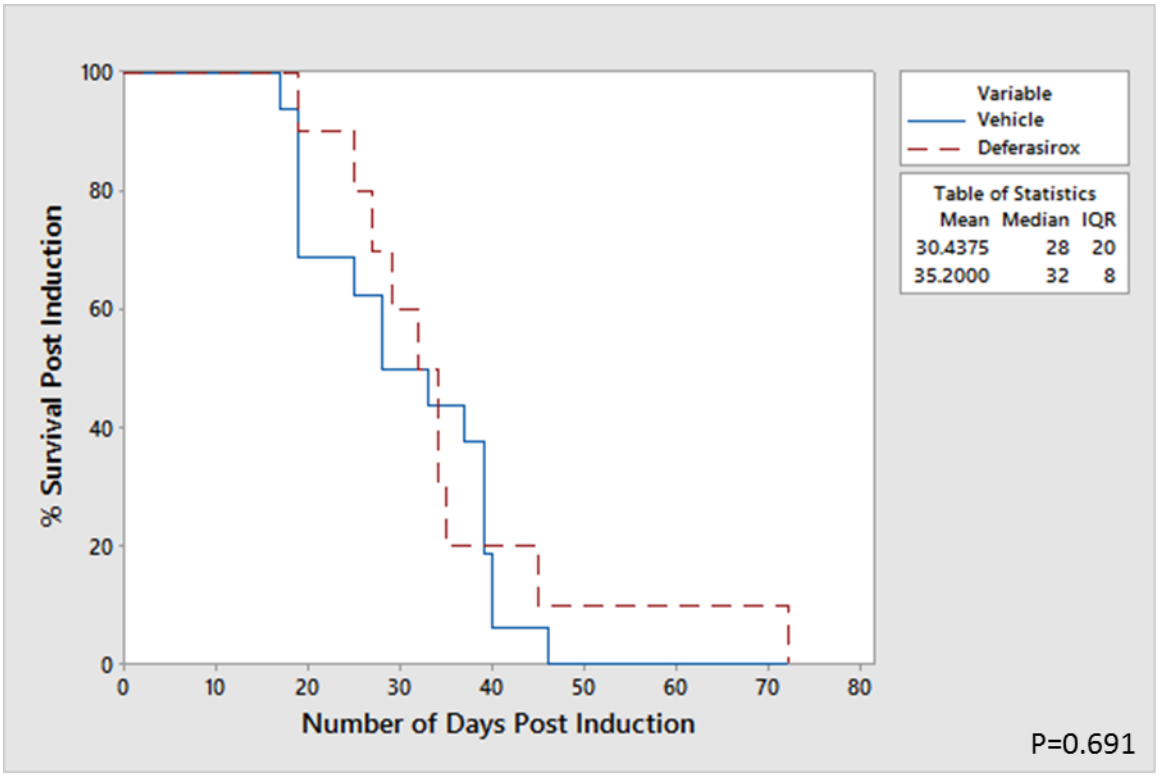

Figure 4.17 Deferasirox did not significantly extend survival when given to Lgr5-CreER^{+} APC$^{fl/fl}$ mice at a dose of 200 mg/kg

Survival plot for Lgr5-CreER^{+} APC$^{fl/fl}$ mice treated with either vehicle or Deferasirox (200 mg/kg) by oral gavage 3 times per week. P value quoted is for log-rank test of survival between the 2 groups.

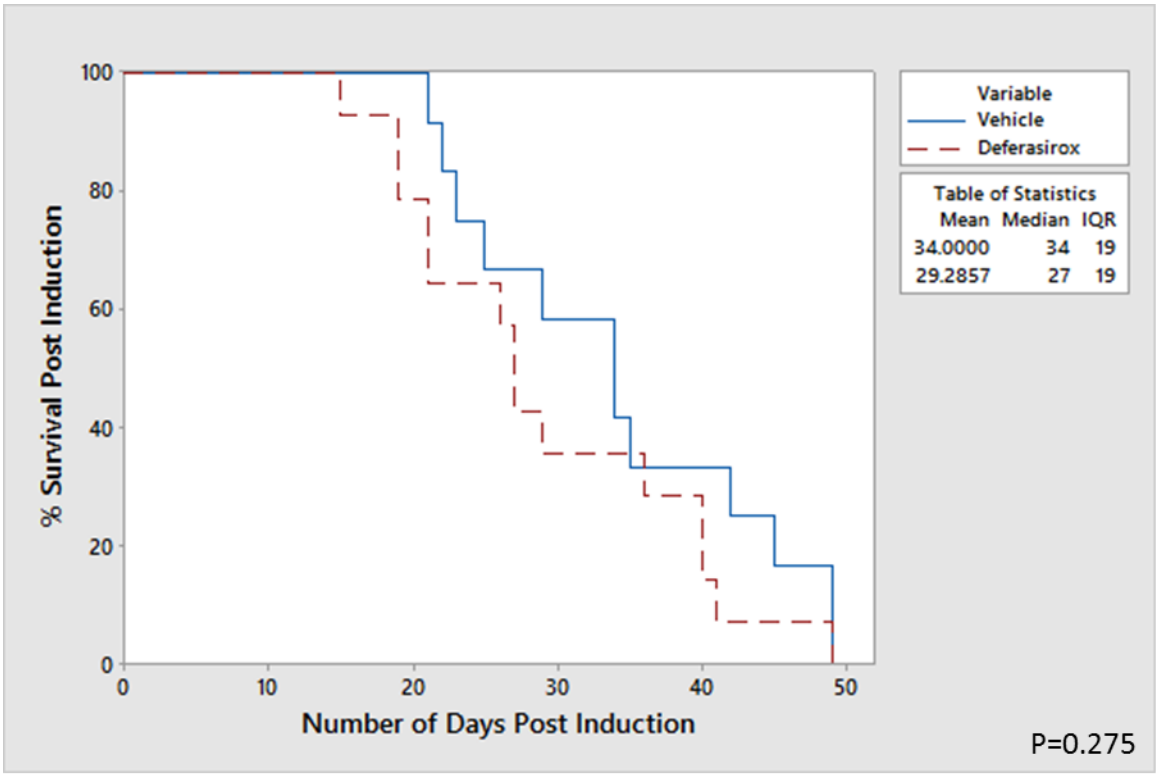

Figure 4.18 Deferasirox did not significantly extend survival when given to Lgr5-CreER^{+} APC$^{fl/fl}$ mice at a dose of 100 mg/kg

Survival plot for Lgr5-CreER^{+} APC$^{fl/fl}$ mice treated with either vehicle or Deferasirox (100 mg/kg) by oral gavage 3 times per week. P value quoted is for log-rank test of survival between the 2 groups.

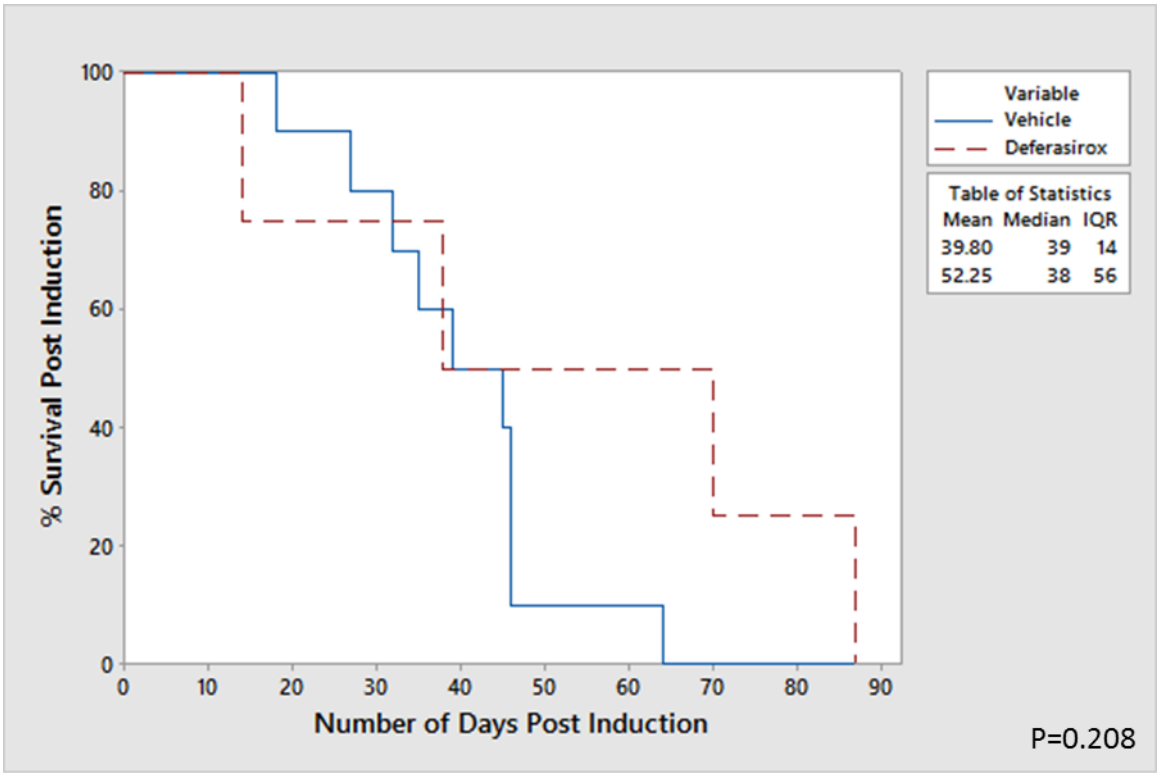

Figure 4.19 Deferasirox did not significantly extend survival when given to Lgr5-CreER^{+} APC$^{fl/fl}$ Pten$^{fl/fl}$ mice at a dose of 100 mg/kg

Survival plot for Lgr5-CreER^{+} APC$^{fl/fl}$ Pten$^{fl/fl}$ mice treated with either vehicle or Deferasirox (100 mg/kg) by oral gavage 3 times per week. P value quoted is for log-rank test of survival between the 2 groups.

4.4 Discussion

Locally advanced and or systemic colorectal cancer is treated with (neo)adjuvant therapy, often with variable response and therefore, as with oesophageal cancer, the development of new agents with increased efficacy is highly desirable. [235]

Cancer cells have an increased requirement for iron and there is now a significant body of evidence linking iron to the propagation of colorectal tumourigenesis. [82, 102] As such, iron chelators represent a promising group of anti-neoplastic agents worthy of further investigation in this setting. [80, 92, 112, 113] It has already been demonstrated in chapter 3 that the orally administered iron chelating agent Deferasirox displays significant anti-neoplastic properties both *in-vitro* and *in-vivo* in oesophageal adenocarcinoma. The main aim of this chapter was therefore to ascertain whether or not these effects were also observed in the colon and rectum as this has not been investigated before.

As in the oesophagus, Deferasirox administration significantly suppressed colorectal adenocarcinoma cell line viability *in-vitro* in a time and dose dependent manner.

The drug significantly inhibited cellular iron uptake (by up to 49.6% compared to control, $p<0.05$) and was also capable of reducing intracellular iron content in cells pre-loaded with iron (as demonstrated by reductions in both total intracellular iron by ferrozine and the iron storage protein ferritin). This ultimately resulted in an accumulation of cells in the G1 phase of the cell cycle, a consequent reduction in cellular proliferation and a subsequent decrease in cell viability. Previous studies of Deferasirox have also demonstrated the induction of cell cycle arrest, although interestingly in S phase rather than G1. [167] The iron chelator Desferrioxamine is also known to induce cell cycle arrest and in particular has been shown to be capable of arresting cells independently in both mid-G1 and S phase. [241]

As stated previously, malignant cells have a higher requirement for iron than their normal counterparts, something that is unsurprising given the element's crucial role in DNA synthesis, ATP generation and cell cycle progression; all activities that by definition are increased in cancer. [112, 113] Cellular iron deprivation is known to cause arrest of the cell cycle at the G1/S checkpoint and subsequent accumulation of cells in the G1 phase (as demonstrated in the current study by a 45.9% increase in cells in G1 phase following treatment with Deferasirox for 48 hours, $p<0.05$ vs. control). [224, 225] Iron deficiency inhibits activity of the R2 subunit of the enzyme ribonucleotide reductase (which catalyzes the conversion of ribonucleotides into deoxyribonucleotides during DNA synthesis) and decreases expression of cyclins A, B and D (all of which are vital for cell cycle progression). [225]

Deferasirox displayed significantly increased efficacy in the colorectal adenocarcinoma cell lines RKO and SW480 compared to the adenoma lines AAC1 and RGC2. This is in part is likely to be explained by the increased metabolic rate of the adenocarcinoma lines and thus an increased requirement for iron, rendering them more sensitive to the effects of cellular iron deprivation through chelation. Previous studies have demonstrated that, although adenomas load iron to a much greater extent than normal colonic mucosa, adenoma iron content is not as great as that of adenocarcinomas. [82, 242] Current chemotherapeutic regimens in colorectal cancer are accompanied by a plethora of well documented side effects resulting from the various drug's non-targeted mechanisms of action. [243] As such, the demonstration that Deferasirox may be more effective against cancer cells than their 'less malignant' counterparts raises the potential that the drug may be selectively targeted to neoplastic cells, thus offering improved efficacy and a reduction in off-target side effects. Previous studies using Deferasirox have also demonstrated that much higher concentrations of the drug were required to induce cytotoxicity in primary hepatocyte cultures compared to hepatoma cells (25 μM vs. >200 μM) again suggesting that malignant lines may be more sensitive to Deferasirox exposure than benign tissues. [167] Similar observations have also been made with alternative iron chelators (DFO, Deferiprone and O-Trensox). [143, 167, 168]

Deferasirox also appears to be more efficacious in the background of an APC mutation, giving further support to the idea that iron chelation therapy may offer targeted treatment of cancer cells. Across the concentrations tested, Deferasirox was up to 35.6% more efficacious (at the equivalent dose) in HT29 cells with an APC mutation compared to their APC wild type counterparts. In part, this may again be explained by the fact the HT29 APC mutant cells had a significantly increased rate of proliferation (55.2% increase vs. APC wild type, $p<0.05$) and hence a higher requirement for iron than HT29 APC wild type cells. There is also, however, an additional explanation for the increase in Deferasirox efficacy seen. Mutation of the tumour suppressor APC permits activation of the Wnt signalling pathway through translocation of accumulated cytosolic β-catenin to the nucleus with subsequent activation of Wnt targets including the proto-oncogene c-Myc. Increased intracellular iron has previously been shown to amplify Wnt signalling in the background of an APC mutation. [132] This in turn results in increased c-Myc, which further increases cellular proliferation (and subsequent requirement for iron) and has also been shown to increase expression of the pertinent cellular iron import proteins TfR1 and DMT1, thus permitting the cell to increase iron acquisition and further exacerbate Wnt signalling (an almost self-perpetuating cycle). Deferasirox therefore may serve to break this cycle through both the induction of intracellular iron deprivation and inhibition of Wnt signalling. Support for this can be found in a previous study identifying Deferasirox as a potent inhibitor of Wnt signalling in SW480 colorectal adenocarcinoma cells. [186] The same study also reported an increase in the expression of genes activated by iron depletion (including HIF-1α) and noted an abrogation of these effects when the iron chelator was subsequently incubated alongside $FeSO_4$, indicating that the inhibition in Wnt signalling seen was achieved entirely through the chelation of iron. [186]

The findings of this latter study, however, despite offering support for the findings made within this thesis, do not agree with all of the results demonstrated here. Firstly, Deferasirox efficacy in reducing colorectal cell line viability was not completely abrogated through pre-incubation alongside

$FeSO_4$ in our study. Secondly, treatment of cells pre-loaded with iron resulted in intracellular ferritin levels that were not only significantly lower than the untreated iron-loaded cells (as may be expected) but that were also significantly lower than the untreated, non iron-loaded control cells. Finally, Deferasirox not only significantly suppressed the induction of proliferation seen in HT29 cells following incubation with iron but actually reduced it to well below baseline control proliferation rates. All of this indicates that Deferasirox may actually be more efficacious at binding iron (and thus suppressing proliferation) in the setting of increased intracellular iron levels (as in colorectal adenocarcinoma). [82]

The tumour suppressor p53 plays a crucial role in mediating cell cycle arrest and functions as a cell-death checkpoint following activation by multiple cellular stresses including DNA damage, oxidative stress and osmotic shock. [244] The protein activates a number of downstream targets, including the cyclin-dependent kinase inhibitor p21 $^{CIP1/WAF1}$, thus initiating cycle arrest at G1/S and ultimately apoptosis if DNA damage cannot be repaired. [244] The gene encoding the p53 protein (TP53) is mutated in around 35-55% of cases of colorectal cancer and is known to influence response to chemotherapy, including 5-Fu. [245, 246] Similar findings were demonstrated in this study, where treatment of the colonic cell line HCT116 p53-/- with 5-Fu resulted in a significantly less efficacious response (in terms of effect on cellular viability) than when the drug was given to HCT116 p53WT cells. Deferasirox efficacy, however, was not significantly altered by cellular p53 status at any of the doses tested. This may be explained by the observation that Deferasirox is primarily exerting its effects through cellular iron deprivation, which is completely independent of p53 activity. In addition, however, previous studies have also demonstrated the ability of Deferasirox to up-regulate p21 $^{CIP1/WAF1}$ expression and also expression of the metastasis suppressor NDRG1, which in turn has been shown to further increase p21 $^{CIP1/WAF1}$ expression in a p53 independent manner. [169, 247] Thus, it would seem that p53 expression is not required for Deferasirox to exert its effects upon the cell

cycle. This is in contrast to previous studies using the iron chelator Desferrioxamine, which has shown decreased efficacy in the context of a p53 deletion in the same cell line. [248]

Deferasirox can overcome chemotherapy resistance (this time to 5-Fu) in colorectal adenocarcinoma cell lines. The adenocarcinoma cell line SW620 (a metastatic clone of the SW480 line) displayed marked resistance to 5-Fu (unlike the SW480 line) but was equally sensitive to Deferasirox. Likewise, a 5-Fu resistant 'clone' of HT29 cells also demonstrated sensitivity to Deferasirox and yielded an additional reduction in cellular viability when Deferasirox was combined with 5-Fu. Again, these findings may merely indicate that Deferasirox is acting through a different mechanism of action to 5-Fu (i.e. iron chelation) thus circumventing the therapy resistance, however, the demonstration of an additive effect by combining 5-Fu and Deferasirox in the HT29 'clone' cell line again raises the possibility that the drug may serve as a chemosensitiser. The mechanism through which this may occur has not been investigated further within this study, however, the NFκB signalling pathway has been shown to be activated in colorectal cancer and therefore its inhibition with Deferasirox may offer a putative mechanism for subsequent chemosensitisation.[249]

The ability of Deferasirox to overcome 5-Fu resistance is somewhat tempered by its reduced efficacy in the context of hypoxia. Hypoxia is a common feature of many solid tumours, including colorectal, and its presence triggers a number of adaptive responses which can promote tumour progression and also resistance to therapy. [250] One explanation for the decrease in efficacy seen is that the exposure of cells to a hypoxic environment results in an initial reduction in cellular proliferation, which is likely to lower their requirement for iron and thus decrease sensitivity to the effects of iron chelation. An alternative explanation is that iron chelation is known to induce expression of HIF-1α, the central protein in the co-ordination of the cellular response to hypoxia, through inhibition of prolyl hydroxylase domain proteins (which require iron for their activity). [251] Elevated levels of HIF-1α are known to activate hypoxia-responsive genes (such as vascular endothelial growth factor,

platelet derived growth factor and nitric oxide synthase) and the initiation of anaerobic glycolysis, which in turn lead to the stimulation of proliferation, metabolism, angiogenesis, invasion, metastasis and therapy resistance. [250] Thus, iron chelation with Deferasirox may serve to exacerbate and enhance the cellular response to hypoxia. In addition, HIF-1α is known to induce cellular iron uptake through increasing the expression of IRP2 and subsequently TfR1 and DMT1. [99] It is also known to up-regulate expression of haem oxygenase 1 (which degrades haem into bilverdin, carbon monoxide and iron) which further increases intracellular iron availability. [99] As such, it may be that under hypoxic conditions increased intracellular iron levels mean a significantly higher dose of chelator is required to generate significant effects (thus overcoming the potential for chelator saturation).

The demonstration of an *in-vivo* effect of Deferasirox administration upon Villin-CreER^{+} Apc$^{fl/fl}$ murine intestinal phenotype (albeit at a significantly higher dose than that used in the previous oesophageal xenograft experiments) is immensely promising. Deferasirox administration significantly increased expression of the apoptotic marker cleaved caspase-3 by 65.2 and 64.3% at doses of 200 mg/kg and 100 mg/kg (in the propylene glycol and sodium carbonate based vehicles respectively, $p<0.05$ vs. control) and also reduced mitosis when used at a dose of 200 mg/kg (52.4% reduction vs. control, $p<0.05$). This result is in agreement with a previous study from our group demonstrating the administration of an iron deficient diet to a similar strain of mice as used here significantly increased rates of intestinal apoptosis (2-3x increase vs. control, $p=0.015$), whilst a diet high in iron significantly stimulated mitosis (4-5x increase vs. control, $p=0.015$). [102] As with the *in-vitro* experiments, it is likely that crypt cellular iron deprivation through chelation results in cell cycle arrest and induction of cellular apoptosis. Deferasirox may also be serving as an inhibitor of the Wnt pathway which is known to be active in these mice (through loss of APC) and exacerbated by iron. [102] This was not investigated in this study but could be through immunohistochemical staining of slides with antibodies against Wnt targets (β-catenin, c-Myc etc.)

Unfortunately, in this study, the increase in intestinal apoptosis seen with Deferasirox administration did not translate into an increase in overall survival when the drug was administered to another spontaneous model of intestinal tumourigenesis, the Lgr5-CreER^{+} APC$^{fl/fl}$ mouse. Again, following induction, these mice lose APC within the intestinal stem cells and develop a hyperproliferative phenotype resulting in adenoma formation. [102] A trend for increased survival with Deferasirox was seen, however, when the drug was given to Lgr5-CreER^{+} APC$^{fl/fl}$ Pten$^{fl/fl}$ mice. Mice given Deferasirox survived for an average of 54.0 days compared to 42.0 days in mice given control vehicle, this was not, however, statistically significant (p=0.621).

The lack of statistical improvement in survival with Deferasirox may be explained by the fact that both of the models utilised result in rapid adenoma formation throughout the whole murine intestine and thus may be too aggressive for Deferasirox to exert an effect. One could repeat the experiment using the APC$^{Min/+}$ murine model where mice develop adenomas at a slower rate, thus allowing smaller differences to be elicited. [102] Another explanation could be that Deferasirox is more efficacious in established tumours that are more phenotypically advanced and possess multiple genetic mutations (not merely just in APC) and as such these models may not be completely appropriate for the testing of the drug. The earlier finding that Deferasirox is more efficacious in adenocarcinoma than adenoma cell lines *in-vitro* would support this latter observation. The final potential explanation for the lack of improvement in survival with Deferasirox therapy is that the drug may exert its effects through a systemic route rather than a luminal one and this may limit its efficacy in the setting of colorectal cancer *in-vivo*. In their previous study, Radulescu and colleagues concluded that it was the luminal pool of iron that was responsible for the propagation of tumourigenesis and not the systemic pool. [102] This may not be true in all cases, however, as an increase in luminal iron is unlikely to explain the increased incidence of colorectal adenocarcinoma seen in patients with Haemochromatosis. [118, 119, 120] Deferasirox clearly exerts a significant proportion of its anti-neoplastic effects through the systemic circulation (as demonstrated by its

marked suppression of OAC subcutaneous xenograft growth in chapter 3), however, although predominantly absorbed in the duodenum (thus not reaching the colon), it is excreted within the bile and, as such, has been shown to retain some of its chelating capacity when it reaches the colon. [252] Therefore, it may actually have the added benefit of being able to chelate iron at both the systemic and luminal levels.

In conclusion, it can be said that the oral iron chelating agent Deferasirox displays marked and significant anti-neoplastic effects against colorectal adenocarcinoma *in-vitro*. The drug effectively inhibits cellular iron uptake and facilitates the removal of iron from within cancer cells precipitating cell cycle arrest and a subsequent reduction in cellular viability. The drug appears to be more efficacious in adenocarcinoma cells than in adenomas and also in the background of an APC mutation. As in oesophageal cancer, Deferasirox can overcome chemotherapy resistance *in-vitro* and its efficacy is not dependent on p53 status. Promisingly, the drug appears to increase rates of intestinal apoptosis and suppress mitosis when administered to APC deficient mice although this has not been shown to translate into an increase in overall survival in the present study. Future experiments should aim to identify markers predictive of response to Deferasirox and also aim to demonstrate an improvement in mouse survival, with a corresponding reduction in tumour burden and abrogation of Wnt targets within the murine intestine. Conclusive demonstration of Deferasirox's safety and tolerability when administered *in-vivo* at the higher doses used in this chapter is also required.

Chapter 5. The role of IRP2 in colorectal adenocarcinoma: A potential biomarker for Deferasirox efficacy?

5.1 Introduction

Tumour iron accumulation has previously been demonstrated along progression through the colorectal adenoma to carcinoma sequence. [82] Furthermore, this is accompanied by increased expression of the key cellular iron import proteins TfR1 and DMT1 with concomitant internalisation of the basolateral iron exporter ferroportin. [82] Expression of the systemic iron regulatory hormone hepcidin (which facilitates the internalisation and degradation of ferroportin) has also been shown. [237] The role of the iron regulatory proteins, the chief regulators of intracellular iron metabolism, within this process of tumour iron accumulation, however, has not been determined.

There are 2 intracellular iron regulatory proteins (IRP1 and IRP2), the function of which is to co-ordinate an adaptive response to iron levels within individual cells. [99] As such, IRPs increase iron uptake when intracellular levels are low and decrease iron import when intracellular levels are high. [99] This process is achieved through IRP-mediated translational regulation of the proteins associated with cellular iron import and storage. [99] In times of cellular iron depletion, IRPs bind to iron responsive elements (IREs) in the 5' untranslated region (UTR) of ferritin and ferroportin mRNA, thus blocking their translation and inhibiting iron storage and efflux. [80, 92, 99] Simultaneously, the IRPs also bind to IREs in the 3' UTR of TfR1 (and to some extent DMT1) mRNA, stabilising its expression and increasing iron import. [80, 92, 99] Conversely, when iron levels are adequate or in excess, IRP1 loses its IRE-binding activity (instead acquiring enzymatic activity as a cytosolic acinotase) and IRP2 is degraded, thus permitting the translation of ferritin and ferroportin mRNA and the degradation of TfR1. [80, 92, 99] In addition to low cellular iron levels, IRP2 has also been shown to be stimulated by

hypoxia and the proto-oncogene c-Myc, whilst also being stabilised by nitric oxide and oxidative stress. [253, 254, 255, 256]

Studies directly investigating the relationship between IRPs and cancer are scarce. In lung cancer, over-expression of IRP1 has been shown to suppress the growth of cell line xenografts, whilst IRP2 was shown to have a stimulatory effect. [254, 257] Micro-array gene expression profiles from breast cancer patients have shown tumour IRP2 over-expression to correlate with high-grade disease whilst the knock down of IRP2 suppresses xenograft growth in mice. [258] In colorectal cancer only 1 previous study has investigated IRP expression, noting a decrease in IRP1 (and TfR1) mRNA expression in cancerous tissue but no difference in IRP2 expression. [259] IRP2 expression was noted to be higher in T3 tumours relative to T1 and T2, however.

As colorectal adenocarcinomas have an excess of intracellular iron, IRP2 (and subsequently TfR1 and DMT1) should be suppressed in tumours relative to normal mucosa, thus preventing the further accumulation of iron. As discussed earlier, this is not the case and thus this feedback mechanism must be perturbed within the process of tumourigenesis. Over or aberrant expression of IRP2 may therefore serve as the driver of excess iron accumulation and subsequent tumour growth.

5.2 Chapter Aims

Colorectal adenocarcinomas load iron rendering them sensitive to the effects of iron deprivation through chelation. Whether or not this increase in iron import is through an IRP2 mediated response is not yet known. If it is, then tumour IRP2 expression could serve as a surrogate marker for iron dependency and thus serve as a predictor of chelation efficacy. Furthermore, the relationship between genetic mutations pertinent to colorectal adenocarcinoma and IRP2 expression has never been determined. As such, the aims for this chapter are:

1. To determine the expression of IRP2 (at both the mRNA and protein level) in human colorectal adenocarcinoma tissue and compare this with normal mucosa.
2. To determine how the expression of IRP2 correlates with the expression of the main iron import protein TfR1 in human colorectal adenocarcinoma tissue.
3. To determine the effect of IRP2 perturbation on TfR1 and ferritin expression *in-vitro*
4. To determine the effect of IRP2 perturbation on cell phenotype *in-vitro.*
5. To determine the relationship between genetic mutations pertinent to colorectal adenocarcinoma and IRP2 expression.

5.3 Results

5.3.1 The expression of IRP2 in colorectal adenocarcinoma

5.3.1.1 Overview

RNA was extracted from the frozen tissue of 41 patients undergoing surgical resection for histologically proven colorectal adenocarcinoma. In addition, paraffin sections were available from a separate cohort of 32 patients with colorectal adenocarcinoma undergoing resection. These samples were processed separately for immunohistochemical analysis of IRP2 protein expression.

5.3.1.2 Results

IRP2 was significantly over-expressed at both the mRNA and protein levels in colorectal adenocarcinoma compared to normal mucosa.

In terms of mRNA, IRP2 expression was significantly higher in adenocarcinoma than in normal mucosa (median fold change 8.80, mean fold change 200.19, $p<0.05$ vs. normal mucosa, Figure 5.1). When sub-group analysis was performed, IRP2 up-regulation appeared to be a colonic (rather than rectal) phenomenon (Figure 5.2) and was greatest in proximal (caecum/ascending colon) and locally advanced (T3 and T4) lesions (Figure 5.3).

At the protein level, IRP2 was ubiquitously but weakly expressed in normal colorectal crypts (Figure 5.4 a-d) with lymphocytes staining strongly throughout. Semi-quantitive scoring of slides demonstrated that colorectal adenocarcinoma sections (Figure 5.4 e-p) showed greater intensity of staining and a larger percentage of cells with positive nuclear staining compared to normal tissue

(tumour median score 5 versus normal mucosa median score 3, p=0.004). Expression was particularly high in tumours of a mucinous phenotype (Figure 5.4 k and l) relative to all other tumours (median score 7.5, p=0.049) and normal tissue (p=0.0027). Normal small bowel tissue showed high intensity staining in the bases of crypts (Figure 5.4 q and r) where proliferation is known to be greatest.

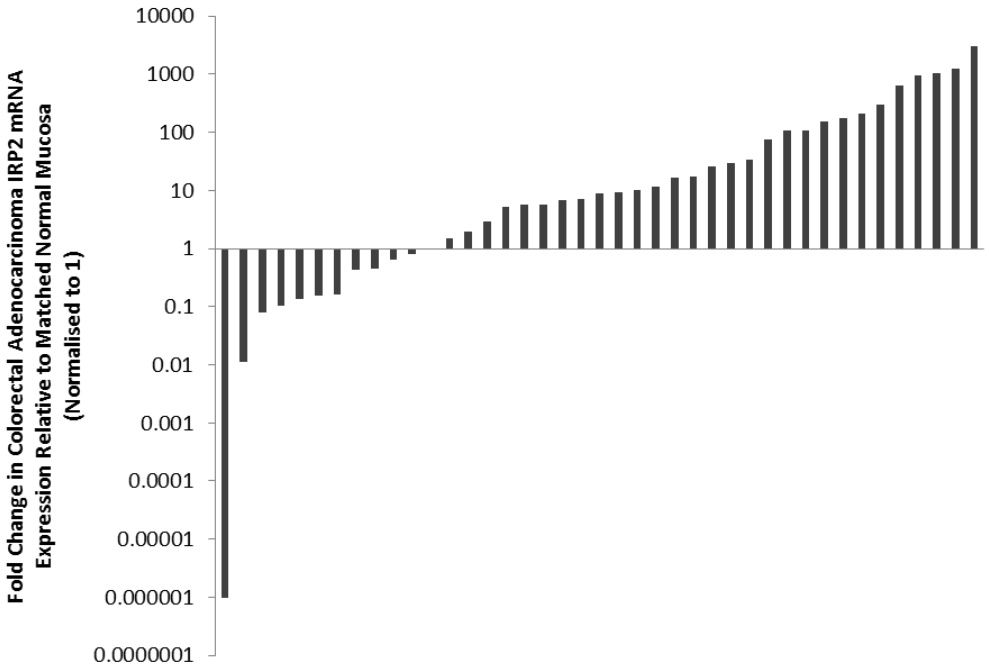

Figure 5.1 IRP2 mRNA expression is significantly up-regulated in colorectal adenocarcinoma tissue relative to matched normal mucosa

qRT-PCR analysis of 41 matched colorectal adenocarcinoma and associated normal mucosa demonstrating significant up-regulation in IRP2 mRNA expression in adenocarcinoma samples relative to control (mean fold change 200.19, $p<0.05$ vs. normal mucosa).

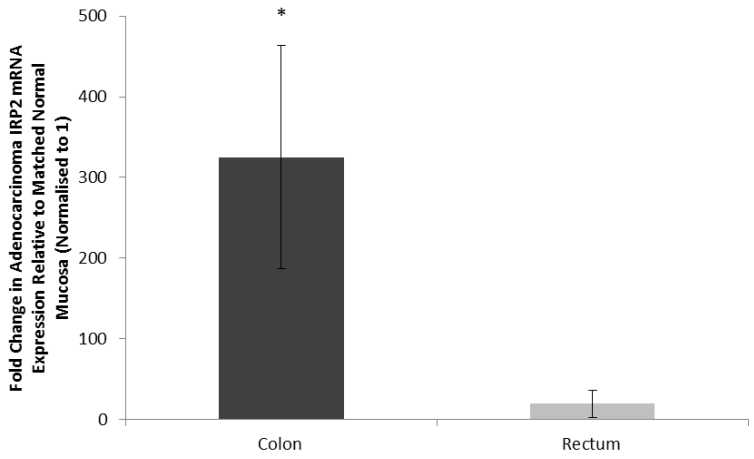

A

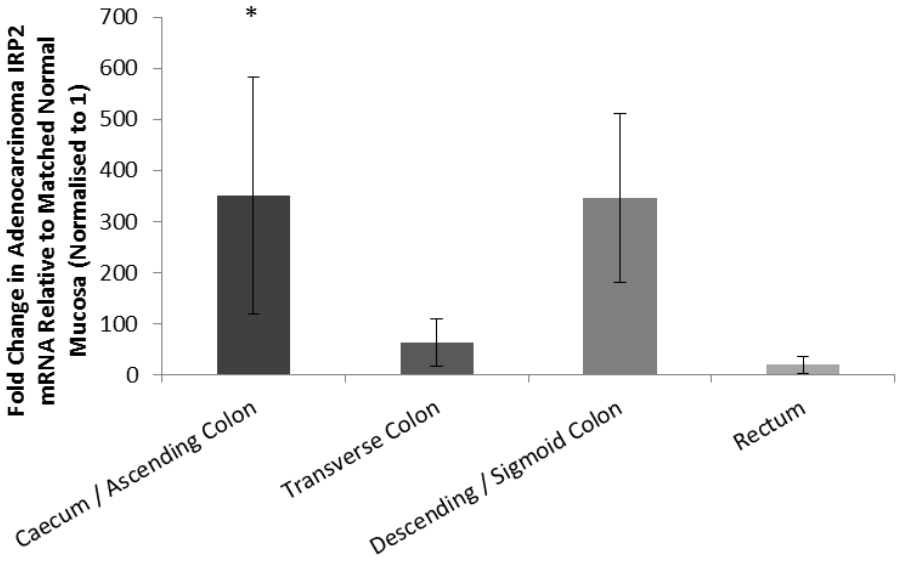

B

Figure 5.2 IRP2 mRNA is significantly up-regulated in the colon but not in the rectum

qRT-PCR (A) demonstrating that IRP2 mRNA is significantly up-regulated compared to matched normal mucosa in the colon (n=24) but not in the rectum (n=9). Proximal (n=13) colonic tumours displayed a significant up-regulation in IRP2 mRNA expression (B) on sub-group analysis. Data points represent mean fold change in IRP2 mRNA relative to matched normal mucosa, error bars denote ±SEM, * $p<0.05$ vs. normal mucosa, $p=0.054$ all colon vs. rectum.

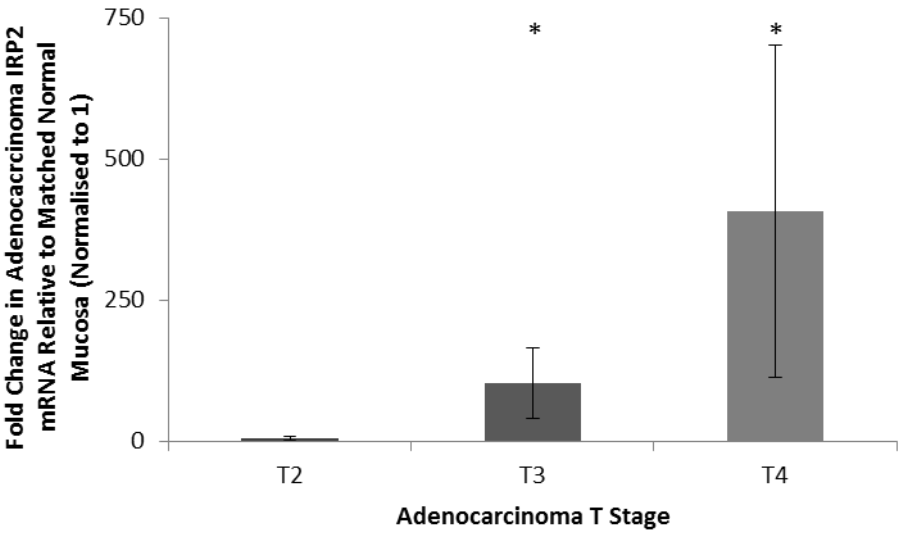

Figure 5.3 IRP2 mRNA is significantly up-regulated in T3 and T4 adenocarcinomas

qRT-PCR demonstrating that IRP2 mRNA is significantly up-regulated compared to matched normal mucosa in T3 (n=20) and T4 (n=10) colorectal adenocarcinomas but not T2 (n=9). Data points represent mean fold change in IRP2 mRNA relative to matched normal mucosa, error bars denote ±SEM, * $p<0.05$ vs. normal mucosa.

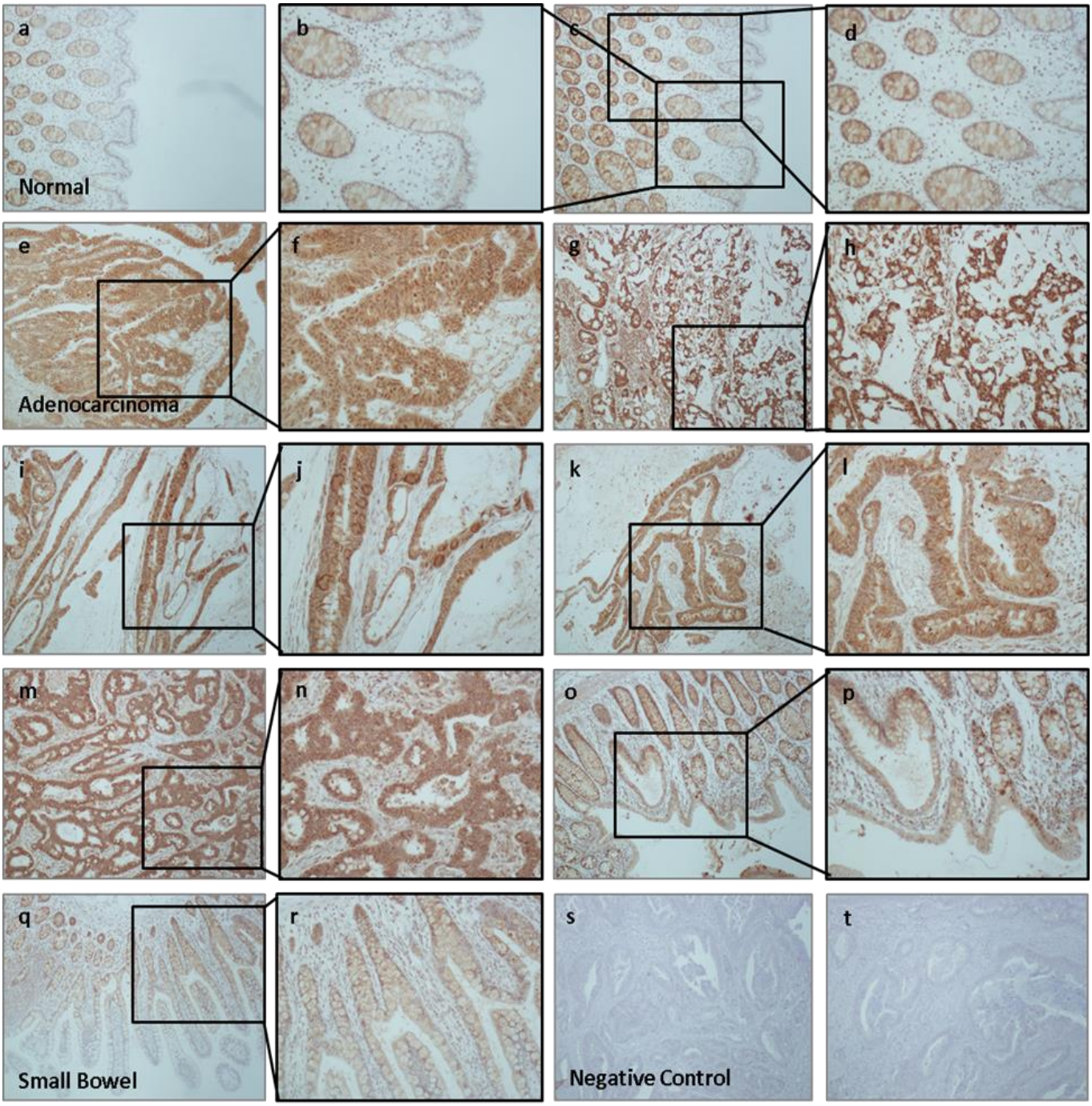

Figure 5.4 IRP2 protein expression is significantly increased in colorectal adenocarcinoma

Immunohistochemistry on paraffin embedded tissue sections taken from colorectal adenocarcinoma (e-p), adjacent normal mucosa (a-d) and small bowel specimens (q and r) stained for expression of IRP2. Low power images taken at magnification x20 or x40, high power images taken at x100.

5.3.2 Correlation of IRP2 expression with that of TfR1

5.3.2.1 Overview

The cDNA generated from the 41 samples of matched adenocarcinoma and normal mucosa in 5.3.1 was utilised to quantify TfR1 mRNA expression by qRT-PCR. This was then also correlated on a sample by sample basis with the IRP2 mRNA expression data using the Spearman's Rank Correlation.

5.3.2.2 Results

TfR1 mRNA expression was significantly up-regulated in samples of colorectal adenocarcinoma compared to matched normal mucosa (median fold change 12.54, mean fold change 314.11 vs. control, $p<0.05$, Figure 5.5A). Expression of TfR1 was positively and significantly correlated with that of IRP2 (Figure 5.5B).

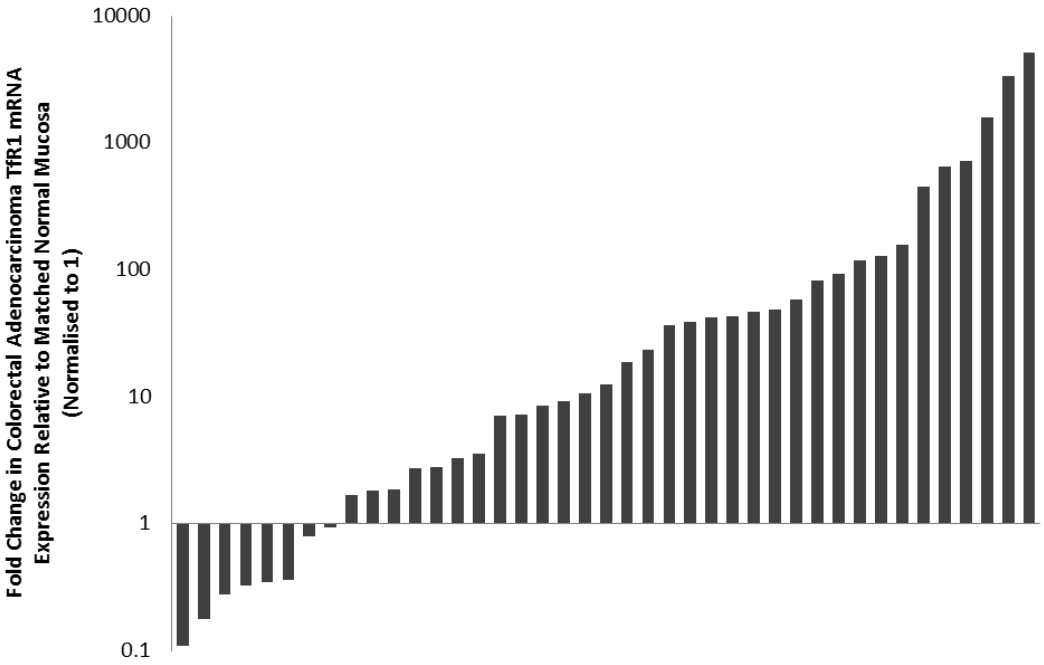
Fold Change in Colorectal Adenocarcinoma TfR1 mRNA Expression Relative to Matched Normal Mucosa (Normalised to 1)
10000
1000
100
10
1
0.1

A

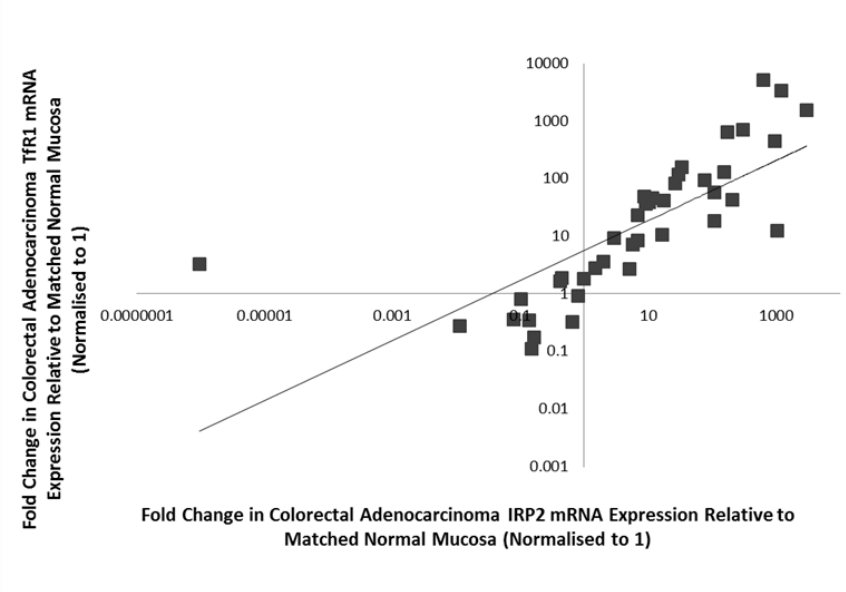
Fold Change in Colorectal Adenocarcinoma TfR1 mRNA Expression Relative to Matched Normal Mucosa (Normalised to 1)
10000
1000
100
10
1
0.1
0.01
0.001
0.0000001
0.00001
0.001
10
1000
Fold Change in Colorectal Adenocarcinoma IRP2 mRNA Expression Relative to Matched Normal Mucosa (Normalised to 1)

B

Figure 5.5 TfR1 mRNA expression is significantly up-regulated and correlates positively with IRP2 mRNA expression in colorectal adenocarcinoma tissue relative to matched normal mucosa

qRT-PCR analysis (A) of 41 matched colorectal adenocarcinoma and associated normal mucosa demonstrating significant up-regulation in TfR1 mRNA expression in adenocarcinoma samples relative to control (mean fold change 314.11, $p<0.05$ vs. normal mucosa). This significant up-regulation in TfR1 expression correlates with IRP2 mRNA expression (B) with a Spearman's Rank Correlation score of 0.908 ($p<0.001$).

5.3.3 The effect of IRP2 perturbation on the expression of TfR1 and ferritin *in-vitro*

5.3.3.1 Overview

IRP2 expression was perturbed in RKO colorectal adenocarcinoma cells using an siRNA knockdown system (see methods chapter for full explanation). qRT-PCR was utilised to confirm successful knockdown of IRP2 at the mRNA level before the subsequent performance of Western blotting to determine the effect on protein expression. In addition, the effect of IRP2 knockdown on TfR1 and ferritin mRNA and protein expression was also delineated again through qRT-PCR and Western blotting respectively. A ferritin ELISA was also utilised to further quantify ferritin protein expression.

5.3.3.2 Results

Significant knockdown in IRP2 expression at the mRNA level was demonstrated after 24 hours incubation with siRNA (46.0% reduction vs. control (Silencer® Select Negative Control siRNA #1), Figure 5.6A). This was accompanied by a significant reduction in the expression of TfR1 (33.7% reduction vs. control, Figure 5.6B).

At the protein level, Western blotting demonstrated that IRP2 expression was significantly reduced by 49.5% following siRNA knockdown (Figure 5.7A) and this was accompanied again by a significant reduction in TfR1 expression (60.8% vs. control, Figure 5.7B). Ferritin expression was increased 18.4 fold (Figure 5.8A) on Western blotting, although this did not reach the threshold for statistical significance on semi-quantitative analysis ($p=0.150$). A significant increase in ferritin protein expression was seen, however, when a ferritin ELISA was performed on samples treated with IRP2 siRNA (Figure 5.8B).

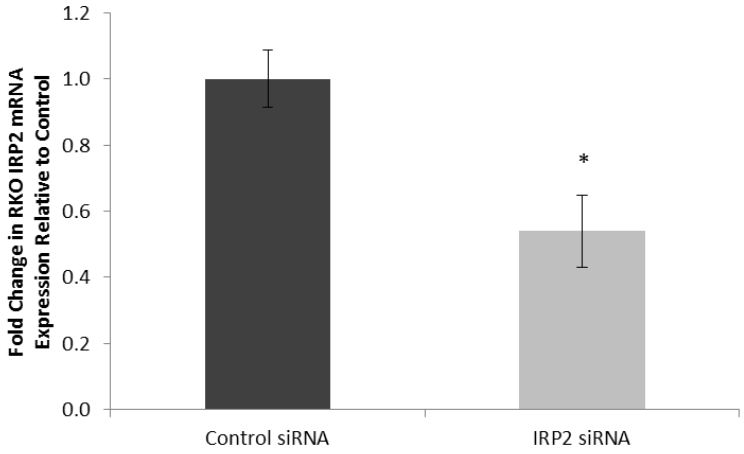

A

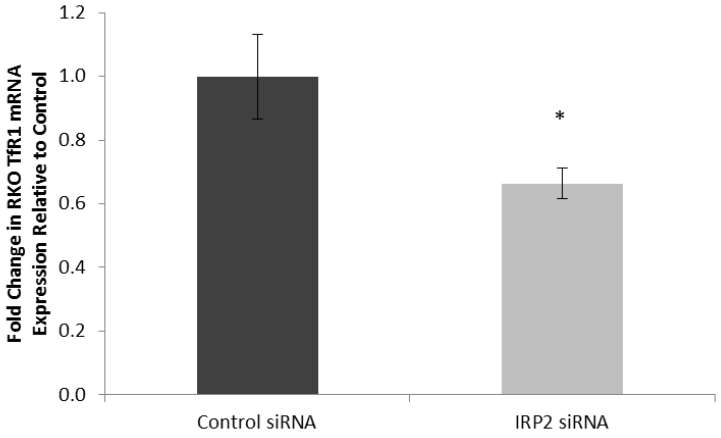

B

Figure 5.6 Reduction of IRP2 mRNA expression through siRNA is associated with decreased TfR1 mRNA expression in colorectal adenocarcinoma cells *in-vitro*

qRT-PCR (A) demonstrating significant knockdown of IRP2 in RKO colorectal adenocarcinoma cell lines after 24 hours using siRNA. This was associated with a significant reduction in TfR1 mRNA expression (B). Data points represent mean fold change in mRNA expression relative to control siRNA, error bars denote ±SEM, * $p<0.05$ vs. control siRNA.

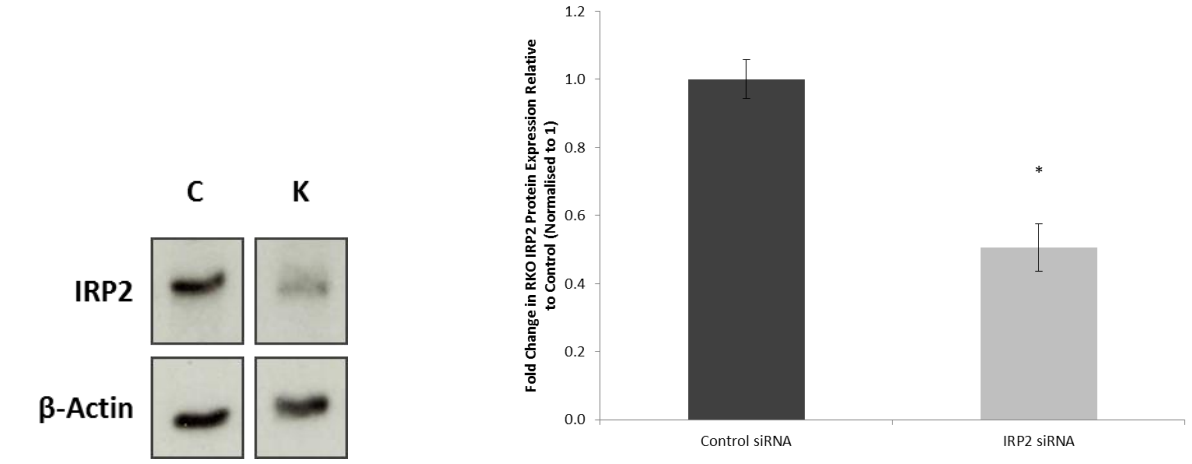

A

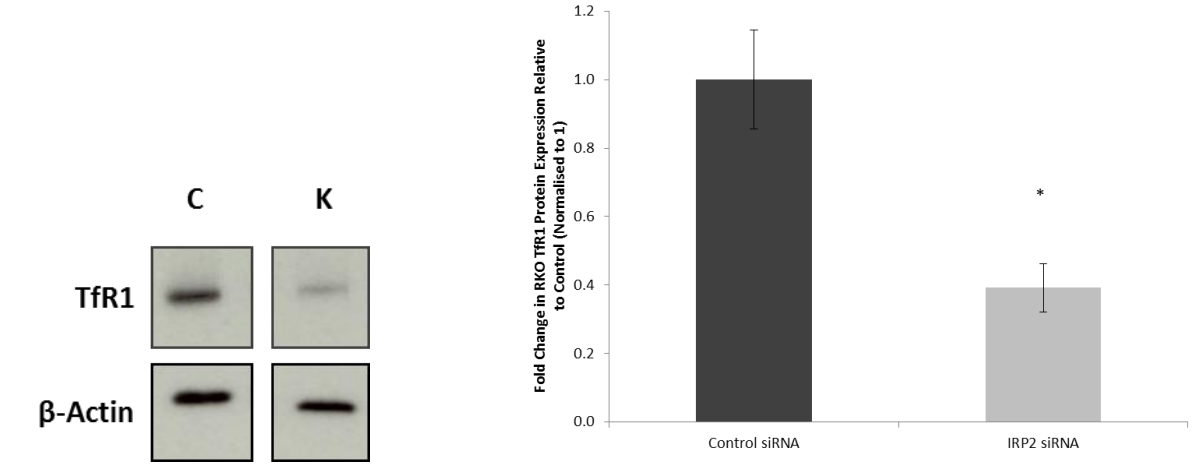

B

Figure 5.7 Reduction in IRP2 mRNA expression through siRNA knockdown is associated with decreased IRP2 and TfR1 protein expression *in-vitro*

Representative Western blot (A) demonstrating significant reduction in IRP2 protein expression in RKO cells following treatment with siRNA (where C=control siRNA, K=knockdown=IRP2 siRNA). This was accompanied by a significant reduction in TfR1 protein expression, as demonstrated by representative Western blot (B). Semi-quantitative analysis of blots was performed through normalisation to β-Actin and subsequent expression as a fold change relative to control siRNA (normalised to 1). Data points represent mean fold change in protein expression relative to control siRNA, error bars denote ±SEM, * $p<0.05$ vs. control siRNA.

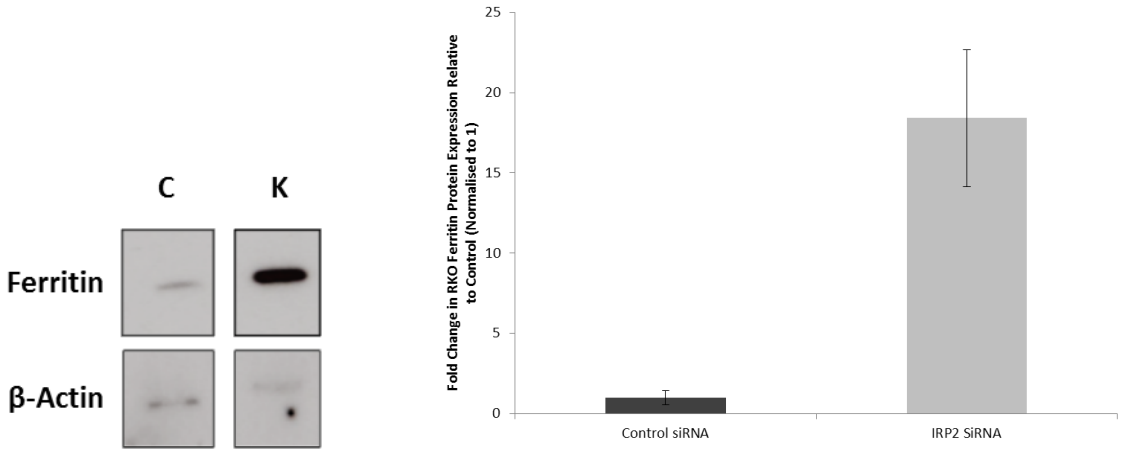

A

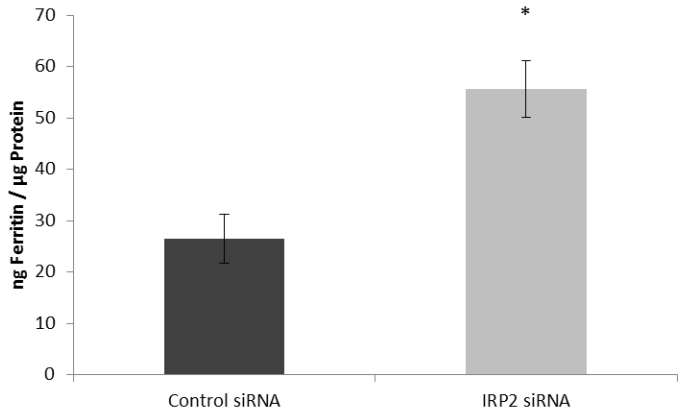

B

Figure 5.8 Reduction in IRP2 mRNA expression through siRNA knockdown is associated with increased ferritin protein expression *in-vitro*

Representative Western blot (A) demonstrating an increase in RKO ferritin protein expression following treatment with IRP2 siRNA (where C=control siRNA, K=knockdown=IRP2 siRNA). This was confirmed through a ferritin ELISA (B). Semi-quantitative analysis of blots was performed through normalisation to β-Actin and subsequent expression as a fold change relative to control siRNA (normalised to 1). Data points in (A) represent mean fold change in protein expression relative to control siRNA, error bars denote ±SEM, * $p<0.05$ vs. control siRNA. Data points in (B) represent mean ng ferritin per µg of cellular protein, error bars denote ±SEM, * $p<0.05$ vs. control siRNA.

5.3.4 The effect of IRP2 perturbation on colorectal adenocarcinoma phenotype *in-vitro*

5.3.4.1 Overview

Following the demonstration that successful knockdown of IRP2 with siRNA at the mRNA level was associated with a reduction in IRP2 and TfR1 protein expression and a paradoxical increase in ferritin protein expression (in keeping with the classical IRP2 response), the effect of IRP2 perturbation on RKO cellular phenotype was assessed.

RKO cells were exposed to the siRNA knockdown regimen for 24 hours as in the previous experiment before being treated with DMEM containing 100 µM $FeSO_4$ (and 500 µM Na Ascorbate) for 1 hour. After this time cellular iron loading was assessed by way of ferrozine assay.

In addition, the effect of IRP2 knockdown on colorectal cell cycle progression was evaluated using FACS. Cells were again treated with the knockdown regimen for 24 hours prior to being harvested. In addition, a 2^{nd} group was included where cells were exposed to 100 µM $FeSO_4$ (and 500 µM Na Ascorbate) for 1 hour immediately prior to being harvested for FACS. All IRP2 knockdown, ferrozine and FACS protocols were performed as outlined in sections 2.2.9 and 2.2.12.

5.3.4.2 Results

RKO cells that had been subjected to the IRP2 knockdown regimen had a significantly lower iron loading capacity than their control counterparts (47.2% reduction in iron loading vs. control, $p<0.05$, Figure 5.9).

IRP2 knockdown also resulted in an increased proportion of cells within G1 of the cell cycle (53.2 vs. 46.9%, $p<0.05$, Figure 5.10) and a corresponding reduction in the proportion in G2/M (21.3 vs. 25.0%, $p<0.05$). This was reversed by the addition of 100 μM iron.

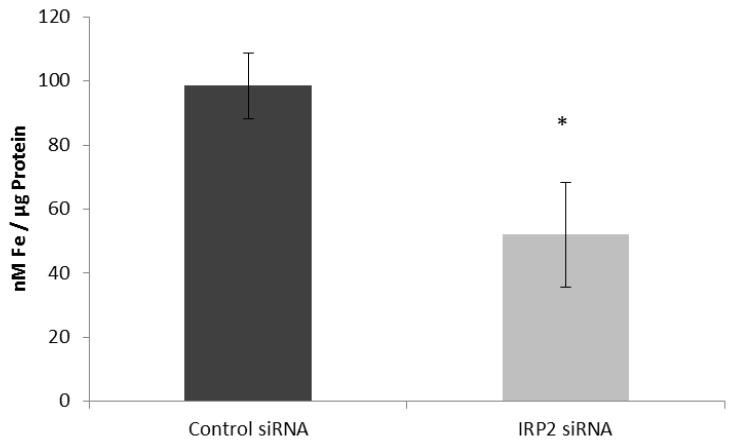

Figure 5.9 Reduction in IRP2 mRNA expression through siRNA knockdown is associated with a reduction in colonic adenocarcinoma cellular iron loading *in-vitro*

Ferrozine assay demonstrating decreased intracellular iron uptake in RKO cells treated with IRP2 siRNA for 24 hours relative to control siRNA. Both groups were exposed to media containing 100 µM $FeSO_4$ for 1 hour prior to the assay being performed. Data points represent mean intracellular iron content (nM Fe / µg cellular protein), error bars denote ±SEM, * $p<0.05$ vs. control.

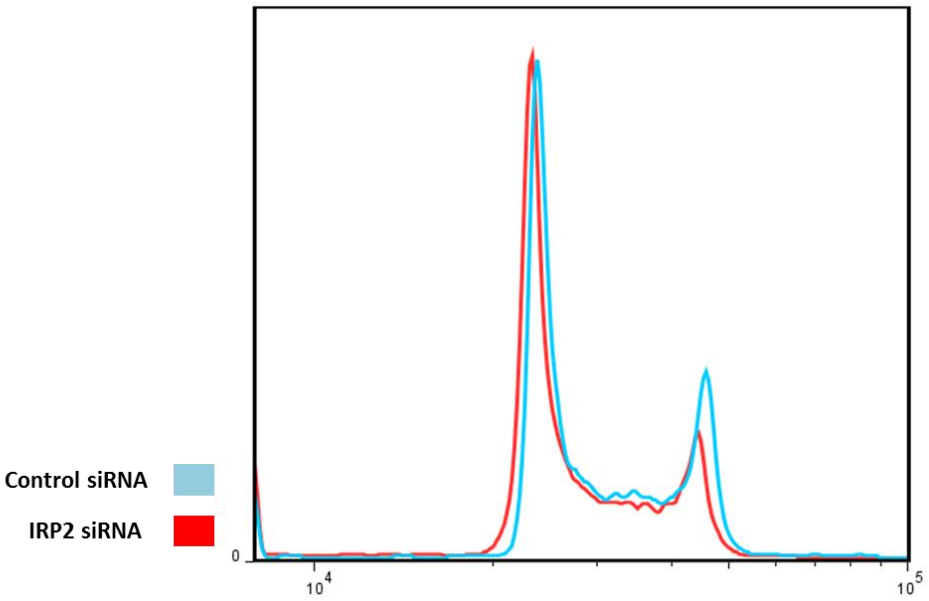
Control siRNA
IRP2 siRNA
0
10^4
10^5

A

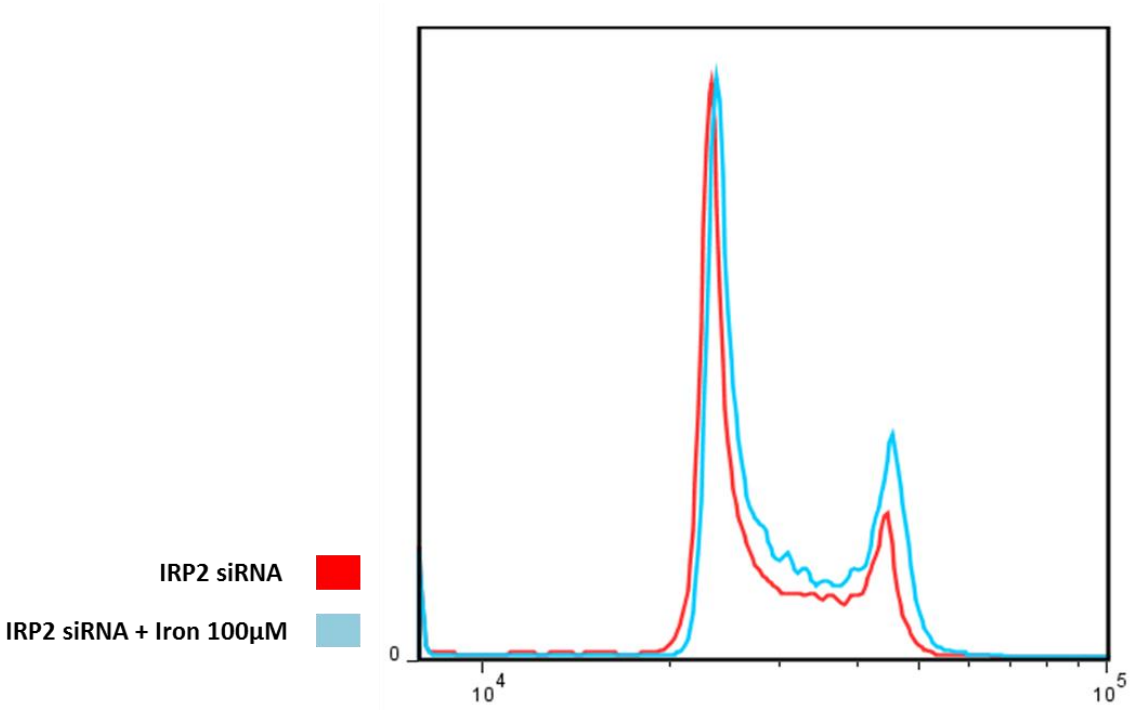
IRP2 siRNA
IRP2 siRNA + Iron 100µM
0
10^4
10^5

B

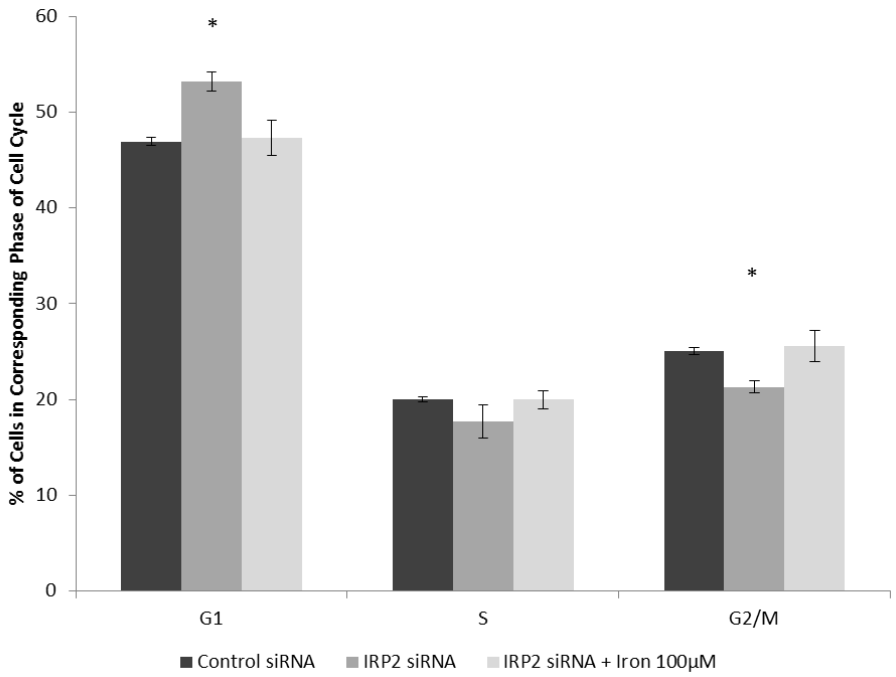

C

Figure 5.10 Reduction in IRP2 mRNA expression through siRNA knockdown is associated with cell cycle perturbation in colorectal adenocarcinoma cells *in-vitro*

Cells cycle analysis through FACS with propidium iodide (A and B) of RKO cells treated with IRP2 siRNA for 24 hours. Successful knockdown of IRP2 at the mRNA level was associated with a significant increase in the proportion of cells in G1 and a corresponding reduction in G2/M compared to control siRNA (C). This phenotype was reversed by the exposure of cells to 100 µM $FeSO_4$. Data points in (C) represent mean % of cells in corresponding phase of cell cycle, error bars denote ±SEM, * $p<0.05$ vs. control siRNA.

5.3.5 The relationship between genetic mutations pertinent to colorectal adenocarcinoma and IRP2 expression

5.3.5.1 Overview

A relationship between the dysregulation of iron metabolism and mutation of the tumour suppressor APC has previously been demonstrated in colorectal cancer. [102, 132] The association of APC with IRP2, however, has not been specifically assessed, nor has its association with other pertinent genetic mutations (p53, K-ras, B-raf, PIK3CA etc.).

The Cancer Genome Atlas (TCGA), an online open-access repository containing tumour genetic mutation and protein expression data sets (cbioportal.org), was explored to identify correlations between gene mutation status and IRP2 protein expression levels. Mutation status was obtained for APC, K-ras, B-raf, c-Myc, PIK3CA and p53 genes while mRNA expression data, presented as z scores, was gathered for IRP2. Any positive trends found were then subjected to univariate and multivariate analysis.

5.3.5.2 Results

The only significant association demonstrated following exploration of the TCGA and subsequent statistical analysis was that between mutation in B-raf and IRP2 over-expression. A significant positive association between IRP2 mRNA expression and B-raf mutation status in 19 CRC samples (odds ratio 1.668 on multivariate analysis, p=0.032) was seen (Figure 5.11).

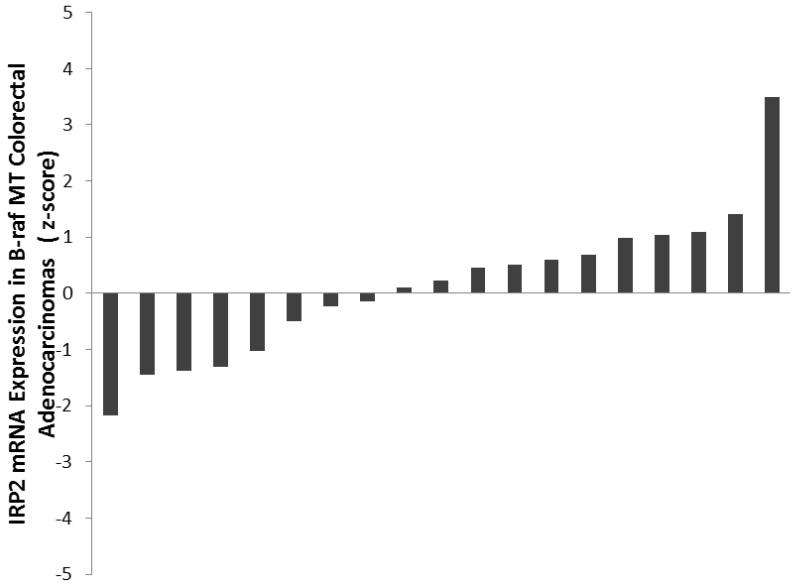

Figure 5.11 B-raf mutations are associated with increased IRP2 mRNA expression in colorectal adenocarcinoma

The Cancer Genome Atlas was interrogated to reveal a significant positive association between IRP2 mRNA expression and B-raf mutation status in 19 CRC samples (odds ratio 1.668 on multivariate analysis, p=0.032).

5.3.6 The influence of B-raf mutation status and MAPK pathway activity on IRP2 expression in colorectal adenocarcinoma *in-vitro*

5.3.6.1 Overview

To further investigate the apparent association between mutations in B-raf and IRP2 protein expression demonstrated in 5.3.5 a doxycycline inducible B-raf V600E construct was created and stably transfected into the HCT116 colorectal adenocarcinoma cell line (as outlined in the methods chapter). Once established, the cell line was utilised to assess the effect of both B-raf V600E induction and subsequent amplification of the MAPK signalling pathway upon IRP2 protein expression. Western blotting was performed following Doxycycline induction of the B-raf V600E vector using antibodies directed against B-raf, IRP2 and p-ERK (a marker of MAPK activitiy). In addition, the dual MEK inhibitor Trametinib and the B-raf inhibitor Sorafenib were utilised to assess the effect of B-raf and or MAPK inhibition on IRP2 expression. Antibodies against TfR1 and ferritin were also utilised to quantify effects on downstream targets of IRP2.

5.3.6.2 Results

Treatment of the HCT116 B-raf V600E transfected cell line with 1µg/ml of Doxycycline resulted in a profound and statistical increase in B-raf expression by Western blotting (12.6 fold induction, $p<0.05$ vs. control, Figure 5.12). This did not, however, alter IRP2 protein expression. Of note, levels of p-ERK were also not statistically changed, indicating activity of the MAPK signalling pathway had not been significantly up-regulated by the increased B-raf expression.

An empty vector construct (HCT116 EV) was also cloned and transfected into HCT116 cells as a negative control. Western blotting was next performed at baseline (in un-stimulated conditions) to assess p-ERK and IRP2 activity in both the EV and V600E cell lines (Figure 5.13). Interestingly, p-ERK activity was 4.5 fold elevated in the V600E cell line compared to the EV and IRP2 levels also exhibited an almost 2 fold increase.

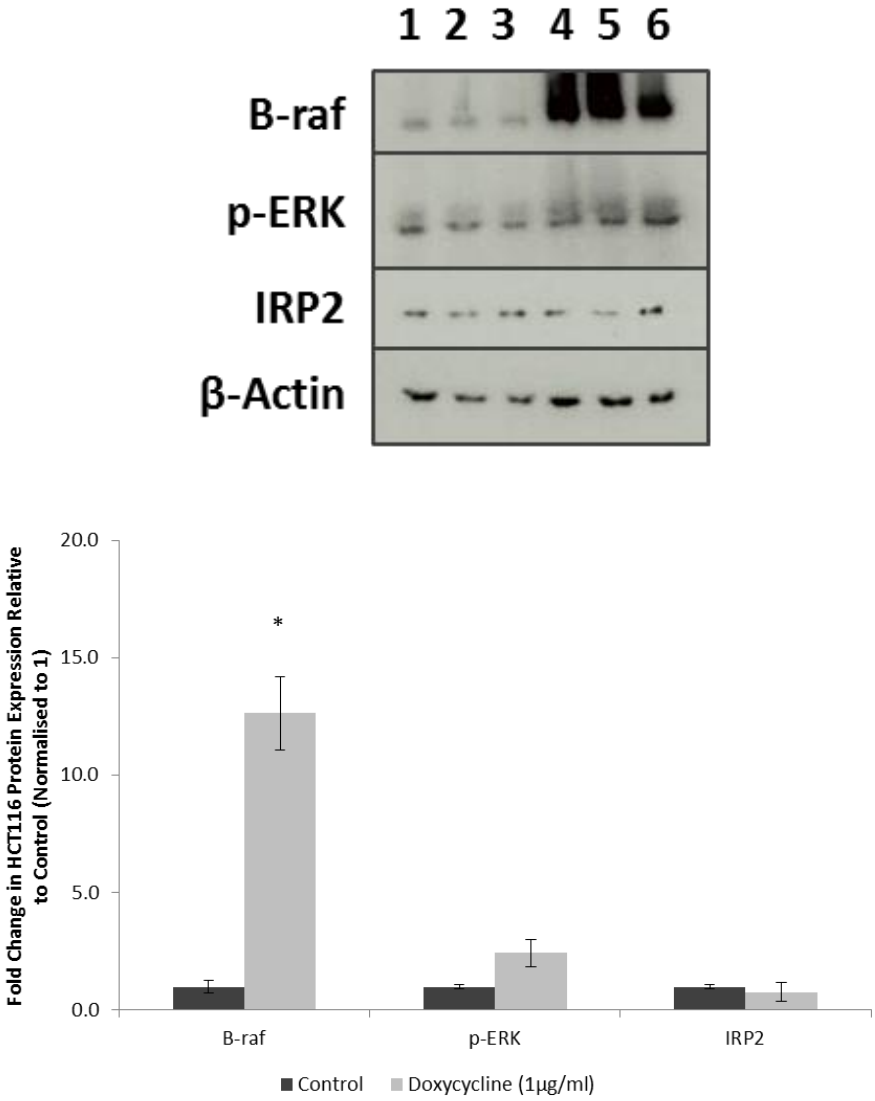

Figure 5.12 B-raf mutations alone are not associated with increased IRP2 protein expression *in-vitro*

Western blot demonstrating significant increase in B-raf protein expression following incubation of HCT116 V600E cells with either standard media (lanes 1-3) or 1 μg/ml of Doxycycline (lanes 4-6). No significant difference was seen, however, in either p-ERK or IRP2 protein expression. Semi-quantitative analysis of blots was performed through normalisation to β-Actin and subsequent expression as a fold change relative to control (normalised to 1). Data points represent mean fold change in protein expression relative to control, error bars denote ±SEM, * $p<0.05$ vs. control.

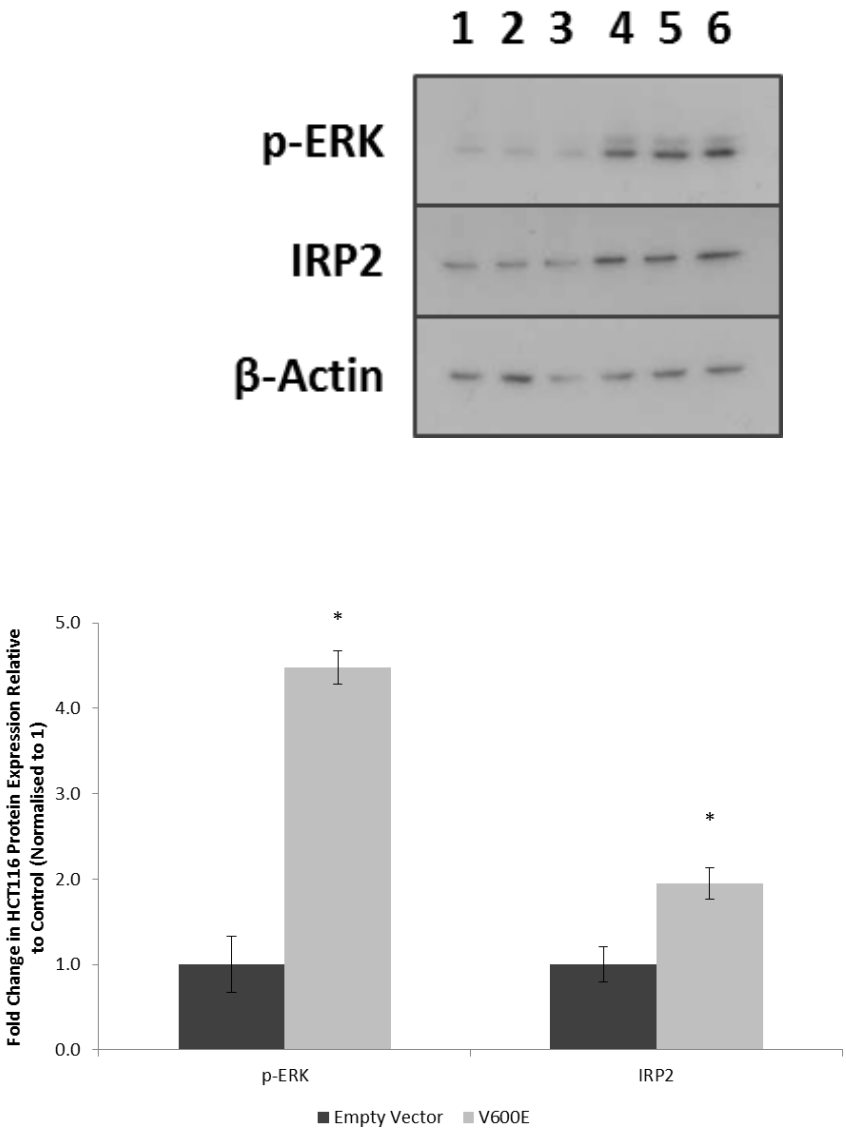

Figure 5.13 B-raf mutations are likely to increase cellular IRP2 protein expression through elevated p-ERK *in-vitro*

Western blot demonstrating baseline p-ERK activity in HCT116 cells transfected with a BRAF V600E inducible vector (lanes 4-6) and those transfected with an empty vector control (lanes 1-3). IRP2 protein expression was significantly increased in the V600E cell line. Semi-quantitative analysis of blots was performed through normalisation to β-Actin and subsequent expression as a fold change relative to control (normalised to 1). Data points represent mean fold change in protein expression relative to control, error bars denote ±SEM, * $p<0.05$ vs. control.

The effect of inhibition of the MAPK signalling pathway on IRP2 expression was next assessed using the dual MEK inhibitor Trametinib on 3 different colorectal cell lines. SW480 and HCT116 cells possess wild type B-raf and a mutant K-ras, whilst the RKO cell line has a mutant B-raf and a wild type K-ras.

Administration of Trametinib resulted in a marked and significant reduction in p-ERK protein expression in all 3 cell lines (66.7, 58.7 and 94.6% reduction in SW480, HCT116 and RKO cells respectively, $p<0.05$ vs. control, Figure 5.14 A-C). IRP2 protein expression was also significantly reduced in the SW480 and HCT116 lines (46.9 and 63.7% respectively, $p<0.05$) but not in the RKOs. TfR1 expression was significantly reduced across all 3 cell lines tested. Both the SW480 and HCT116 cell lines demonstrated a trend towards increased ferritin expression, although this did not reach statistical significance on semi-quantitative analysis. A profound induction in ferritin expression (over 30 fold) was seen, however, in the RKO cell line.

Treatment of the RKO cell line with Sorafenib resulted in a significant reduction in p-ERK, IRP2 and TfR1 expression (Figure 5.15). Ferritin expression was not significantly altered on this occasion, however.

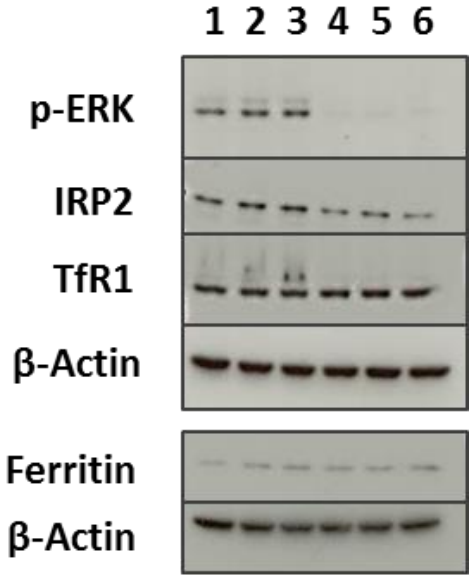
1 2 3 4 5 6
p-ERK
IRP2
TfR1
β-Actin
Ferritin
β-Actin

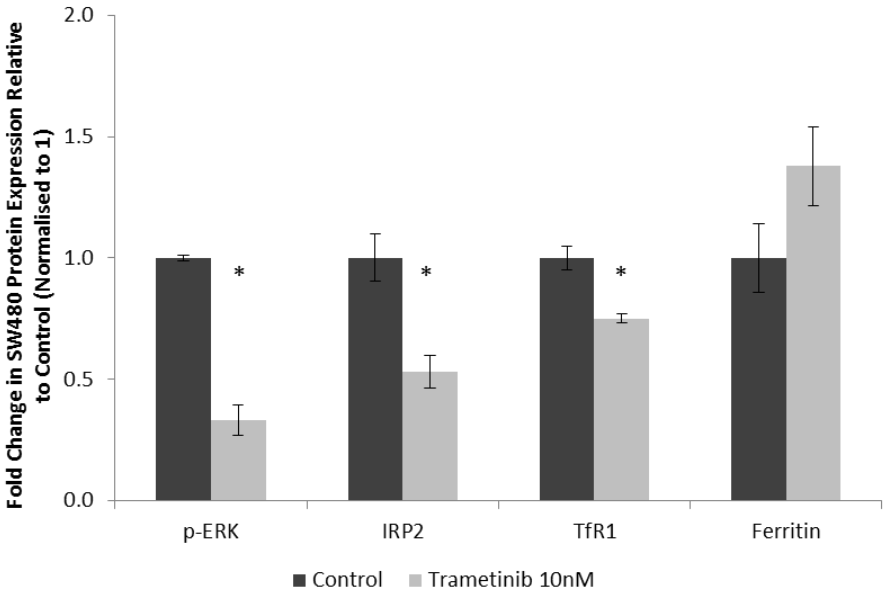
Fold Change in SW480 Protein Expression Relative to Control (Normalised to 1)
2.0
1.5
1.0
0.5
0.0
*
*
*
p-ERK
IRP2
TfR1
Ferritin
Control
Trametinib 10nM

A

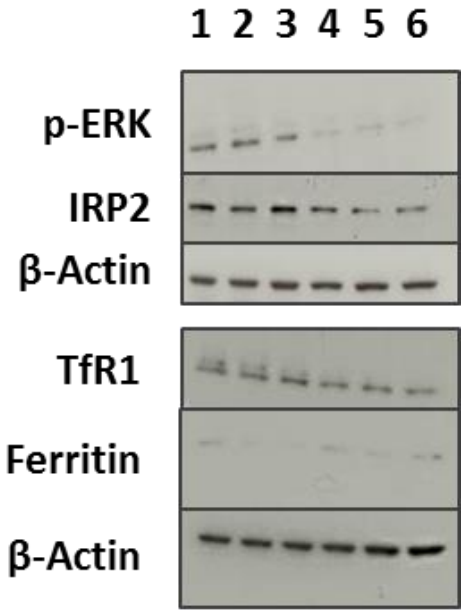
1 2 3 4 5 6
p-ERK
IRP2
β-Actin
TfR1
Ferritin
β-Actin

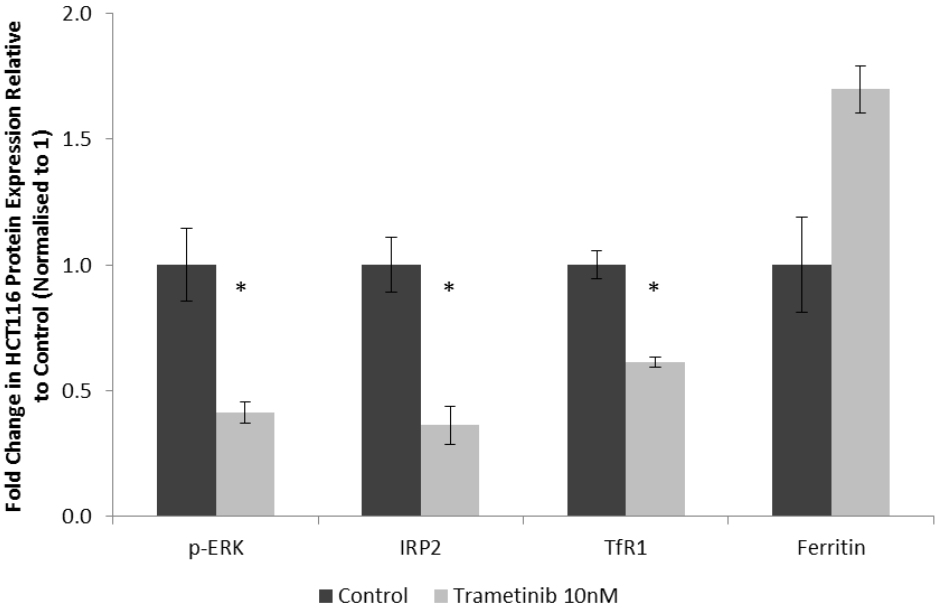
Fold Change in HCT116 Protein Expression Relative to Control (Normalised to 1)
2.0
1.5
1.0
0.5
0.0
*
*
*
p-ERK
IRP2
TfR1
Ferritin
Control
Trametinib 10nM

B

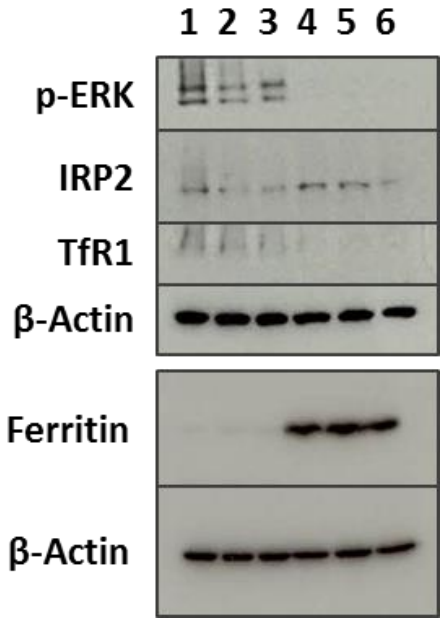
1 2 3 4 5 6
p-ERK
IRP2
TfR1
β-Actin
Ferritin
β-Actin

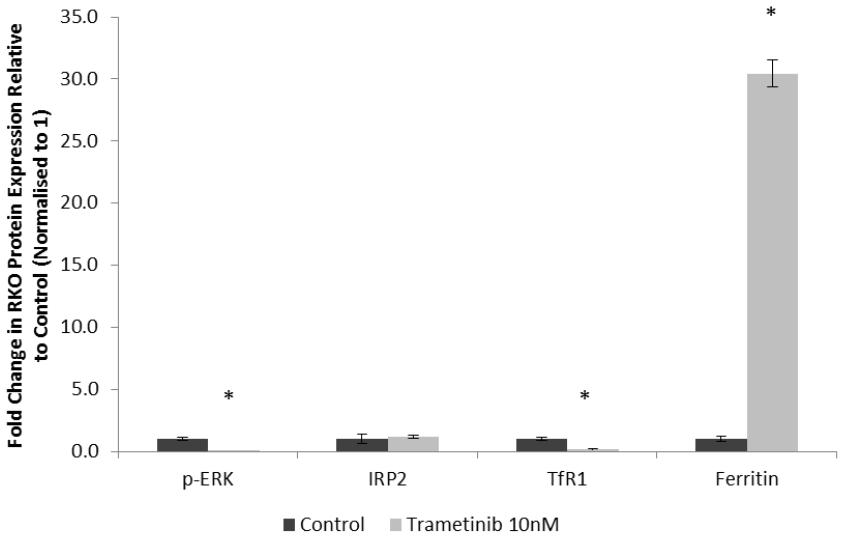
Fold Change in RKO Protein Expression Relative to Control (Normalised to 1)
35.0
30.0
25.0
20.0
15.0
10.0
5.0
0.0
*
*
*
p-ERK
IRP2
TfR1
Ferritin
Control
Trametinib 10nM

C

Figure 5.14 Treatment of colorectal adenocarcinoma cells with the MEK inhibitor Trametinib is associated with a reduction in IRP2 protein expression *in-vitro*

Western blots demonstrating the effect of the MEK inhibitor Trametinib (10 nM for 48 hours, lanes 4-6) upon protein expression in the SW480 (A), HCT116 (B) and RKO (C) colorectal adenocarcinoma cell lines compared to standard media control (lanes 1-3). P-ERK was measured as a marker of MEK inhibition, TfR1 and ferritin were blotted for as downstream markers of IRP2 activity. Semi-quantitative analysis of blots was performed through normalisation to β-Actin and subsequent expression as a fold change relative to control (normalised to 1). Data points represent mean fold change in protein expression relative to control, error bars denote ±SEM, * $p<0.05$ vs. control.

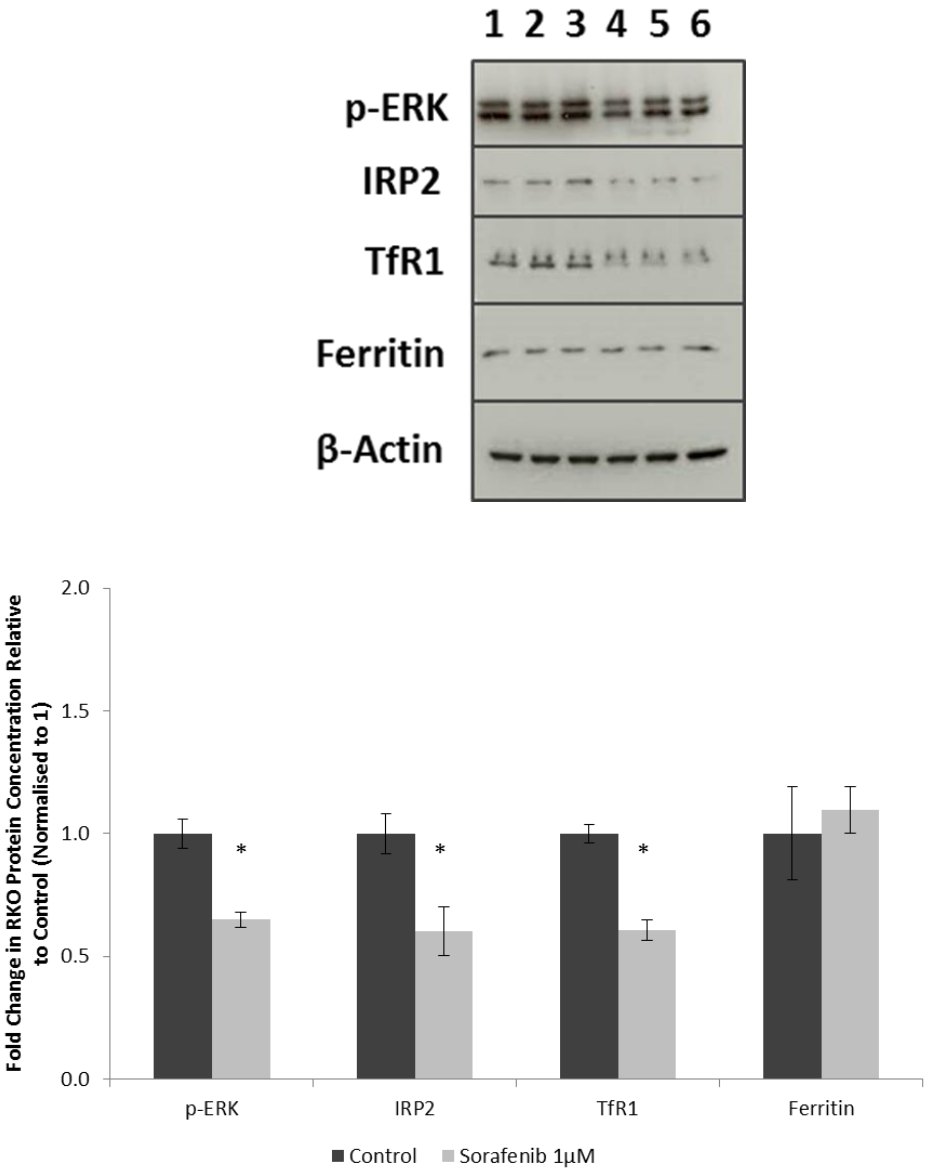

Figure 5.15 Treatment of colorectal adenocarcinoma cells with the B-raf kinase inhibitor Sorafenib is associated with a reduction in IRP2 protein expression *in-vitro*

Western blot demonstrating change in IRP2, TfR1 and ferritin expression in RKO cells following exposure to either standard media (lanes 1-3) or media containing 1 μM Sorafenib (lanes 4-6) for 48 hours. Semi-quantitative analysis of blots was performed through normalisation to β-Actin and subsequent expression as a fold change relative to control (normalised to 1). Data points represent mean fold change in protein expression relative to control, error bars denote ±SEM, * $p<0.05$ vs. control.

5.4 Discussion

Iron is intimately involved in the propagation of colorectal tumourigenesis. Adenocarcinomas accumulate iron, a process aided by the increased expression of key cellular iron import proteins (TfR1 and DMT1) and decreased iron export through the perturbation of the basolateral transporter ferroportin. [82] This increased intracellular iron serves as a 'fuel source' for DNA synthesis, ATP generation and cell cycle progression; which then in turn drive cellular proliferation. Iron has also been shown to amplify the Wnt signalling pathway, resulting in elevated levels of downstream targets including c-Myc, which further serves to aid cellular proliferation and survival. [102, 132]

Iron metabolism is co-ordinated at the cellular level by the iron regulatory proteins IRP1 and IRP2. [99] IRPs facilitate the increased availability of intracellular iron in times of iron depletion through stabilising the translation of TfR1 (and to some extent DMT1) and inhibiting translation of ferritin. In times of iron repletion, the IRPs are inactive (IRP1 acting instead as a cytosolic acinotase whilst IRP2 is degraded). [99]

The role of the IRPs within the up-regulation of iron metabolism seen in colorectal adenocarcinoma has not previously been conclusively determined and thus the findings discussed herein are novel. IRP2 over-expression has been linked to the propagation of both lung and breast cancer and hence the expression (and subsequent consequences) of it were selected to be determined in colorectal adenocarcinoma. [254, 258]

In this study, IRP2 was shown to be markedly and significantly over-expressed in samples of colorectal adenocarcinoma compared to matched normal mucosa at the mRNA level (mean fold change 200.19 vs. normal tissue, p=0.000). TfR1 mRNA levels were also markedly elevated in tumour samples (mean fold change 314.11 vs. normal tissue, p=0.000) and correlated positively with IRP2

mRNA expression. On sub-group analysis the up-regulation of IRP2 mRNA appeared to be a colonic rather than rectal phenomenon and was greatest in tumours that were proximally located (caecum or ascending colon) and locally advanced (T3 or T4).

Similarly, immunohistochemical staining revealed IRP2 expression to be significantly increased at the protein level in adenocarcinomas compared to normal tissue. Interestingly, mucinous tumours were shown to stain strongest for IRP2.

The finding of increased IRP2 expression in colorectal cancer is novel and contradicts the findings of a recent study by Hamara and colleagues which demonstrated no significant change in IRP2 mRNA levels between tumour and normal mucosa in 73 matched samples.[259] Interestingly, the authors of the same study also demonstrated a statistical decrease in both IRP1 and TfR1 mRNA expression (the opposite to our findings). In agreement with our results, however, it was demonstrated that IRP2 was up-regulated in T3 tumours (compared to T1 and T2). [259] Increased IRP2 expression has also previously been demonstrated to correlate with grade of disease in breast cancer. [258]

The positive correlation between IRP2 and TfR1 mRNA expression demonstrates that the functionality of the IRE-IRP interaction persists despite the over-expression of IRP2 in colorectal cancer. Hamara and colleagues also demonstrated the correlation of IRP2 with TfR1 expression, albeit limited to early stage disease. [259]

IRP2 expression results in stabilisation of TfR1 translation and inhibition of ferritin mRNA translation. This interaction permits an increase in the amount of iron that is free for use within the cell (the so called labile iron pool) through increased iron acquisition and a reduction in iron storage. As expected, perturbation of IRP2 in this study (through the use of siRNA) resulted in significantly decreased TfR1 expression (at both the mRNA and protein levels) and a marked increase in ferritin

expression (at the protein level). In turn, this resulted in a significant decrease in the ability of colorectal cells to load iron (47.2% reduction vs. control, $p<0.05$ by ferrozine assay) and a subsequent increase in the proportion of cells in G1 of the cell cycle. Again, similar findings have been noted previously in breast cancer (where knockdown of IRP2 inhibited cell proliferation and stimulated apoptosis) and points to the vital role IRP2 is likely to play in facilitating both the increased iron acquisition required for proliferation in cancerous tissue and the amplification of oncogenic signalling pathways (such as Wnt). [132, 258] It would therefore be useful in future studies to investigate the effect of IRP2 perturbation on Wnt signalling and intracellular free radical formation, both processes known to be stimulated by increased labile iron.

Ideally, the use of a more stable knockdown system (e.g. shRNA) would also have facilitated further investigation of the effects of IRP2 perturbation on cell proliferation, migration, invasion and sensitivity to chemotherapeutic agents (including iron chelation with Deferasirox). Unfortunately, this system was not available during the course of this study and therefore investigations were limited to the effects of transient IRP2 knockdown within a 24 hour window.

In an attempt to delineate whether the increase in tumour IRP2 expression is merely a response to the increased cellular requirement for iron present in malignant tissue or is somehow initiated by factors within the tumour itself, exploration of the Cancer Genome Atlas was next performed in order to assess the relationship between genetic mutations pertinent to colorectal cancer and IRP2. A potential relationship between B-raf mutation and IRP2 protein overexpression (odds ratio 1.7, $p=0.032$) was subsequently demonstrated.

Oncogenic mutations in B-raf occur in approximately 13% of colorectal cancers. [245] B-raf mutations signal B-raf serine-threonine kinase activity thus activating the mitogen-activated protein kinase (MAPK) signalling cascade (EGFR→RAS→RAF→MEK→ERK1/2) which is involved in the subsequent

activation of a significant number of downstream targets involved in cellular proliferation, including c-Myc. [245, 260] Interestingly, c-Myc has previously been shown to up-regulate IRP2 expression (but not TfR1) and suppress ferritin expression in B cells. [261] Of note, in the same study, the subsequent restoration of intracellular ferritin levels (through a vector expressing H-ferritin) inhibited cell clonogenicity, indicating the importance of free iron to cell growth and proliferation. In a separate study using B-cell lymphoma cell lines, c-Myc was shown to increase the expression of TfR1, subsequently leading to an increase in cellular proliferation. [133] Increased c-Myc and ERK 1/2 phosphorylation has also been demonstrated in lung tumour xenografts expressing increased levels of IRP2. [254]

B-raf mutant colorectal adenocarcinomas are associated with proximal location, increasing age, female gender, microsatellite instability, high grade and mucinous histology. [262] Anecdotally, in this study, IRP2 expression was greatest in proximal tumours, those that were locally advanced and in tumours of a mucinous appearance, all features found in B-raf mutant tumours.

The successful generation of a cell line transfected with an inducible B-raf V600E construct permitted *in-vitro* assessment of the interaction between B-raf and IRP2. The B-raf V600E mutation is the most common B-raf mutation in cancer (accounting for around 90% of mutations) and derives from a DNA point mutation (1799 T→A). [262] Within the limits of this study, it was demonstrated that induction of B-raf V600E (by almost 13 fold) did not significantly alter IRP2 expression at the protein level. Of note, p-ERK levels were also unaltered; a phenomenon that may be partially explained by the presence of a constitutively active K-ras mutation within the same cell line thus raising the possibility that the MAPK signalling may have already been pre-saturated and was not amenable to further stimulation by B-raf, an undoubted limitation of this model. [263] An attempt was made to circumvent this problem by repeating the transfection in Colo320 cells (expressing wild type B-raf

and K-ras), however, this process was unsuccessful owing to profound puromycin resistance within the Colo320 line. Other appropriate cell lines were unavailable within the study time period.

On further investigation, however, using the HCT116 V600E and HCT116 empty vector cell lines it was demonstrated that elevated p-ERK signalling at base line was associated with increased IRP2 protein expression.

Further confirmation of a link between MAPK signalling and IRP2 expression in colorectal cancer was sought through administration of the MEK 1/2 inhibitor Trametinib and the B-raf kinase inhibitor Sorafenib to a panel of colorectal cell lines. MEK inhibition was associated with decreased IRP2 and TfR1 expression in the SW480 and HCT116 cell lines (both with mutant K-ras). In the RKO line (displaying mutant B-raf), however, MEK inhibition suppressed TfR1 expression but did not significantly alter IRP2 levels. Interestingly, ferritin expression was markedly increased (30 fold). Treatment of the RKO cell line with the B-raf inhibitor Sorafenib, however, did significantly suppress both IRP2 and TfR1 protein expression.

It is likely that the link between increased MAPK signalling and elevated IRP2 expression is through the proto-oncogene c-Myc. IRP2 has previously been shown to correlate with c-Myc expression in studies using lung and haematological cell lines. [254, 261] Interestingly, mutation of the tumour suppressor APC is also known to elevate levels of c-Myc. [102] Further work looking at the effect of c-Myc perturbation (either through knockout or over expression) on the link between MAPK and IRP2 would undoubtedly be useful in delineating this relationship further. Furthermore, the effect of stimulation of colorectal cells with MAPK ligands (e.g. epidermal growth factor or amphiregulin) and subsequent effect on iron metabolism could be assessed. Anecdotally, preliminary experiments within this study period have indicated a dose dependent increase in IRP2 mRNA expression

following stimulation of RKO cells with EGF (data not shown). Further work is needed, however, before any conclusions can be drawn from this.

It has been demonstrated in this chapter that IRP2, an important regulator of intracellular iron acquisition, is markedly over expressed at both the mRNA and protein levels in colorectal cancer. Furthermore, this over expression results in increased potential for the acquisition of iron through elevated levels of the iron import protein TfR1. IRP2 expression appears to be greatest in colonic tumours (particularly those arising proximally, that are locally advanced and of a mucinous type). Knockdown of IRP2 results in the classical IRE-IRP response of decreased TfR1 and increased ferritin expression. In turn, this decreases the ability of the cell to acquire iron and results in perturbation of the cell cycle that is over turned through the subsequent administration of iron.

Furthermore, IRP2 over expression appears to be linked to over activity of the MAPK signalling cascade, a pathway known to be constitutively active in a significant proportion of colorectal cancers. [260] Much research has been conducted into this signalling cascade and has led to the development of a number of monoclonal antibodies (e.g. Cetuximab) and small molecule tyrosine kinase inhibitors (e.g. Sorafenib) that already serve as adjuncts to existing chemotherapeutic regimens. [260] Unfortunately, acquired and primary resistance to therapy with these agents is a problem and therefore the demonstration of a link between MAPK signalling and IRP2 protein expression raises the possibility that iron chelation therapy with Deferasirox could serve as an additional therapy adjunct. [264] Furthermore, if MAPK activation (be it through K-ras or B-raf mutation) is a marker of IRP2 expression (which in turn is a surrogate marker for cellular iron requirement) then this offers the potential for selective therapy based on the genetic status of the tumour at the time of therapy initiation.

Further work is undoubtedly required in this area before affirmative conclusions can be drawn, however, the work undertaken in this chapter has led to a number of novel findings which offer direction for future research into iron chelation as a potential treatment for colorectal cancer.

Chapter 6. Drug redeployment: A useful tool in gastrointestinal cancer?

6.1 Introduction

Owing to the known dysregulation of iron metabolism within neoplastic cells, there is significant interest in the potential of iron chelators to act as anti-cancer agents in their own right. [80, 92] Furthermore, there is also evidence that iron chelators may be capable of both overcoming established chemotherapy resistance and of acting as chemosensitising agents. [139, 177] At present, however, much of this work has been carried out using experimental agents that (in part owing to significant side effects in pre-clinical models) are not currently licensed for use in humans. [139, 140, 141] Thus, the demonstration here (in chapters 3 and 4) that a licensed chelator (Deferasirox) possesses potent anti-neoplastic and chemosensitising properties in gastrointestinal cancer is of great promise.

At present, the use of Deferasirox in clinical practice is restricted to the treatment of conditions associated with chronic iron overload (such as β-thalassaemia) and it has never before been used as a direct treatment for any form of cancer. As such, the discovery in the current study that Deferasirox possesses potential efficacy as an anti-cancer therapy can also be said to represent a form of drug repurposing or redeployment.

The development of novel anti-cancer therapies is an immensely expensive and time-consuming process. [265] On average, it takes 13 years of research and over $1.8 billion to bring a single drug from the laboratory bench to the patient's bedside.[266] In addition, studies have demonstrated that only 1 in every 5-10,000 prospective anti-cancer agents receives formal clinical approval and only 5% of oncology drugs entering Phase I clinical trials are ever approved for use. [265, 267] Even if a drug proceeds to clinical trials, the final product is often extremely expensive (in part due to the costs incurred by the drug companies in reaching that point) and may be associated with a number of

significant side effects. Furthermore, they may ultimately make only marginal improvements in overall disease survival. [265] As such, the approval of new anti-cancer agents for routine clinical use can be an immensely emotive subject as health service providers are forced to weigh up cost benefit ratios prior to advocating widespread adoption. Examples of this in the UK include the introduction of the monoclonal antibody Trastuzumab (Herceptin) for the treatment of breast cancer and, more recently, its successor Trastuzumab emtansine (Kadcyla), which at present has been rejected for clinical use by the National Institute for Health and Care Excellence (NICE) on the grounds of cost. [268]

Thus, alternative routes for the discovery of new agents effective against cancer are required. One such avenue now being extensively employed is that of drug redeployment. The field of drug redeployment involves the systematic screening of existing licensed compounds for efficacy in diseases other than those for which they are traditionally used to treat (i.e. cancer). [200] This process is based on the knowledge that, owing to the common molecular origins of diverse diseases, approximately 90% of approved drugs may possess secondary indications and could be used for other purposes.[269] The major advantage of this approach to cancer drug development is that prior knowledge of the pharmacological and toxicity profiles of existing drugs (gained through their current use) is likely to permit entry into phase II and III trials at a much faster rate. [265] Indeed, recent studies have estimated that, whilst only 10 and 50% of new agents make it to market having entered phase II and III trials respectively, the figure is closer to 25 and 65% for redeployed agents. [265, 270] As well as reducing the time it takes for new agents to come to market, drug redeployment also has the advantage that, as agents are often older and thus off patent, final market costs are likely to be significantly reduced.

The process of drug repurposing typically takes one of two forms: ‘on-target repurposing’ attempts to utilise drugs which are known to act through a relevant mechanism of action but which currently have a different clinical indication, whilst ‘off-target repurposing’ or systematic serendipity involves

the random screening of drugs with no known association, in the hope of demonstrating efficacy and a subsequent novel mechanism of action. [271]

Redeployed drugs that have been successfully shown to possess marked anti-cancer effects include thalidomide (which has been shown to possess anti-angiogenic and NFκB inhibiting properties in a number of haematological malignancies), aspirin (through inhibition of platelet aggregation, cyclooxygenase enzymes, Wnt signalling and also NFκB amongst other mechanisms), statins (again through NFκB inhibition), metformin (through inhibition of the mTOR pathway) and finally methotrexate. [265]

Of note, systematic drug redeployment screens have also revealed agents that may be ineffective solely yet become highly efficacious in combination with other redeployed agents. An example of this includes the combination of the lipid-lowering drug Bezafibrate and the sex hormone Medroxyprogesterone acetatate in the treatment of acute myeloid leukaemia and Burkitt's lymphoma. [272, 273] This raises the potential that combining agents with an iron chelator (such as Deferasirox) may also yield efficacious combinations.

The use of drug redeployment approaches within gastrointestinal cancer, however, has thus far been limited. As stated previously, systemic therapy is utilised in the treatment of both oesophageal and colorectal cancer with variable tumour response. [41, 42, 235] Agents are typically used in combination in an attempt to exert effects on a number of pathways simultaneously and also in some instances to illicit synergy between compounds (e.g. Leucovorin and 5-Fu in colon cancer). [274] As such, it seems logical to assess the usefulness of adopting a drug redeployment approach for the identification of new agents that may be effective either alone or in combination with Deferasirox against these diseases.

6.2 Chapter Aims

Having already demonstrated a form of drug redeployment using the iron chelator Deferasirox (an on-target approach using the knowledge that cancer cells have a higher requirement for iron and that iron metabolism itself is dysregulated in gastrointestinal cancer), it was decided to next serendipitously screen a library of 99 licensed, off-patent reagents both alone and in combination with Deferasirox against a panel of gastrointestinal cell lineages to identify agents or combinations that may display anti-neoplastic properties in this area. As such, the aims for this chapter are:

1. To identify any synergistic combinations between a panel of redeployed drugs and the iron chelating agent Deferasirox in oesophageal and colorectal carcinoma *in-vitro.*
2. To identify agents with potential anti-neoplastic properties against colorectal adenocarcinoma *in-vitro* using a drug redeployment approach.
3. To determine the effect of p53 status on the efficacy of redeployed agents in colorectal adenocarcinoma *in-vitro.*
4. To determine the effect of hypoxia on the efficacy of redeployed agents in colorectal adenocarcinoma *in-vitro.*
5. To identify agents with potential anti-neoplastic properties against oesophageal carcinoma *in-vitro.*
6. To validate any promising agents *in-vivo* using a murine xenograft model of oesophageal adenocarcinoma.

6.3 Results

6.3.1 The determination of any synergy between the redeployed drugs and the iron chelating agent Deferasirox in colorectal adenocarcinoma *in-vitro*

6.3.1.1 Overview

Deferasirox has previously shown potential synergy (particularly at sub-therapeutic doses) in studies in this thesis when given with common chemotherapeutic agents in both oesophageal (Figure 3.3C) and colorectal (Figure 4.7D) carcinoma. As such, the potential for Deferasirox to form synergistic combinations was investigated using a selection of redeployed drugs (Table 2.2) in colorectal adenocarcinoma.[200]

The whole drug redeployment library was initially screened against the HCT116 p53WT cell line, with or without the presence of Deferasirox at the sub-therapeutic concentration of 1 μM. MTT assays were performed to determine effect on cell viability. Deferasirox was utilised at a sub-therapeutic concentration as it had previously proved to be so potent in isolation at higher doses that any potential synergy could be masked in these experiments.

6.3.1.2 Results

Following provisional screening of the redeployed library with or without the presence of Deferasirox (1 µM) against the HCT116 p53WT cell line (which did not identify any statistically significant synergistic relationships, data not shown here) promising agents were re-tested against a broader panel of colorectal lines (Figure 6.1). Of note, Valproic acid demonstrated synergy with Deferasirox across all of the lines tested. Furthermore, an additional reduction in cellular viability was also seen in 2 of the cell lines tested when Niclosamide was cultured alongside Deferasirox.

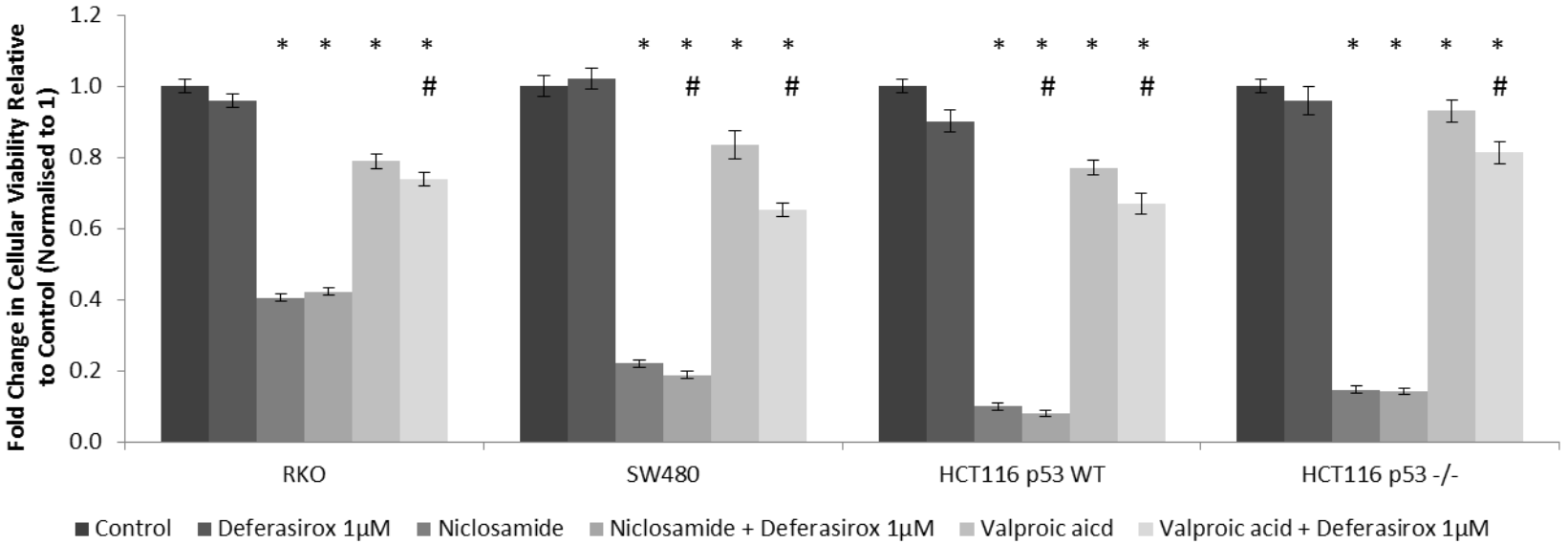

Figure 6.1 The redeployed drugs Niclosamide and Valproic acid are efficacious against colorectal adenocarcinoma cell lines *in-vitro* and demonstrate synergy when combined with a low dose of the iron chelator Deferasirox

Cell viability assay (MTT) demonstrating the efficacy of the redeployed agents Niclosamide and Valproic acid against the colorectal adenocarcinoma cell lines RKO, SW480 and HCT116. In addition, it appears the respective efficacy of each drug can be improved further by co-incubation with Deferasirox (1 µM). Data points represent mean fold change relative to control (normalised to 1), error bars denote ±SEM, * $p<0.05$ vs. control, # $p<0.05$ vs. equivalent drug without Deferasirox.

6.3.2 The efficacy of redeployed drugs against colorectal adenocarcinoma *in-vitro*

6.3.2.1 Overview

The library of redeployed drugs was screened alone for efficacy against a panel of colorectal adenocarcinoma cell lines *in-vitro* (RKO, SW480 and HT29). In addition, agents were also screened against the colorectal cell line SW620 (which is a metastatic clone arising from the same patient as the SW480 cell line) to see if there were any differences in efficacy between primary and metastatic lines.

6.3.2.2 Results

A number of agents demonstrated a significant effect on colorectal cell line viability (Figure 6.2 A-C). Of note, the anti-gout agent Colchicine and the anti-helminthic Mebendazole demonstrated marked effects across all 3 lines tested.

Both Colchicine and Mebendazole were equally effective in the SW620 cells as they were in the SW480 (Figure 6.3). This was not the case with the existing chemotherapeutic agent 5-Fu, which did not exert a significant suppression of cellular viability compared to control and was also significantly less effective than in the SW480 line.

Figure 6.2 The effect of redeployed drugs on colorectal adenocarcinoma cell line viability *in-vitro*

Drug	Fold Change (vs. Control)	P Value	Chloroquine	0.717	0.014
Control	1.000		Valproic acid	0.718	0.140
Mebendazole	0.213	0.001	Zinc acetate	0.719	0.204
Methotrexate	0.232	0.002	Propantheline	0.722	0.030
Colchicine	0.236	0.001	Alverine citrate	0.723	0.046
5-Fluorouracil	0.372	0.003	Fluoxetine	0.726	0.138
Nicotine	0.391	0.048	Norethisterone	0.726	0.114
Desferrioxamine	0.439	0.075	Acitretin	0.732	0.148
Trimethoprim	0.449	0.050	Thalidomide	0.732	0.125
Danazol	0.461	0.130	Artemisinin	0.733	0.160
Calciferol/ergocalciferol	0.476	0.085	Carbamazepine	0.742	0.037
Omeprazole	0.494	0.141	Chlorpheniramine	0.743	0.249
Mifepristone	0.521	0.051	Pravastatin	0.744	0.170
Naloxone	0.552	0.214	Thiamine	0.747	0.002
Domperidone	0.556	0.166	Vitamin K1	0.752	0.338
Bezafibrate	0.573	0.092	Ascorbic acid	0.755	0.277
Testosterone	0.587	0.087	Clobetasol propionate	0.755	0.052
Paroxetine	0.587	0.086	Metformin	0.756	0.058
Dantrolene sodium	0.592	0.166	Alpha tocopheryl acetate	0.757	0.075
Medroxyprogesterone acetate	0.599	0.094	Ritodrine	0.766	0.079
Acipimox	0.609	0.097	Flecainide	0.782	0.376
Nortryptyline	0.612	0.112	Paracetamol	0.784	0.060
Chlorambucil	0.616	0.046	Nicotinamide	0.787	0.135
Prochlorperazine	0.617	0.015	Praziquantel	0.787	0.473
Imatinib	0.620	0.100	Finasteride	0.788	0.153
Diltiazem	0.622	0.062	Rifampicin	0.789	0.179
Fluconazole	0.633	0.095	Methanol	0.799	0.262
Niclosamide	0.633	0.066	Ampicillin	0.801	0.259
Water	0.635	0.100	Acyclovir	0.816	0.453
Clofibric acid	0.638	0.242	Neostigmine	0.821	0.286
Itraconazole	0.640	0.027	Amantidine	0.824	0.014
Amphotericin b	0.648	0.108	Ranitidine	0.824	0.042
Mefenamic acid	0.654	0.000	DMSO	0.828	0.097
Fenofibrate	0.663	0.106	Allopurinol	0.829	0.289
Selegiline	0.674	0.039	Propanolol	0.833	0.296
Vitamin B12	0.675	0.159	Metronidazole	0.834	0.488
DMEM (2)	0.676	0.086	Doxycycline	0.840	0.125
Simvastatin	0.680	0.190	Ibuprofen	0.843	0.061
Erythromycin	0.686	0.037	Imipramine	0.849	0.086
DMEM (1)	0.690	0.175	Cyclophosphamide	0.852	0.566
Levothyroxine	0.690	0.108	Prednisolone	0.857	0.113
Methyldopa	0.698	0.030	Theophylline	0.873	0.375
Ethanol	0.703	0.279	Flutamide	0.875	0.515
Clomipramine	0.704	0.128	Bromocriptine	0.880	0.536
Penicillin V	0.705	0.047	Folic acid	0.886	0.274
Diclofenac	0.710	0.055	Nicotinic acid	0.887	0.137
Flupentixol	0.712	0.140	Dexamethasone	0.908	0.198
Mesalazine	0.713	0.124	Bendroflumethiazide	0.937	0.818
Pilocarpine	0.714	0.276	Retinol	0.967	0.804
Cefaclor	0.717	0.108	Propylthiouracil	0.973	0.846
Metoclopromide	0.717	0.220	Aspirin	1.032	0.827

A. RKO

Drug	Fold Change (vs. Control)	P Value	Rifampicin	0.786	0.251
Control	1.000		Erythromycin	0.788	0.225
Colchicine	0.104	0.000	Zinc acetate	0.789	0.025
Mebendazole	0.119	0.000	DMEM (1)	0.789	0.067
Desferrioxamine	0.372	0.033	Methanol	0.789	0.105
Nicotine	0.438	0.109	Nicotinamide	0.790	0.047
Methotrexate	0.472	0.010	Praziquantel	0.793	0.073
Niclosamide	0.472	0.060	Flutamide	0.803	0.091
Calciferol/ergocalciferol	0.508	0.026	Neostigmine	0.806	0.050
Omeprazole	0.517	0.092	Ampicillin	0.809	0.023
Acipimox	0.528	0.065	Chlorpheniramine	0.814	0.187
Naloxone	0.530	0.160	Diclofenac	0.815	0.072
Danazol	0.537	0.174	Thiamine	0.820	0.258
Trimethoprim	0.552	0.014	Thalidomide	0.821	0.102
5-Fluorouracil	0.557	0.012	Propantheline	0.823	0.077
Mifepristone	0.577	0.153	Metoclopromide	0.834	0.198
Ethanol	0.578	0.164	Prednisolone	0.836	0.175
Flupentixol	0.588	0.018	Prochlorperazine	0.839	0.033
Mefenamic acid	0.622	0.093	Vitamin K1	0.846	0.006
Clomipramine	0.636	0.011	DMSO	0.847	0.163
Testosterone	0.640	0.015	Fluoxetine	0.851	0.228
Dantrolene sodium	0.647	0.033	Chloroquine	0.852	0.289
Bezafibrate	0.662	0.006	Acitretin	0.852	0.214
Amphotericin b	0.663	0.038	Vitamin B12	0.857	0.420
Clofibric acid	0.673	0.027	Folic acid	0.860	0.093
Nortryptyline	0.676	0.166	Mesalazine	0.861	0.588
Medroxyprogesterone acetate	0.694	0.050	Ranitidine	0.864	0.004
Norethisterone	0.703	0.008	Amantidine	0.867	0.032
Methyldopa	0.703	0.157	Penicillin V	0.870	0.467
Domperidone	0.707	0.160	Cefaclor	0.875	0.502
Paroxetine	0.708	0.014	Paracetamol	0.876	0.610
Itraconazole	0.724	0.051	Aspirin	0.877	0.419
Metformin	0.724	0.064	Metronidazole	0.878	0.212
Diltiazem	0.726	0.136	Bendroflumethiazide	0.879	0.315
Imatinib	0.726	0.067	Ibuprofen	0.880	0.304
Selegiline	0.727	0.018	Simvastatin	0.888	0.508
Valproic acid	0.727	0.189	Bromocriptine	0.888	0.122
Water	0.729	0.024	Dexamethasone	0.889	0.215
Fluconazole	0.734	0.142	Propanolol	0.890	0.271
Chlorambucil	0.739	0.147	Pilocarpine	0.891	0.373
Alpha tocopheryl acetate	0.742	0.065	Theophylline	0.892	0.046
Levothyroxine	0.748	0.014	Clobetasol propionate	0.892	0.522
Fenofibrate	0.753	0.024	Ascorbic acid	0.900	0.343
Alverine citrate	0.755	0.189	Acyclovir	0.922	0.172
Pravastatin	0.756	0.057	Propylthiouracil	0.928	0.227
Cyclophosphamide	0.757	0.002	Imipramine	0.928	0.615
Carbamazepine	0.758	0.090	Nicotinic acid	0.938	0.225
Artemisinin	0.760	0.009	Allopurinol	0.940	0.101
DMEM (2)	0.767	0.021	Doxycycline	0.959	0.768
Finasteride	0.785	0.095	Flecainide	1.030	0.896
Ritodrine	0.785	0.013	Retinol	1.065	0.292

B. SW480

Drug	Fold Change (vs. Control)	P Value	Paroxetine	0.969	0.906
Control	1.000		Chlorambucil	0.971	0.900
Desferrioxamine	0.156	0.014	Bromocriptine	0.980	0.924
Mebendazole	0.164	0.000	Selegiline	0.984	0.914
Colchicine	0.164	0.001	Ranitidine	0.987	0.917
Danazol	0.235	0.060	Diltiazem	0.993	0.968
Nicotine	0.255	0.075	Clomipramine	0.997	0.990
Omeprazole	0.262	0.026	Ascorbic acid	0.998	0.980
Dantrolene sodium	0.321	0.042	Imipramine	1.004	0.898
Ethanol	0.342	0.108	Doxycycline	1.006	0.976
Prochlorperazine	0.407	0.049	Methyldopa	1.009	0.971
Alverine citrate	0.414	0.059	Vitamin K1	1.010	0.933
Imatinib	0.433	0.046	Propantheline	1.014	0.942
Domperidone	0.443	0.108	Levothyroxine	1.017	0.940
Methotrexate	0.469	0.007	Vitamin B12	1.018	0.944
Naloxone	0.487	0.158	Norethisterone	1.023	0.938
Amphotericin b	0.506	0.228	DMEM (2)	1.024	0.895
Zinc acetate	0.510	0.033	Bezafibrate	1.026	0.930
Mifepristone	0.511	0.286	Clobetasol propionate	1.026	0.915
Nortryptyline	0.525	0.140	Chlorpheniramine	1.037	0.872
Acipimox	0.560	0.162	Nicotinamide	1.041	0.773
Calciferol/ergocalciferol	0.603	0.161	Finasteride	1.045	0.829
Clofibric acid	0.643	0.176	Medroxyprogesterone acetate	1.046	0.877
5-Fluorouracil	0.666	0.100	Alpha tocopheryl acetate	1.049	0.820
Thalidomide	0.700	0.066	Mefenamic acid	1.055	0.882
Methanol	0.721	0.051	Metronidazole	1.057	0.810
Fluoxetine	0.756	0.091	Thiamine	1.064	0.591
Testosterone	0.762	0.378	Rifampicin	1.070	0.779
Acyclovir	0.762	0.067	Folic acid	1.074	0.583
Itraconazole	0.766	0.326	Carbamazepine	1.080	0.588
Pravastatin	0.775	0.410	Paracetamol	1.086	0.793
Flupentixol	0.783	0.209	Ibuprofen	1.087	0.795
Cefaclor	0.800	0.074	Neostigmine	1.088	0.693
Water	0.823	0.520	Acitretin	1.092	0.709
Simvastatin	0.827	0.176	Mesalazine	1.094	0.737
Metoclopromide	0.834	0.251	Fluconazole	1.095	0.682
Penicillin V	0.874	0.052	Ritodrine	1.098	0.678
Trimethoprim	0.882	0.727	Aspirin	1.103	0.730
Fenofibrate	0.884	0.440	DMSO	1.107	0.594
Metformin	0.899	0.755	Prednisolone	1.109	0.636
Niclosamide	0.902	0.704	Propanolol	1.111	0.381
Diclofenac	0.905	0.360	Dexamethasone	1.113	0.608
Chloroquine	0.913	0.702	Amantidine	1.113	0.623
Allopurinol	0.922	0.666	Retinol	1.117	0.594
Ampicillin	0.929	0.628	DMEM (1)	1.120	0.652
Flutamide	0.943	0.818	Flecainide	1.124	0.543
Artemisinin	0.948	0.730	Theophylline	1.127	0.524
Valproic acid	0.955	0.775	Pilocarpine	1.140	0.598
Erythromycin	0.955	0.705	Propylthiouracil	1.158	0.595
Praziquantel	0.961	0.846	Nicotinic acid	1.161	0.535
Cyclophosphamide	0.968	0.769	Bendroflumethiazide	1.219	0.521

C. HT29

Figure 6.2 The effect of redeployed drugs on colorectal adenocarcinoma cell line viability *in-vitro*

Cell viability assay (MTT) demonstrating the effects of the same panel of redeployed drugs on the colorectal adenocarcinoma cell lines RKO (A), SW480 (B) and HT29 (C) after 72 hours incubation. Data presented as mean fold change relative to control (normalised to 1), p value quoted represents drug vs. control.

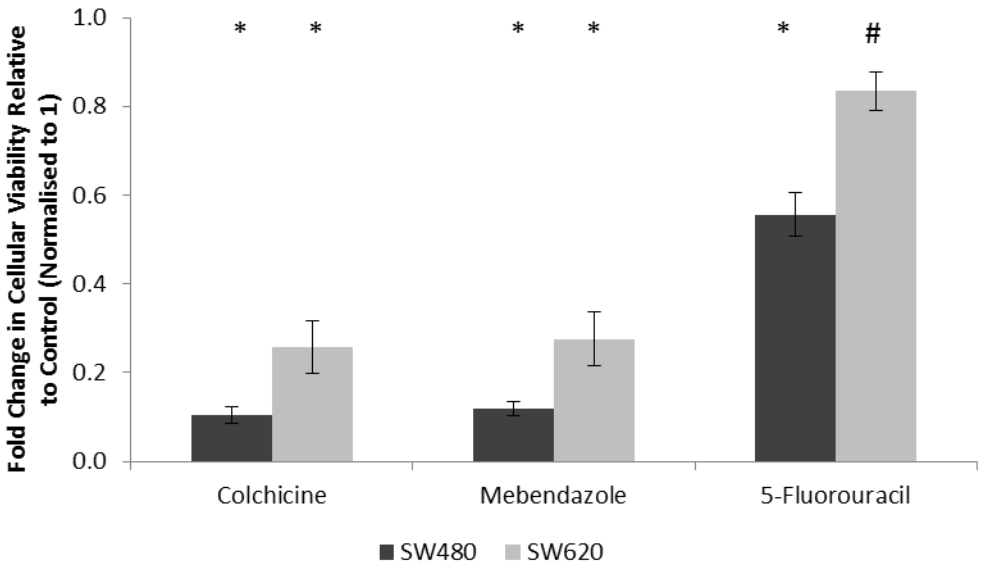

Figure 6.3 Colchicine and Mebendazole are efficacious against metastatic colorectal adenocarcinoma cell lines *in-vitro* whereas 5-Fluorouracil is not

Cell viability assay (MTT) demonstrating the effects of Colchicine, Mebendazole and 5-fluorouracil on the colorectal adenocarcinoma cell line SW480 and its metastatic clone SW620 after 72 hours incubation. Data presented as mean fold change relative to control (normalised to 1), error bars denote ±SEM, * $p<0.05$ vs. control, # $p<0.05$ vs. equivalent drug in SW480 cell line.

6.3.3 The effect of p53 status and hypoxia upon redeployed drug efficacy in colorectal adenocarcinoma *in-vitro*

6.3.3.1 Overview

The redeployed library of drugs was next screened against the HCT116 p53WT cell line and its isogenic counterpart HCT116 p53-/-. As previously demonstrated, these lines differ only in p53 status (Figure 4.10). The library was also administered to HCT116 p53WT cells in hypoxia to identify potentially efficacious agents that were then re-screened against a broader panel of colorectal cell lines (RKO, SW480, HCT116 p53WT and HCT116 p53-/-) to confirm efficacy.

Hypoxia was induced by the use of a 1% O_2 chamber and confirmed through Western blotting for HIF-1α expression (Figure 6.4A). Effect on cellular phenotype was assessed in normoxia by use of the MTT cell viability assay and in hypoxia using the SRB assay.

6.3.3.2 Results

Mebendazole and Colchicine were again both markedly efficacious in the HCT116 p53WT cell line, reducing cellular viability by 68.5 and 50.7% respectively ($p<0.05$ vs. control). In addition, Niclosamide also significantly decreased viability by 74.9% ($p<0.05$ vs. control). No drugs, however, within the redeployed library demonstrated a significant difference in efficacy based upon p53 status alone.

Screening of the entire redeployed library against the HCT116 p53WT cell line in the presence of hypoxia did not demonstrate any targets that were statistically efficacious in their own right (data not shown here). Promisingly, however, a number of agents demonstrated a non-significant trend

towards efficacy and therefore experiments were repeated with these in a broader panel of colorectal cell lines to confirm the results (Figure 6.4). Both Niclosamide and Valproic acid were subsequently found to significantly impede cellular proliferation across all 4 lines tested by 81.3 and 23.1% respectively ($p<0.05$ vs. control).

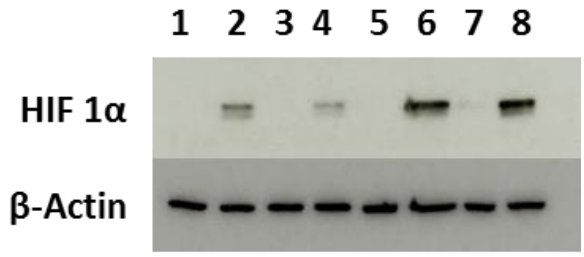
1 2 3 4 5 6 7 8
HIF 1α
β-Actin

A

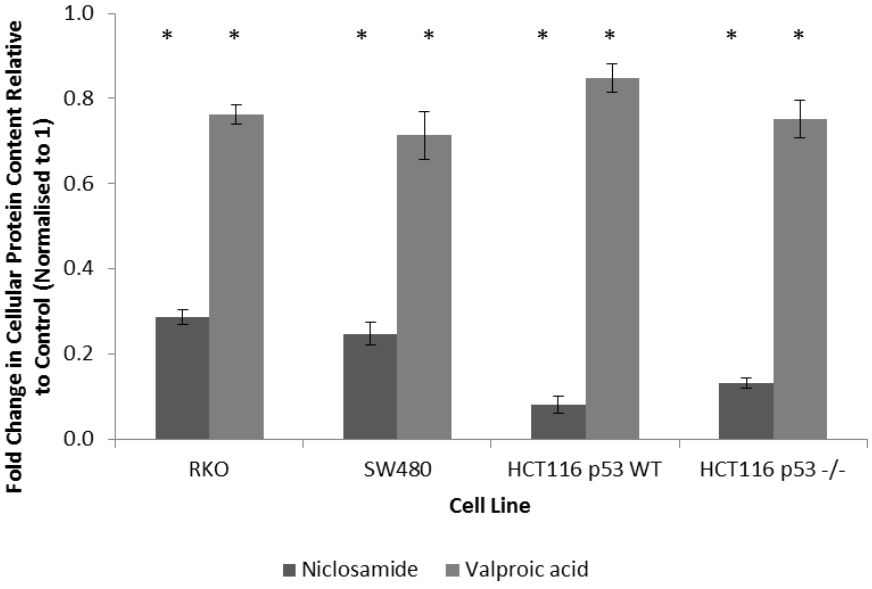
Fold Change in Cellular Protein Content Relative to Control (Normalised to 1)
1.0
0.8
0.6
0.4
0.2
0.0
RKO
SW480
HCT116 p53 WT
HCT116 p53 -/-
Cell Line
Niclosamide
Valproic acid

B

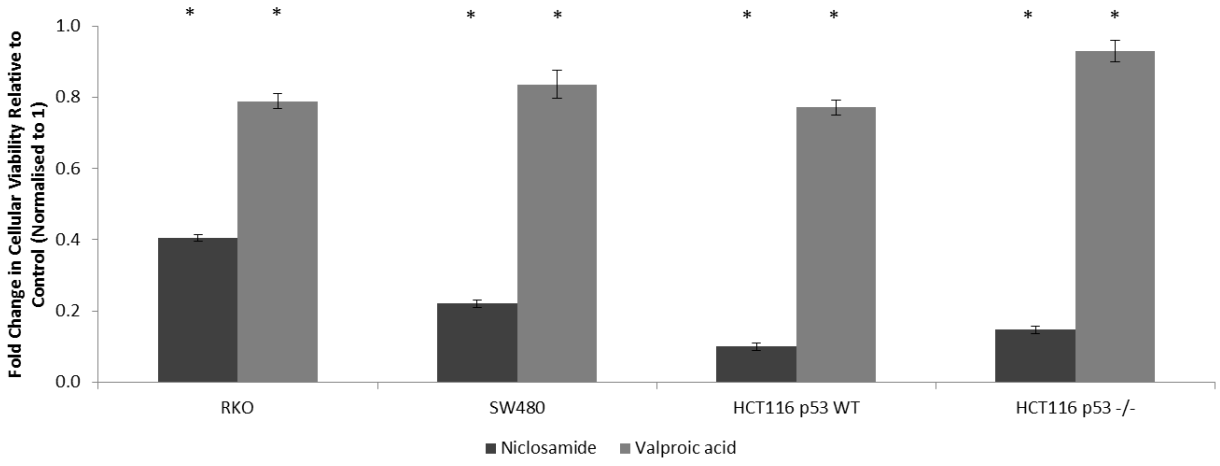
Fold Change in Cellular Viability Relative to Control (Normalised to 1)
1.0
0.8
0.6
0.4
0.2
0.0
RKO
SW480
HCT116 p53 WT
HCT116 p53 -/-
Niclosamide
Valproic acid

C

Figure 6.4 The redeployed drugs Niclosamide and Valproic acid are efficacious against colorectal adenocarcinoma cell lines in the presence of hypoxia

Western blot (A) demonstrating the increase in HIF-1α seen when a panel of colorectal cell lines (RKO lanes 1-2, SW480 lanes 3-4, HCT116 p53 WT lanes 5-6 and HCT116 p53 -/- lanes 7-8) are exposed to 1% O_2 for 24 hours. Lanes 1, 3, 5 and 7 represent normoxia, lanes 2, 4, 6 and 8 denote hypoxia. The drugs Niclosamide and Valproic acid were both efficacious against the same panel of cell lines despite this induction of hypoxia (SRB assay, B). The reagents were also efficacious in normoxia (C). Data points represent mean fold change compared to control, error bars denote ±SEM, * $p<0.05$ vs. control.

6.3.4 The efficacy of redeployed drugs against oesophageal carcinoma *in-vitro*

6.3.4.1 Overview

In order to assess whether or not agents within the same redeployed drug library were efficacious in oesophageal carcinoma the OAC cell lines OE19 and OE33 and the SCC line OE21 were next screened against the library. Cell growth was monitored over 72 hours prior to the performance of an MTT assay to assess drug effect on cell viability. The experiment was then repeated using the most efficacious agents to permit determination of cellular proliferation using the BrdU assay.

6.3.4.2 Results

A number of agents within the redeployed drug library demonstrated a significant reduction in oesophageal cell line viability within the 72 hour time period (Figure 6.5 A-C).

Of note, the iron chelating agent Desferrioxamine significantly reduced cellular viability by 69.6, 77.7 and 75.9% in the OE19, OE33 and OE21 lines respectively (Figure 6.6A). Other agents shown to have a profound effect on cellular viability included Prochlorperazine (mean reduction across all 3 lines 76.7% vs. control), methotrexate (75.7% reduction), Mebendazole (73.7% reduction), mifepristone (65.4% reduction) and Colchicine (62.1% vs. control).

Subsequent validation of these agents using the BrdU assay demonstrated that Prochlorperazine, Mebendazole and Colchicine all significantly reduced cellular proliferation in the OE19 and OE33 OAC lines. The same agents also reduced proliferation in the OE21 SCC line (Figure 6.6B). The iron chelator Desferrioxamine also reduced proliferation across all 3 lines tested, but owing to variability within experimental repeats, did not reach the required threshold for statistical significance.

Figure 6.5 The effect of redeployed drugs on oesophageal adenocarcinoma and squamous cell carcinoma cell line viability *in-vitro*

Drug	Fold Change (vs. Control)	P Value	Fluoxetine	0.757	0.042
Control	1.000		Allopurinol	0.757	0.244
Mebendazole	0.285	0.002	Simvastatin	0.757	0.440
Prochlorperazine	0.288	0.026	Pravastatin	0.759	0.266
Methotrexate	0.301	0.007	Penicillin V	0.765	0.138
Desferrioxamine	0.304	0.000	Acyclovir	0.775	0.033
Colchicine	0.430	0.012	Vitamin B12	0.776	0.255
Naloxone	0.434	0.004	Clobetasol	0.778	0.123
Omeprazole	0.489	0.103	Erythromycin	0.779	0.123
Danazol	0.537	0.009	Carbamazepine	0.782	0.060
Mifepristone	0.540	0.010	Valproic acid	0.784	0.264
Domperidone	0.555	0.028	Mesalazine	0.785	0.225
Nicotine	0.574	0.045	Nicotinic acid	0.790	0.221
Clofibric acid	0.586	0.041	Thalidomide	0.794	0.135
Fenofibrate	0.587	0.016	Retinol	0.795	0.323
Itraconazole	0.603	0.069	Paracetamol	0.799	0.214
Paroxetine	0.611	0.094	Chlorpheniramine	0.802	0.428
Flecainide	0.613	0.103	Alpha tocopheryl acetate	0.809	0.208
Pilocarpine	0.614	0.020	Clomipramine	0.814	0.121
Ampicillin	0.636	0.040	Vitamin K1	0.815	0.034
Levothyroxine	0.637	0.095	Testosterone	0.815	0.075
Water	0.644	0.077	Nicotinamide	0.817	0.269
Niclosamide	0.653	0.104	Chloroquine	0.821	0.155
Diltiazem	0.663	0.049	Diclofenac	0.824	0.214
Trimethoprim	0.663	0.101	Cefaclor	0.825	0.364
Bezafibrate	0.664	0.089	Propanolol	0.827	0.022
Dantrolene	0.667	0.154	DMEM (1)	0.834	0.438
Amphotericin b	0.667	0.048	Ritodrine	0.835	0.372
Ethanol	0.669	0.075	DMEM (2)	0.839	0.349
Chlorambucil	0.671	0.105	Neostigmine	0.840	0.142
Methanol	0.681	0.061	Theophylline	0.841	0.277
Fluconazole	0.684	0.057	Ranitidine	0.857	0.079
Alverine citrate	0.685	0.097	Propylthiouracil	0.860	0.133
Acipimox	0.695	0.115	Doxycycline	0.866	0.181
Flupentixol	0.698	0.047	Norethisterone	0.867	0.415
Cisplatin	0.702	0.001	Bendroflumethiazide	0.872	0.327
Flutamide	0.703	0.098	Dexamethasone	0.876	0.321
Metformin	0.704	0.060	Imatinib	0.883	0.510
Selegiline	0.715	0.105	Zinc acetate	0.885	0.512
Nortryptyline	0.720	0.228	Imipramine	0.888	0.193
Metoclopromide	0.722	0.085	Ibuprofen	0.895	0.521
Ergocalciferol	0.728	0.166	Acitretin	0.896	0.617
Cyclophosphamide	0.728	0.112	Thiamine	0.897	0.044
Mefenamic acid	0.729	0.106	Metronidazole	0.904	0.458
Finasteride	0.736	0.111	Aspirin	0.912	0.457
Propantheline bromide	0.738	0.096	Bromocriptine	0.926	0.685
Methyldopa	0.741	0.136	DMSO	0.931	0.422
Ascorbic acid	0.743	0.021	Prednisolone	0.945	0.485
Medroxyprogesterone acetate	0.749	0.208	Folic acid	0.960	0.658
Artemisinin	0.757	0.219	Rifampicin	0.986	0.927
Praziquantel	0.757	0.141	Amantidine	0.998	0.970

A. OE19

Drug	Fold Change (vs. Control)	P Value	Norethisterone	0.806	0.059
Control	1.000		Finasteride	0.807	0.095
Desferrioxamine	0.223	0.002	Imipramine	0.807	0.091
Prochlorperazine	0.226	0.008	Ascorbic acid	0.811	0.079
Methotrexate	0.251	0.002	Levothyroxine	0.818	0.010
Mebendazole	0.277	0.001	Thalidomide	0.820	0.001
Mifepristone	0.293	0.007	Diltiazem	0.824	0.147
Colchicine	0.411	0.001	Diclofenac	0.827	0.391
Nicotine	0.526	0.139	Doxycycline	0.827	0.424
Danazol	0.553	0.196	Flecainide	0.828	0.230
Omeprazole	0.554	0.008	Cefaclor	0.835	0.280
Niclosamide	0.568	0.069	Chloroquine	0.845	0.216
Domperidone	0.583	0.104	Cyclophosphamide	0.845	0.072
Clofibric acid	0.607	0.125	Methyldopa	0.846	0.360
Fluoxetine	0.609	0.109	Mesalazine	0.857	0.305
Water	0.620	0.219	Selegiline	0.859	0.134
Pilocarpine	0.626	0.020	Theophylline	0.859	0.047
Naloxone	0.633	0.216	Penicillin V	0.863	0.196
Ergocalciferol	0.673	0.237	Bezafibrate	0.865	0.292
Ampicillin	0.676	0.259	Zinc acetate	0.866	0.226
Cisplatin	0.684	0.002	Clomipramine	0.869	0.562
Nortryptyline	0.698	0.006	Ritodrine	0.878	0.600
Metformin	0.698	0.017	Aspirin	0.882	0.449
Itraconazole	0.701	0.221	Pravastatin	0.882	0.341
Vitamin K1	0.710	0.168	Praziquantel	0.883	0.624
Amphotericin b	0.718	0.462	Nicotinamide	0.888	0.143
Simvastatin	0.721	0.066	Methanol	0.891	0.294
Valproic acid	0.725	0.235	Dexamethasone	0.893	0.504
Fenofibrate	0.726	0.293	Imatinib	0.899	0.126
Acyclovir	0.728	0.219	Propanolol	0.902	0.182
Artemisinin	0.730	0.022	Ethanol	0.914	0.744
Flutamide	0.733	0.107	DMEM (1)	0.917	0.715
Vitamin B12	0.734	0.169	Chlorpheniramine	0.922	0.665
Alverine citrate	0.738	0.089	Flupentixol	0.923	0.756
Clobetasol	0.740	0.076	Carbamazepine	0.924	0.379
Erythromycin	0.742	0.082	Alpha tocopheryl acetate	0.936	0.560
Metoclopromide	0.752	0.242	Paracetamol	0.937	0.698
Medroxyprogesterone acetate	0.756	0.312	DMSO	0.947	0.767
Propantheline bromide	0.756	0.016	Propylthiouracil	0.952	0.712
Dantrolene	0.761	0.092	Metronidazole	0.955	0.854
Chlorambucil	0.761	0.193	Folic acid	0.955	0.287
Mefenamic acid	0.762	0.055	Prednisolone	0.964	0.789
Acitretin	0.771	0.323	Acipimox	0.969	0.875
Trimethoprim	0.780	0.419	Retinol	0.972	0.807
Fluconazole	0.784	0.189	Rifampicin	0.983	0.923
Allopurinol	0.787	0.326	Bendroflumethiazide	0.991	0.961
Ibuprofen	0.788	0.055	Thiamine	1.002	0.975
DMEM (2)	0.791	0.230	Amantidine	1.011	0.846
Paroxetine	0.792	0.219	Nicotinic acid	1.033	0.879
Testosterone	0.792	0.409	Ranitidine	1.045	0.826
Neostigmine	0.796	0.132	Bromocriptine	1.069	0.512

B. OE33

Drug	Fold Change (vs. Control)	P Value	Simvastatin	0.777	0.249
Control	1.000		Ampicillin	0.779	0.144
Methotrexate	0.178	0.001	Norethisterone	0.799	0.045
Prochlorperazine	0.185	0.007	Bezafibrate	0.800	0.422
Mifepristone	0.206	0.009	Nortryptyline	0.802	0.269
Mebendazole	0.228	0.000	Chlorpheniramine	0.805	0.404
Desferrioxamine	0.241	0.002	Bendroflumethiazide	0.810	0.208
Colchicine	0.296	0.001	Acitretin	0.810	0.205
Naloxone	0.330	0.046	Pravastatin	0.815	0.092
Nicotine	0.417	0.073	Flutamide	0.815	0.069
Amphotericin b	0.490	0.115	Praziquantel	0.817	0.077
Danazol	0.533	0.133	Vitamin B12	0.821	0.391
Niclosamide	0.541	0.083	Propantheline bromide	0.822	0.320
Omeprazole	0.550	0.069	Nicotinamide	0.823	0.297
Cisplatin	0.608	0.047	Levothyroxine	0.824	0.223
Itraconazole	0.627	0.028	Selegiline	0.828	0.269
Metoclopromide	0.635	0.012	Finasteride	0.830	0.325
Imatinib	0.638	0.108	Artemisinin	0.844	0.287
Dantrolene	0.641	0.046	Metronidazole	0.848	0.174
Alverine citrate	0.647	0.064	Paracetamol	0.849	0.311
Domperidone	0.647	0.067	Aspirin	0.853	0.130
Zinc acetate	0.651	0.118	Theophylline	0.856	0.209
Water	0.669	0.178	Clobetasol	0.860	0.317
Fluconazole	0.674	0.016	Ritodrine	0.860	0.305
Valproic acid	0.679	0.072	DMSO	0.862	0.109
Ascorbic acid	0.684	0.049	Bromocriptine	0.865	0.038
Paroxetine	0.688	0.333	Dexamethasone	0.866	0.224
Acyclovir	0.689	0.109	Allopurinol	0.871	0.287
Clofibric acid	0.693	0.164	Cefaclor	0.877	0.433
Chlorambucil	0.697	0.034	Chloroquine	0.877	0.423
Methyldopa	0.703	0.046	Clomipramine	0.882	0.523
Fenofibrate	0.703	0.087	Propylthiouracil	0.884	0.425
Testosterone	0.704	0.100	Nicotinic acid	0.896	0.463
Propanolol	0.704	0.147	Mesalazine	0.901	0.564
Vitamin K1	0.719	0.117	Ibuprofen	0.905	0.553
Ethanol	0.725	0.171	DMEM (2)	0.907	0.514
Medroxyprogesterone acetate	0.728	0.224	Metformin	0.918	0.737
Trimethoprim	0.730	0.255	Alpha tocopheryl acetate	0.923	0.667
Ergocalciferol	0.732	0.319	Flupentixol	0.940	0.842
Flecainide	0.734	0.112	Penicillin V	0.943	0.643
Mefenamic acid	0.735	0.213	Thiamine	0.944	0.741
Methanol	0.736	0.150	DMEM (1)	0.946	0.564
Cyclophosphamide	0.737	0.136	Diclofenac	0.951	0.658
Fluoxetine	0.739	0.251	Thalidomide	0.961	0.849
Ranitidine	0.742	0.070	Prednisolone	0.967	0.824
Pilocarpine	0.750	0.182	Rifampicin	0.976	0.705
Erythromycin	0.753	0.123	Doxycycline	0.981	0.892
Diltiazem	0.754	0.097	Amantidine	0.982	0.899
Carbamazepine	0.760	0.113	Retinol	0.982	0.816
Neostigmine	0.764	0.185	Imipramine	1.010	0.938
Acipimox	0.768	0.306	Folic acid	1.024	0.899

C. OE21

Figure 6.5 The effect of redeployed drugs on oesophageal adenocarcinoma and squamous cell carcinoma cell line viability *in-vitro*

Cell viability assay (MTT) demonstrating the effects of the redeployed drugs on oesophageal adenocarcinoma (OE19, A and OE33, B) and squamous cell carcinoma (OE21, C) cell lines after 72 hours incubation. Data presented as mean fold change relative to control (normalised to 1), p value quoted represents drug vs. control.

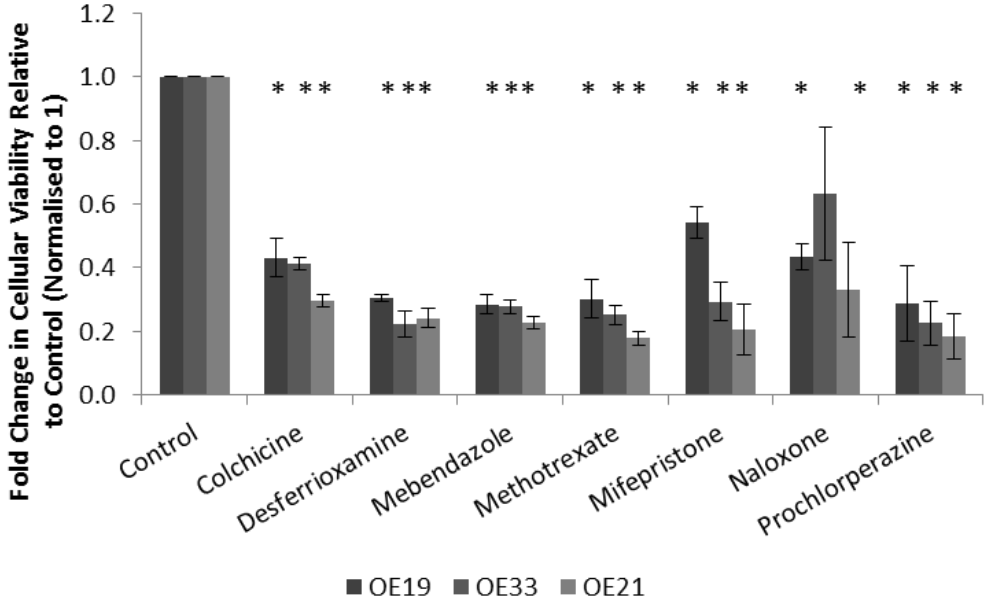
Fold Change in Cellular Viability Relative to Control (Normalised to 1)
1.2
1.0
0.8
0.6
0.4
0.2
0.0
* * *
* * *
* * *
* * *
* * *
*
*
* * *
Control
Colchicine
Desferrioxamine
Mebendazole
Methotrexate
Mifepristone
Naloxone
Prochlorperazine
OE19
OE33
OE21

A

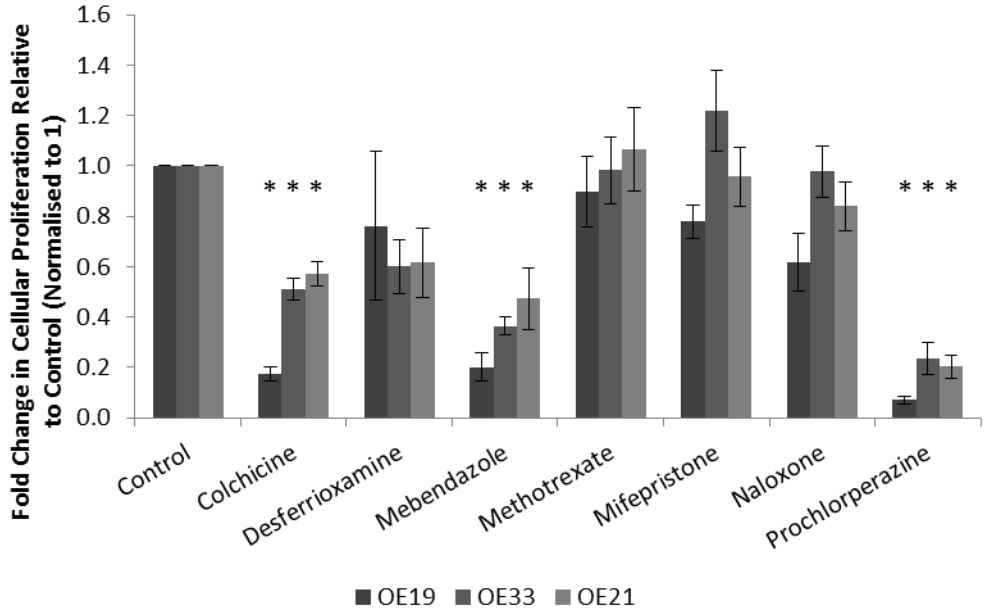
Fold Change in Cellular Proliferation Relative to Control (Normalised to 1)
1.6
1.4
1.2
1.0
0.8
0.6
0.4
0.2
0.0
* * *
* * *
* * *
Control
Colchicine
Desferrioxamine
Mebendazole
Methotrexate
Mifepristone
Naloxone
Prochlorperazine
OE19
OE33
OE21

B

Figure 6.6 The effect of redeployed drugs on oesophageal adenocarcinoma and squamous cell carcinoma cell line proliferation *in-vitro*

The effect of the top 7 redeployed agents on oesophageal adenocarcinoma (OE19 and OE33) and squamous cell carcinoma (OE21) was assessed by cell viability (MTT, A) and cell proliferation (BrdU, B) assays. Cells were incubated alongside the reagents for 72 hours. Data points represent mean fold change compared to control, error bars denote ±SEM, * $p<0.05$ vs. control.

6.3.5 The efficacy of redeployed agents in oesophageal adenocarcinoma *in-vivo*

6.3.5.1 Overview

Following the demonstration that the redeployed agents Prochlorperazine, Mebendazole and Colchicine significantly suppressed both cellular viability and cellular proliferation *in-vitro*, an OE19 OAC murine xenograft model (the same as was previously used in chapter 3) was generated to investiagate the efficacy of these compounds *in-vivo*.

NOD-SCID mice were divided into groups and given one of 4 treatment regimens as an oral gavage on alternate days for 3 weeks:

1. Sterile distilled water (100 µl)
2. Mebendazole (40 mg/kg as a suspension in a total volume of 100 µl)
3. Prochlorperazine (1 mg/kg as a suspension in a total volume of 100 µl)
4. Colchicine (1 mg/kg as a suspension in a total volume of 100 µl)

Doses were decided upon using a combination of previously published literature (in the case of Mebendazole) and manufacturer's pre-clinical drug safety data. [275] [276]

Drug efficacy was assessed by comparing final xenograft volume (mm^3) with the control group (water). The modified ellipsoid formula, volume = (maximal length x maximal $width^2$) / 2, was utilised to calculate tumour volume (mm^3). [277]

6.3.5.2 Results

Both Mebendazole and Colchicine significantly suppressed final xenograft size (56.7 and 72.1% reduction in final volume vs. control respectively, $p<0.05$, Figure 6.7).

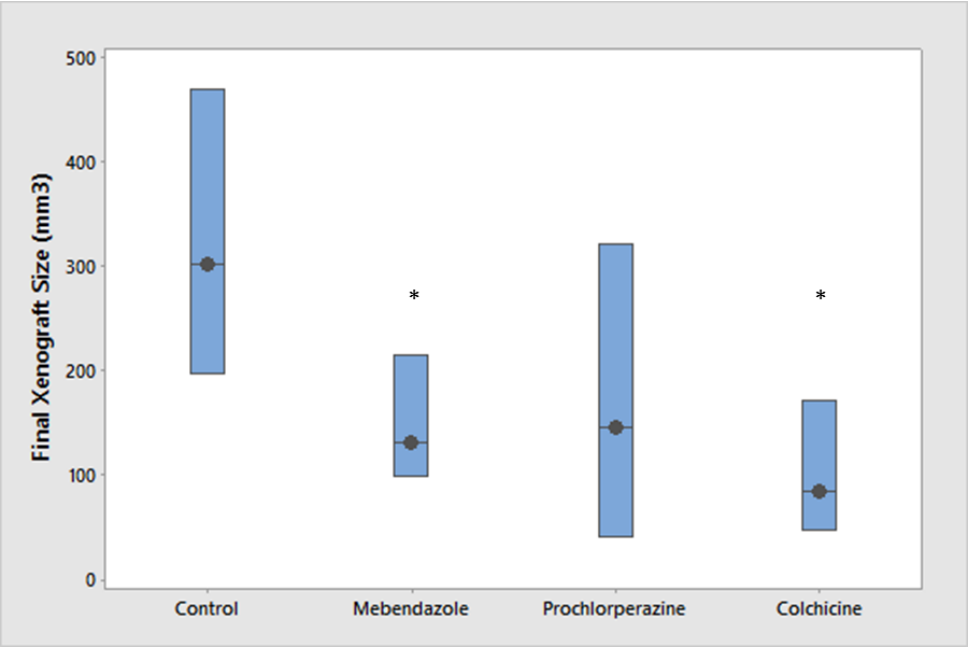

Figure 6.7 Mebendazole and Colchicine suppress oesophageal adenocarcinoma xenograft growth *in-vivo*

NOD-SCID mice with established OE19 OAC cell line xenografts were given 3 weeks of oral water (control), Mebendazole, Prochlorperazine or Colchicine on alternate days. Data presented as median xenograft volume (mm^3) post treatment. 95% confidence range for median displayed as bars around median, * $p<0.05$ vs. control.

6.3.6 The determination of any synergy between the redeployed drugs and the iron chelating agent Deferasirox in oesophageal carcinoma *in-vitro*

6.3.6.1 Overview

The OE19 OAC cell line was next screened against varying concentrations of Mebendazole, Colchicine and Prochlorperazine with or without the presence of Deferasirox (at the sub-therapeutic concentration of 1 μM) for 72 hours. Cell viability assays were then performed as previously outlined. Mebendazole, Colchicine and Prochlorperazine were selected at they had shown the most promise in the earlier oesophageal screen. Deferasirox was again utilised at a sub-therapeutic concentration of 1 μM. MTT assays were performed to determine effect on cell viability.

6.3.7.2 Results

The combination of low dose Mebendazole (0.43 μM, approximately 25% of the standard dose used in the previous experiments) with low dose Deferasirox (1 μM) generated a marked additional reduction of 60.4% compared to the redeployed drug alone at that concentration. This was statistically significant ($p<0.05$) against control, Mebendazole alone and Deferasirox alone at the same concentrations (Figure 6.8A). In contrast, no additional benefits were seen by combining Deferasirox with either Prochlorperazine or Colchicine (Figure 6.8 B and C).

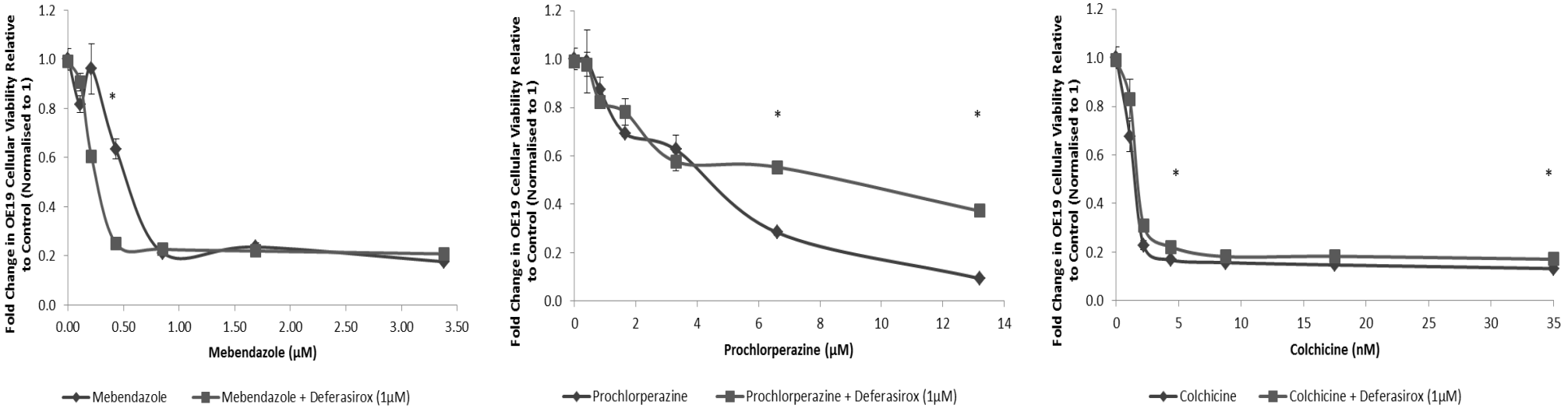

A **B** **C**

Figure 6.8 Mebendazole and Deferasirox demonstrate evidence of synergy *in-vitro* when utilised at concentrations below the peak serum levels obtained with their respective conventional dosing regimens

Cell viability assay (MTT) demonstrating dose response profile of Mebendazole (A), Prochlorperazine (B) and Colchicine (C) with or without the presence of the iron chelator Deferasirox (1 µM). Data points represent mean fold change compared to control (normalised to 1), error bars denote ±SEM, * $p<0.05$ vs. equivalent concentration of drug + Deferasirox 1 µM.

6.4 Discussion

The overall aim of this chapter was to ascertain whether or not the systematic screening of a library of redeployed drugs could identify novel agents with potential efficacy against oesophageal and colorectal cancer (either in synergy with the iron chelator Deferasirox or alone).

In terms of synergy between Deferasirox and redeployed agents, this study has demonstrated that the combination of Valproic acid with a sub-therapeutic dose of the iron chelator Deferasirox (1 μM) resulted in a significant additional reduction in cellular viability across a panel of colorectal cell lines (mean additional reduction 6.5-22.0% vs. Valproic acid alone). This finding is of interest and agrees with the findings of a recent study demonstrating synergy between the histone deacetylase (HDAC) inhibitor Trichostatin A and the iron chelators DFO and Phenanthroline in breast cancer cell lines. [278] The authors of this study speculated that the synergy seen was likely to be a consequence of iron chelator inhibition of the endoplasmic reticulum chaperone protein glucose-regulated protein 78 (which was increased by the HDAC inhibitor and appears to inhibit its anti-neoplastic effects).

A number of reagents demonstrated efficacy against oesophageal adenocarcinoma and squamous cell carcinoma cell lines *in-vitro*. Of note, the traditional iron chelator Desferrioxamine (an alternative to Deferasirox) significantly reduced cell viability across all 3 lines tested by an average of 74.4%.

The agents Colchicine (currently used to treat acute attacks of gout), Mebendazole (an anti-helminthic used to treat parasitic infections) and Prochlorperazine (a phenothiazine prescribed as an anti-emetic and anti-psychotic) induced a profound reduction in both cellular viability and proliferation in OAC and SCC *in-vitro*. Furthermore, when administered to mice harbouring

established OE19 OAC xenografts both Mebendazole and Colchicine demonstrated suppression of tumour growth compared to control.

Screening of the same redeployed library against the colorectal cell lines *in-vitro* also demonstrated that Colchicine, Mebendazole and Prochlorperazine were efficacious, reducing cellular viability by an average of 83.2, 83.5 and 37.9% respectively. In support of previous findings, Desferrioxamine was again also efficacious, inducing an average reduction in cellular viability of 67.8% across the 3 lines tested.

Colchicine was originally discovered as an extract from plants of the *Colhicum autumnale* (autumn crocus) genus. The anti-cancer properties of Colchicine demonstrated here are likely to stem from its known action against microtubules. [279] Along with actin microfilaments and intermediate filaments, microtubules comprise the cytoskeleton and play a significant role in the process of mitosis. [279] During the majority of the cell cycle, microtubules form an intracellular lattice-like structure, however, when cells enter mitosis, this microtubule network is reorganised into the mitotic spindle. [279] The processes of depolymerizing the interphase microtubule structure and forming the mitotic spindle, as well as finding, attaching and separating chromosomes, require highly coordinated microtubule dynamics. [279, 280] Therefore, agents that interfere with microtubule dynamics inhibit the ability of cells to successfully complete mitosis thus limiting proliferation. [279]

Microtubules are comprised of α and β-tubulin heterodimers that polymerise head-to-tail to form protofilaments. [279] Colchicine is known to bind to tubulin at a location adjacent to a GTP-binding site on the α-tubulin heterodimer leading to microtubule de-polymerisation through the inhibition of lateral contacts between protofilaments. [279, 281, 282] Thus, the drug is a potent inhibitor of mitosis, which by definition means it is effective at inhibiting the proliferation of rapidly dividing cancer cells. Widespread adoption of Colchicine as an anti-neoplastic agent to date, however, has been largely

limited due to its significant toxicity (it should be noted that Colchicine was well tolerated by the mice at the dose used in this study, however). [279] As such, much work has been carried out into the development, synthesis and pre-clinical evaluation of less toxic Colchicine analogues. [279, 283, 284]

Mebendazole is a broad spectrum anti-helminthic drug from the benzimadazole class (which also includes albendazole and flubendazole amongst others). [285] At present, it is commonly prescribed to treat a range of parasitical worm infections, including threadworm, tapeworms, roundworms and other nematode and trematode infections in humans and domestic animals. [285] It is available in an off-patent generic form and can be administered as both an acute (days) or longer-term (several months) prescription. [285] As with Colchicine, the anti-neoplastic effects seen with Mebendazole are likely to be exerted through the inhibition of microtubule polymerisation and the subsequent arrest of mitosis. [286] Indeed, both Mebendazole and the other benzimadazole drugs are known to bind to the Colchicine binding domain on the α-tubulin heterodimer. [287] Unlike Colchicine, however, the drug has a good safety and tolerability profile. [285]

A number of pre-clinical studies have demonstrated the anti-neoplastic action of Mebendazole. [285] Of note, the drug has been shown to suppress the growth of lung, adrenal, melanoma and glioblastoma xenografts. [275, 276, 288, 289] Mebendazole has also demonstrated efficacy in leukaemic, breast, and osteosarcoma cell lines. [285, 290, 291] Furthermore, in a recent study Nygren and colleagues screened a panel of 1600 existing drugs for activity against two colon cancer cell lines (HCT116 and RKO) and found 64 candidate drugs, including a cluster of benzimidazoles. [290] Further analysis performed with Mebendazole (across a broader panel of colonic lines including HCT116, RKO, HT29, HT-8 and SW626) demonstrated that all displayed an IC50 of <5 μM (as in this study) and that the drug was largely inactive against non-malignant cell lines. [290] Of note, Mebendazole has never been studied before in the context of oesophageal cancer.

The inhibition of tubulin polymerisation by Mebendazole has been shown to result in G2/M cell cycle arrest and the subsequent induction of apoptosis. [275] In melanoma lines, apoptosis has been shown to be activated through Bcl-2 phosphorylation and a reduction in the expression of X-linked inhibitor of apoptosis (XIAP). [288, 292] Mebendazole has also been shown to function in a p53 independent manner. [292]

It has been postulated in previous studies that Mebendazole offers the potential to act as a synergistic agent with both existing chemotherapeutic drugs and other redeployed agents under investigation in a number of cancers. [285] Thus, it is of interest (and certainly worthy of further investigation) that a potentially synergistic relationship was demonstrated in the current study between low dose Mebendazole and a low (sub-therapeutic) dose of the iron chelator Deferasirox.

No clinical trials of Mebendazole as an anti-neoplastic agent have been completed to date (although there are 2 currently underway for the treatment of glioma). [285] There are however, case reports demonstrating evidence of disease regression following Mebendazole therapy in both adrenal and metastatic colorectal cancer. [293, 294]

The phenothiazine prolchlorperazine demonstrated significant *in-vitro* effects in this study against both oesophageal and colorectal lines. Prochlorperazine was originally used as an anti-psychotic and is also commonly used as an anti-emetic (particularly during chemotherapy). Phenothiazines (as a broad class) have been studied previously as potential anti-cancer agents, although there are no studies using Prochlorperazine specifically nor in the context of oesophageal or colorectal cancer. [295] Ancedotally, a decreased risk of cancer has been noted previously amongst patients with Schizophrenia treated long-term with phenothiazines. [296]Phenothiazines have been shown to induce G1 cell cycle arrest with the subsequent induction of apoptosis. [297] Furthermore, in ovarian carcinoma xenografts, the phenothiazine derivative thioriadazine inhibited neo-vascularisation

resulting in a significant suppression of tumour growth. [298] The authors demonstrated that this was likely to be through inhibition of the PI3K signalling cascade (via suppression of Akt, PDK1 and mTOR phosphorylation) secondary to inhibition of VEGFR-2 phosphorylation. Phenothiazines have also been shown to inhibit c-Myc, Wnt, MAPK signalling and lysosomal function, whilst demonstrating increased efficacy in cell lines displaying B-raf mutations. [298] [299] [300] [301] Of note, studies have also demonstrated the ability of phenothiazines to reverse drug resistance and act as chemosensitisers, likely through the inhibition of P-glycoprotein. [295, 302, 303]

Whilst the redeployed agents Niclosamide and Valproic acid demonstrated significant efficacy when utilised in this study in the context of normoxia, they were also significantly effective in hypoxia (unlike Deferasirox). Niclosamide, like Mebendazole, is also used primarily as an anti-helminthic drug and belongs to the teniacide family of compounds. Its mechanism of action is through the inhibition of oxidative phosphorylation within mitochondria (via uncoupling of the electron transport chain from oxidative phosphorylation by increasing the proton permeability of the mitochondrial membrane thereby decreasing the proton electrochemical potential). [200] It is known to also inhibit anaerobic metabolism. [304] Niclosamide has demonstrated anti-neoplastic effects in a number of different cancer cell lines (including colorectal), and, in addition to its effects on cellular oxidative phosphorylation, has been postulated to perturb function of Wnt, NFκB, mTOR, Notch and Stat3 signalling. [304, 305] Its efficacy in hypoxia therefore, is likely to be explained through both the direct effect on anaerobic metabolism and the inhibition of Stat3, a known stimulator of the cellular response to hypoxia. [306]

Valproic acid is used at present for the treatment of epilepsy. It is a HDAC inhibitor and has shown promise as an anti-neoplastic agent in a number of pre-clinical cancer models. [307] Of note, the drug has been shown to cause cellular accumulation in G1 of the cell cycle as well as decreased cellular motility and metastasis. [307] It has also been shown to inhibit the proto-oncogene n-Myc, suppress

NFκB signalling and impede angiogenesis. [307] HDACs are involved in chromatin modification, which plays a crucial role in the regulation of gene transcription. The addition of charge-neutralizing acetyl groups to lysine residues disrupts DNA-histone interaction, resulting in a more open DNA conformation and a transcriptionally active state. [307] It is hypothesized that, by this mechanism, HDAC inhibitors can achieve de-repression of silenced tumor suppressor genes.

Furthermore, HDAC inhibitors have previously been shown to block the expression of HIF-1α (the master regulator of the cellular response to hypoxia). [308] Of note, therefore, in this study it was demonstrated that Valproic acid was effective against colorectal cell lines under hypoxic conditions, decreasing cellular proliferation by an average of 15.2-28.6% vs. control ($p<0.05$).

In summary, it has been demonstrated within this chapter that a drug redeployment based screening approach does indeed offer the potential to identify targets with potential efficacy against both oesophageal and colorectal carcinoma.

Colchicine, Mebendazole and Prochlorperazine demonstrated significant *in-vitro* effects against the oesophageal and colorectal cancer lines tested and (in the cases of Colchicine and Mebendazole) also evidence of *in-vivo* efficacy in a xenograft model of OAC. Both Niclosamide and Valproic acid were effective against colorectal adenocarcinoma cell lines under hypoxic conditions, whilst Mebendazole and Valproic acid also demonstrated evidence of synergy when cultured with sub-therapeutic concentrations of Deferasirox against OAC and colorectal adenocarcinoma cell lines respectively.

A thorough search of the literature demonstrated that all of the agents identified as potential 'hits' had plausible primary mechanisms of action conducive to an anti-neoplastic effect and furthermore, appeared to have additional effects on pathways common within cancer.

Much further work is needed to build on the results highlighted within this chapter. In particular, delineation of the top target's mechanisms of action (particularly in the context of OAC where much of these findings are novel) and their potential to synergise with lower doses of Deferasirox is certainly worthy of further investigation. In addition, the characterisation of their *in-vivo* effects would begin to pave the way towards future human trials in cancer therapy.

Chapter 7. Discussion

7.1 Conclusions

It is now clear that iron is implicated in the propagation of both oesophageal and colorectal carcinoma and therefore a strategy to deplete tumour cells of iron by chelation represents an attractive and logical therapeutic option. [24, 82, 92, 99, 102] After all, iron is essential for a plethora of cellular processes including DNA synthesis, ATP generation and cell cycle progression; all activities that are increased in cancer. [112] Furthermore, the increased requirement of malignant cells for iron offers the potential that iron chelation may offer a selective therapy, sparing normal cells (and the patient) from the deleterious side effects associated with existing chemotherapeutic regimens. [92, 112]

Within this thesis it has been demonstrated that the licensed and orally administered iron chelating agent Deferasirox possesses significant anti-neoplastic efficacy both *in-vitro* and *in-vivo* in the context of oesophageal carcinoma. The drug exerted its effects in a time and dose dependent manner and was well tolerated when given to mice at a relatively low dose. Furthermore, Deferasirox was also capable of inhibiting the growth of oesophageal cells that were resistant to conventional therapy with Cisplatin and, through inhibition of the NFκB signalling pathway, showed evidence for an anti-neoplastic and chemosensitising mode of action extending beyond that of just cellular iron deprivation by chelation alone. This is highly relevant, as tumours are often heterogeneous and can develop resistance to mono-modal therapy over time.

In addition to the demonstration of Deferasirox's efficacy in the oesophagus, the finding that the drug is equally efficacious against colorectal adenocarcinoma is highly novel. In addition to a higher basal requirement for iron (that is generic across almost all tumours), colorectal adenocarcinomas are known to acquire iron during their development. [82, 102, 242] Furthermore, iron has been shown to

drive tumour proliferation both *in-vitro* and *in-vivo*. [82, 102] Here, it was demonstrated for the first time that Deferasirox therapy inhibits the uptake and storage of cellular iron within colorectal adenocarcinoma cells leading to cell cycle arrest, significantly reduced rates of proliferation and ultimately a reduction in colorectal cellular viability. Of note, the drug appears to be more efficacious in adenocarcinoma cell lines than it was in those derived from adenomas and, as in the oesophagus, it was capable of suppressing the viability of cells that were otherwise resistant to the effects of existing chemotherapeutic reagents. In contrast to previous studies using the iron chelator DFO, Deferasirox efficacy was not dependent on cellular p53 status and appeared to actually be enhanced by the presence of an APC mutation. [248] In murine models of colorectal tumourigenesis following APC loss, Deferasirox administration was again well-tolerated and significantly up-regulated rates of apoptosis. Unfortunately, this did not translate into an increase in murine survival within the current study, although further work is ongoing within the laboratory group to investigate this further.

The finding that the IRP-IRE interaction is maintained but inappropriately active within colorectal adenocarcinoma is also highly novel. IRP2 over-expression now serves as an explanation for the increased iron accumulation seen with malignant colorectal tissue (an increase that is above what is merely required to maintain adequate levels of cellular growth). Furthermore, elevated expression of IRP2 facilitates not only an increase in total intracellular iron levels (through increased TfR1 expression) but also an increase in the labile or free intracellular iron pool (by the concomitant suppression of ferritin translation). [99, 258] This iron is thus available to drive both cellular proliferation and oncogenic signalling pathways, such as Wnt. [102, 132] The demonstration of an association between over-activity of the MAPK signalling pathway and increased IRP2 protein expression (probably through activation of the proto-oncogene c-Myc) in colorectal adenocarcinoma cells is of interest and further adds to the existing body of evidence implicating iron in both the amplification of Wnt signalling and the suppression of functioning p53 levels. [102] [132] [248] The fact that IRP2

expression was greatest in locally advanced, proximal colonic lesions and may be associated with perturbation of the MAPK signalling cascade (e.g. mutations in constituents such as B-raf) offers the potential that it may serve (either directly or indirectly) as a biomarker for Deferasirox efficacy, offering the potential for personalised medicine and a reduction in needless side effects.

Finally, it was demonstrated that drug redeployment offers a valid area worthy of further investigation for the identification of potential new agents that are effective against both oesophageal and colorectal carcinoma. A number of drugs demonstrated significant efficacy within the *in-vitro* and *in-vivo* models utilised, particularly Colchicine and Mebendazole. Of note, the anti-helminthic drug Niclosamide and the HDAC inhibitor Valproic acid were also significantly effective under hypoxic conditions and, in the case of Valproic acid, demonstrated evidence of synergy when administered with sub-therapeutic doses of Deferasirox. This adds further weight to the argument that iron chelators may act as chemosensitising agents.

7.2 Further Work

7.2.1 Laboratory Studies

In terms of the oesophagus, further *in-vitro* exploration of the drug's effects on other pathways (such as mTOR) would be beneficial. The conclusive demonstration that Deferasirox's anti-neoplastic efficacy is not restricted to merely iron deprivation through chelation alone and is actually achieved through a multi-modal mechanism of action would be extremely interesting and highly relevant to any future potential for clinical translation. With this in mind, the analysis of existing stored OE19 OAC xenograft specimens for markers of Deferasirox's effect on the NFκB signalling pathway *in-vivo* would be particularly important as it would help to conclusively determine the interaction of the drug with it.

In terms of the colon, again *in-vitro* assessment of Deferasirox's ability to act through iron independent channels would be interesting (particularly on Wnt signalling and downstream targets of it such as c-Myc). Determining the effects of Deferasirox upon intra-cellular ROS levels would also be relevant. Of greatest importance, however, would be the further exploration and demonstration of the drug's *in-vivo* efficacy. Although a murine xenograft type model could easily be utilised (as in the oesophagus) and is likely to demonstrate a positive result (in the opinion of the author), transgenic models of sporadic intestinal tumourigenesis now represent the gold standard for the investigation of colorectal cancer development and progression. [102] [201] [202] As such, future experiments should persist with this approach and re-evaluate the drug's effect on survival in models such as the $Apc^{Min/+}$ mouse. In addition, the drug's effect on Wnt targets (such as c-Myc) could also be evaluated through immunohistochemical and qRT-PCR based approaches.

The construction of a stable IRP2 'knockdown' cell line (using shRNA) would permit valuable further investigation into the effect of IRP perturbation on colorectal adenocarcinoma cell line phenotype (both *in-vitro* and *in-vivo* using xenograft models). It would also allow the effect of IRP2 expression on Deferasirox efficacy to be formally assessed (something that has not been attempted thus far). Furthermore, the successful transfection of the inducible B-raf V600E construct that was created during this thesis into a colorectal cell line that had a normal MAPK signalling cascade (i.e. wild type K-ras and B-raf) would permit further analysis of the interaction with IRP2. This could then be further augmented through the perturbation of c-Myc thus identifying whether it is a c-Myc dependent phenomenon.

7.2.2 Clinical Studies

In terms of the oesophagus, the next step would be to design and initiate a clinical trial of Deferasirox therapy. The demonstration that patients presenting with oesophageal adenocarcinoma (both resectable and advanced) are systemically iron replete is a crucial finding en-route to the design of any future trial of Deferasirox in this setting. Preliminary protocols are at present being designed for a Phase 1 safety and tolerability study of the drug in palliative patients. If this is successful then further more advanced trials could be planned.

In both the oesophagus and the colon, other than the obvious requirement for the demonstration that Deferasirox is safe and well-tolerated amongst patients with cancer, the next crucial step would be the demonstration of an effect of the drug at the level of the tumour. This could be achieved through the obtaining of a pre and post-therapy biopsy (or the surgically resected specimen), almost as a window study. Markers of iron metabolism, apoptosis and Wnt targets could be assessed within the tumour. Ultimately, if the drug was given after staging but before surgical resection, a pathological response to therapy scoring system could also be applied. [309]

In conclusion, iron metabolism and iron chelation therapy represents an important novel therapeutic avenue for the treatment of gastrointestinal cancer that is worthy of ongoing and further investigation to improve outcome in this clinically important disease.

8. Appendix

8.1 Full papers published to date relating to this thesis

A comparative study of the iron status of patients with oesophageal adenocarcinoma to determine suitability for a clinical trial of iron chelation therapy
Ford SJ, **Bedford M,** Pang W, Wood A, Iqbal T, Tselepis C, Tucker O
Annals of the Royal College of Surgeons of England 2014; **96(4):** 275-8

Iron chelators in the treatment of cancer: A new role for Deferasirox?
Bedford MR, Ford SJ, Horniblow RD, Iqbal TH, Tselepis C
Journal of Clinical Pharmacology 2013; **53(9):** 885-91

Deferasirox (ICL670A) effectively inhibits oesophageal cancer growth in vitro and in vivo
Ford S, Obeidy P, Lovejoy D, **Bedford M,** Nichols L, Chadwick C, Tucker O, Lui G, Kalinowski D, Jansson P, Iqbal T, Alderson D, Richardson D, Tselepis C
British Journal of Pharmacology 2013; **168(6):** 1316-28

8.2 Abstracts published to date relating to this thesis

Iron chelation as a novel strategy for the treatment of colorectal adenocarcinoma
Bedford MR, Evans S, Radulescu S, Stavrou V, Iqbal T, Ford SJ, Alderson D, Tselepis C
British Journal of Surgery 2015; 102(S5): 41

Iron metabolism in colorectal adenocarcinoma: A novel therapeutic target?
Evans S, **Bedford MR,** Lal N, Beggs AD, Iqbal T, Tucker O, Tselepis C
British Journal of Surgery 2015; 102(S5): 39

Drug repurposing in oesophageal adenocarcinoma: New tricks for old dogs?
Bedford MR, Gill J, Iqbal T, Ford SJ, Alderson D, Khanim F, Tselepis C
British Journal of Surgery 2014; 101(S4): 18

Pre-treatment with the oral chelating agent ICL670A may enhance chemotherapy response in oesophageal adenocarcinoma

Bedford MR, Ford SJ, Tucker O, Iqbal T, Alderson D, Tselepis C

American Journal of Haematology 2013; **88(5):** E182

Iron chelators as chemotherapy adjuncts in oesophageal adenocarcinoma: In-vitro and in-vivo effects of Deferasirox

Bedford MR, Ford SJ, Tucker O, Iqbal T, Alderson D, Tselepis C

British Journal of Surgery 2013; **100(S2):** 13-16.

Iron chelation in the treatment of oesophageal adenocarcinoma – in-vivo action of Deferasirox on a xenograft model

Ford SJ, **Bedford MR,** Tucker O, Iqbal T, Alderson D, Richardson DR, Tselepis C

British Journal of Surgery 2013; **100(S2):** 13-16.

8.3 Presentations to learned societies to date relating to this thesis

Iron chelation as a novel strategy for the treatment of colorectal adenocarcinoma

Bedford MR, Evans S, Radulescu S, Stavrou V, Iqbal T, Ford SJ, Alderson D, Tselepis C

Oral presentation at the Society of Academic and Research Surgery (SARS) annual meeting (Durham), January 2015

Iron metabolism in colorectal adenocarcinoma: A novel therapeutic target?

Evans S, **Bedford MR,** Lal N, Beggs AD, Iqbal T, Tucker O, Tselepis C

Oral presentation at the Society of Academic and Research Surgery (SARS) annual meeting (Durham), January 2015 (shortlisted for Medical Student prize)

Drug repurposing in oesophageal adenocarcinoma: New tricks for old dogs?

Bedford MR, Gill J, Iqbal T, Ford SJ, Alderson D, Khanim F, Tselepis C

Oral presentation at the Society of Academic and Research Surgery (SARS) annual meeting (Cambridge), January 2014

Pre-treatment with the oral chelating agent ICL670A may enhance chemotherapy response in oesophageal adenocarcinoma

Bedford MR, Ford SJ, Tucker O, Iqbal T, Alderson D, Tselepis C

Poster presentation at the 5th Congress of the International BioIron Society (IBIS) Biennial World Meeting (London), April 2013

Iron chelators as chemotherapy adjuncts in oesophageal adenocarcinoma: In-vitro and in-vivo effects of Deferasirox

Bedford MR, Ford SJ, Tucker O, Iqbal T, Alderson D, Tselepis

Oral presentation at the Society of Academic and Research Surgery (SARS) annual meeting (London), January 2013

Iron chelation in the treatment of oesophageal adenocarcinoma – in-vivo action of Deferasirox on a xenograft model

Ford SJ, **Bedford MR,** Tucker O, Iqbal T, Alderson D, Richardson DR, Tselepis C

Oral presentation at the Society of Academic and Research Surgery (SARS) annual meeting (London), January 2013 (shortlisted for Patey prize)

Anti-neoplastic effect of iron chelators: In-vivo effects of Deferasirox (ICL670A) in a murine xenograft model of oesophageal adenocarcinoma

Bedford MR, Ford SJ, Chadwick C, Tucker O, Iqbal T, Alderson D, Tselepis C

Poster presentation at the British Association for Cancer Research / Royal Society of Medicine's 'Development of cancer medicines: Preclinical in vivo models to interrogate cancer biology, biomarkers and therapeutic response' meeting (London), November 2012

Iron chelators as anti-neoplastic and chemosensitising agents in oesophageal adenocarcinoma: In-vitro and in-vivo effects of Deferasirox

Bedford MR, Ford SJ, Tucker O, Iqbal T, Alderson D, Tselepis C

Oral presentation at the Midlands Gastroenterology Society Winter Meeting (Keele), November 2012

9. References

[1] Tanaka T. Colorectal carcinogenesis: Review of human and experimental studies. J Carcinog 2009; 8: 5.

[2] Cancer Research UK. Worldwide cancer statistics. Available at http://www.cancerresearchuk.org/cancer-info/cancerstats/world/. First accessed 16 August 2013.

[3] Cancer Research UK. Cancer incidence statistics. Available at http://www.cancerresearchuk.org/cancer-info/cancerstats/incidence/. First accessed 16 August 2013.

[4] Cancer Research UK. Cancer statistics report. Available at http://publications.cancerresearchuk.org/downloads/Product/CS_CS_MORTALITY.pdf. First accessed 16 August 2013.

[5] Snell RS. Clinical anatomy for medical students (6th edition). Lippincott, Williams and Wilkins 2000; 5: 191-282.

[6] Ohio State University. Gastrointestinal cancer. Available at http://cancer.osu.edu/patientsandvisitors/cancerinfo/cancertypes/gi/Pages/index.aspx. First accessed 19 August 2013.

[7] Cancer Research UK. Oesophageal cancer statistics. Available at http://www.cancerresearchuk.org/cancer-info/cancerstats/types/oesophagus/incidence/. First accessed 19 August 2013.

[8] Cancer Research UK. Cancer survival for common cancers. Available at http://www.cancerresearchuk.org/cancer-info/cancerstats/survival/common-cancers/#One-. First accessed 21 August 2014.

[9] Dixon MF. The alimentary system. In: Underwood JCE. General and systemic pathology (4th edition). Churchill Livingstone 2004; 15: 359-99.

[10] Enzinger PC, Mayer RJ. Esophageal cancer. N Engl J Med 2003; 349: 2241-52.

[11] Parkin DM, Bray F, Ferlay J, Pisani P. Global cancer statistics 2002. CA Cancer J Clin 2005; 55: 74-108.

[12] Crepsi M, Bogomoletz VW, Munoz N, Peracchia A, Savary M. Cancer of the oesophagus. Gastroenterol Int 1994; 7: 24-35.

[13] Jemal A, Siegel R, Ward E, Hao Y, Xu J, Thun MJ. Cancer statistics 2009. CA Cancer J Clin 2009; 59: 225-49.

[14] Cancer Research UK. Oesophageal cancer statistics. Available at http://www.cancerresearchuk.org/cancer-info/cancerstats/types/oesophagus/incidence/. First accessed 19 August 2013.

[15] Yang S, Wu S, Huang Y, Shao Y, Chen XY, Xian L, *et al*. Screening for oesophageal cancer (review). The Cochrane Collaboration 2012; 12. Available at www.thecochranelibrary.com. First accessed 15 August 2013.

[16] Burkitt HG, Quick CRG. Essential surgery (3rd edition). Churchill Livingstone 2002; 15: 227-37.

[17] Pennathur A, Gibson MK, Jobe BA, Luketich JD. Oesophageal carcinoma. The Lancet 2013; 381: 400-12.

[18] Lagergren J, Bergstrom R, Lindgren A, Nyren O. Symptomatic gastrooesophageal reflux as a risk factor for oesophageal adenocarcinoma. N Engl J Med 1999; 340: 825-31.

[19] Kubo A, Corley DA. Body mass index and adenocarcinomas of the oesophagus or gastric cardia: a systematic review and meta-analysis. Cancer Epidemiol Biomarkers Prev 2006; 295: 1549-55.

[20] Fisher BI, Pennathur A, Mutnick JL. Little AG. Obesity correlates with gastroesophageal reflux. Dig Dis Sci 1999; 44: 2290-4.

[21] Ronkainen J, Aro P, Storskrubb T, Johansson SE, Lind T, Bolling-Sternevald E, *et al.* Prevalence of Barrett's esophagus in the general population: an endoscopic study. Gastroenterology 2005; 129: 1825-31.

[22] Voutilainen M, Sippronen P, Mecklin JP, Juhola M, Farkkla M. Gastresophageal reflux disease: prevalence, clinical, endoscopic and histopathological findings in 1,128 consecutive patients referred for endoscopy due to dyspeptic and reflux symptoms. Digestion 2000; 61: 6-13.

[23] Edelstein ZR, Farrow DC, Bronner MP, Rosen SN, Vaughan TL. Central adiposity and risk of Barrett's esophagus. Gastroenterology 2007; 133: 403-11.

[24] Boult J, Roberts K, Brookes MJ, Hughes S, Bury JP, Cross SS, *et al*. Overexpression of cellular iron import proteins is associated with malignant progression of esophageal adenocarcinoma. Clin Cancer Res 2008; 14: 379-387.

[25] Solaymani-Dodaran M, Logan RF, West J, Card T, Coupland C. Risk of oesophageal cancer in Barrett's oesophagus and gastro-oesophageal reflux. Gut 2004; 53: 1070-4.

[26] Hage M, Siersema PD, van Dekken H, Steyerberg EW, Dees J, Kuipers EJ. Oesophageal cancer incidence and mortality in patients with long-segment Barrett's oesophagus after a mean follow-up of 12.7 years. Scand J Gastroenterol 2004; 39: 1175-9.

[27] Pennathur A, Landreneau RJ, Luketich JD. Surgical aspects of the patient with high-grade dysplasia. Semin Thorac Cardiovasc Surg 2005; 17: 326-32.

[28] Reid BJ, Weinstein WM, Lewin KJ, Haggitt RC, VanDeventer G, DenBesten L, *et al*. Endoscopic biopsy can detect high-grade dysplasia or early adenocarcinoma in Barrett's esophagus without grossly neoplastic lesions. Gastroenterology 1988; 94: 81-90.

[29] Schnell TG, Sontag SJ, Chejfec G, Aranha G, Metz A, O'Connell S, *et al*. Long-term nonsurgical management of Barrett's esophagus with high-grade dysplasia. Gastroenterology 2001; 120: 1607-19.

[30] Tselepis C, Morris CD, Wakelin D, Hardy R, Perry I, Luong QT, *et al*. Upregulation of the oncogene c-myc in Barrett's adenocarcinoma: induction of c-myc by acidified bile acid in vitro. Gut 2003; 52: 174-80.

[31] Watanabe M. Risk factors and molecular mechanisms of esophageal cancer: differences between the histologic subtypes. J Cancer Metastasis Treat 2015; 1: 1-7.

[32] Hollstein M, Sidransky D, Vogelstein B, Harris CC. p53 mutations in human cancers. Science 1991; 253: 49-53.

[33] Samuels Y, Velculescu VE. Oncogenic mutations of PIK3CA in human cancers. Cell Cycle 2004; 3: 1221-4.

[34] Weaver JM, Ross-Innes CS, Shannon N, Lynch AG, Forshew T, Barbera M, *et al.* Ordering of mutations in preinvasive disease stages of esophageal carcinogenesis. Nat Genet 2014; 46: 837-43.

[35] Hechtman JF, Polydorides AD. HER2/neu gene amplification and protein overexpression in gastric and gastroesophageal junction adenocarcinoma: A review of histopathology, diagnostic testing, and clinical implications. Arch Pathol Lab Med 2012; 136: 691-7.

[36] Rice TW. Diagnosis and staging of esophageal cancer. In: Pearson FG, Patterson GA. Pearson's thoracic and esophageal surgery (3rd edition). Churchill Livingstone 2008; 454-63.

[37] American Joint Committee on Cancer. AJCC cancer staging handbook (6th edition). Lippincott-Raven 2002; 91-103.

[38] NCCN clinical practice guidelines in oncology. Oesophageal and oesophagogastric junction cancers. Available at http://www.nccn.org/professionals/physician_gls/pdf/esophageal.pdf. First accessed 1 September 2013.

[39] Pennathur A, Luketich JD, Landreneau RJ, Ward J, Christian NA, Gibson MK, *et al*. Long-term results of a phase II trial of neoadjuvant chemotherapy followed by esophagectomy for locally advanced esophageal neoplasm. Ann Thorac Surg 2008; 85: 1930–6.

[40] Medical Research Council Oesophageal Cancer Working Group. Surgical resection with or without preoperative chemotherapy in oesophageal cancer: a randomised controlled trial. Lancet 2002; 359: 1727–33.

[41] Cunningham D, Allum WH, Stenning SP, Thompson JN, Van de Velde CJ, Nicolson M, *et al* and the MAGIC Trial Participants. Perioperative chemotherapy versus surgery alone for resectable gastroesophageal cancer. N Engl J Med 2006; 355: 11–20.

[42] Le Prise E, Etienne PL, Meunier B, Maddern G, Ben Hassel M, Gedouin D, *et al*. A randomized study of chemotherapy, radiation therapy, and surgery versus surgery for localized squamous cell carcinoma of the esophagus. Cancer 1994; 73: 1779–84.

[43] Bosset JF, Gignoux M, Triboulet JP, Tiret E, Mantion G, Elias D, *et al*. Chemoradiotherapy followed by surgery compared with surgery alone in squamous-cell cancer of the esophagus. N Engl J Med 1997; 337: 161–7.

[44] Urba SG, Orringer MB, Turrisi A, Iannettoni M, Forastiere A, Strawderman M. Randomized trial of preoperative chemoradiation versus surgery alone in patients with locoregional esophageal carcinoma. J Clin Oncol 2001; 19: 305–13.

[45] Apinop C, Puttisak P, Preecha N. A prospective study of combined therapy in esophageal cancer. Hepatogastroenterology 1994; 41: 391–93.

[46] Walsh TN, Noonan N, Hollywood D, Kelly A, Keeling N, Hennessy TP. A comparison of multimodal therapy and surgery for esophageal adenocarcinoma. N Engl J Med 1996; 335: 462–67.

[47] Tepper J, Krasna MJ, Niedzwiecki D, Hollis D, Reed CE, Goldberg R, *et al*. Phase III trial of trimodality therapy with cisplatin, fl uorouracil, radiotherapy, and surgery compared with surgery alone for esophageal cancer: CALGB 9781. J Clin Oncol 2008; 26: 1086–92.

[48] Gebski V, Burmeister B, Smithers BM, Foo K, Zalcberg J, Simes J, and the Australasian Gastro-Intestinal Trials Group. Survival benefits from neoadjuvant chemoradiotherapy or chemotherapy in oesophageal carcinoma: a meta-analysis. Lancet Oncol 2007; 8: 226–34.

[49] Macdonald JS, Smalley SR, Benedetti J, Hundahl SA, Estes NC, Stemmermann GN, *et al*. Chemoradiotherapy after surgery compared with surgery alone for adenocarcinoma of the stomach or gastroesophageal junction. N Engl J Med 2001; 345: 725–30.

[50] Polednak AP. Trends in survival for both histologic types of esophageal cancer in US surveillance, epidemiology and end results areas. Int J Cancer 2003; 105: 98–100.

[51] Homs MY, v d Gaast A, Siersema PD, Steyerberg EW, Kuipers EJ. Chemotherapy for metastatic carcinoma of the esophagus and gastro-esophageal junction. Cochrane Database Syst Rev 2006; 4: CD004063.

[52] Cunningham D, Starling N, Rao S, Iveson T, Nicolson M, Coxon F, *et al*, and the UpperGastrointestinal Clinical Studies Group of the National Cancer Research Institute of the United Kingdom. Capecitabine and oxaliplatin for advanced esophagogastric cancer. N Engl J Med 2008; 358: 36–46.

[53] Shah MA, Ramanathan RK, Ilson DH, Levnor A, D'Adamo D, O'Reilly E, *et al*. Multicenter phase II study of irinotecan, cisplatin, and bevacizumab in patients with metastatic gastric or gastroesophageal junction adenocarcinoma. J Clin Oncol 2006; 24: 5201–06.

[54] Waddell T, Chau I, Cunningham D, Gonzalez D, Okines AF, Okines C, *et al*. Epirubicin, oxaliplatin, and capecitabine with or without panitumumab for patients with previously untreated advanced oesophagogastric cancer (REAL3): a randomised, open-label phase 3 trial. Lancet Oncol. 2013; 14(6): 481-9.

[55] Bang YJ, Van Cutsem E, Feyereislova A, Chung HC, Shen L, Sawaki A, *et al*. Trastuzumab in combination with chemotherapy versus chemotherapy alone for treatment of HER2-positive advanced gastric or gastro-oesophageal junction cancer (ToGA): a phase 3, open-label, randomised controlled trial. Lancet. 2010; 376: 687-97.

[56] Okines AF, Cunningham D. Trastuzumab: a novel standard option for patients with HER-2-positive advanced gastric or gastro-oesophageal junction cancer. Therap Adv Gastroenterol. 2012; 5(5): 301-18.

[57] Cancer Research UK. Bowel cancer survival statistics. Available at http://www.cancerresearchuk.org/cancer-info/cancerstats/types/bowel/survival/. First accessed 21 August 2014.

[58] Cancer Research UK. Bowel cancer incidence statistics. Available at http://www.cancerresearchuk.org/cancer-info/cancerstats/types/bowel/incidence/#distribution. First accessed 9 September 2014.

[59] The National Cancer Institute. Genetics of colorectal cancer. Available at http://www.cancer.gov/cancertopics/pdq/genetics/colorectal/HealthProfessional/page1. First accessed 9 September 2014.

[60] Tárraga López PJ, Albero JS, Rodríguez-Montes JA. Primary and secondary prevention of colorectal cancer. Clin Med Insights Gastroenterol. 2014; 7: 33-46.

[61] Chan DS, Lau R, Aune D, Vieira R, Greenwood DC, Kampman E, *et al*. Red and processed meat and colorectal cancer incidence: meta-analysis of prospective studies. PLoS One. 2011; 6(6): e20456.

[62] Markowitz SD, Bertagnolli MM. Molecular basis of colorectal cancer. N Engl J Med 2009; 361(25): 2449-60.

[63] Morin PJ, Vogelstein B, Kinzler KW. Apoptosis and APC in colorectal tumorigenesis. Proc Natl Acad Sci U S A. 1996; 93(15): 7950-4.

[64] Walther A, Johnstone E, Swanton C, Midgley R, Tomlinson I, Kerr D.. Genetic prognostic and predictive markers in colorectal cancer. Nat Rev Cancer. 2009; 9(7): 489-99.

[65] Anastas JN, Moon RT. WNT signalling pathways as therapeutic targets in cancer. Nature Reviews Cancer 2013; 13: 11-25

[66] Myant K, Sansom OJ. Wnt/Myc interactions in intestinal cancer: Partners in crime. Experimental Cell Research 2011; 317: 2725-31.

[67] Narayan S, Roy D. Role of APC and DNA mismatch repair genes in the development of colorectal cancers. Mol Cancer 2003; 2: 41.

[68] Baker SJ, Preisinger AC, Jessup JM, Paraskeva C, Markowitz S, Willson JK, *et al*. Gene mutations occur in combination with 17p allelic deletions as late events in colorectal tumourigenesis. Cancer Res 1990; 50: 7717-22.

[69] Roberts PJ, Der CJ. Targeting the Raf-MEK-ERK mitogen-activated protein kinase cascade for the treatment of cancer. Oncogene 2007; 26: 3291-310.

[70] Chin L. The genetics of malignant melanoma: lessons from mouse and man. Nature Reviews Cancer 2003; 3**:** 559-570.

[71] Kearns B, Whyte S, Chilcott J, Patnick J. Guaiac faecal occult blood test performance at initial and repeat screens in the English Bowel Cancer Screening Programme. Br J Cancer. 2014 Sep 2. doi: 10.1038/bjc.2014.469.

[72] The National Institute for Health and Clinical Excellence (NICE). Guideline CG131 Colorectal Cancer, November 2011. Available at http://guidance.nice.org.uk/CG131/Guidance/pdf/English. First accessed 21 August 2014.

[73] The National Institute for Health and Care Excellence. Staging colorectal cancer. Available at http://pathways.nice.org.uk/pathways/colorectal-cancer. First accessed 9 September 2014.

[74] Tanis PJ, Buskens CJ, Bemelman WA. Laparoscopy for colorectal cancer. Best Pract Res Clin Gastroenterol. 2014; 28(1): 29-39.

[75] Sajid MS, Farag S, Leung P, Sains P, Miles WF, Baig MK. Systematic review and meta-analysis of published trials comparing the effectiveness of transanal endoscopic microsurgery and radical resection in the management of early rectal cancer. Colorectal Dis. 2014; 16(1): 2-14.

[76] Rahbari NN, Elbers H, Askoxylakis V, Motschall E, Bork U, Büchler MW, *et al*. Neoadjuvant radiotherapy for rectal cancer: meta-analysis of randomized controlled trials. Ann Surg Oncol. 2013; 20: 4169–4182.

[77] Foxtrot Collaborative Group. Feasibility of preoperative chemotherapy for locally advanced, operable colon cancer: the pilot phase of a randomised controlled trial. Lancet Oncol. 2012; 13(11): 1152-60.

[78] Brezden-Masley C, Polenz C. Current practices and challenges of adjuvant chemotherapy in patients with colorectal cancer. Surg Oncol Clin N Am. 2014; 23(1): 49-58.

[79] Ciombor KK, Berlin J. Targeting metastatic colorectal cancer – present and emerging treatment options. Pharmgenomics Pers Med. 2014; 7: 137–144.

[80] Kalinowski DS, Richardson DR. The Evolution of Iron Chelators for the Treatment of Iron Overload Disease and Cancer. Pharmacological Reviews 2005; 57: 547-83.

[81] Miret S, Simpson RJ, and McKie AT. Physiology and molecular biology of dietary iron absorption. Annu Rev Nutr 23: 283-301, 2003.

[82] Brookes MJ, Hughes S, Turner FE, Reynolds G, Sharma N, Ismail T, *et al*. Modulation of iron transport proteins in human colorectal carcinogenesis. Gut 2006; 55(10): 1449-60.

[83] McKie AT, Barrow D, Latunde-Dada GO, Rolfs A, Sager G, Mudaly E, *et al*. An iron-regulated ferric reductase associated with the absorption of dietary iron. Science 2001; 291: 1755–9.

[84] Gruenheid S, Cellier M. Vidal S, Gros P. Identification and characterization of a second mouse Nramp gene. Genomics 1995; 25: 514–25.

[85] Gunshin H, Mackenzie B, Berger U, Gunshin Y, Romero MF, Boron WF, *et al*. Cloning and characterization of a mammalian proton-coupled metal-ion transporter. Nature 1997; 388: 482–8.

[86] Torti SV, Kwak EL, Miller SC, Miller LL, Ringold GM, Myambo KB, *et al*. The molecular cloning and characterization of murine ferritin heavy chain, a tumor necrosis factor-inducible gene. J Biol Chem 1988; 263: 12638–44.

[87] Frazer DM, Vulpe CD, McKie AT, Wilkins SJ, Trinder D, Cleghorn GJ, *et al*. Cloning and gastrointestinal expression of rat hephaestin: relationship to other iron transport proteins. Am J Physiol Gastrointest Liver Physiol 2001; 281: G931–9.

[88] Vulpe CD, Kuo YM, Murphy TL, Cowley L, Askwith C, Libina N, *et al*. Hephaestin, a ceruloplasmin homologue implicated in intestinal iron transport, is defective in the sla mouse. Nat Genet 1999; 21: 195–9.

[89] McKie AT, Marciani P, Rolfs A, Brennan K, Wehr K, Barrow D, *et al*. A novel duodenal iron-regulated transporter, IREG1, implicated in the basolateral transfer of iron to the circulation. Mol Cell 2000; 5: 299–309.

[90] Aisen P. Transferrin receptor 1. Int J Biochem Cell Biol 2004; 36: 2137–43.

[91] Rizvi S, Robert E Schoen RE. Supplementation with oral vs. intravenous iron for anaemia with IBD or gastrointestinal bleeding: Is oral Iron getting a bad rap? The American Journal of Gastroenterology 2011; 106: 1872-1879.

[92] Merlot AM, Kalinowski DS, Richardson DR. Novel chelators for cancer treatment: Where are we now? Antioxid Redox Signal. 2013; 18(8): 973-1006.

[93] Shayeghi M, Latunde-Dada GO, Oakhill JS, Laftah AH, Takeuchi K, Halliday N, *et al*. Identification of an intestinal heme transporter. Cell 2005; 122: 789-801.

[94] Qiu A, Jansen M, Sakaris A, Min SH, Chattopadhyay S, Tsai E, *et al*. Identification of an intestinal folate transporter and the molecular basis for hereditary folate malabsorption. Cell 127: 917-928, 2006.

[95] Raffin SB, Woo CH, Roost KT, Price DC, Schmid R. Intestinal absorption of hemoglobin iron-heme cleavage by mucosal heme oxygenase. J Clin Invest 1974; 54: 1344-1352.

[96] De Domenico I, McVey Ward D, Kaplan J. Regulation of iron acquisition and storage: consequences for iron-linked disorders. Nat Rev Mol Cell Biol 9: 72-81, 2008.

[97] Hentze MW, Kuhn LC. Molecular control of vertebrate iron metabolism: mRNA-based regulatory circuits operated by iron, nitric oxide and oxidative stress. Proc Natl Acad Sci USA 1996; 93: 8175-82.

[98] Hentze MW, Muckenthaler MU, Andrews NC. Balancing acts: molecular control of mammalian iron metabolism. Cell 2004; 117: 285-97.

[99] Torti SV, Torti FM. Iron and cancer: more ore to be mined. Nat Rev Cancer. 2013; 13(5): 342-55.

[100] Park CH, Valore EV, Waring AJ, Ganz T. Hepcidin, a urinary antimicrobial peptide synthesized in the liver. J Biol Chem 2001; 276: 7806-7810.

[101] Nemeth E, Tuttle MS, Powelson J, Vaughn MB, Donovan A, Ward DM, *et al*. Hepcidin regulates cellular iron efflux by binding to ferroportin and inducing its internalization. Science 2004; 306: 2090-93.

[102] Radulescu S, Brookes MJ, Salgueiro P, Ridgway RA, McGhee E, Anderson K, *et al*. Luminal iron levels govern intestinal tumorigenesis after Apc loss in vivo. Cell Reports 2012; 2: 270-82.

[103] Cavill I, Auerbach M, Bailie GR, Barrett-Lee P, Beguin Y, Kaltwasser P, *et al*. Iron and the anaemia of chronic disease: a review and strategic recommendations. Curr Med Res Opin 2006; 22: 731-7.

[104] Kortman GA, Boleij A, Swinkels DW, Tjalsma H. Iron availability increases the pathogenic potential of Salmonella typhimurium and other enteric pathogens at the intestinal epithelial interface. PLoS One 2012; 7(1): e29968.

[105] Flaten TP, Aaseth J, Andersen O, Kontoghiorghes G J. Iron mobilization using chelation and phlebotomy. J Trace Elem Med Biol 2012; 26(2-3): 127-30.

[106] Olivieri NF, Brittenham GM. Iron-chelating therapy and the treatment of thalassemia. Blood 1997; 89: 739–761.

[107] Schrier SL, Centis F, Verneris M, Ma L, Angelucci E. The role of oxidant injury in the pathophysiology of human thalassemias. Redox Rep 2003; 8:241–245.

[108] Corti MC, Gaziano M, Hennekens C H. Iron status and risk of cardiovascular disease. Ann Epidemiol 1997; 7: 62-8.

[109] Fernandez-Real JM, Ricart-Engel W, Arroyo E, Balançá R, Casamitjana-Abella R, Cabrero D, *et al*. Serum ferritin as a component of the insulin resistance syndrome. Diabetes Care 1998; 21: 62-8.

[110] Bush AI. The metallobiology of Alzheimer's disease. Trends Neurosci 2003; 26: 207-14.

[111] Huang, X. Iron overload and its association with cancer risk in humans: evidence for iron as a carcinogenic metal. Mutat Res 2003; 533: 153-71.

[112] Kwok JC, Richardson DR. The iron metabolism of neoplastic cells: alterations that facilitate proliferation? Crit Rev.Oncol.Hematol. 2002; 42: 65-78.

[113] Andrews NC. Forging a field: the golden age of iron biology. Blood 2008; 9: 72-81.

[114] Stevens RG, Graubard BI, Micozzi MS, Neriishi, Blumberg BS. Moderate elevation of body iron level and increased risk of cancer occurrence and death. Int. J. Cancer 1994; 56: 364–369.

[115] Stevens RG, Jones DY, Micozzi MS, Taylor PR. Body iron stores and the risk of cancer. New Engl. J. Med. 1998; 319: 1047–1052.

[116] Nelson RL, Davis FG, Persky V, Becker E. Risk of neoplastic and other diseases among people with heterozygosity for hereditary hemochromatosis. Cancer 1995; 76: 875–879.

[117] Shaheen NJ, Silverman LM, Keku T, Lawrence LB, Rohlfs EM, Martin CF, *et al*. Association between hemochromatosis (HFE) gene mutation carrier status and the risk of colon cancer. J. Natl. Cancer Inst. 2003; 95: 154–159.

[118] Bradbear RA, Bain C, Siskind V, Schofield FD, Webb S, Axelsen EM, *et al*. Cohort study of internal malignancy in genetic hemochromatosis and other chronic nonalcoholic liver diseases. J. Natl Cancer Inst. 1985; 75**:** 81–84.

[119] Hsing AW, McLaughlin JK, Olsen JH, Mellemkjar L, Wacholder S, Fraumeni JF Jr.Cancer risk following primary hemochromatosis: a population-based cohort study in Denmark. Int. J. Cancer 1995; 60: 160–162.

[120] Osborne NJ, Gurrin LC, Allen KJ, Constantine CC, Delatycki MB, McLaren CE, *et al*. HFE C282Y homozygotes are at increased risk of breast and colorectal cancer. Hepatology 2010; 51**:** 1311–1318.

[121] Zacharski LR, Chow BK, Howes PS, Shamayeva G, Baron JA, Dalman RL, *et al*. Decreased cancer risk after iron reduction in patients with peripheral arterial disease: results from a randomized trial. J. Natl. Cancer Inst. 2008; 100: 996–1002.

[122] Edgren G, Reilly M, Hjalgrim H, Tran TN, Rostgaard K, Adami J, *et al*. Donation frequency, iron loss, and risk of cancer among blood donors. J. Natl. Cancer Inst. 2008; 100: 572–579.

[123] Nelson RL. Iron and colorectal cancer risk: human studies. Nutr. Rev. 2001; 59**:** 140–148.

[124] Ward MH, Cross AJ, Abnet CC, Sinha R, Markin RS, Weisenburger DD. Heme iron from meat and risk of adenocarcinoma of the esophagus and stomach. Eur J Cancer Prev. 2012; 21(2): 134-8.

[125] Pinnix ZK, Miller LD, Wang W, D'Agostino R Jr, Kute T, Willingham MC, *et al*. Ferroportin and iron regulation in breast cancer progression and prognosis. Sci Transl Med. 2010; 2(43): 43ra56.

[126] Han HS, Lee SY, Seong MK, Kim JH, Sung IK, Park HS, *et al*. Presence of iron in colorectal adenomas and adenocarcinomas. Gut Liver. 2008; 2(1): 19-22.

[127] Siegers CP, Bumann D, Trepkau HD, Schadwinkel B, Baretton G. Influence of dietary iron overload on cell proliferation and intestinal tumorigenesis in mice. Cancer Lett 1992; 65: 245-9.

[128] Kim JH, Hue JJ, Kang BS. Effects of selenium on colon carcinogenesis induced by azoxymethane and dextran sodium sulfate in mouse model with high-iron diet. Lab Anim Res 2011; 27: 9-18.

[129] Chen X, Yang G, Ding WY, Bondoc F, Curtis SK, Yang CS. An esophagogastroduodenal anastomosis model for esophageal adenocarcinogenesis in rats and enhancement by iron overload. Carcinogenesis. 1999; 20: 1801-8.

[130] Xue X, Taylor M, Anderson E, Hao C, Qu A, Greenson JK, *et al*. Hypoxia-inducible factor-2α activation promotes colorectal cancer progression by dysregulating iron homeostasis. Cancer Res. 2012; 72(9): 2285-93.

[131] Torti SV, Torti FM. Ironing out cancer. Cancer Res 2011: 71; 1511-1514.

[132] Brookes MJ, Boult J, Roberts K, Cooper BT, Hotchin NA, Matthews G, *et al*. A role for iron in Wnt signalling. Oncogene 2008; 27(7): 966-75.

[133] O'Donnell KA, Yu D, Zeller KI, Kim JW, Racke F, Thomas-Tikhonenko A, *et al*. Activation of transferrin receptor 1 by c-Myc enhances cellular proliferation and tumorigenesis. Mol Cell Biol. 2006; 26(6): 2373-86.

[134] Cheng Z, Dai LL, Song YN, Kang Y, Si JM, Xia J, *et al*. Regulatory effect of iron regulatory protein-2 on iron metabolism in lung cancer. Genet Mol Res. 2014; 13(3):5514-22.

[135] Wang W, Deng Z, Hatcher H. IRP2 regulates breast tumor growth. Cancer Res. 2014; 74(2): 497-507.

[136] Maffettone C, Chen G, Drozdov I, Ouzounis C, Pantopoulos K..Tumorigenic properties of iron regulatory protein 2 (IRP2) mediated by its specific 73-amino acids insert. PLoS One. 2010; 5(4): e10163.

[137] Shpyleva SI, Tryndyak VP, Kovalchuk O, Starlard-Davenport A, Chekhun VF, Beland FA, *et al*. Role of ferritin alterations in human breast cancer cells. Breast Cancer Res Treat. 2011; 126(1): 63-71.

[138] Chekhun VF, Lukyanova NY, Burlaka CA, Bezdenezhnykh NA, Shpyleva SI, Tryndyak VP, *et al*. Iron metabolism disturbances in the MCF-7 human breast cancer cells with acquired resistance to doxorubicin and cisplatin. Int J Oncol. 2013; 43(5): 1481-6.

[139] Whitnall M, Howard J, Ponka P, Richardson DR. A Class of iron chelators with a wide spectrum of potent antitumor activity that overcomes resistance to chemotherapeutics. Proc Natl Acad Sci U S A 2006; 103: 14901–14906.

[140] Chen Z, Zhang D, Yue F, Zheng M, Kovacevic Z, Richardson DR. The iron chelators Dp44mT and DFO inhibit TGF-β-induced epithelial-mesenchymal transition via up-regulation of N-Myc downstream-regulated gene 1 (NDRG1).J Biol Chem 2012; 17016-28.

[141] Kalinowski DS, Yu Y, Sharpe PC, Islam M, Liao YT, Lovejoy DB, *et al*. Design, synthesis, and characterization of novel iron chelators: structure-activity relationships of the 2-benzoylpyridine thiosemicarbazone series and their 3-nitrobenzoyl analogues as potent antitumor agents. J Med Chem 2007; 50: 3716-29.

[142] Yu Y, Suryo Rahmanto Y, Richardson DR. Bp44mT: an orally active iron chelator of the thiosemicarbazone class with potent anti-tumour efficacy.Br J Pharmacol 2012; 165: 148-66.

[143] Becton DL, Bryles P. Deferoxamine inhibition of human neuroblastoma viability and proliferation. Cancer Res. 1988; 48: 7189-92.

[144] Simonart T, Boelaert JR, Mosselmans R, Andrei G, Noel JC, De Clercq E, *et al*. Antiproliferative and apoptotic effects of iron chelators on human cervical carcinoma cells. Gynecol Oncol 2002; 85: 95-102.

[145] Brard L, Granai CO, Swamy N. Iron chelators deferoxamine and diethylenetriamine pentaacetic acid induce apoptosis in ovarian carcinoma. Gynecol Oncol 2006; 100: 116-127.

[146] Becton DL, Roberts B. Antileukemic effects of deferoxamine on human myeloid leukemia cell lines. Cancer Res 1989; 49: 4809-4812.

[147] Yamasaki T, Terai S, Sakaida I. Deferoxamine for advanced hepatocellular carcinoma. N Engl J Med 2011; 365: 576-578.

[148] Blatt J, Taylor SR, Kontoghiorghes GJ. Comparison of activity of deferoxamine with that of oral iron chelators against human neuroblastoma cell lines. Cancer Res 1989; 49: 2925-7.

[149] Chenoufi N, Drenou B, Loreal O, Pigeon C, Brissot P, Lescoat G. Antiproliferative effect of deferiprone on the Hep G2 cell line. Biochem Pharmacol 1998; 56: 431-7.

[150] Yasumoto E, Nakano K, Nakayachi T, Morshed SR, Hashimoto K, Kikuchi H, *et al*. Cytotoxic activity of deferiprone, maltol and related hydroxyketones against human tumor cell lines. Anticancer Res 2004; 24: 755-62.

[151] Selig RA, White L, Gramacho C, Sterling-Levis K, Fraser IW, Naidoo D. Failure of iron chelators to reduce tumor growth in human neuroblastoma xenografts. Cancer Res 1998; 58: 473-8.

[152] Simonart T, Boelaert JR, Andrei, G, Clercq ED, Snoeck R. Iron withdrawal strategies fail to prevent the growth of SiHa-induced tumors in mice. Gynecol Oncol 2003; 90: 91-5.

[153] Veci A, Baiardi P, Felisi M, Cappellini MD, Carnelli V, De Sanctis V, *et al*. The safety and effectiveness of deferiprone in a large-scale, 3-year study in Italian patients. Br J Haematol 2002; 118: 330-6.

[154] Cappellini MD. Exjade(R) (deferasirox, ICL670) in the treatment of chronic iron overload associated with blood transfusion. Ther Clin Risk Manag 2007; 3: 291-9.

[155] Galanello R, Piga A, Cappellini MD, Forni GL, Zappu A, Origa R, *et al*. Effect of food, type of food, and time of food intake on deferasirox bioavailability: recommendations for an optimal deferasirox administration regimen. J Clin Pharmacol 2008; 48: 428-35.

[156] Nick H, Ackmann P, Lattmann R, Buehlmayer P, Hauffe S, Schupp J, *et al*. Development of tridentate iron chelators: from desferrithiocin to ICL670. Curr Med Chem 2003; 10: 1065-76.

[157] Nick H, Wong A, Acklin P, Faller B, Jin Y, Lattmann R, *et al*. ICL670A: preclinical profile. Adv Exp Med Biol 2002; 509: 185-203.

[158] Galanello R, Piga A, Alberti P, Rouan MC, Bigler H, Séchaud R. *et al*. Safety, tolerability, and pharmacokinetics of ICL670, a new orally active iron-chelating agent in patients with transfusion-dependent iron overload due to beta-thalassemia. J Clin Pharmacol 2003; 43: 565-72.

[159] Nisbet-Brown E, Olivieri NF, Giardina PJ, Grady RW, Neufeld EJ, Séchaud R, *et al*. Effectiveness and safety of ICL670 in iron-loaded patients with thalassaemia: a randomised, double-blind, placebo-controlled, dose-escalation trial. Lancet 2003; 361: 1597-602.

[160] Piga A, Galanello R, Forni G, Cappellini MD, Origa R, Zappu A, *et al*. Randomized phase II trial of deferasirox (Exjade, ICL670), a once-daily, orally-administered iron chelator, in comparison to deferoxamine in thalassemia patients with transfusional iron overload. Haematologica 2006; 91: 873-80.

[161] Cappellini MD, Cohen A, Piga A, Bejaoui M, Perrotta S, Agaoglu L, *et al*. A phase 3 study of deferasirox (ICL670), a once-daily oral iron chelator, in patients with beta-thalassemia. Blood 2006; 107: 3455-62.

[162] List AF, Baer MR, Steensma DP, Raza A, Esposito J, Martinez-Lopez N, *et al*. Deferasirox Reduces Serum Ferritin and Labile Plasma Iron in RBC Transfusion-Dependent Patients With Myelodysplastic Syndrome. J Clin Oncol. 2012; 30(17): 2134-9.

[163] Galanello R, Piga A, Forni G, Bertrand Y, Foschini ML, Bordone E, *et al*. Phase II clinical evaluation of deferasirox, a once-daily oral chelating agent, in pediatric patients with beta-thalassemia major. Haematologica 2006; 91: 1343-51.

[164] Gattermann N, Finelli C, Porta MD, Fenaux P, Ganser A, Guerci-Bresler A, *et al*. Deferasirox in iron-overloaded patients with transfusion-dependent myelodysplastic syndromes: Results from the large 1-year EPIC study. Leuk Res 2010; 34: 1143-50.

[165] Gattermann N, Jarisch A, Schlag R, Blumenstengel K, Goebeler M, Groschek M, *et al*. Deferasirox treatment of iron-overloaded chelation-naïve and prechelated patients with myelodysplastic syndromes in medical practice: results from the observational studies eXtend and eXjange. Eur J Haematol 2012; 88: 260-8.

[166] Breccia M, Alimena G. Efficacy and safety of deferasirox in myelodysplastic syndromes. Ann Hematol 2013. Epub ahead of print.

[167] Chantrel-Groussard K, Gaboriau F, Pasdeloup N, Havouis R, Nick H, Pierre JL, *et al*. The new orally active iron chelator ICL670A exhibits a higher antiproliferative effect in human hepatocyte cultures than O-trensox. Eur J Pharmacol 2006; 541: 129-37.

[168] Kicic A, Chua AC, Baker E. Effect of iron chelators on proliferation and iron uptake in hepatoma cells. Cancer 2001; 92: 3093-110.

[169] Lui GY, Obeidy P, Ford SJ, Tselepis C, Sharp DM, Jansson PJ, *et al*. The iron chelator, deferasirox, as a novel strategy for cancer treatment: oral activity against human lung tumor xenografts and molecular mechanism of action. Mol Pharmacol 2013; 83: 179-90.

[170] Di Tucci AA, Murru B, Alberti D, Rabault B, Deplano S, Angelucci E. Correction of anemia in a transfusion-dependent patient with primary myelofibrosis receiving iron chelation therapy with deferasirox (Exjade, ICL670). Eur J Haematol 2007; 78: 540-2.

[171] Messa E, Cilloni D, Messa F, Arruga F, Roetto A, Saglio G.. Deferasirox treatment improved the hemoglobin level and decreased transfusion requirements in four patients with the myelodysplastic syndrome and primary myelofibrosis. Acta Haematol 2008; 120: 70-4.

[172] Okabe H, Suzuki T, Omori T, Mori M, Uehara E, Hatano K, *et al*. Hematopoietic recovery after administration of deferasirox for transfusional iron overload in a case of myelodysplastic syndrome. Rinsho Ketsueki. 2009; 50(11): 1626-9.

[173] Lescoat G, Chantrel-Groussard, K, Pasdeloup N, Nick H, Brissot P, Gaboriau F.. Antiproliferative and apoptotic effects in rat and human hepatoma cell cultures of the orally active iron chelator ICL670 compared to CP20: a possible relationship with polyamine metabolism. Cell Prolif 2007; 40: 755-67.

[174] Wallace HM, Fraser AV, Hughes A. A perspective of polyamine metabolism. Biochem. J. 2003; 376: 1–14.

[175] Kim JL, Kang HN, Kang MH, Yoo YA, Kim JS, Choi CW.. The oral iron chelator deferasirox induces apoptosis in myeloid leukemia cells by targeting caspase. Acta Haematol. 2011; 126(4): 241-5.

[176] Alnemri ES, Livingston DJ, Nicholson DW, Salvesen G, Thornberry NA, Wong WW, *et al*. Human ICE/CED-3 protease nomenclature. Cell 1996; 87(2): 171.

[177] Messa E, Carturan S, Maffe C, Pautasso M, Bracco E, Roetto A, *et al*. Deferasirox is a powerful NF-kappaB inhibitor in myelodysplastic cells and in leukemia cell lines acting independently from cell iron deprivation by chelation and reactive oxygen species scavenging. Haematologica 2010; 95: 1308-16.

[178] Aggarwal BB. Nuclear factor-kappaB: the enemy within. Cancer Cell 2004; 6: 203-8.

[179] Feinman R, Koury J, Thames M, Barlogie B, Epstein J, Siegel DS.. Role of NF-κB in the rescue of multiple myeloma cells from glucocorticoid-induced apoptosis by bcl-2. Blood 1999; 93: 3044–3052.

[180] Baron F, Turhan AG, Giron-Michel J, Azzarone B, Bentires-Alj M, Bours V, *et al*. Leukemic target susceptibility to natural killer cytotoxicity: Relationship with BCRABL expression. Blood 2002; 99: 2107–2113.

[181] Palayoor ST, Youmell MY, Calderwood SK, Coleman CN, Price BD. Constitutive activation of IκB kinase α and NF-κB in prostate cancer cells is inhibited by ibuprofen. Oncogene 199; 18: 7389–7394.

[182] Nakshatri H, Bhat-Nakshatri P, Martin DA, Goulet RJ, Sledge GW. Constitutive activation of NF-κB during progression of breast cancer to hormone-independent growth. Mol. Cell. Biol. 1997; 17: 3629–3639.

[183] Ohyashiki JH, Kobayashi C, Hamamura R, Okabe S, Tauchi T, Ohyashiki K.. The oral iron chelator deferasirox represses signaling through the mTOR in myeloid leukemia cells by enhancing expression of REDD1. Cancer Sci 2009; 100: 970-7.

[184] Easton JB, Houghton PJ. mTOR and cancer therapy. Oncogene 2006; 25: 6436-46.

[185] Schwarzer R, Tondera D, Arnold W, Giese K, Klippel A, Kaufmann J. *et al*. REDD1 integrates hypoxia-mediated survival signalling downstream of phosphatidylinositol 3-kinase. Oncogene 2005; 24: 1138-49.

[186] Song S, Christova T, Perusini S, Alizadeh S, Bao RY, Miller BW, *et al*. Wnt inhibitor screen reveals iron dependence of β-catenin signaling in cancers. Cancer Res. 2011 Dec 15; 71(24):7628-39.

[187] Guariglia R, Martorelli M, Villani O, Pietrantuono G, Mansueto G, D'Auria F, *et al*. Positive effects on hematopoiesis in patients with myelodysplastic syndrome receiving deferasirox as oral iron chelation therapy: A brief review. Leukemia Research 2011; 35: 566-570.

[188] Fukushima T, Kawabata H, Nakamura T, Iwao H, Nakajima A, Miki M, *et al*. Iron chelation therapy with deferasirox induced complete remission in a patient with chemotherapy-resistant acute monocytic leukemia. Anticancer Res. 2011; 31(5): 1741-4.

[189] Vreugdenhil G, Smeets M, Feelders RA. Iron chelators may enhance erythropoiesis by increasing iron delivery to haematopoietic tissue and erythropoietin response in iron-loading anaemia. Acta Haematol 1993; 89.

[190] Ghoti H, Fibach E, Merkel D, Perez-Avraham G, Grisariu S, Rachmilewitz EA. Changes in parameters of oxidative stress and free iron biomarkers during treatment with Deferasirox in iron-overloaded patients with Myelodysplastic syndromes. Haematologica 2010; 95: 1433-4.

[191] Rockett JC, Larkin K, Darnton SJ, Morris AG, Matthews HR. Five newly established oesophageal carcinoma cell lines: phenotypic and immunological characterization. Br J Cancer. 1997; 75(2): 258-63.

[192] Takashima N, Ishiguro H, Kuwabara Y, Kimura M, Mitui A, Mori Y, *et al*. Gene expression profiling of the response of esophageal carcinoma cells to cisplatin. Dis Esophagus. 2008; 21(3): 230-5.

[193] American Tissue Culture Collection (ATCC). Colon cancer and normal cell lines. Available at http://www.atcc.org/~/media/PDFs/Cancer%20and%20Normal%20cell%20lines%20tables/Colon%20cancer%20and%20normal%20cell%20lines.ashx. First accessed 28 August 2013.

[194] Hsi LC, Angerman-Stewart J, Eling TE. Introduction of full-length APC modulates cyclooxygenase-2 expression in HT-29 human colorectal carcinoma cells at the translational level. Carcinogenesis. 1999; 20(11): 2045-9.

[195] Chung CS, Jiang Y, Cheng D, Birt DF. Impact of adenomatous polyposis coli (APC) tumor supressor gene in human colon cancer cell lines on cell cycle arrest by apigenin. Mol Carcinog. 2007; 46(9): 773-82.

[196] Bunz F, Dutriaux A, Lengauer C, Waldman T, Zhou S, Brown JP, *et al*. Requirement for p53 and p21 to sustain G_2 arrest after DNA damage. Science 1998; 282: 1497-1501.

[197] Hidalgo IJ, Raub TJ, Borchardt RT. Characterization of the human colon carcinoma cell line (Caco-2) as a model system for intestinal epithelial permeability. Gastroenterology. 1989; 96(3): 736-49.

[198] Watson SA, Morris TM, McWilliams DF, Harris J, Evans S, Smith A, *et al*. Potential role of endocrine gastrin in the colonic adenoma carcinoma sequence. British Journal of Cancer 2002; 87: 567–573.

[199] Williams AC, Harper SJ, Paraskeva C. Neoplastic transformation of a human colonic epithelial cell line: in vitro evidence for the adenoma to carcinoma sequence. Cancer Res. 1990; 50(15): 4724-30.

[200] Khanim FL, Merrick BA, Giles HV, Jankute M, Jackson JB, Giles LJ, *et al*. Redeployment-based drug screening identifies the anti-helminthic niclosamide as anti-myeloma therapy that also reduces free light chain production. Blood Cancer J. 2011; 1(10): e39.

[201] Sansom OJ, Reed KR, Hayes AJ, Ireland H, Brinkmann H, Newton IP, *et al*. Loss of Apc in vivo immediately perturbs Wnt signaling, differentiation and migration. Genes Dev. 2004; 18: 1385–1390.

[202] Barker N, van Es JH, Kuipers J, Kujala P, van den Born M, Cozijnsen M, *et al*. Identification of stem cells in small intestine and colon by marker gene Lgr5. Nature 2007; 449: 1003–1007.

[203] Marsh V, Winton DJ, Williams GT, Dubois N, Trumpp A, Sansom OJ, *et al*. Epithelial Pten is dispensable for intestinal homeostasis but suppresses adenoma development and progression after Apc mutation. Nat Genet. 2008; 40(12): 1436-44.

[204] Vichai V, Kirtikara K. Sulforhodamine B colorimetric assay for cytotoxicity screening. *Nature Protocols 2006;* 1**:** 1112-16.

[205] Jemal A, Bray F, Center MM, Ferlay J, Ward E, Forman D. Global cancer statistics. CA Cancer J Clin 2011; 61(2): 69-90.

[206] Devesa SS, Blot WJ, Fraumeni Jr JF. Changing patterns in the incidence of esophageal and gastric carcinoma in the United States. Cancer 1998; 83(10): 2049–53.

[207] Medical Research Council Oesophageal Cancer Working Party. Surgical resection with or without preoperative chemotherapy in oesophageal cancer: a randomised controlled trial. Lancet 2002; 359: 1727-1733.

[208] Koppert LB, Wijnhoven BP, van Dekken H, Tilanus HW, Dinjens WN.. The molecular biology of esophageal adenocarcinoma [review]. J Surg Oncol 2005; 92: 169-90.

[209] Chen X, Ding YW, Yang G, Bondoc F, Lee MJ, Yang CS.. Oxidative damage in an esophageal adenocarcinoma model with rats. Carcinogenesis 2000; 21: 257-63.

[210] Goldstein SR, Yang GY, Chen X, Curtis SK, Yang CS.. Studies of iron deposits, inducible nitric oxide synthase and nitrotyrosine in a rat model for esophageal adenocarcinoma. Carcinogenesis 1998; 19: 1445-9.

[211] Lee DH, Anderson KE, Folsom AR, Jacobs DR Jr. Heme iron, zinc and upper digestive tract cancer: the Iowa Women's Health Study. Int J Cancer 2005; 117: 643-7.

[212] Huang W, Han Y, Xu J, Zhu W, Li Z. Red and processed meat intake and risk of esophageal adenocarcinoma: a meta-analysis of observational studies. Cancer Causes Control 2013; 24(1): 193-201.

[213] Di Maso M, Talamini R, Bosetti C, Montella M, Zucchetto A, Libra M, *et al*. Red meat and cancer risk in a network of case-control studies focusing on cooking practices. Ann Oncol 2013; 24(12): 3107-12.

[214] Jakszyn P, Lujan-Barroso L, Agudo A, Bueno-de-Mesquita HB, Molina E, Sánchez MJ, *et al*. Meat and heme iron intake and esophageal adenocarcinoma in the European Prospective Investigation into Cancer and Nutrition study. Int J Cancer 2013; 133(11): 2744-50.

[215] Ford S, Obeidy P, Lovejoy D, Bedford M, Nichols L, Chadwick C, *et al*. Deferasirox (ICL670A) effectively inhibits oesophageal cancer growth in vitro and in vivo. British Journal of Pharmacology 2013; 168(6): 1316-28.

[216] Abdel-Latif MM, O'Riordan J, Windle HJ, Carton E, Ravi N, Kelleher D, *et al*. NF-kappaB activation in esophageal adenocarcinoma: relationship to Barrett's metaplasia, survival, and response to neoadjuvant chemoradiotherapy. Ann Surg 2004; 239(4): 491-500.

[217] Izzo JG, Correa AM, Wu TT, Malhotra U, Chao CK, Luthra R, *et al*. Pretherapy nuclear factor-kappaB status, chemoradiation resistance, and metastatic progression in oesophageal carcinoma. Mol Cancer Therapy 2006; 5(11): 2844-50.

[218] Li J, Minnich DJ, Camp ER, Brank A, Mackay SL, Hochwald SN.. Enhanced sensitivity to chemotherapy in esophageal cancer through inhibition of NF-kappaB. J Surg Res 2006; 132(1): 112-20.

[219] Yang YH, Zhou H, Binmadi NO, Proia P, Basile JR. Plexin-B1 activates NF-κB and IL-8 to promote a pro-angiogenic response in endothelial cells. PLoS One. 2011; 6(10): e25826.

[220] Knight K, Wade S, Balducci L. Prevalence and outcomes of anemia in cancer: A systematic review of the literature. The American Journal of Medicine 2004; 116(7A): 11S-26S.

[221] Zhao KL, Liu G, Jiang GL, Wang Y, Zhong LJ, Wang Y, *et al*. Association of haemoglobin level with morbidity and mortality of patients with locally advanced oesophageal carcinoma undergoing radiotherapy--a secondary analysis of three consecutive clinical phase III trials. Clin Oncol (R Coll Radiol). 2006; 18(8): 621-7.

[222] Tanswell I, Steed H, Butterworth J, Townson G. Anaemia is of prognostic significance in patients with oesophageal adenocarcinoma. J R Coll Physicians Edinb 2011; 41:206–10.

[223] Suominen P, Punnonen K, Rajamaki A, Irjala K. Serum transferring receptor and transferring-receptor-ferritin index identify healthy subjects with subclinical iron deficits. Blood 1998; 92(8): 2934-9.

[224] Fu D, Richardson D. Iron chelation and regulation of the cell cycle: 2 mechanisms of posttranscriptional regulation of the universal cyclin-dependent kinase inhibitor p21CIP1/WAF1 by iron depletion. Blood 2007; 110(2): 752-761.

[225] Le NT, Richardson DR. The role of iron in cell cycle progression and the proliferation of neoplastic cells. Biochim Biophys Acta 2002; 1603(1) 31-46.

[226] Li B, Li YY, Tsao SW, Cheung AL. Targeting NF-kappaB signalling pathwat suppresses tumour growth, angiogenesis and metastasis of human espohageal cancer. Mol Cancer Ther 2009; 8(9): 2635-44.

[227] Karin M. Nuclear factor-kappaB in cancer development and progression. Nature. 2006; 441(7092): 431-6.

[228] Ruddell RG, Hoang-Le D, Barwood JM, Rutherford PS, Piva TJ, Watters DJ, *et al*. Ferritin functions as a proinflammatory cytokine via iron-independent protein kinase C zeta/nuclear factor kappaB-regulated signaling in rat hepatic stellate cells. Hepatology. 2009; 49(3):887-900.

[229] Shpyleva SI, Tryndyak VP, Kovalchuk O, Starlard-Davenport A, Chekhun VF, Beland FA, *et al*. Role of ferritin alterations in human breast cancer cells. Breast Cancer Res Treat. 2011; 126(1): 63-71.

[230] Chekhun VF, Lukyanova NY, Burlaka CA *et al*. Iron metabolism disturbances in the MCF-7 human breast cancer cells with acquired resistance to doxorubicin and cisplatin. Int J Oncol. 2013; 43(5): 1481-6.

[231] Mueller S, Schittenhelm M, Honecker F, Malenke E, Lauber K, Wesselborg S, *et al*. Cell-cycle progression and response of germ cell tumours to cisplatin in vitro. Int J Oncol 2006; 29(2): 471-9.

[232] Cancer Research UK. Cancer survival for common cancers. Available at http://www.cancerresearchuk.org/cancer-info/cancerstats/survival/common-cancers/#One-. First accessed 21 August 2014.

[233] Cancer Research UK. Bowel cancer survival statistics. Available at http://www.cancerresearchuk.org/cancer-info/cancerstats/types/bowel/survival/. First accessed 21 August 2014.

[234] The National Institute for Health and Clinical Excellence (NICE). Guideline CG131 Colorectal Cancer, November 2011. Available at http://guidance.nice.org.uk/CG131/Guidance/pdf/English. First accessed 21 August 2014.

[235] Kuremsky JG, Tepper JE, McLeod HL. Biomarkers for response to neoadjuvant chemoradiation for rectal cancer. Int J Radiat Oncol Biol Phys 2009; 74: 673–88.

[236] Cho KR, Vogelstein B. Genetic alterations in the adenoma – carcinoma sequence. Cancer 1992; 70(6 Suppl): 1727-31.

[237] Ward D, Roberts K, Brookes MJ, Joy H, Martin A, Ismail T, *et al*. Increased hepcidin expression in colorectal carcinogenesis. World J Gastroenterol 2008; 14(9): 1339-45.

[238] Okazaki F, Matsunaga N, Okazaki H, Utoguchi N, Suzuki R, Maruyama K, *et al*. Circadian rhythm of transferrin receptor 1 gene expression controlled by c-Myc in colon cancer-bearing mice. Cancer Res 2010; 70(15): 6238-46.

[239] Nelson RL, Yoo SJ, Tanure JC, Andrianopoulos G, Misumi A. The effect of iron on experimental colorectal carcinogenesis. Anticancer Res 1989; 9(6): 1477-82.

[240] Wilson WR, Hay MP.Targeting hypoxia in cancer therapy. Nat Rev Cancer. 2011; 11(6):3 93-410.

[241] Siriwardana G, Seligman PA. Two cell cycle blocks caused by iron chelation of neuroblastoma cells: separating cell cycle events associated with each block. Physiol Rep. 2013;1(7): e00176. doi: 10.1002/phy2.176. eCollection 2013.

[242] Han HS, Lee SY, Seong MK, Kim JH, Sung IK, Park HS, *et al*. Presence of iron in colorectal adenomas and adenocarcinomas. Gut Liver. 2008; 2(1): 19-22.

[243] Mohelnikova-Duchonova B, Melichar B, Soucek P. FOLFOX/FOLFIRI pharmacogenetics: The call for a personalized approach in colorectal cancer therapy. World J Gastroenterol. 2014; 20(30): 10316-30.

[244] Vasquez A, Bond EE, Levine AJ, Bond GL. The genetics of the p53 pathway, apoptosis and cancer therapy. Nat Rev Drug Discov 2008; 7: 979-87.

[245] Markowitz SD, Bertagnolli MM. Molecular basis of colorectal cancer. N Engl J Med 2009; 361(25): 2449-60.

[246] Yang B, Eshleman JR, Berger NA, Markowitz SD. Clin Cancer Res. 1996; 2(10): 1649-57. Wild-type p53 protein potentiates cytotoxicity of therapeutic agents in human colon cancer cells.

[247] Kovacevic Z, Sivagurunathan S, Mangs H, Chikhani S, Zhang D, Richardson DR. The metastasis suppressor, N-myc downstream regulated gene 1 (NDRG1), upregulates p21 via p53-independent mechanisms. Carcinogenesis. 2011; 32(5): 732-40.

[248] Shen J, Sheng X, Chang Z, Wu Q, Wang S, Xuan Z, *et al*. Iron metabolism regulates p53 signaling through direct heme-p53 interaction and modulation of p53 localization, stability, and function. Cell Rep. 2014; 7(1): 180-93.

[249] Fan Y, Mao R, Yang J. NF-κB and STAT3 signaling pathways collaboratively link inflammation to cancer. Protein Cell. 2013; 4(3): 176-85.

[250] Luo D, Wang Z, Wu J, Jiang Wu J. The role of hypoxia inducible factor-1 in hepatocellular carcinoma. Biomed Res Int. 2014; 2014: 409272.

[251] Lihong F, Jia L, Zefeng Y, Xiaoqian D, Kunzheng W. The hypoxia-inducible factor pathway, prolyl hydroxylase domain protein inhibitors and their roles in bone repair and regeneration. BioMed Research International 2014; Article ID 239356. doi:10.1155/2014/239356. First accessed 29 August 2014.

[252] Bruin GJ, Faller T, Wiegand H, Schweitzer A, Nick H, Schneider J, *et al*. Pharmacokinetics, distribution, metabolism, and excretion of deferasirox and its iron complex in rats. Drug Metab Dispos. 2008; 36(12): 2523-38.

[253] Sanchez M, Galy B, Muckenthaler MU, Hentze MW. Iron-regulatory proteins limit hypoxia-inducible factor-2alpha] expression in iron deficiency. Nat Struct Mol Biol 2007 print;14(5):420-426.

[254] Maffettone C, Chen G, Drozdov I, Ouzounis C, Pantopoulos K.Tumorigenic properties of iron regulatory protein 2 (IRP2) mediated by its specific 73-amino acids insert. PLoS One. 2010; 5(4): e10163.

[255] Oexle H, Gnaiger E, Weiss G. Iron-dependent changes in cellular energy metabolism: influence on citric acid cycle and oxidative phosphorylation. Biochimica et Biophysica Acta (BBA) - Bioenergetics 1999 11/10;1413(3):99-107.

[256] Rouault TA. The role of iron regulatory proteins in mammalian iron homeostasis and disease. Nat Chem Biol 2006 print; 2(8):406-414.

[257] Chen G, Fillebeen C, Wang J, Pantopoulos K. Overexpression of iron regulatory protein 1 suppresses growth of tumor xenografts. Carcinogenesis. 2007; 28(4): 785-91.

[258] Wang W, Deng Z, Hatcher H, Miller LD, Di X, Tesfay L, *et al*. IRP2 regulates breast tumor growth. Cancer Res. 2014; 74(2): 497-507.

[259] Hamara K, Bielecka-Kowalska A, Przybylowska-Sygut K, Sygut A, Dziki A, Szemraj J. Alterations in expression profile of iron-related genes in colorectal cancer. Mol Biol Rep. 2013; 40(10): 5573-85.

[260] Roberts PJ, Der CJ. Targeting the Raf-MEK-ERK mitogen-activated protein kinase cascade for the treatment of cancer. Oncogene 2007; 26: 3291-310.

[261] Wu K, Polack A, Dalla-Favera R. Coordinated regulation of iron-controlling genes, H-ferritin and IRP2, by c-MYC. Science 199; 9; 283(5402): 676-679.

[262] Thiel A, Ristimaki A. Toward a molecular classification of colorectal cancer: the role of BRAF. Frontiers in oncology 2013; 3(281): 1-7.

[263] American Tissue Culture Collection (ATCC). Colon cancer and normal cell lines.

Available at

http://www.atcc.org/~/media/PDFs/Cancer%20and%20Normal%20cell%20lines%20tables/Colon%20cancer%20and%20normal%20cell%20lines.ashx. First accessed 28 August 2013.

[264] Yokota T. Are KRAS/BRAF mutations potent prognostic markers and/or predictive biomarkers in colorectal cancers? Anticancer Agents Med Chem. 2012; 12(2): 163-71.

[265] Gupta SC, Sung B, Prasad S, Webb LJ, Aggarwal BB. Cancer drug discovery by repurposing: teaching new tricks to old dogs. Trends in Pharmacological Sciences 2013; 34(9): 508-17.

[266] Paul SM, Mytelka DS, Dunwiddie CT, Persinger CC, Munos BH, Lindborg SR, *et al*. How to improve R&D productivity: the pharmaceutical industry's grand challenge. Nat Rev Drug Discov. 2010; 9(3): 203-14.

[267] Zamboni WC, Torchilin V, Patri AK, Hrkach J, Stern S, Lee R, *et al*. Best practices in cancer nanotechnology: perspective from NCI nanotechnology alliance. Clin Cancer Res. 2012; 18(12): 3229-41.

[268] The National Institute for Health and Care Excellence (NICE). Breast cancer (HER2 positive, unresectable) - trastuzumab emtansine (after trastuzumab & taxane) [ID603]. Available at https://www.nice.org.uk/Guidance/InDevelopment/GID-TAG350/Documents. First accessed 3 September 2014.

[269] Gelijns AC, Rosenberg N, Moskowitz AJ. Capturing the unexpected benefits of medical research. N Engl J Med. 1998; 339(10): 693-8

[270] Thayer AM. Drug repurposing. Chem Eng News 2012; 90: 15-25. Available at http://cen.acs.org/articles/90/i40/Drug-Repurposing.html?h=-1031248274. First accessed 3 September 2014.

[271] Li YY, Jones SJ. Drug repositioning for personalized medicine. Genome Med. 2012 Mar 30;4(3):27. doi: 10.1186/gm326. eCollection 2012.

[272] Khanim FL, Hayden RE, Birtwistle J, Lodi A, Tiziani S, Davies NJ, *et al*. Combined bezafibrate and medroxyprogesterone acetate: Potential novel therapy for acute myeloid leukaemia. PLoS One. 2009; 4(12): e8147.

[273] Molyneux E, Merrick B, Khanim FL, Banda K, Dunn JA, Iqbal G, *et al*. Bezafibrate and medroxyprogesterone acetate in resistant and relapsed endemic Burkitt lymphoma in Malawi; an open-label, single-arm, phase 2 study (ISRCTN34303497). Br J Haematol. 2014; 164(6): 888-90.

[274] Taieb J, Tabernero J, Mini E, Subtil F, Folprecht G, Van Laethem JL, *et al*. Oxaliplatin, fluorouracil, and leucovorin with or without cetuximab in patients with resected stage III colon cancer (PETACC-8): an open-label, randomised phase 3 trial. Lancet Oncol. 2014; 15(8): 862-73.

[275] Mukhopadhyay T, Sasaki J, Ramesh R, Roth JA. Mebendazole elicits a potent antitumor effect on human cancer cell lines both in vitro and in vivo. Clin Cancer Res. 2002; 8(9): 2963-9.

[276] Martarelli D, Pompei P, Baldi C, Mazzoni G. Mebendazole inhibits growth of human adrenocortical carcinoma cell lines implanted in nude mice. Cancer Chemother Pharmacol. 2008; 61(5): 809-17.

[277] Euhus DM, Hudd C, LaRegina MC, Johnson FE: Tumor measurement in the nude mouse. J Surg Oncol 1986; 31: 229-234.

[278] Kilinc V, Bedir A, Okuyucu A, Salis O, Alacam H, Gulten S.. Do iron chelators increase the antiproliferative effect of trichostatin A through a glucose-regulated protein 78 mediated mechanism? Tumour Biol. 2014; 35(6): 5945-51.

[279] Risinger AL, Giles FJ, Mooberry SL. Microtubule dynamics as a target in oncology. Cancer Treat Rev. 2009;35(3): 255-61.

[280] Rusan NM, Fagerstrom CJ, Yvon AM, Wadsworth P. Cell cycle-dependent changes in microtubule dynamics in living cells expressing green fluorescent protein-alpha tubulin. Mol Biol Cell. 2001; 12(4): 971–80.

[281] Ravelli RB, Gigant B, Curmi PA, Jourdain I, Lachkar S, Sobel A, *et al*. Insight into tubulin regulation from a complex with colchicine and a stathmin-like domain. Nature. 2004; 428(6979): 198–202.

[282] Bhattacharyya B, Panda D, Gupta S, Banerjee M. Anti-mitotic activity of colchicine and the structural basis for its interaction with tubulin. Med Res Rev. 2008; 28(1): 155–83.

[283] Sivakumar G. Colchicine semisynthetics: chemotherapeutics for cancer? Curr Med Chem. 2013; 20(7): 892-8.

[284] Cosentino L, Redondo-Horcajo M, Zhao Y, Santos AR, Chowdury KF, Vinader V, *et al*. Synthesis and biological evaluation of colchicine B-ring analogues tethered with halogenated benzyl moieties. J Med Chem. 2012; 55(24): 11062-6.

[285] Pantziarka P, Bouche G, Meheus L, Sukhatme V, Sukhatme VP. Repurposing Drugs in Oncology (ReDO)-mebendazole as an anti-cancer agent. Ecancermedicalscience. 2014; 8: 443.

[286] Laclette JP, Guerra G, Zetina C. Inhibition of tubulin polymerization by mebendazole Biochem Biophys Res Commun 1980; 92(2): 417–23.

[287] Friedman PA and Platzer EG (1980) Interaction of anthelmintic benzimidazoles with Ascaris suum embryonic tubulin Biochim Biophys Acta 1980; 630(2): 271–8.

[288] Doudican NA, Byron SA, Pollock PM, Orlow SJ. XIAP downregulation accompanies mebendazole growth inhibition in melanoma xenografts. Anticancer Drugs. 2013; 24(2): 181-8.

[289] Bai RY, Staedtke V, Aprhys CM, Gallia GL, Riggins GJ. Antiparasitic mebendazole shows survival benefit in 2 preclinical models of glioblastoma multiforme. Neuro Oncol. 2011; 13(9): 974-82.

[290] Nygren P, Fryknäs M, Agerup B, Larsson R. Repositioning of the anthelmintic drug mebendazole for the treatment for colon cancer J Cancer Res Clin Oncol 2013; 139(12): 2133–40.

[291] Coyne CP, Jones T, Bear R. Gemcitabine-(C4-amide)-[anti-HER2/neu] anti-neoplastic cytotoxicty in dual combination with mebendazole against chemotherapeutic-resistant mammary adenocarcinoma. J Clin Exp Oncol 2013; 02(02).

[292] Doudican N, Rodriguez A, Osman I, Orlow SJ. Mebendazole induces apoptosis via Bcl-2 inactivation in chemoresistant melanoma cells Mol Cancer Res 2008; 6(8): 1308–15.

[293] Dobrosotskaya IY, Hammer GD, Schteingart DE, Maturen KE, Worden FP. (2011) Mebendazole monotherapy and long-term disease control in metastatic adrenocortical carcinoma Endocr Prac 2011; 17(3): e59–62.

[294] Nygren P, Larsson R. Drug repositioning from bench to bedside: Tumour remission by the antihelmintic drug mebendazole in refractory metastatic colon cancer Acta Oncol 2013; 57(3): 427–8.

[295] Jaszczyszyn A, Gąsiorowski K, Świątek P, Malinka W, Cieślik-Boczula K, Petrus J, *et al*. Chemical structure of phenothiazines and their biological activity. Pharmacol Rep. 2012; 64(1):16-23.

[296] Fond G, Macgregor A, Attal J, Larue A, Brittner M, Ducasse D, *et al*. Antipsychotic drugs: pro-cancer or anti-cancer? A systematic review. Med Hypotheses. 2012; 79(1): 38-42.

[297] Byun HY, Lee JH, Kim BR, Kang S, Dong SM, Park MS, *et al*. Anti-angiogenic effects of thioridazine involving the FAK-mTOR pathway. Microvasc. Res. 2012; 84: 227–234.

[298] Park MS, Dong SM, Kim BR, Seo SH, Kang S, Lee EJ, *et al*.Thioridazine inhibits angiogenesis and tumor growth by targeting the VEGFR-2/PI3K/mTOR pathway in ovarian cancer xenografts. Oncotarget. 2014; 5(13): 4929-34.

[299] Qi L, Ding Y. Potential antitumor mechanisms of phenothiazine drugs. Sci China Life Sci. 2013; 56(11): 1020-7.

[300] Zong D, Zielinska-Chomej K, Juntti T, Mörk B, Lewensohn R, Hååg P, *et al*. Harnessing the lysosome-dependent antitumor activity of phenothiazines in human small cell lung cancer. Cell Death Dis. 2014; 5: e1111.

[301] Ikediobi ON, Reimers M, Durinck S, Blower PE, Futreal AP, Stratton MR, *et al*. In vitro differential sensitivity of melanomas to phenothiazines is based on the presence of codon 600 BRAF mutation. Mol Cancer Ther. 2008; 7(6): 1337-46.

[302] Spengler G, Takács D, Horváth A, Riedl Z, Hajós G, Amaral L, *et al*. Multidrug resistance reversing activity of newly developed phenothiazines on P-glycoprotein (ABCB1)-related resistance of mouse T-lymphoma cells. Anticancer Res. 2014; 34(4): 1737-41.

[303] Zong D, Hååg P, Yakymovych I, Lewensohn R, Viktorsson K. Chemosensitization by phenothiazines in human lung cancer cells: impaired resolution of γH2AX and increased oxidative stress elicit apoptosis associated with lysosomal expansion and intense vacuolation. Cell Death Dis. 2011; 2: e181.

[304] Pan JX, Ding K, Wang CY. Niclosamide, an old antihelminthic agent, demonstrates antitumor activity by blocking multiple signaling pathways of cancer stem cells. Chin J Cancer. 2012; 31(4): 178-84.

[305] Li Y, Li PK, Roberts MJ, Arend RC, Samant RS, Buchsbaum DJ. Multi-targeted therapy of cancer by niclosamide: A new application for an old drug. Cancer Lett. 2014; 349(1): 8-14.

[306] Kang SH, Yu MO, Park KJ, Chi SG, Park DH, Chung YG.. Activated STAT3 regulates hypoxia-induced angiogenesis and cell migration in human glioblastoma. Neurosurgery. 2010; 67(5): 1386-95.

[307] Kuendgen A, Gattermann N. Valproic acid for the treatment of myeloid malignancies. Cancer. 2007; 110(5): 943-54.

[308] Hutt DM, Roth DM, Vignaud H, Cullin C, Bouchecareilh M. The histone deacetylase inhibitor, vorinostat, represses hypoxia inducible factor 1 alpha expression through translational inhibition. PLoS One. 2014; 9(8): e106224.

[309] Mandard, A.-M., Dalibard, F., Mandard, J.-C, Marnay J, Henry-Amar M, Petiot JF, *et al*. Pathologic assessment of tumor regression after preoperative chemoradiotherapy of esophageal carcinoma. Clinicopathologic correlations. Cancer 1994; 73: 2680–2686.